Taxonomy, Phylogeny, Molecular Dating and Ancestral State Reconstruction of *Xylariomycetidae* (*Sordariomycetes*)

Milan C. Samarakoon
School of Life Science and Technology, Center for Informational Biology, University of Electronic Science and Technology of China, Chengdu 611731, P.R. China
Kevin D Hyde (kdhyde3@gmail.com)
Center of Excellence in Fungal Research
Sajeewa S. N. Maharachchikumbura
School of Life Science and Technology, Center for Informational Biology, University of Electronic Science and Technology of China, Chengdu 611731, P.R. China
Marc Stadler
Institute of Microbiology, Technische Universität Braunschweig, Spielmannstraβe 7, 38106 Braunschweig, Germany
E. B. Gareth Jones
Department of Botany and Microbiology, College of Science, King Saud University, P.O Box 2455, Riyadh 11451, Kingdom of Saudi Arabia
Itthayakorn Promputtha
Department of Biology, Faculty of Science, Chiang Mai University, Chiang Mai 50200, Thailand
Nakarin Suwannarach
Department of Biology, Faculty of Science, Chiang Mai University, Chiang Mai 50200, Thailand
Erio Camporesi
A.M.B. Gruppo, Micologico Forlivese "Antonio Cicognani", Via Roma 18, Forlí, Italy
Timur S. Bulgakov
Department of Plant Protection, Federal Research Centre the Subtropical Scientific Centre of the Russian Academy of Sciences, Yana Fabritsiusa Street 2/28, Sochi 354002, Krasnodar Region, Russia
Jian-Kui Liu
School of Life Science and Technology, Center for Informational Biology, University of Electronic Science and Technology of China, Chengdu 611731, P.R. China

Research Article

Keywords: 33 new taxa, Amphisphaeriales, Appendicosporaceae, Evolution, Stromata, Xylariales

Posted Date: October 1st, 2021

DOI: https://doi.org/10.21203/rs.3.rs-935829/v1

Version of Record: A version of this preprint was published at Fungal Diversity on January 16th, 2022. See the published version at https://doi.org/10.1007/s13225-021-00495-5.

Abstract

Xylariomycetidae (Ascomycota) is a highly diversified group with variable stromatic characters. Our research focused on inconspicuous stromatic xylarialean taxa from China, Italy, Russia, Thailand and the United Kingdom. Detailed morphological descriptions, illustrations and combined ITS-LSU- rpb 2- tub 2- tef 1 phylogenies revealed 38 taxa from our collections belonging to Amphisphaeriales and Xylariales . A new family (Appendicosporaceae), five new genera (Magnostiolata , Melanostictus , Neoamphisphaeria , Nigropunctata and Paravamsapriya), 27 new species (Acrocordiella photiniicola , Allocryptovalsa sichuanensis , Amphisphaeria parvispora , Anthostomella lamiacearum , Apiospora guiyangensis , Ap. sichuanensis , Biscogniauxia magna , Eutypa camelliae , Helicogermslita clypeata , Hypocopra zeae , Magnostiolata mucida , Melanostictus longiostiolatus , Me. thailandicus , Nemania longipedicellata , Ne. delonicis , Ne. paraphysata , Ne. thailandensis , Neoamphisphaeria hyalinospora , Neoanthostomella bambusicola , Nigropunctata bambusicola , Ni. nigrocircularis , Ni. thailandica , Occultitheca rosae , Paravamsapriya ostiolata , Peroneutypa leucaenae , Seiridium italicum and Vamsapriya mucosa) and seven new host/geographical records are introduced and reported. Divergence time estimates indicate that Delonicicolales diverged from Amphisphaeriales + Xylariales at 161 (123–197) MYA. Amphisphaeriales and Xylariales diverged 154 (117–190) MYA with a crown age of 127 (92–165) MYA and 147 (111–184) MYA, respectively. Appendicosporaceae (Amphisphaeriales) has a stem age of 89 (65–117) MYA. Ancestral character state reconstruction indicates that astromatic, clypeate ascomata with aseptate, hyaline ascospores that lack germ slits may probably be ancestral Xylariomycetidae having plant-fungal endophytic associations. The Amphisphaeriales remained mostly astromatic with common septate, hyaline ascospores. Stromatic variations may have developed mostly during the Cretaceous period. Brown ascospores are common in Xylariales , but they first appeared in Amphisphaeriaceae , Melogrammataceae and Sporocadaceae during the early Cretaceous. The ascospore germ slits appeared only in Xylariales during the Cretaceous after the divergence of Lopadostomataceae . Hyaline, filiform and apiospores may have appeared as separate lineages providing the basis to Xylariaceae , which may have diverged independently. The future classification of polyphyletic xylarialean taxa will not be based on stromatic variations, but the type of ring, the colour of the ascospores, and the presence or absence of the type of germ slit.

Introduction

Eriksson and Winka (1997) introduced *Xylariomycetidae* with a single order *Xylariales*, based on morphology and SSU phylogeny. Eriksson (1983) suggested to treat *Amphisphaeriales* as accommodating *Amphisphaeriaceae*, *Cainiaceae*, *Clypeosphaeriaceae* and *Hyponectriaceae* based on ascospore morphology. Barr (1990), however, arranged *Amphisphaeriales*, *Diatrypales*, *Phyllachorales* and *Trichosphaeriales* in *Xylariales*. Kang et al. (1998) revived *Amphisphaeriales* based on 5.8S-ITS2 molecular phylogeny and coelomycetous asexual morphs and accepted *Clypeosphaeriaceae* and *Cainiaceae* in the order. Subsequently, Kang et al. (2002) revised their previous conclusion, and *Amphisphaeriaceae* and *Xylariaceae* were accepted in *Xylariales* based on a combined SSU-ITS molecular phylogeny. Kirk et al. (2008) documented *Xylariales* as the only order in *Xylariomycetidae* with nine families (*Amphisphaeriaceae*, *Cainiaceae*, *Clypeosphaeriaceae*, *Diatrypaceae*, *Graphostromataceae*, *Hyponectriaceae*, *Iodosphaeriaceae*, *Myelospermataceae* and *Xylariaceae*). A revision with additional collections and the morpho-phylogenetic study revealed that *Xylariomycetidae* consisted of two orders; *Amphisphaeriales* (*Amphisphaeriaceae*, *Bartaliniaceae*, *Clypeosphaeriaceae*, *Discosiaceae*, *Pestalotiopsidaceae* and *Phlogicylindriaceae*) and *Xylariales* (*Apiosporaceae*, *Cainiaceae*, *Coniocessiaceae*, *Diatrypaceae*, *Graphostromataceae*, *Hyponectriaceae*, *Iodosphaeriaceae*, *Lopadostomataceae*, *Melogrammataceae*, *Pseudomassariaceae*, *Vialaeaceae* and *Xylariaceae*) (Senanayake et al. 2015). In an outline of *Sordariomycetes*, Maharachchikumbura et al. (2016) treated *Amphisphaeriales* as a synonym of *Xylariales* due to inadequate statistical support in the phylogenetic analyses by Senanayake et al. (2015), and accepted 22 families in *Xylariales* based on morphology and combined LSU-SSU-*tef*1-*rpb*2 phylogeny. With divergence time estimates as additional information for the standardizing of higher ranks, Samarakoon et al. (2016) and Hongsanan et al. (2017) accepted *Xylariales* and *Amphisphaeriales* in *Xylariomycetidae*, which may have diverged around 152–187 MYA.

Perera et al. (2017) introduced *Delonicicolales* as the third order in *Xylariomycetidae*, which diverged from the *Amphisphaeriales*+*Xylariales* clade at 181 (133–234) MYA. Following several consecutive morpho-molecular studies, Hyde et al. (2020b) provided an outline for the *Sordariomycetes*, including *Xylariomycetidae* with three orders as *Amphisphaeriales* (17 families), *Delonicicolales* (2 families) and *Xylariales* (15 families). In addition, *Myelospermataceae* is treated as a *Xylariomycetidae* families *incertae sedis* due to lack of molecular data.

Species in *Xylariomycetidae* are distributed worldwide with dynamic nutritional relationships as endophytes (U'Ren et al. 2016; Rashmi et al. 2019), pathogens and saprobes (Zhang et al. 2006; Daranagama et al. 2018; Hyde et al. 2020b). *Xylariomycetidae* comprises species with conspicuous and inconspicuous, superficial or immersed stromata, usually black and thick-walled ascomata with periphysate, papillate ostioles; unitunicate or rarely bitunicate-like asci with or without apical ring bluing in Melzer's reagent, and mostly pigmented ascospores in their sexual state and hyphomycetous or coelomycetous asexual morphs (Smith et al. 2003; Wang et al. 2004; Zhang et al. 2006; Jaklitsch and Voglmayr 2012; Senanayake et al. 2015; Hyde et al. 2020b). Conspicuous massive, stalked or sessile stromata are commonly found among xylarialean taxa (Daranagama et al. 2016b). Daranagama et al. (2016b) reviewed the stromatic diversity of xylarialean taxa and considered the collection of taxa with inconspicuous form to be sparse.

As a result, the taxonomic placement of many taxa lacking distinct stromata are uncertain (Daranagama et al. 2018; Wendt et al. 2018). Several recent studies have focused on the morphology and phylogeny of inconspicuous xylarialean taxa, including the re-examination of herbarium specimens (Daranagama et al. 2018). Those studies not only focused on providing morpho-molecular information but also placed them in higher ranks (e.g. *Barrmaeliaceae*, *Induratiaceae*, *Fasciatisporaceae* and *Oxydothidaceae*) (Konta et al. 2016; Voglmayr et al. 2018; Hyde et al. 2020a; Samarakoon et al. 2020c). The genera, which have been introduced in new families were previously accepted with uncertain morphologies and phylogenies. They are morphologically unique in having inconspicuous, immersed ascomata, that do not have key characters for delimiting higher ranks as compared to conspicuous stromatic xylarialean taxa. However, the asci and ascospore morphologies were cardinal characters coupled with molecular phylogenies towards establishing new higher ranks. There are many taxonomic uncertainties of xylarialean taxa that are not yet resolved.

We are researching xylarialean taxa towards resolving taxonomic uncertainties. Here we provided new collections with their morphology, analysed their DNA sequences and investigated their phylogenetic relationships to better identify and classify them. We evaluated different stromatic characters of selected taxa

in *Xylariomycetidae* to reconstruct the ancestral state. In addition, ascospore characters i.e. colour, septation and the presence or absence of a germ slit were evaluated to understand the ancestral state of the xylarialean taxa.

Materials And Methods

Collection, isolation and morphological studies

Fresh specimens were collected and received from China, Italy, Russia, Thailand and the United Kingdom during 2016–2020. External examinations were made as described in Samarakoon et al. (2020b). Indian ink, Congo red and Melzer's reagent were used where necessary. The Tarosoft (R) Image Frame Work (v 0.9.7) program and Adobe Photoshop CS6 software (Adobe Systems, USA) were used for measuring and processing images.

Axenic cultures were obtained from single spores or tissues by the method described in Senanayake et al. (2020). Germinating spores were observed with a Motic SMZ 168 Stereo Zoom microscope and transferred to potato dextrose agar (PDA; 39 g/l distilled water, Difco potato dextrose). The cultures were incubated at 25–30°C for 4–6 weeks, with frequent observations. The herbarium specimens were deposited in the Mae Fah Luang University Herbarium (MFLU), Chiang Rai, Thailand and the Cryptogamic Herbarium of Kunming Institute of Botany Academia Sinica (HKAS), Chinese Academy of Sciences, Kunming, China. Ex-type cultures were deposited in the Mae Fah Luang University Culture Collection (MFLUCC), the Guizhou Culture Collection (GZCC), Guizhou, and China General Microbiological Culture Collection Center (CGMCC), Institute of Microbiology Chinese Academy of Sciences, Beijing, China. New taxa were linked with Facesoffungi and Index Fungorum databases as explained in Jayasiri et al. (2015) and Index Fungorum (http://www.indexfungorum.org; accessed at 9 September 2021).

In addition, selected cultures deposited in MFLUCC were loaned for regenerating missing sequences. Subcultures were obtained and incubated them at 25–30°C for 4–6 weeks with frequent observations. Those cultures were used for total DNA extraction and PCR amplification.

DNA extraction, PCR amplification and sequencing

Fresh mycelium was scraped from the margins of colonies on PDA plates, incubated at 25–30°C for four weeks. When fungi failed to grow in culture, DNA was extracted directly from the fruiting bodies. Total DNA extraction kits were used according to the manufacturer's instructions [Sangon Biotech (Shanghai) Co. Ltd. China]. The primers and PCR protocols are summarised in Table 1. The total volume of 25 µl containing 12.5 µl of 2× PCR Master Mix with dye [0.1 U Taq Polymerase/µl, 500 µM dNTP each, 20 mM Tris-HCl (pH 8.3), 100 mM KCl, 3 mM $MgCl_2$], 1 µl of each primer, 9.5 µl of double-distilled water and 1 µl (100–500 ng) of DNA template. All the PCR products were immediately subjected to 4°C and were visualised on 1% agarose electrophoresis gels stained with GoldView I nuclear staining dye (1 µL/10 mL of agarose) with D2000 DNA ladder (Realtimes Biotech, Beijing, China). DNA sequencing was performed at Sangon Biotech (Shanghai) Co. Ltd., China.

Phylogenetic analyses

All the assembled sequences were used for BLAST search (https://www.ncbi.nlm.nih.gov) (Altschul et al. 1990). Related sequences for newly obtained sequences were downloaded from the GenBank (Supplementary Table 1). Individual loci were aligned using FFT-NS-2 Tree-based progressive method, 20 PAM/ k = 2 Scoring matrix for nucleotide sequences and 1.0 Gap opening penalty settings of MAFFT V.7.036 (http://mafft.cbrc.jp/alignment/server/) (Katoh et al. 2019) and improved manually when necessary, using BioEdit v. 7.0 (Hall 1999). ITS and LSU sequences were trimmed with TrimAl [(v.1.0) Gappyout option] (Capella-Gutierrez et al. 2009). Exon regions of *rpb*2, *tub*2 and *tef*1 were extracted with reference to *Amphirosellinia nigrospora* (HAST 91092308) and *Graphostroma platystomum* (CBS 270.87).

Characters were assessed to be unordered and equally weighted. MrModeltest 2.3 was performed for each locus to estimate the best-fit evolutionary model under the Akaike Information Criterion (AIC) (Nylander 2004). Phylogenies were generated using maximum-likelihood (ML) and Bayesian Inference (BI) analyses using single and ITS-LSU-*rpb*2-*tub*2 and ITS-LSU-*rpb*2-*tub*2-*tef*1 combined alignments. For future studies, all the newly generated sequences were deposited in GenBank (Dissanayake et al. 2020) (Table 2).

The ML analyses were performed with IQ-TREE (Nguyen et al. 2015, Trifinopoulos et al. 2016) using the ML+rapid bootstrap setting with 1,000 replicates. The Bayesian tree was generated using MCMC sampling in MrBayes v3.1.2 (Huelsenbeck and Ronquist 2001; Zhaxybayeva and Gogarten 2002) for 10,000,000 MCMC generations using four chains and partition analysis with 100 sample frequencies. The first 25,000 (25% from total) trees were in the burn-in phase and were discarded. The remaining 75,000 trees were used to calculate the posterior probability (PP). The resulting trees were viewed with FigTree v.1.4.0 (Rambaut 2012), and the final layout was done with Adobe Illustrator® CS5 (Version 15.0.0, Adobe®, San Jose, CA). The final alignment and tree were registered in TreeBASE (http://www.treebase.org/) under the submission ID: XXXX.

Divergence time estimation

Divergence time estimation among the families in *Xylariomycetidae* was performed using the BEAST.v1.10.4 program. Combined LSU, ITS, *rpb*2, *tub*2 and *tef*1 DNA loci were used for the analysis, representing 240 taxa (Supplementary Table 2). The XML file was obtained, including the partitioned alignment, using the BEAUti (BEAST package). The crown age of *Xylariomycetidae* was used as the secondary calibration node (mean = 168 MYA, SD = 16, Normal distribution) (Samarakoon et al. 2016; Hongsanan et al. 2017). The analysis was performed for 80,000,000 generations using BEAST.v1.10.4 (Suchard et al. 2018), obtaining logging parameters and trees for every 5000 generations. Effective sample sizes (ESS) of parameters were checked using Tracer v.1.6 (Rambaut et al. 2013) (ESS > 200). The first 20% trees were discarded based on the ESS values, and the remaining trees were used to generate a maximum clade credibility tree by using TreeAnnotator v1.10.4. The resulted tree was viewed with FigTree v.1.4.0 (Rambaut 2012), and the final layout was done with Adobe Illustrator® CS5 (Version 15.0.0, Adobe®, San Jose, CA). The geographical timescale was followed as in Walker (2019).

Ancestral character state analyses

Bayesian Binary MCMC was performed in RASP 3.2.1 (Reconstruct Ancestral State in Phylogenies) to construct ancestral character state (Yu et al. 2015). Time-calibrated maximum clade credibility tree reconstructed in BEAST was used for the analysis and exported to RASP 3.2.1. Each terminal in the tree was coded for seven stromatic characters (Table 3), and undetermined sexual morphs were treated as separate undetermined characters for the family level. In addition, characters of ascospore septation (aseptate/septate/apiosporous/undetermined), ascospore colour (hyaline/brown/undetermined) and ascospore germ slit (presence/absence/undetermined) were evaluated (Supplementary Table 2). Bayesian Binary MCMC trees were performed and visualised in RASP 3.2.1 using default settings as follows: 1,010,000 iterations for BayesTraits with a burnin of 10,000, sampling 1000 trees and with 10 ML trees; 50,000 generations for Bayesian Binary MCMC, with 10 chains, a sampling frequency of 100, a temperature of 0.1, state frequencies fixed (JC), and among-site rate variation equal.

Results

Phylogenetic analyses

All gene regions resulted in GTR+I+G model. Maximum likelihood tree topologies for each gene dataset and combined datasets were compared, and the overall tree topology was congruent to those obtained from the combined dataset. The RAxML analysis of the combined ITS-LSU-*rpb2*-*tub2*-*tef*1 dataset yielded the best-scoring tree (Fig. 1). Bayesian posterior probabilities from MCMC were evaluated with a final average standard deviation of split frequencies less than 0.01.

Delonicicolales clusters as basal to the *Amphisphaeriales* and *Xylariales* clades, with 100%/1.00 PP statistical support. *Amphisphaeriales* and *Xylariales* form distinct clades with 99%/0.92 PP statistical support, similar to a previous study in Hyde et al. (2020b). *Amphisphaeriales* comprised 27 clades (Clade Am) including 21 families, while *Xylariales* (Clade Xy) comprised 31 clades including 16 families. Uncertain clades with a single or few taxa are identified as six in *Amphisphaeriales* and 15 in *Xylariales*. Forty-nine of newly generated sequences from our study group with *Xylariales* and nine with *Amphisphaeriales*.

One of our collections (HKAS 107015) is similar to *Appendicospora hongkongensis* and is introduced here as a reference specimen. Two isolates (MFLU 19-2131, HKAS 106988), *Neoamphisphaeria hyalinospora gen. et sp. nov*. form a sister clade to *Appendicospora*, and here we introduce *Appendicosporaceae fam. nov*. in *Amphisphaeriales* to accommodate *Appendicospora* and *Neoamphisphaeria*. New species for the families *Amphisphaeriaceae* (*Amphisphaeria parvispora sp. nov*. MFLU 18-0767), *Apiosporaceae* (*Apiospora guiyangesnsis sp. nov*. HKAS 102403, *Ap. sichuanensis sp. nov*. HKAS 107008) and *Sporocadaceae* (*Seiridium italicum sp. nov*. MFLU 16-1315) are introduced with high statistical support.

Seven newly generated sequences group in *Diatrypaceae* and identify them as, *Allocryptovalsa sichuanensis sp. nov*. (HKAS 107017), *Diatrype disciformis* (MFLU 17-1549), *Eutypa camelliae sp. nov*. (HKAS 107022, MFLU 20-0182HT), *Melanostictus longiostiolatus gen. et sp. nov*. (MFLU 19-2146), *Me. thailandicus sp. nov*. (MFLU 19-2123) and *Peroneutypa leucaenae sp. nov*. (MFLU 18-0816). Twelve taxa cluster in *Xylariaceae* sensu stricto. *Helicogermslita clypeata sp. nov*. (MFLU 18-0852, HKAS 102321) clusters in *Astrocystis*+*Collodiscula* clade. Four *Nemania* species, *Ne. longipedicellata sp. nov*. (MFLU 18-0819), *Ne. delonicis sp. nov*. (MFLU 19-2124), *Ne. paraphysata sp. nov*. (MFLU 19-2121) and *Ne. thailandensis sp. nov*. (MFLU 19-2122, MFLU 19-2117) are supported with high statistical support. A single taxon, MFLU 18-0809, clusters with *Stromatoneurospora phoenix* (BCC 82040) sister to the *Hypocopra* clade. Three newly generated sequences cluster in *Vamsapriyaceae*. *Paravamsapriya ostiolata gen. et sp. nov*. (MFLU 18-0761, MFLU 18-0813) and *Vamsapriya mucosa sp. nov*. (MFLU 18-0103) are described here.

Anthostomella-like taxa collected in this study group in seven clades (Xy3, Xy4, Xy22, Xy23, Xy24, Xy25 and Xy26) in *Xylariales*. *Magnostiolata mucida gen. et sp. nov*. (MFLU 19-2133) and *Occultitheca rosae sp. nov*. (HKAS 102393) cluster between *Clypeosphaeriaceae* and *Induratiaceae* as distinct clades. *Neoanthostomella bambusicola sp. nov*. (MFLU 18-0796) is accommodated in Clade Xy22 with *Neo. pseudostromatica*, the generic type with high statistical support (100%/1.00 PP). Clade Xy23 comprises *Calceomyces*, *Ceratocladium*, *Circinotrichum*, *Gyrothrix* and *Xenoanthostomella*. Our new collection, MFLU 18-0840, clusters as a sister to *Xe. chromolaenae* (MFLUCC 17-1484) with 100%/1.00 PP statistical support. *Anthostomella lamiacearum*, "*Neoathostomella ficl*" and "*Neo. viticola*" cluster group in Clade Xy24 (*Anthostomella helicofissa* clade), which is distinct from *Neo. pseudostromatica*. Our new collections, *Anthostomella lamiacearum sp. nov*. (MFLU 18-0101, HKAS 102325) clustered in Clade Xy24.

Several *Anthostomella*, *Alloanthostomella* and *Pseudoanthostomella* taxa cluster in Clade Xy25. Three newly generated sequences cluster in *Pseudoanthostomella*. Based on morphological similarities and phylogeny, we accepted those collections as *Ps. pini-nigrae*. Clade Xy26 accommodates five taxa (three species): *Nigropunctata bambusicola gen. et sp. nov*. (MFLU 19-2134, MFLU 19-2145), *Ni. nigrocircularis sp. nov*. (MFLU 19-2130) and *Ni. thailandica sp. nov*. (MFLU 19-2118, HKAS 106975). Thirteen sequences of our collections clustered in other families'; viz. *Coniocessiaceae* (*Paraxylaria xylostei* MFLU 17-1645, MFLU 17-1636, HKAS 102313), *Fasciatisporaceae* (*Fasciatispora cocoes* MFLU 19-2143, HKAS 107000), *Graphostromataceae* (*Biscogniauxia magna sp. nov*. MFLU 18-0850, *Bi. Petrensis* HKAS 102388, *Camillea tinctor* MFLU 18-0786), *Lopadostomataceae* (*Lopadostoma quercicola* MFLU 17-0843, MFLU 17-0731, MFLU 17-0940) and *Requienellaceae* (*Acrocordiella photiniicola sp. nov*. MFLU 17-1552, HKAS 102287).

Divergence time estimation

Three clades were obtained in *Xylariomycetidae*, including 39 families representing the orders *Amphisphaeriales*, *Delonicicolales* and *Xylariales* (Fig. 2). According to the estimates, *Delonicicolales* diverged from *Amphisphaeriales*+*Xylariales* 161 (123–197) MYA. *Amphisphaeriales* and *Xylariales* diverged 154 (117–190) MYA with a crown age of 127 (92–165) MYA and 147 (111–184) MYA, respectively, with similar results to Hyde et al. (2020b) and Samarakoon et al. (2020c). The new family *Appendicosporaceae* diverged from *Hyponectriaceae* and *Nothodactylariaceae* 89 (65–117) MYA.

Character analysis

Ancestral character state analyses resulting from Bayesian Binary MCMC (BBM) are shown in Figs. 2 and 3. *Xylariomycetidae* was reconstructed as derived from inconspicuous, immersed or semi-immersed ascomata with a prominent or rudimentary carbonaceous clypeus (Character 6) and shared a high percentage among *Amphisphaeriales*, *Delonicicolales* and *Xylariales*. *Xylariaceae* includes highly variable stromatic characters, and is a diversified group as compared to all the other families in *Xylariomycetidae*. *Hypoxylaceae* was reconstructed as having a conspicuous, unipartite, carbonaceous stroma (Character 3) and diversified into a conspicuous, stalked or sessile, carbonaceous stroma (Character 1). The conspicuous, erumpent, bipartite, carbonaceous stromatic development (Character 2) and semi-immersed, erumpent or superficial, pseudostromatic development (Character 4) were mostly distributed in *Graphostromataceae* and *Diatrypaceae,* respectively. Even though the sexual morphs of *Beltraniaceae* and *Castanediellaceae* are undetermined, there is a high possibility that they will have inconspicuous, immersed or semi-immersed ascomata with a prominent or rudimentary carbonaceous clypeus stromata (Character 6), based on evidence from recent ancestors of the clade. It is therefore possible to predict characters of the sexual morphs in some families that lack known sexual morphs through their ancestral characters. In addition, septate, hyaline ascospores and the absence of a germ slit are ancestral characters of *Xylariomycetidae*. Apiospores have evolved independently in several clades. Brown ascospores are often found in *Xylariales*, while *Induratiaceae* and *Vamsapriyaceae* have hyaline apiospores. Several xylarialean taxa have ascospores with germ slits, but these are not found in *Amphisphaeriales* and *Delonicicolales*. The *Amphisphaeriales* clade comprises a variety of characters and several groups with undetermined sexual morphs.

Taxonomy

In this paper, we follow the classifications in the studies of Hyde et al. (2020b) and Wijayawardene et al. (2020), and are updated according to recent relevant literature.

Ascomycota R.H. Whittaker, Quarterly Review of Biology 34: 220 (1959)

Sordariomycetes O.E. Erikss. & Winka, Myconet 1: 10 (1997)

Xylariomycetidae O.E. Erikss & Winka

Notes: For the latest treatments of this subclass, we follow Hyde et al. (2020b) and Wijayawardene et al. (2020). *Myelospermataceae* is accepted in *Xylariomycetidae* families *incertae sedis* due to lack of molecular data.

Amphisphaeriales D. Hawksw. & O.E. Erikss.

Amphisphaeriaceae G. Winter [as 'Amphisphaerieae'], Rabenh. Krypt.-Fl., Edn 2 (Leipzig) 1.2: 259 (1885)

Amphisphaeriaceae was introduced by Winter (1887), which mainly consists of saprobes in terrestrial, aquatic and marine habitats and occasionally hemibiotrophic or necrotrophic species (Wang et al. 2004; Senanayake et al. 2015; Jaklitsch et al. 2016). Hyde et al. (2020b) and Wijayawardene et al. (2020) accepted *Amphisphaeriaceae* in *Amphisphaeriales* with three genera as *Amphisphaeria*, *Griphosphaerioma*, and *Lepteutypa*. Samarakoon et al. (2020b) revised the morphology and phylogeny of *Amphisphaeria* and *Lepteutypa*, and synonymised *Lepteutypa* under *Amphisphaeria*. In addition, the monospecific genus *Trochilispora*, which had been accepted in *Amphisphaeriaceae*, is revised and synonymised under *Hymenopleella* (*Sporocadaceae*) (Samarakoon et al. 2020b). As a result of these studies, only *Amphisphaeria* and *Griphosphaerioma* are accepted in *Amphisphaeriaceae*.

Amphisphaeria Ces. & De Not., Comm. Soc. crittog. Ital. 1(4): 223 (1863)

Notes: *Amphisphaeria* is the type genus of *Amphisphaeriaceae*, with *A. umbrina* as the type species (Cesati and de Notaris 1863). *Amphisphaeria* species are saprobes on woody branches and some monocotyledons, including grasses (Wang et al. 2004). *Amphisphaeria* accommodates 27 species (Samarakoon et al. 2020b), which are characterised by solitary or aggregated ascomata under a poorly-developed clypeus or clypeus lacking; unitunicate asci with J+ or J-, apical rings and light brown to dark brown, ellipsoid to fusiform, 1–3-septate ascospores and coelomycetous asexual morphs.

Amphisphaeria parvispora Samarak. & K.D. Hyde, ***sp. nov***.

Index Fungorum number: IF558710; *Facesoffungi number*: FoF 10186; Fig. 4

Etymology: The specific epithet reflects the small ascospores.

Holotype: MFLU 18-0767

Saprobic on a dead branch. **Sexual morph**: *Ascomata* 230–260 × 300–400 µm ($\bar{x}$ = 245 × 360 µm, n = 10), immersed, visible as raised, black dots, solitary, in cross-section, conical with mostly flattened base. *Ostioles* centric, prominent, conical, wide, ostiolar canal periphysate. *Peridium* 8.5–23 µm ($\bar{x}$ = 16.5 µm, n = 10) wide, wider at the apex, multi-layered, outer layer comprising reddish brown, thick-walled cells of *textura angularis*, inner layer composed of hyaline, thin-walled cells of *textura angularis*. *Paraphyses* 2.5–5 µm ($\bar{x}$ = 3.6 µm, n = 15) wide, longer than asci, cellular, septate, constricted at septa, guttulate, embedded in a gelatinous matrix. *Asci* 62–105 × 5–6.5 µm ($\bar{x}$ = 83.5 × 5.7 µm, n = 20), 8-spored, unitunicate, cylindrical, with a bifurcate pedicel, with a 0.7–0.9 × 1.8–2.2 µm ($\bar{x}$ = 0.8 ×2 µm, n = 5), discoid, apical ring, J+ in Melzer's reagent, apically rounded. *Ascospores* 9.5–11.5 × 3–4 µm ($\bar{x}$ = 10.5 × 3.5 µm, n = 30), L/W 3, uniseriate, hyaline when young, light brown to grayish when mature, ellipsoid, 1-septate, constricted at septa, bi-guttulate, smooth-walled, lack of mucilaginous sheath. **Asexual morph**: Undetermined.

Material examined: Thailand, Phayao Province, Phu Sang, on dead branch, 20 July 2017, M.C. Samarakoon, SAMC060 (MFLU 18-0767, **holotype**), (HKAS 102328, **isotype**).

Notes: *Amphisphaeria parvispora* shares similar morphologies to other species in the genus in having solitary, immersed ascomata with two-layered peridium, unitunicate asci with J+, discoid, apical ring, and brown ascospores. Our novel taxon is similar to *Am. curvaticonidia*, *Am. thailandica* (Thailand) and *Am. sorbi* (Italy) in having conical to subglobose, solitary ascomata with a short, periphysate and a narrow ostiolar canal. *Amphisphaeria curvaticonidia* possesses 2-distoseptate ascospores with a median, slightly constricted euseptum and thin mucilaginous sheath, while *Am. parvispora* possesses 1-septate ascospores lacking a mucilaginous sheath. *Amphisphaeria thailandica* and *Am. sorbi* have J-, apical rings, while *Am. parvispora* has a J+, apical ring. Compared to all *Amphishaeria* species, our new collection has the smallest asci (83.5 × 5.7 µm) and ascospores (10.5 × 3.5 µm) among J+, apical ring bearing species. The LSU sequence of *Am. parvispora* is similar to *Am. curvaticonidia* MFLU 18-0789 (98.5%, 4/732 gaps), *Am. fuckelii* CBS 140409 (98%, 1/873 gaps) and *Am. thailandica* MFLU 18-0794 (98%, 0/869 gaps), while *rpb*2 is similar to *Am. fuckelii* CBS 140409 (87%, 0/1067 gaps), *Am. qujingensis* KUMCC 19-0187 (86%, 0/1067 gaps) and *Am. curvaticonidia* MFLU 18-0789 (85%, 2/880 gaps). In combined gene phylogeny, *Am. parvispora* clusters with *Am. sorbi* (MFLUCC 13-0721) and *Am. thailandica* (MFLU 18-0767), as a basal clade with 84% statistical support. Based on distinct morphology and phylogeny, *Am. parvispora* is introduced as a new species.

Apiosporaceae K.D. Hyde, J. Fröhl., Joanne E. Taylor & M.E. Barr, in Hyde, Fröhlich & Taylor, Sydowia 50(1): 23 (1998)

Hyde et al. (1998) established *Apiosporaceae* with five genera as *Appendicospora*, *Arthrinium* (= *Apiospora*), *Dictyoarthrinium*, *Endocalyx* and *Spegazzinia* based only on morphology. Species accommodated in *Apiosporaceae* are saprobic, pathogenic or endophytic on plant tissues, lichens, and marine algae, occasionally infecting humans or isolated from soil (Hyde et al. 2020b). Tanaka et al. (2015) provided the phylogenetic affinity of *Spegazzinia* in *Didymosphaeriaceae* (*Pleosporales*). A taxonomic and phylogenetic revision of *Nigrospora* showed that the genus has a close affinity to *Apiosporaceae* (Wang et al. 2017). Samarakoon et al. (2020a) revised the morphology and phylogeny of *Dictyoarthrinium* (*D. musae* and *D. sacchari*), and transferred it into *Didymosphaeriaceae* (*Pleosporales*) sister to *Spegazzinia*. Moreover, Konta et al. (2021) introduced *Endocalyx metroxyli* and transferred *Endocalyx* to *Cainiaceae* based on morphology and multigene phylogeny. Pintos and Alvarado (2021) re-evaluated the multigene phylogeny and the morphology of *Arthrinium* and suggested accepting *Arthrinium sensu stricto* and *Apiospora* as independent lineages within *Apiosporaceae*. *Appendicosporaceae* is introduced as a new family to accommodate *Appendicospora* in this study. At present, only the genera *Apiospora*, *Arthrinium* and *Nigrospora* remain in *Apiosporaceae* (Hyde et al. 2020b; Samarakoon et al. 2020a; Konta et al. 2021).

Apiospora Sacc., Atti Soc. Veneto-Trent. Sci. Nat., Padova, Sér. 4 4: 85 (1875)

Notes: Crous and Groenewald (2013) re-evaluated the morphology and phylogeny of *Arthrinium* (= *Apiospora*). *Arthrinium* species have densely arranged perithecial ascomata in a longitudinal stroma; clavate to broadly cylindrical asci and apiospores in the sexual and coelomycetous or hyphomycetous asexual morphs. The genus is widely distributed as endophytes, epiphytes, saprobes and plant pathogens on commercial crops and ornamentals (Crous and Groenewald 2013; Hyde et al. 2020b). *Arthrinium* was expanded with abundant sampling and isolation with morpho-phylo studies while accepting > 70 species in recent years (Hyde et al. 2020b). Pintos and Alvarado (2021) provided molecular data for the type species *Ar. cariciola* and accepted two genera as *Apiospora* and *Arthrinium*. *Arthrinium* species have variously shaped conidia and inhabit *Cyperaceae* or *Juncaceae* in temperate, cold or alpine habitats. *Apiospora* species have rounded/lenticular conidia and inhabit mainly on *Poaceae* (and many other plant host families) in a wide range of habitats, including tropical and subtropical regions. Nearly 20 *Apiospora*/ *Arthrinium* species have been recorded from China (Senanayake et al. 2020; Farr and Rossman 2021; Feng et al. 2021).

Apiospora guiyangensis Samarak., Jian K. Liu & K.D. Hyde, ***sp. nov***.

Index Fungorum number: IF558711; *Facesoffungi number*: FoF 10187; Fig. 5

Etymology: The specific epithet reflects the location, Guiyang, from where the species was first collected.

Holotype: HKAS 102403

Saprobic on dead culm of grass. **Sexual morph**: *Stromata* 3.6–6 × 0.9–4.6 × 0.16–1.2 mm ($\bar{x}$ = 4.4 × 2.2 × 0.4 mm), scattered to gregarious, partially immersed, becoming erumpent to superficial, raised, dark brown, in linear rows, with a slit-like opening, multi-loculate. *Ascomata* 150–210 × 100–230 µm ($\bar{x}$ = 170 × 180 µm, n = 10), with 2–12 ascomata forming groups immersed in stromata, arranged in rows, clustered, gregarious, to erumpent through host surface, dark brown, in cross-section ellipsoidal to subglobose. *Ostioles* centric, ostiolar canal periphysate. *Peridium* 20–30 µm ($\bar{x}$ = 23.7 µm, n = 15) wide, multi-layered, outer layer comprising dark brown or reddish brown to lightly pigmented cells of *textura angularis*, inner layer very thin, composed of hyaline cells of *textura angularis*. *Paraphyses* 3.5–6 µm ($\bar{x}$ = 4.5 µm, n = 20) wide, septate, branched, smooth-walled, constricted at septa, embedded in a gelatinous matrix. *Asci* 80–110 × 12–15 µm ($\bar{x}$ = 94 × 13.5 µm, n = 20), 8-spored, unitunicate, clavate, with short basal pedicel, thin-walled, lacking an apical ring, with obtusely rounded apex. *Ascospores* 26–29 × 5.5–7 µm ($\bar{x}$ = 28 × 6.5 µm, n = 25), L/W 4.3, 2–3-seriate, hyaline, ellipsoid to reniform, straight to curved, apiosporous, not constricted at septa, large cell 21–24 µm ($\bar{x}$ = 22.7 µm) long, small cell 5–5.6 µm ($\bar{x}$ = 5.2 µm) long, covered with a 4–8 µm ($\bar{x}$ = 6 µm, n = 10) wide mucilaginous sheath. **Asexual morph**: On PDA, *Hyphae* 1.5–3.5 µm ($\bar{x}$ = 2.4 µm, n = 10) wide, branched, septate, hyaline. *Conidiophores* reduced to conidiogenous cells. *Conidiogenous cells* 3.5–7.5 × 3–6 ($\bar{x}$ = 5.3 × 4.5 µm, n = 8), solitary on hyphae, integrated, branched, ampuliform, cylindrical, hyaline to brown. *Conidia* 10–13 × 7–10.5 ($\bar{x}$ = 11.3 × 8.9 µm, n = 15), brown, smooth, guttulate, globose to ellipsoid in surface view, lenticular with a paler equatorial slit in side view. *Sterile cells* 13–20 × 6–11 ($\bar{x}$ = 16.7 × 8.7 µm, n = 10), elongated, mixed among conidia.

Culture characteristics: Colonies on PDA reaching 55 mm diam. after two weeks at 25°C, cottony, flat, spreading, with moderate aerial mycelium, circular, dense, entire margin, and light brown; reverse brown at center and dirty white.

Material examined: China, Guizhou, Guiyang, Guizhou Academy of Agricultural Sciences (GZAAS) premises, on dead culm of grass (*Poaceae*), 7 July 2018, M.C. Samarakoon, SAMC173 (HKAS 102403, **holotype**), (MFLU 19-2113, **isotype**); ex-type living cultures GZCC 21-0041 = CGMCC3.20365.

Notes: *Apiospora guiyangensis* differs from *Ap. cyclobalanopsidis* in its small conidiogenous cells (3.5–7.5 × 3–6 µm vs 6–19 × 2.5–7 µm). *Apiospora guiyangensis* clustered in a distinct well-supported clade closely related to *Ap. camelliae-sinensis* CGMCC 3.18333 (98% sequence similarity in ITS, 2/584 gaps; 92% in *tub*2, 11/760 gaps), *Ap. cyclobalanopsidis* (99% sequence similarity in ITS, 1/572 gaps; 93% in *tub*2, 11/786 gaps) and *Ap. jiangxiense* (97% sequence similarity in ITS; 3/541 gaps, 93% in *tub*2; 6/736 gaps).

Apiospora sichuanensis Samarak., Jian K. Liu & K.D. Hyde, ***sp. nov***.

Index Fungorum number: IF558712; *Facesoffungi number*: FoF 10188; Fig. 6

Etymology: The specific epithet reflects the location, Sichuan, from where the species was first collected.

Holotype: HKAS 107008

Saprobic on dead culm of grass. **Sexual morph**: *Stromata* 1.1–5.1 × 0.3–0.7 × 0.2–0.4 mm ($\bar{x}$ = 2.2 × 0.47 × 0.28 mm, n=10), scattered to gregarious, partially immersed, becoming erumpent to superficial, raised, dark brown, in linear rows, with a slit-like opening, multi-loculate. *Ascomata* 160–205 × 205–270 µm ($\bar{x}$ = 182.5 × 241.6 µm, n = 10), with 5–15 ascomata forming in groups immersed in stromata, arranged in rows, clustered, gregarious, to erumpent through host surface, dark brown, in cross-section ellipsoidal to subglobose. *Ostioles* centric, ostiolar canal periphysate. *Peridium* 11–20 µm ($\bar{x}$ = 16.7 µm, n = 15) wide, thinner at the base, multi-layered, outer layer comprising dark brown or reddish brown to lightly pigmented cells of *textura angularis*, inner layer very thin, composed of hyaline cells of *textura angularis*. *Paraphyses* 3.6–6.5 µm ($\bar{x}$ = 5.1 µm, n = 20) wide, septate, branched, smooth-walled, constricted at septa, embedded in a gelatinous matrix. *Asci* 72–125 × 18–30 µm ($\bar{x}$ = 100.2 × 23.7 µm, n = 20), 8-spored, unitunicate, clavate, with short basal pedicel, thin-walled, lacking an apical ring, with obtusely rounded apex. *Ascospores* 29–48 × 7–10.5 µm ($\bar{x}$ = 39.7 × 9 µm, n = 25), L/W 4.4, 2–3-seriate, hyaline, ellipsoid to reniform, straight to curved, apiosporous, not constricted at septa, large cell 34–43 µm ($\bar{x}$ = 38 µm) long, small cell 3.5–7.5 µm ($\bar{x}$ = 5.3 µm) long, covered with a 13–24 µm ($\bar{x}$ = 19 µm, n = 10) wide, up to 30 µm, mucilaginous sheath. **Asexual morph**: Undetermined.

Material examined: China, Sichuan, Chengdu, Flowing Water Park, Huaxing Road 5, Jinjiang, on dead culm of grass (*Poaceae*), 1 October 2019, M.C. Samarakoon, SAMC241 (HKAS 107008, **holotype**), (MFLU HT20-0168, **isotype**).

Notes: *Apiospora sichuanensis* clustered with *Ap. pseudoparenchymatica* in the combined gene phylogeny. Morphological comparison is not possible due to the lack of a similar morph for both species (Wang et al. 2018). The ITS sequence of *Ap. sichuanensis* is similar to *Ap. pseudoparenchymatica* CGMCC 3.18336 (97.5%, 3/559 gaps) and *Ap. hyphopodii* MFLUCC 15-0003 (93%, 13/585 gaps), and *tub*2 to *Ap. pseudoparenchymatica* CGMCC 3.18336 (94.5%, 17/705 gaps) and *Ap. marii* (86%, 30/959 gaps).

Appendicosporaceae Samarak. & K.D. Hyde, ***fam. nov***.

Index Fungorum number: IF558713; *Facesoffungi number*: FoF 06297

Etymology: Named after the type genus, *Appendicospora*.

Saprobic on dead rachis/fronds of palms and dicotyledonous twigs. **Sexual morph**: *Ascomata* immersed, under slightly raised areas, visible as brown or black dots, solitary or aggregated in clusters, in cross-section, conical to subglobose with mostly flattened base. *Ostioles* centric, ostiolar canal periphysate or filled with white amorphous tissues. *Peridium* multi-layered, outer layer comprising brown, thick-walled, flattened cells of *textura angularis*, inner layer composed of hyaline, thin-walled cells of *textura angularis*. *Paraphyses* wider at the base, septate, embedded in a gelatinous matrix. *Asci* 8-spored, unitunicate, clavate to cylindrical, short pedicellate or sessile, lacking an apical ring, apically rounded. *Ascospores* uniseriate or 2–3-seriate, hyaline, clavate to broadly ellipsoidal, 1-septate, not constricted at septa, with or without appendages at one end. **Asexual morph**: Undetermined.

Type genus: *Appendicospora* K.D. Hyde

Notes: *Appendicospora* shares similar morphologies with *Apiospora* and *Pseudomassaria* with an uncertain taxonomic placement (Hyde 1995; Bahl 2006). Several morpho-phylo studies suggested that *Appendicospora* consistently grouped with *Hyponectria* and was best placed within the *Hyponectriaceae*, although further work to confirm the taxonomic placement was suggested (Wang and Hyde 1999; Smith et al. 2003; Bahl 2006). The only available LSU sequence of *Appendicospora sp.* (HKUCC 1120) links the morphology and phylogeny of this group. Combined gene phylogeny in our study shows that *Appendicospora* forms a distinct clade to *Apiosporaceae* in *Amphisphaeriales*. In addition, an inconspicuous taxon introduced as *Neoamphisphaeria* in this study clustered with *Appendicospora* with high statistical support (100%/1.00 PP). *Appendicosporaceae* clustered in the clade comprising *Anungitiomycetaceae*, *Iodosphaeriaceae* and *Pseudosporidesmiaceae* with strong statistical support (95%). In addition, the divergence time estimates show that *Appendicosporaceae* has diverged at 89 (65–117) MYA (*Amphisphaeriales*), which is comparable with the common divergence trend in family level (50–150 MYA) as described in Hyde et al. (2017). Based on distinct morphologies, phylogeny and divergence time estimates, we introduce *Appendicosporaceae* with the type genus *Appendicospora* and tentatively accommodate *Neoamphisphaeria*.

Appendicospora K.D. Hyde, Sydowia 47(1): 31 (1995)

Notes: *Appendicospora* was introduced by Hyde (1995), which is distinguished from *Apiospora* by ascospores with basal bifurcate appendages. *Appendicospora coryphae* (≡ *Apiosporella coryphae*), the generic type, was described on dead rachides of *Corypha elata* from the Philippines. Hyde and Fröhlich (1997) introduced the second species as *App. hongkongensis*, occurring on fronds of *Livistona chinensis* in Hong Kong.

Appendicospora hongkongensis Yanna, K.D. Hyde & J. Fröhl., Mycoscience 38(4): 395 (1997)

Index Fungorum number: IF442936; *Facesoffungi number*: FoF 10189; Fig. 7

Reference specimen: HKAS 107015 designated here

Saprobic on dead frond of *Livistona chinensis*. **Sexual morph**: *Ascomata* 70–125 × 105–145 µm ($\bar{x}$ = 95 × 125 µm, n = 10), immersed in the host tissue (subepidermal) under slightly raised areas, irregular in outline, individually light brown in the middle and dark at the periphery, solitary or aggregated in clusters, or evenly distributed, in cross-section conical to subglobose with mostly flattened base. *Ostioles* centric, ostiolar canal periphysate, filled with bright yellow pigmented drops when immature, blackish when mature, deteriorating when overmature. *Peridium* 5.5–13 µm ($\bar{x}$ = 9.2 µm, n = 10) wide, multi-layered, outer layer comprising light brown, flattened cells of *textura angularis*, inner layer composed of hyaline cells of *textura angularis*. *Paraphyses* 5–9 µm ($\bar{x}$ = 6.5 µm, n = 20) wide, septate, smooth-walled, constricted at septa, difficult to distinguish, embedded in a gelatinous matrix. *Asci* 55–70 × 15–19.5 µm ($\bar{x}$ = 60 × 17.5 µm, n = 15), few, 8-spored, unitunicate, clavate, short pedicellate, or pedicel lacking, thin-walled, lacking an apical ring, deliquescing early and releasing spores, developing from the base and lower sides of the ascomata, apically rounded. *Ascospores* 18–24.5 × 6–7 µm ($\bar{x}$ = 22 × 6.5 µm, n = 25), L/W 3.4, 2–3-seriate, hyaline, clavate, unequally 2-celled, not constricted at septa, large cell 10.5–18 µm ($\bar{x}$ = 14 µm) long, small cell 10.5–18 µm ($\bar{x}$ = 14 µm) long with a bifurcated (moustache-shaped) appendage, lacking a mucilaginous sheath. **Asexual morph**: Undetermined.

Culture characteristics: Colonies on PDA reaching 45 mm diam. after three weeks at 25°C, flat, powdery, with an outer radiating margin, hyphae embedded in the media, greenish white; reverse yellowish brown in the center, greenish brown marginal area, media becoming light brown.

Material examined: China, Sichuan Province, Chengdu, University of Electronic Science and Technology of China (Qingshuihe Campus), on dead frond of *Livistona chinensis* (*Arecaceae*), 30 September 2019, M.C. Samarakoon, SAMC247 (HKAS 107015, **reference specimen** designated here), (MFLU HT20-0175); living cultures GZCC 21-0044 = CGMCC3.20364.

Notes: The type of *Appendicospora hongkongensis* (HKU(M) 5301) was collected on fronds of *Livistona chinensis* in Hong Kong. Our specimen is similar to *App. hongkongensis* with overlapping size of height of ascomata (70–125 µmvs 108–128 µm), asci (55–70 × 15–19.5 µmvs 70–80 × 16–24 µm), ascospores (18–24.5 × 6–7 µmvs 70–80 × 17–24 × 5–8 µm) and brown peridium. *Appendicospora coryphae* possesses a hyaline peridium, which allows for discrimination of the species from *App. hongkongensis* (Hyde 1995; Hyde and Fröhlich 1997). Apart from similar morphology, both (HKU(M) 5301) and our specimen were collected from the same host and similar geography. In the multigene phylogeny, our strain clusters with an *Appendicospora sp*. (HKUCC 1120), which has only LSU sequence data (Smith et al. 2003). However, HKU(M) 5301 does not have molecular data. Based on similar morphology, host and geographical distribution, here we propose a reference specimen for *App. hongkongensis* on the dead frond of *Livistona chinensis* from Sichuan, China.

Neoamphisphaeria Samarak. & K.D. Hyde, ***gen. nov***.

Index Fungorum number: IF558714; *Facesoffungi number*: FoF 10190

Etymology: After its morphological similarities to *Amphisphaeria*.

Saprobic on dead twigs. **Sexual morph**: *Ascomata* immersed, slightly raised, visible as black dots, solitary, in cross-section conical with mostly flattened base or less globose. *Ostioles* centric, filled with white amorphous tissue. *Peridium* multi-layered, outer layer comprising reddish brown, thick-walled cells of *textura angularis*, inner layer composed of hyaline, thin-walled cells of *textura angularis*. *Paraphyses* wider at the base, long, septate, branched. *Asci* 8-spored, unitunicate, cylindrical, short pedicel, with a bilobed or dome-shaped apical ring, J- in Melzer's reagent, apically rounded. *Ascospores* uniseriate, hyaline, broadly ellipsoidal, aseptate when immature, 1-septate when mature, guttulate, lacking a mucilaginous sheath. **Asexual morph**: Undetermined.

Type: *Neoamphisphaeria hyalinospora* Samarak. & K.D. Hyde

Notes: *Neoamphisphaeria* is similar to *Amphisphaeria* in having immersed ascomata with a brown peridium, long hyaline paraphyses, cylindrical asci and ellipsoid, 1-septate, mature ascospores. The distinct characters of *Neoamphisphaeria* are the ostiolar canal filled with amorphous hyaline cells, asci with a bilobed or dome-shaped apical ring and hyaline ascospores. In the phylogeny, *Neoamphisphaeria* clusters with *Appendicospora* with 100%/1.00 PP statistical support, which has a periphysate ostiolar canal, clavate asci and 2–3-seriate, hyaline, clavate ascospores with a bifurcated (moustache-shaped) appendage. With inconspicuous, immersed ascomata, asci with short or lacking pedicels with J-, apical ring and 2-celled hyaline ascospores and strong phylogenetic evidence, we accept *Neoamphisphaeria* as a new genus in *Appendicosporaceae*.

Neoamphisphaeria hyalinosporaSamarak. & K.D. Hyde, ***sp. nov***.

Index Fungorum number: IF558715; *Facesoffungi number*: FoF 10191; Fig. 8

Etymology: The specific epithet reflects the hyaline ascospores.

Holotype: MFLU 19-2131

Saprobic on dead twigs. **Sexual morph**: *Ascomata* 220–280 × 335–365 µm ($\bar{x}$ = 250 × 350 µm, n = 8), immersed, under slightly raised areas, visible as black dots, solitary, in cross-section conical with mostly flattened base or subglobose. *Ostioles* prominent, centric, filled with white amorphous tissues. *Peridium* 25–34 µm ($\bar{x}$ = 30 µm, n = 10) wide, wider in upper regions, multi-layered, outer layer comprising reddish brown, thick-walled cells of *textura angularis*, inner layer composed of hyaline, thin-walled cells of *textura angularis*. *Paraphyses* 5–9 µm ($\bar{x}$ = 6.5 µm, n = 15) wide, wider at the base, long, cellular, septate, branched, guttulate, constricted at septa, embedded in a gelatinous matrix. *Asci* 105–130 × 7.5–9.5 µm ($\bar{x}$ = 118 × 8.5 µm, n = 20), 8-spored, unitunicate, cylindrical, with a short pedicel, with a bilobed or dome-shaped apical ring, J- in Melzer's reagent, apically rounded. *Ascospores* 14.5–17.5 × 6–8 µm ($\bar{x}$ = 16 × 6.5 µm, n = 30),

L/W 2.5, uniseriate, hyaline, broadly ellipsoidal, aseptate when immature, 1-septate when mature, guttulate, lacking a mucilaginous sheath or any appendage. **Asexual morph**: Undetermined.

Material examined: Thailand, Phrae Province, on dead twigs, 24 January 2019, M.C. Samarakoon, SAMC209 (MFLU 19-2131, **holotype**), (HKAS 106988, **isotype**).

Notes: *Neoamphisphaeria hyalinospora* is similar to *Amphisphaeria* with its subglobose to conical ascomata, cylindrical asci with a short pedicel and 2-celled ascospores, but differs in the amorphous cells in the ostiolar canal and hyaline ascospores. Asci and ascospores size and shape of *Neoa. hyalinospora* are similar to *Keissleriella hyalinospora* (formerly known as *Am. hyalinospora*) (Müller and von Arx 1962). However, *Am. hyalinospora* has dark brown, sparsely bristly hairs in the ostiolar canal, whereas *Neoa. hyalinospora* has hyaline amorphous cells. Combined gene phylogenies showed that *Neoamphisphaeria* is not related to *Amphisphaeria*, but clustered with *Appendicospora* with high statistical support (100%/1.00 PP). Based on unique morphology and distinct phylogeny, we introduce *Neoa. hyalinospora* as a new species.

Melogrammataceae G. Winter [as 'Melogrameae'], Rabenh. Krypt.-Fl., Edn 2 (Leipzig) 1.2: 797 (1886)

Melogrammataceae was introduced by Winter (1887) to accommodate *Melogramma*. Species of the family are saprobes or hemibiotrophs on the bark of woody plants. Based on morphology and phylogenetic revisions, Jaklitsch and Voglmayr (2012) accepted *Melogrammataceae* in *Xylariales*. Senanayake et al. (2015) re-evaluated the phylogeny of *Melogrammataceae* and accepted it in *Amphispheriales*, and this has been confirmed in the later studies by Hongsanan et al. (2017) and Hyde et al. (2020b).

Melogramma Fr., Summa veg. Scand., Section Post. (Stockholm): 386 (1849)

Notes: *Melogramma* was established by Fries (1849) with *Mel. campylosporum* as the type species, which is a commonly and abundantly reported species. *Melogramma* is characterised by reddish brown stromata, unitunicate asci with J-, apical ring and 3-septate, brown ascospores, and a coelomycetous asexual morph (Jaklitsch and Voglmayr 2012; Maharachchikumbura et al. 2016). Seventeen *Melogramma* epithets are accepted (Hyde et al. 2020b).

Melogramma campylosporum Fr., Summa veg. Scand., Sectio Post. (Stockholm): 386 (1849)

Index Fungorum number: IF150772; *Facesoffungi number*: FoF 00841; Fig. 9

Saprobic dead aerial branch of *Corylus avellana*. **Sexual morph**: *Stromata* 1–2.5 × 0.6–1.4 × 0.3–1 mm ($\bar{x}$ = 1.6 × 1 × 0.7 mm, n=10), erumpent from bark, solitary, scattered or aggregated, pulvinate or discoid, smooth to slightly velutinous, surface brown with slightly papillate black ostiolar dots. *Ascomata* 315–400 × 225–360 µm ($\bar{x}$ = 341 × 274 µm, n = 10), 2–12 per stroma, immersed, in cross-section globose to subglobose. *Ostioles* centric, ostiolar canal periphysate. *Peridium* 21–30 µm ($\bar{x}$ = 25 µm, n = 15) wide, multi-layered, outer layer comprising reddish brown, flattened cells of *textura angularis*, thin inner layer comprising hyaline cells of *textura angularis*. *Paraphyses* 3–5 µm ($\bar{x}$ = 4.2 µm, n = 20) wide, numerous, septate, smooth-walled, apically blunt. *Asci* 100–140 × 13–16 µm ($\bar{x}$ = 122 × 14.5 µm, n = 25), 8-spored, unitunicate, clavate or fusoid, straight, curved or sigmoid, with short and narrow pedicel, lacking an apical ring, apically rounded. *Ascospores* 38–50 × 4–6 µm ($\bar{x}$ = 44 × 5 µm, n = 25), L/W 8.8, 2–3-seriate, hyaline, straight and 0–1-septate when immature, brown, 3 equidistant septa when mature, end cells slightly lighter entirely or only at their tips, falcate, often strongly curved or slightly straight, tips narrowly rounded to subacute, with a smooth narrow hyaline perispore, often with one large guttule in each cell. **Asexual morph**: Undetermined.

Culture characteristics: Colonies on PDA, very slow growing, reaching 9 mm diam. after three months at 25°C, convex and a papillate surface, compact, lobate with zonate margin, hyphae embedded in the media, dark greenish brown; reverse dark brown in the center, yellowish brown marginal area, media becoming reddish brown.

Material examined: Italy, Province of Forlì-Cesena, Tontola di Predappio, on the dead aerial branch of *Corylus avellana*(*Betulaceae*), 5 February 2017, E. Camporesi, IT3241 (MFLU 17-0348, HKAS 102324); living culture MFLUCC 17-2674. Russia, Krasnodar region, Sochi, Central city district, park “Riviera”, on dead aerial branchs and twigs of *Corylus avellana* (*Betulaceae*), 10 October 2016, T.S. Bulgakov, SC-101 (MFLU 18-0778, HKAS 102312); living culture MFLUCC 18-0612.

Notes: *Melogramma campylosporum* has been described on *Alnus glutinosa subsp. glutinosa* (Turkey), *Carpinus betulus* (Austria, Poland, Sweden), *Carpinus sp.* (Ukraine, United Kingdom), *Corylus avellana* (Austria, Poland) and *Fagus sylvatica* (Italy) (Farr and Rossman 2021). LSU and ITS sequences of our two collections are 100% identical to the ITS-LSU of acc. JF440978 (CBS 141086). The microscopic characters of our two collections are similar to *Mel. campylosporum*,described by Jaklitsch and Voglmayr (2012). This is the first record of *Mel. campylosporum* on *Corylus avellane* in Italy.

Sporocadaceae Corda [as 'Sporocadeae'], Icon. fung. (Prague) 5: 34 (1842)

Sporocadaceae species typically possess appendage bearing conidia and are important as saprobes or pathogens on leaves, twigs, branches, fruits of flowering plants and gymnosperms, and as endophytes or parasites on humans and animals (Liu et al. 2019; Hyde et al. 2020b). Following the recent revision of the morphology and multigene phylogeny, there are 23 genera in *Sporocadaceae* (Liu et al. 2019).

Seiridium Nees, Syst. Pilze (Würzburg): 22 (1816) [1816-17]

Notes: *Seiridium* was introduced by Nees (1816) with the type species *Se. marginatum*. The sexual morph of *Seiridium* is characterised by immersed to semi-erumpent ascomata, a dark peridium, centric, slightly papillate, periphysate ostiolar canals, cylindrical, 8-spored asci with J+, apical rings and cylindrical-

oblong, euseptate, yellow to dark brown ascospores (Bonthond et al. 2018). The coelomycetous asexual morph of *Seiridium* differs from closely related *Nothoseiridium* and *Nonappendiculata* in having versicolorous, 5-septate conidia with appendages. There are 44 *Seiridium* species (Bonthond et al. 2018).

Seiridium italicum Samarak., Camporesi & K.D. Hyde, ***sp. nov***.

Index Fungorum number: IF558716; *Facesoffungi number*: FoF 10192; Fig. 10

Etymology: The specific epithet reflects Italy, from where the species was first collected.

Holotype: MFLU 16-1315

Saprobic on dead aerial branch of *Laurus nobilis*. **Sexual morph**: *Ascomata* 185–205 × 275–450 µm ($\bar{x}$ = 195 × 365 µm, n = 10), immersed, visible as raised, black dots, solitary or aggregated, in cross-section conical with mostly flattened base or sub-globose. *Ostioles* prominent, centric or eccentric, conical, wide, ostiolar canal periphysate. *Peridium* 13–21 µm ($\bar{x}$ = 17.3 µm, n = 10) wide, multi-layered, outer layer comprising yellowish brown, thick-walled cells of *textura angularis*, inner layer composed of hyaline, thin-walled cells of *textura angularis*. *Paraphyses* 3.3–5.4 µm ($\bar{x}$ = 4 µm, n = 20) wide, longer than asci, cellular, septate, rarely branched, guttulate, constricted at septa, embedded in a gelatinous matrix. *Asci* 110–130 × 8–11 µm ($\bar{x}$ = 120 × 10 µm, n = 20), 8-spored, unitunicate, cylindrical, short pedicellate, J- in Melzer's reagent, apically rounded. *Ascospores* 14.8–18.5 × 5.5–8 µm ($\bar{x}$ = 16.3 × 7.3 µm, n = 30), L/W 2.3, uniseriate, hyaline, light to dark brown when mature, ellipsoid, 2–3-septate, constricted at septa, lacking a mucilaginous sheath. **Asexual morph**: Undetermined.

Culture characteristics: Colonies on PDA reaching 23–25 mm diam. after four weeks at 25°C, circular, flat, entire margin, white and yellowish brown as concentric zones; yellowish orange center, salmon pink marginal area.

Material examined: Italy, Forlì-Cesena Province, Camposonaldo - Santa Sofia, on dead aerial branch of *Laurus nobilis*, 6 April 2016, E. Camporesi, IT2945 (MFLU 16-1315, **holotype**), (HKAS 102342, **isotype**); ex-type living culture MFLUCC 18-0510.

Notes: *Seiridium italicum* is only known from its sexual morph and is similar to the generic description except in having J-, apical rings (Bonthond et al. 2018). However, the morphological comparisons are difficult due to the availability of sexual characteristics. In addition, *Nonappendiculata* and *Nothoseiridium* are close to *Se. italicum* in phylogeny but lack sexual morphologies (Liu et al. 2019; Crous et al. 2020). ITS sequence of *Se. italicum* is close to *Se. papillatum* CBS 340.97 (93%, 22/580 gaps), *Se. persooniae* CBS 143445 (93%, 19/568 gaps) and *Se. podocarpi* CBS 137995 (91%, 35/594 gaps), while the LSU sequence is close to *Se. phylicae* CPC 19962 (99%), *Se. rosarum* MFLUCC 17-0654 (99%, 1/888 gaps) and *Notho. podocarpi* CPC 36967 (99%, 0/866 gaps). Combined gene phylogenies show that *Se. italicum* clusters apart from other species, and here we introduce *Se. italicum* as a new species.

Xylariales Nannf.

Coniocessiaceae Asgari & Zare, Mycol. Progr. 10(2): 195 (2011)

Coniocessiaceae was introduced by Asgari and Zare (2011) to accommodate *Coniocessia*, which comprises saprobes in plants, soil and dung. *Coniocessiaceae* is placed in *Xylariales* based on morphology and phylogeny and divergence time estimations (Asgari and Zare 2011; Maharachchikumbura et al. 2016; Hyde et al. 2020).

Paraxylaria Wanas., Gafforov, E.B.G. Jones & K.D. Hyde, in Wanasinghe et al., Fungal Diversity: 89; 1-236, [200] (2018)

≡ *Rosellinia* subgen. *Amphisphaerella* Sacc., Syll. fung. (Abellini) 1: 262 (1882)

= *Amphisphaerella* (Sacc.) Kirschst., Trans. Br. mycol. Soc. 18(4): 306 (1934) [1933] (Nom. illegit., Art. 53.1), non-*Amphisphaerella* Henn., Hedwigia 41: 13 (1902)

Paraxylaria was introduced by Wanasinghe et al. (2018) to accommodate *Pa. rosacearum*, a saprobe on trunks and branches of *Rosa sp*. from Uzbekistan. *Paraxylaria* has asci with J+, apical ring and uniseriate, ellipsoid, mostly symmetrical, aseptate, brown ascospores, which lack germ slits (Wanasinghe et al. 2018). We re-examined the holotype and observed germ pores in ascospores of *Pa. rosacearum* (Fig. 136, Wanasinghe et al. 2018). Molecular phylogeny also supported *Paraxylaria* as a basal clade, but distinct from *Coniocessia* in *Coniocessiaceae*.

Kirschstein (1934) introduced *Amphisphaerella* to accommodate *Amp. amphisphaerioides*. *Amphisphaerella* was introduced to accommodate a micro-fungal group, which is characterised by immersed to semi-immersed ascomata, often beneath a clypeus, globose to subglobose in section, 8-spored, cylindrical, pedicellate asci with apically rounded, J+/J-, apical rings and ellipsoidal, brown, aseptate ascospores with two to six germ pores arranged equatorially or scattered or in groups towards the poles (Kirschstein 1934; Barr 1994). However, this introduction is invalid according to the Art. 53.1 since Hennings (1902) introduced *Amphisphaerella* with the type of *Amp. hypoxyloides*. Petrini (2013) synonymised and accepted the monospecific *Amphisphaerella* (*Amp. hypoxyloides*) in *Rosellinia* (*Ro. hypoxyloides*) based on morphology. Only the invalidly published *Amphisphaerella* has been considered thereafter. Munk (1953) proposed *Amphisphaerellaceae* for *Amphisphaerella.* However, Eriksson (1966), Barr (1990) and Lumbsch and Huhndorf (2010) retained *Amphisphaerella* in *Amphisphaeriaceae* until more information was available. There are 13 *Amphisphaerella* epithets that have been accepted. Lu and Hyde (2000) observed that the holotype of *Amp. dispersella* and ascospores with germ pores are identified as a unique character of the genus. Here we accept *Paraxylaria* as the valid name to accommodate species similar to *Amphisphaerella*.

Paraxylaria xylostei (Pers.) Samarak. & K.D. Hyde, ***comb. nov***.

≡ *Sphaeria xylostei* Pers., Neues Mag. Bot. 1: 84 (1794)

= *Amphisphaerella xylostei* (Pers.) Munk, 1953 (this Index 5: 278), nom. inval., Art. 41.5

= *Amphisphaerella xylostei* (Pers.) Rulamort, Bull. Soc. bot. Centre-Ouest, Nouv. sér. 17(2): 192 (1986)

Index Fungorum number: IF558404; *Facesoffungi number*: FoF 10193; Fig. 11

Saprobic on dead aerial branch of *Lonicera sp*. **Sexual morph**: *Ascomata* 200–250 × 250–310 µm ($\bar{x}$ = 225 × 275 µm, n = 10), immersed beneath the clypeus, visible as black patches, solitary or aggregated in small numbers, in cross-section conical with rounded base or subglobose. *Ostioles* prominent, centric or eccentric, conical, more or less acute, shiny black, periphasate ostiolar canal. *Peridium* 17–26 µm ($\bar{x}$ = 22 µm, n = 10) wide at base, thickened to 27–44 µm ($\bar{x}$ = 36 µm, n = 10) wide near to ostiole, hard in upper regions, multi-layered, outer layer comprising brown, thick-walled cells of *textura angularis*, inner layer composed of hyaline, thin-walled cells of *textura angularis*. *Paraphyses* 2–3.5 µm ($\bar{x}$ = 2.6 µm, n = 15) wide, long, numerous, filamentous, flexuous, septate, rarely branched, guttulate. *Asci* 75–140 × 9.5–13.5 µm ($\bar{x}$ = 105 × 11.3 µm, n = 20), 8-spored, unitunicate, cylindrical, pedicellate up to 20 µm long, with a 1.5–2 × 3.5–5 µm ($\bar{x}$ = 1.7 × 4.3 µm, n = 10), wedge-shaped apical ring, J+ in Melzer's reagent. *Ascospores* 15–19 × 7–10 µm ($\bar{x}$ = 17.8 × 8.7 µm, n = 25), L/W 2.1, uniseriate, initially hyaline to yellowish brown, becoming blackish brown at maturity, ellipsoid, mostly symmetrical, aseptate, with rounded ends, guttulate, with 3–5 equatorial germ pores surrounded by thick, dark brown margin, lacking a mucilaginous sheath, lacking a germ slit. **Asexual morph**: Undetermined.

Material examined: Italy, Province of Forlì-Cesena, Campigna - Santa Sofia, on dead aerial branch of *Lonicera sp*. (*Caprifoliaceae*), 5 February 2017, E. Camporesi, IT3479 (MFLU 17-1636, HKAS 102371). *ibid*. IT3479A (MFLU 17-1645, HKAS 102313).

Notes: *Paraxylaria xylostei* is common in temperate regions and is variable in both ascus and ascospore characters, amyloid/nonamyloid and size, probably due to geographical variation and the different hosts (Mathiassen 1993). The morphological variations are higher in the *Lonicera* materials compared to *Salix* (Mathiassen 1993). *Paraxylaria xylostei* is known from *Lonicera microphylla*, *L. tatarica*, *L. xylosteum*, *Salix glauca ssp. glauca*, *S. lanata ssp. lanata* and *S. phylicifolia* (Mathiassen 1993; Gafforov 2017). *Paraxylaria xylostei* possesses J+ asci and 14–18 × 6–9 µm ascospores with (3)5–6 equatorial germ pores, while *Pa. rosacea* has 16–20 × 9–11 µm ascospores with 7–11 scattered germ pores. Here we provide another collection of *Pa. xylostei* from Italy as a new geographical record and update the phylogenetic affinity of *Paraxylaria* in *Coniocessiaceae*.

Diatrypaceae Nitschke [as 'Diatrypeae'], Verh. naturh. Ver. preuss. Rheinl. 26: 73 (1869)

Diatrypaceae was introduced by Nitschke (1869), which comprises saprobes, pathogens and endophytes on economic crops and forest trees worldwide occurs in aquatic and terrestrial habitats (Hyde et al. 2020b; Konta et al. 2020a). Based on phylogeny and divergence time estimations, *Diatrypaceae* is accepted as a well-supported family in *Xylariales* (Hongsanan et al. 2017). With the addition of several new genera, there are 25 genera accommodated in *Diatrypaceae* as; *Allocryptovalsa*, *Allodiatrype*, *Anthostoma*, *Cryptosphaeria*, *Cryptovalsa*, *Diatrypasimilis*, *Diatrype*, *Diatrypella*, *Dothideovalsa*, *Echinomyces*, *Endoxylina*, *Eutypa*, *Eutypella*, *Halocryptosphaeria*, *Halocryptovalsa*, *Halodiatrype*, *Leptoperidia*, *Libertella*, *Monosporascus*, *Neoeutypella*, *Paraeutypella*, *Pedumispora*, *Peroneutypa*, *Quaternaria* and *Rostronitschkia* (Hyde et al. 2020b; Konta et al. 2020a; Dissanayake et al. 2021a).

Allocryptovalsa Senwanna, Phookamsak & K.D. Hyde, in Senwanna et al., Mycosphere 8(10): 1839 (2017)

Notes: *Allocryptovalsa* was introduced by Senwanna et al. (2017) with the type species *Al. polyspora* on a dead twig of *Hevea brasiliensis* from Thailand. *Allocryptovalsa* has immersed ascomata, polysporous asci, and allantoid ascospores and forms a distinct phylogenetic affinity in *Diatrypaceae* with ITS-*tub*2 phylogeny. There are five *Allocryptovalsa* species.

Allocryptovalsa sichuanensis Samarak., Jian K. Liu & K.D. Hyde, ***sp. nov***.

Index Fungorum number: IF558717; *Facesoffungi number*: FoF 10194; Fig. 12

Etymology: The specific epithet reflects the location, Sichuan, from where the fungus was first collected.

Holotype: HKAS 107017

Saprobic on dead branch. **Sexual morph**: *Stromata* 0.7–4.1 mm ($\bar{x}$ = 1.9 mm, n = 10) length, 0.8–1.75 mm ($\bar{x}$ = 1.1 mm, n = 10) high, erumpent through host epidermis, with bark adhering to stromata, visible as black, rounded to irregular dots on host surface, solitary to aggregated, scattered. *Ascomata* 460–755 × 300–420 µm ($\bar{x}$ = 579 × 367 µm, n = 10), immersed to semi-immersed in stroma, black, 2–9 ascomata per stroma, thin black pseudoparenchymatous tissue around the white entostroma, in cross-section ovoid to subglobose. *Ostioles* cylindrical, sulcate, ostiolar canal periphysate, with yellowish pigment around ostioles, with or without papilla. *Peridium* 34–56 µm ($\bar{x}$ = 43.5 µm, n = 10) wide, multi-layered, outer layer comprising dark brown, thick-walled cells of *textura angularis*, a thin inner layer composed of hyaline cells of *textura angularis*. *Paraphyses* 2.4–4.4 µm ($\bar{x}$ = 3.4 µm, n = 20) wide, wider at the base, long, septate, filamentous, smooth-walled, constricted at septa, narrowing and tapering towards the blunt apex, embedded in a gelatinous matrix. *Asci* 100–142 × 16–24 µm ($\bar{x}$ = 122 × 19.4 µm, n = 15), spore bearing part 60–75 µm ($\bar{x}$ = 68 µm, n = 10) long, polysporous, unitunicate, clavate to cylindric-clavate, long pedicellate, thin-walled, with an indistinct, J-, apical ring, apically rounded to truncate. *Ascospores* 6–11 × 2–3 µm (= 8.5 × 2.7 µm, n = 35), L/W 3.2, crowded, initially hyaline, becoming pale yellowish to brown when mature, oblong to allantoid, aseptate, slightly curved, smooth-walled, mostly with small guttules. **Asexual morph**: Undetermined.

Culture characteristics: Colonies on PDA reaching 55 mm diam. after one week at 25°C, irregular, flat or effuse, cottony, medium dense, margin fimbriate, and dirty white; reverse yellowish brown.

Material examined: China, Sichuan Province, Chengdu, University of Electronic Science and Technology of China (Qingshuihe Campus), on the dead branch, 30 September 2019, M.C. Samarakoon, SAMC249 (HKAS 107017, **holotype**), (MFLU HT20-0177, **isotype**); ex-type living cultures MFLUCC T20-0653 = GZCC 21-0043 = CGMCC3.20363.

Notes: *Allocryptovalsa sichuanensis* has stromata with 2–9 ascomata, which distinguishes it from *Al. elaeidis* (1–2), *Al. polyspora* (1–3) and *Al. rabenhorstii* (5–25) (Mehrabi et al. 2016; Senwanna et al. 2017; Konta et al. 2020a). The LSU, ITS and *tub*2 sequences of *Al. sichuanensis* are similar to *Al. elaeidis* MFLUCC 15-0707 (LSU 99%, 0/892 gaps; ITS 99%, 0/532 gaps; *tub*2 99%, 1/1064 gaps) and *Al. polyspora* MFLU 17-1218 (LSU 100%, 0/823 gaps; ITS 99%, 1/486 gaps). Combined ITS-*tub*2 (data not shown) and ITS-LSU-*rpb*2-*tub*2-*tef*1 (Fig. 1) phylogenies showed our taxon is basal to *Allocryptovalsa* with 97%/1.00 PP statistical support. Here we introduce *Al. sichuanensis* as a new species.

Diatrype Fr., Summa veg. Scand., Section Post. (Stockholm) 384 (1849)

Notes: *Diatrype* was introduced with the type *D. disciformis* by Fries (1849). Species in the genus are characterised by discoid or widely effuse, erumpent stromata with embedded ascomata in their sexual morph and libertella-like asexual morph (Vasilyeva and Stephenson 2009; Senanayake et al. 2015).

Diatrype disciformis (Hoffm.) Fr., Summa veg. Scand., Sectio Post. (Stockholm): 385 (1849)

Index Fungorum number: IF233766; *Facesoffungi number*: FoF 00691; Fig. 13

Saprobic on the dead branch. **Sexual morph**: *Stromata* 3.3–5.6 mm ($\bar{x}$ = 4.1 mm, n = 10) length, 3–4.8 mm ($\bar{x}$ = 3.7 mm, n = 10) high, scattered, erumpent to superficial, orbicular, somewhat convex, edges of cracks remaining as pointed, angular parts, margin thick, black, composed of an outer, dark brown, small, tightly packed, thin parenchymatous cell layer and inner, yellowish white, large, loosely packed, parenchymatous cell layer. *Ascomata* 590–700 × 280–430 µm ($\bar{x}$ = 636 × 357 µm, n = 15), immersed in stromatic tissues, aggregated, in cross-section globose to subglobose, narrowing towards the apex and very narrow at the base of ostiolar canal, pale brown, thin-walled, ostiolate. *Ostioles* short, centric, compressed, apex wider than base, ostiolar canal periphysate, ostiolar opening covered with carbonaceous, black cells. *Peridium* 17–20 µm ($\bar{x}$ = 18.8 µm, n = 8) wide, multi-layered, outer layer comprising dark brown cells of *textura angularis*, a thin inner layer composed of hyaline cells of *textura angularis*. *Paraphyses* 2–5 µm ($\bar{x}$ = 3.2 µm, n = 20) wide, wider at the base, long, septate, smooth-walled, constricted at septa, tapering towards the blunt apex. *Asci* 55–80 × 3.5–5 µm ($\bar{x}$ = 69 × 4.5 µm, n = 25), 8-spored, unitunicate, clavate, thin-walled, pedicel 37–53 µm ($\bar{x}$ = 44 µm, n = 15) long, apex flat, J- in Melzer's reagent. *Ascospores* 4.5–7 × 0.8–1.3 µm ($\bar{x}$ = 5.7 × 1.1 µm, n = 30), L/W 5.2, overlapping, cylindrical or elongate-allantoid, hyaline, aseptate, guttulate, smooth-walled. **Asexual morph**: Undetermined.

Material examined: UK, on dead branch, 2015, E.B.G. Jones, GJ384 (MFLU 17-1549; HKAS 107036).

Notes: Senanayake et al. (2015) designated a reference specimen for *Diatrype disciformis* (MFLU 15–0722) on a branch of *Ostrya carpinifolia* from Italy. In this study, we provide another specimen collected from the UK, which is morphologically similar with overlapping measurements of ascomata, asci and ascospores. However, our collection has larger stromata (3.3–5.6 mm vs 1.5–2 mm length) and a thinner peridium (17–20 µm vs 20–30 µm) as compared to MFLU 15–0722. Mehrabi et al. (2016) also described *D. disciformis*, which has up to 8 mm diam. of stromata. The known distribution of the fungus is on *Alnus* and *Fagus* from Europe and lead-contaminated soils from abandoned firing range USA (Acero et al. 2004; Vasilyeva and Stephenson 2009; 2014; Sullivan et al. 2012; Vasilyeva and Ma 2014; Mehrabi et al. 2016).

Eutypa Tul. & C. Tul., Select. fung. carpol. (Paris) 2: 52 (1863)

Notes: *Eutypa* is an important plant pathogenic group on fruit crops that causes eutypa dieback (Hyde et al. 2020b). *Eutypa* species have superficial, irregular stromata with scattered, roundish to prominent ostioles, clavate asci with a round to truncate apex and allantoid to ellipsoidal, aseptate ascospores. Hyde et al. (2020b) and Wijayawardene et al. (2020) estimated the genus contains 66 species, with 17 with sequence data.

Eutypa camelliae Samarak., Jian K. Liu & K.D. Hyde, ***sp. nov***.

Index Fungorum number: IF558718; *Facesoffungi number*: FoF 10195; Fig. 14

Etymology: The specific epithet reflects the host genus *Camellia*.

Holotype: HKAS 107022

Saprobic on decayed stem of *Camellia japonica*. **Sexual morph**:Underestimated. *Immture sromata* 8.5–9.9 × 0.84–1.9 × 0.35–0.5 mm ($\bar{x}$ = 9.2 × 1.3 × 0.45 mm, n = 4), incrusted with superficial, effuse, confluent into irregularly elongated, surface greyish black to dull black, carbonaceous tissues, as with yellowish white dots on the surface, two sac-like structures. *Type one sac-like structure* 180–380 × 100–165 µm ($\bar{x}$ = 270 × 123 µm, n = 8), arranged in one layer, ovoid, filled with white crystalline substances, peridium 12–16.5 µm ($\bar{x}$ = 14.4 µm, n = 8) wide, multi-layered, of yellowish brown cells of *textura angularis*. *Type two sac-like structure* 380 × 220 µm, ovoid, filled with amorphous cells, peridium 31–43 µm ($\bar{x}$ = 37.4 µm, n = 3) wide, multi-layered of reddish brown cells of *textura angularis*. No other structures observed. **Asexual morph**: Observed on the stroma. *Conidiophores* 10–22.7 × 3.4–6 µm ($\bar{x}$ = 16.5 × 4.7 µm, n = 6), branched, arising from pseudoparenchymatous cells or interwoven hyphae, hyaline. *Conidiogenous cells* 5.5–9 × 0.9–1.6 µm ($\bar{x}$ = 7.3 × 1.3 µm, n = 5), cylindrical, holoblastic, straight or curved, apically distorted with conidial secession. *Conidia* 33.7–42.6 × 1.1–1.7 µm ($\bar{x}$ = 38.2 × 1.4 µm, n = 30), hyaline, lunate to fusiform, curved at the apex, rarely straight, with flattened base and blunt apex.

Culture characteristics: Colonies on PDA reaching 30 mm diam. after one week at 25°C, irregular, flat or effuse, fluffy to fairly fluffy, medium dense, margin fimbriate, and dirty white; reverse yellowish brown.

Material examined: China, Sichuan Province, Chengdu, University of Electronic Science and Technology of China (Qingshuihe Campus), on a dead stem of *Camellia japonica* (*Theaceae*), 30 September 2019, M.C. Samarakoon, SAMC254X (HKAS 107022, **holotype**), (MFLU HT20-0182, **isotype**); ex-type living cultures MFLUCC T20-0643 = GZCC 21-0042.

Notes: Our new isolates were obtained through the internal tissue isolation of the stromata. We did not observe any spores in those stromata, but observed an asexual morph, which is similar to diatrypaceous asexual morphs on the stromata. Two areas on the stroma produced ascoma-like structures with a brown peridium filled with amorphous cells, probably immature ascomata. However, these observations did not provide enough morphology for the complete identification of the strain. Our two isolates are phylogenetically similar to each other and form a distinct single clade in *Eutypa*. The ITS and LSU sequences of our strains are 98% (4/559 gaps) and 99% (3/887 gaps) similar to *E. lata* respectively. Combined ITS-*tub*2 (data not shown) and ITS-LSU-*rpb*2-*tub*2-*tef*1 (Fig. 1) phylogenies showed that our new isolates clustered in *Eutypa sensu stricto* and is sister to *E. armeniacae* (ATCC 28120) with poor statistical support (58%/0.99 PP). Here we propose *E. camelliae* as a new species.

Melanostictus Samarak. & K.D. Hyde, ***gen. nov***.

Index Fungorum number: IF558719; *Facesoffungi number*: FoF 10196

Etymology: The generic epithet refers to the Greek: melano- “black” + stictus “spot”.

Saprobic on dead branch. **Sexual morph**: *Ascomata* immersed, visible as black, raised dots, solitary or aggregated, in cross-section globose. *Ostioles* centric, ostiolar canal periphysate, sulcate on top. *Ectostroma* yellow to white. *Peridium* multi-layered, outer layer comprising dark brown, flattened cells of *textura angularis*, inner layer comprising hyaline cells of *textura angularis*. *Paraphyses* septate. *Asci* 8-spored, unitunicate, clavate, with a long pedicel, apical ring minute, apically flattened. *Ascospores* overlapping, hyaline, cylindrical or elongate-allantoid, aseptate, smooth-walled. **Asexual morph**: Undetermined.

Type: *Melanostictus longiostiolatus* Samarak. & K.D. Hyde

Notes: *Melanostictus* is characterised by immersed ascomata appearing as black dots on the host surface, long papillate ostioles with a sulcate top, yellow to white ectostroma, 8-spored asci with cylindrical or elongate-allantoid ascospores. Several genera are phylogenetically close to *Melanostictus* bear 8-spored asci with diversified stromatic characters. *Cryptosphaeria*, *Eutypa* and *Neoeutypella* have effused stromata and aggregated ascomata on the host surface, while *Allodiatrype* has well-developed, erumpent stromata (Trouillas et al. 2015; de Almeida et al. 2016; Phookamsak et al. 2019; Konta et al. 2020a). *Halodiatrype* and *Pedumispora* are the closest genera to our new genus. *Halodiatrype* has immersed ascomata, papillate ostioles with a brown outer amorphous layer and inner yellow cells of *textura porrecta*, 8-spored, unitunicate asci with oblong to allantoid or sub-inaequilateral, aseptate to septate, light brown ascospores (Dayarathne et al. 2016), while *Pedumispora* has 1–4 immersed ascomata per stroma, papillate ostioles, 8-spored, fusiform asci with filiform, multi-septate, curved, longitudinally striate ascospores (Hyde and Jones 1992). *Melanostictus* clustered sister to *Halodiatrype* and *Pedumispora* as a distinct group in morphology and phylogeny; hence we introduce our two new collections in the new genus.

Melanostictus longiostiolatus Samarak. & K.D. Hyde, ***sp. nov***.

Index Fungorum number: IF558720; *Facesoffungi number*: FoF 10197; Fig. 15

Etymology: The specific epithet reflects the papillate ostioles.

Holotype: MFLU 19-2146

Saprobic on dead branch. **Sexual morph**: *Ascomata* 550–630 × 300–370 µm ($\bar{x}$ = 585 × 345 µm, n = 10), immersed in the host tissue under slightly raised areas, visible as black dots, surrounded by black periphery, solitary or aggregated, mostly in pairs, with clusters or evenly distributed, in cross-section globose. *Ostioles* 300–390 × 110–180 µm ($\bar{x}$ = 340 × 145 µm, n = 5), centric, ostiolar canal periphysate, sulcate on top. *Ectostroma* yellow. *Peridium* 30–38 µm ($\bar{x}$ = 35 µm, n = 10) wide, multi-layered, outer layer comprising dark brown, flattened cells of *textura angularis*, inner layer comprising hyaline cells of *textura angularis*. *Paraphyses* 3–7.5 µm ($\bar{x}$ = 5.4 µm, n = 20) wide, wider at the base, septate, rarely branched, constricted at septa, smooth-walled, with a blunt end. *Asci* 50–65 × 5.5–8 µm ($\bar{x}$ = 56 × 6.5 µm, n = 25), 8-spored, unitunicate, clavate, thin-walled, pedicel 19–35 µm ($\bar{x}$ = 26 µm, n = 25) long, apical ring minute, deliquescing early and releasing spores, developing from the base and lower sides of the ascomata, apically flattened. *Ascospores* 3.5–5.5 × 1–1.5 µm ($\bar{x}$ = 4.5 × 1.2 µm, n = 30), L/W 3.75, overlapping, hyaline, cylindrical or elongate-allantoid, aseptate, smooth-walled. **Asexual morph**: Undetermined.

Material examined: Thailand, Chiang Rai Province, Amphoe Mueang Chiang Rai, on dead branch, 15 June 2019, M.C. Samarakoon, SAMC229 (MFLU 19-2146, **holotype**), (HKAS 107003, **isotype**).

Notes: Please see the notes of *Melanostictus thailandicus*.

Melanostictus thailandicus Samarak. & K.D. Hyde, ***sp. nov***.

Index Fungorum number: IF558721; *Facesoffungi number*: FoF 10198; Fig. 16

Etymology: The specific epithet reflects Thailand, where the species was first collected.

Holotype: MFLU 19-2123

Saprobic on dead branch. **Sexual morph**: *Ascomata* 415–580 × 300–410 µm ($\bar{x}$ = 512 × 362 µm, n = 10), immersed in the host tissue under slightly raised areas, visible as black dots, solitary or aggregated, with clusters or evenly distributed, in cross-section globose or subglobose, base rarely flattened. *Ostioles* 185–280 × 85–145 µm ($\bar{x}$ = 235 × 115 µm, n = 5), centric, ostiolar canal periphysate, sulcate on top. *Ectostroma* yellowish white. *Peridium* 27–40 µm ($\bar{x}$ = 33 µm, n = 10) wide, multi-layered, outer layer comprising dark brown, flattened cells of *textura angularis*, inner layer composed of hyaline cells of *textura angularis*, *Paraphyses* 2.4–4 µm ($\bar{x}$ = 3.1 µm, n = 20) wide, long, septate, constricted at septa, smooth-walled, ends blunt. *Asci* 50–64 × 3.8–5 µm ($\bar{x}$ = 56 × 4.2 µm, n = 25), 8-spored, unitunicate, clavate, thin-walled, pedicel 24–30 µm ($\bar{x}$ = 26.5 µm, n = 15) long, apical ring minute, deliquescing early and releasing spores. *Ascospores* 5–6.2 × 1–1.6 µm ($\bar{x}$ = 5.5 × 1.4 µm, n = 30), L/W 3.9, overlapping, cylindrical or elongate-allantoid, hyaline, aseptate, guttulate, smooth-walled. **Asexual morph**: Undetermined.

Material examined: Thailand, Lampang Province, Wang Nuea, on the dead branch, 7 December 2018, M.C. Samarakoon, SAMC190 (MFLU 19-2123, **holotype**), (HKAS 106980, **isotype**).

Notes: Two *Melanostictus* species are introduced, namely *Me. longiostiolatus* and *Me. thailandicus*. *Melanostictus longiostiolatus* has longer and wider papillate ostioles (300–390 × 110–180 µm), and yellow ectostroma as compared to *Me. thailandicus* (185–280 × 85–145 µm), which has a white ectostroma. The LSU and ITS bp (base pair) comparisons show only 3 and 2 bp differences respectively, among *Me. longiostiolatus* and *Me. thailandicus*, while 35 bp differences (including gaps) among *tub*2 sequences (4.6%). Combined gene phylogeny (Fig. 1) showed that *Me. longiostiolatus* is sister to *Me. thailandicus* with 100%/1.00 PP statistical support. In addition, we observed few asci of both *Me. longiostiolatus* and *Me. thailandicus* collections with J+, apical ring, mildly bluing in Melzer's reagent. However, it is not constant throughout the study, and further observations are needed in future studies.

Peroneutypa Berl., Icon. fung. (Abellini) 3(3-4): 80 (1902)

Notes: *Peroneutypa* is typified by *Pe. bellula* and characterised by valsoid stromata with long-necked ascomata; 8-spored, clavate asci and allantoid, hyaline or yellowish ascospores (Carmarán et al. 2006; Senwanna et al. 2017; Shang et al. 2017). Hyde et al. (2020b) listed 28 species, including 11 species with sequence data.

Peroneutypa leucaenae Samarak. & K.D. Hyde, ***sp. nov***.

Index Fungorum number: IF558722; *Facesoffungi number*: FoF 10199; Fig. 17

Etymology: The specific epithet reflects the host genus *Leucaena leucocephala*.

Holotype: MFLU 18-0816

Saprobic on dead branch of *Leucaena leucocephala*. **Sexual morph**: *Ascomata* (including neck) 635–680 × 480–580 µm ($\bar{x}$ = 655 × 525 µm, n = 10), immersed in the host tissue under slightly raised areas, black, mostly solitary or sometimes aggregated, with clusters or evenly distributed, in cross-section globose or subglobose, delimited by a black zone in host tissues, glabrous. *Ostioles* with 275–350 µm ($\bar{x}$ = 310 µm, n = 5) long neck, centric, ostiolar canal periphysate. *Peridium* 22–43 µm ($\bar{x}$ = 34 µm, n = 10) wide, multi-layered, outer layer comprising thick, dark brown cells of *textura angularis*, inner layer composed of hyaline, thin-walled cells of *textura angularis*. *Paraphyses* 3.2–7 µm ($\bar{x}$ = 5.2 µm, n = 20) wide, wider at the base, long, septate, smooth-walled, constricted at septa. *Asci* 30–37 × 3.8–4.5 µm ($\bar{x}$ = 33 × 4.2 µm, n = 25), 8-spored, unitunicate, clavate, pedicel 17–27 µm ($\bar{x}$ = 22 µm, n = 10) long, thin-walled, with wedge-shaped, apical ring, J+ in Melzer's reagent. *Ascospores* 2.9–3.7 × 0.9–1.3 µm ($\bar{x}$ = 3.2 × 1.1 µm, n = 30), L/W 2.9, overlapping, yellowish brown, ellipsoidal to cylindrical or elongate-allantoid, aseptate, smooth-walled. **Asexual morph**: Undetermined.

Culture characteristics: Colonies on PDA reaching 50–52 mm diam. after one week at 25°C, fast growing, irregular, flat or effuse, slightly raised, margin fimbriate, with aerial mycelium, and dirty white; reverse yellow to pale brown at the center, white at the margin.

Material examined: Thailand, Lampang Province, Wang Nuea, on dead branch of *Leucaena leucocephala* (*Fabaceae*), 18 August 2017, M.C. Samarakoon, SAMC048 (MFLU 18-0816, **holotype**), (HKAS 102352, **isotype**); ex-type living culture MFLUCC 18-0522.

Notes: *Peroneutypa leucaenae* has stromata with stromatic tissues developing only between perithecial necks, urn-shaped asci with J+, apical rings and allantoid, slightly to moderately curved ascospores similar to *Pe. diminutispora*. However, *Pe. diminutispora* has protruded necks and up to seven ascomata per stroma and lacks paraphyses, which differs from *Pe. leucaenae* in having one ascoma per stroma and raised neck on the surface with free hyphae and thick paraphyses (de Almeida et al. 2016). *Peroneutypa leucaenae* has asci with a J+, apical ring similar to *Pe. cosmosa*, but differs in having larger asci (30–37 vs 18–25 µm) and smaller ascospores (2.9–3.7 vs 6–8 µm) (Carmarán et al. 2006). The LSU sequence of *Pe. leucaenae* is similar to *Pe. mangrovei* PUFD526 (99%, 0/862 gaps) and *Pe. scoparia* MFLUCC 11-0615 (97%, 0/886 gaps), while the ITS sequence is similar to *Pe. polysporae* NFCCI 4392 (93%, 10/394 gaps) and *E. microasca* BAFC51550 (89%, 14/444 gaps). Combined ITS-*tub*2 and ITS-LSU-*rpb*2-*tub*2-*tef*1 gene phylogeny also supports *Pe. leucaenae* as distinct, forming an independent lineage (Fig. 1).

Fasciatisporaceae S.N. Zhang, J.K. Liu & K.D. Hyde, in Hyde et al., Fungal Diversity 100: 227 (2020)

Hyde et al. (2020a) introduced *Fasciatisporaceae* to accommodate *Fasciatispora* with distinctive morphology of aseptate ascospores with a central pallid band, and on a multigene phylogeny, thus distinguishing it from other members of *Xylariales*. Fasciatisporaceous species are saprobes on palms and other monocotyledons (from *Arecaceae* and *Pandanaceae*) distributed in terrestrial and coastal habitats.

Fasciatispora K.D. Hyde, Trans. Mycol. Soc. Japan 32(2): 265 (1991)

Notes: *Fasciatispora* was introduced by Hyde (1991) with *F. nypae* as the type species with clypeate ascomata; asci with J +/J-, wedge-shaped apical ring, and pale brown to brown, ellipsoidal, ovoid or rhomboid, aseptate ascospores with a central pallid band (Hyde et al. 2020a). Liu et al. (2015) proposed a reference specimen for *F. nypae* and accepted it in *Xylariales* based on molecular data. Thus, following several consecutive studies, 11 *Fasciatispora* species have been accepted, five with molecular data.

Fasciatispora cocoes S.N. Zhang, K.D. Hyde & J.K. Liu, in Hyde et al., Fungal Diversity 100: 231 (2020)

Index Fungorum number: IF557000; *Facesoffungi number*: FoF 06503; Fig. 18

Saprobic on dead leaflets of *Cocos nucifera*. **Sexual morph**: *Ascomata* 200–230 × 160–210 µm ($\bar{x}$ = 220 × 185 µm, n = 7), immersed beneath the clypeus, visible as black, circular dots, ostioles slightly protruding outside, indistinct, mostly solitary, sometimes aggregated into small groups, in cross-section subglobose or globose, with a rounded or flattened base. *Ostioles* centric, ostiolar canal periphysate. *Peridium* 7–14.5 µm ($\bar{x}$ = 10.3 µm, n = 10) wide, multi-layered, outer layer comprising brown, thick-walled cells of *textura angularis*, inner layer composed of hyaline, thin-walled cells of *textura angularis*. *Paraphyses* 2–3.5 µm ($\bar{x}$ = 2.7 µm, n = 15) wide, long, numerous, filamentous, flexuous, septate, rarely branched, tapering. *Asci* 70–100 × 8–11 µm ($\bar{x}$ = 82.5 × 9.5 µm, n = 20), 8-spored, unitunicate, cylindrical, short pedicellate, with a 0.5–0.8 × 2.2–3.1 µm ($\bar{x}$ = 0.7 × 2.6 µm, n = 10), wedge-shaped apical ring, J+ in Melzer's reagent, apex rounded. *Ascospores* 9–12 × 4.5–6.5 µm ($\bar{x}$ = 10.8 × 5.5 µm, n = 25), L/W 2, uniseriate, hyaline when immature, yellowish brown, with wide equatorial pallid band when mature, ellipsoidal to obovoid, aseptate, 1–2-guttulate, surrounded by a 3.5–6 µm ($\bar{x}$ = 4.5 µm, n = 10) wide mucilaginous sheath, lacking a germ slit. **Asexual morph**: Undetermined.

Material examined: Thailand, Chiang Rai Province, Amphoe Mueang Chiang Rai, on the dead leaflets of *Cocos nucifera* (*Arecaceae*), 6 June 2019, M.C. Samarakoon, SAMC226 (MFLU 19-2143, HKAS 107000).

Notes: Our collection is similar to *Fasciatispora cocoes* (MFLU 18-1589) in asci (70–100 × 8–11 µm vs 78–110 × 6–12 µm) and ascospore (9–12 × 4.5–6.5 µmvs 10–15 × 4.5–6 µm) and has the same host *Cocos nucifera*. Combined gene phylogenetic analyses show that our collection clusters with the type of *F. cocoes* (MFLUCC 18-1445) with 100%/1.00 PP statistical support.

Graphostromataceae M.E. Barr, J.D. Rogers & Y.M. Ju, Mycotaxon 48: 533 (1993)

Graphostromataceae was introduced by Barr et al. (1993), which comprises saprobes, endophytes and pathogens on trunks, branches, and twigs of angiosperms (Hyde et al. 2020b). *Biscogniauxia*, *Camillea*, *Graphostroma*, *Obolarina* and *Vivantia* have been accepted in this family (Hyde et al. 2020b; Wijayawardene et al. 2020).

Biscogniauxia Kuntze, Revis. Gen. Pl. (Leipzig) 2: 398 (1891)

Notes: *Biscogniauxia* (type species *Bi. nummularia*) species are characterised by bipartite stromata lacking KOH-extractable pigments, and short pedicellate cylindrical asci and ellipsoid to short fusoid ascospores in their sexual and nodulisporium-like or periconiella-like asexual morphs (Daranagama et al. 2018). *Biscogniauxia* appears paraphyletic with *Camillea*, *Obolarina* and *Graphostoma* (Daranagama et al. 2018). There are 76 *Biscogniauxia* species and 23 have molecular data (Hyde et al. 2020b).

Biscogniauxia magna Samarak. & K.D. Hyde, ***sp. nov***.

Index Fungorum number: IF558723; *Facesoffungi number*: FoF 10200; Fig. 19

Etymology: The specific epithet refers to the Latin word that means "large" because of the large ascomata.

Holotype: MFLU 18-0850

Saprobic on dead branch. **Sexual morph**: *Stromata* 3–18 × 2–7 mm, applanate, dull brown to black, carbonaceous. *Ascomata* 475–700 × 265–375 µm ($\bar{x}$ = 595 × 320 µm, n = 15), ovoid to obpyriform, laterally compressed. *Ostioles* pointed, raised. *Paraphyses* 2.5–6.5 µm ($\bar{x}$ = 4 µm, n = 15) wide, long, numerous, filamentous, flexuous, septate, apex rounded. *Asci* 72–100 × 8–10 µm ($\bar{x}$ = 85.5 × 9.3 µm, n = 20), 8-spored, unitunicate, cylindrical, short pedicellate, with a 1.9–3.3 × 3.3–4.5 µm ($\bar{x}$ = 2.8 × 3.9 µm, n = 10), wedge-shaped apical ring, J+ in Melzer's reagent, apex rounded. *Ascospores* 11.5–14 × 6.5–8.5 µm ($\bar{x}$ = 12.5 × 7.5 µm, n = 35), L/W 1.6, uniseriate, hyaline when immature, dark brown to black when mature, ellipsoid, ends rounded, 1–2-guttulate, aseptate, with straight germ slit along the entire spore length. **Asexual morph**: *Hyphae* 1.5–2.5 µm ($\bar{x}$ = 1.9 µm, n = 15) wide, hyaline to brown, septate, branched, thin-walled aerial mycelia abundant. *Conidiophores* 2.5–5.5 µm ($\bar{x}$ = 3.8 µm, n = 15) wide, composed of main axis, rough-walled, light brown to dark brown, sometimes one or more major branches, with conidiogenous cells arising terminally or laterally. *Conidiogenous cells* 7–11 × 2.5–4.5 µm ($\bar{x}$ = 8.5 × 3.5 µm, n = 20), swollen at the apex and with conidial secession scars, thin- and rough-walled, cylindrical to oblong, hyaline. *Conidia* 5.5–7.5 × 2–3 µm ($\bar{x}$ = 6.5 × 2.6 µm, n = 20), holoblastic, ovoid to clavate, obtuse tip and acute truncated base, hyaline, smooth.

Culture characteristics: Colonies on PDA reaching 55 mm diam. after one week at 25°C, growing fast, flat, circular, dense, margin entire, aerial mycelia, light brown; reverse brown at center with dirty white edges, becoming yellowish brown when mature.

Material examined: Thailand, Chiang Rai Province, Mae Suai, on dead wood, 18 August 2017, M.C. Samarakoon, SAMC011 (MFLU 18-0850, **holotype**), (HKAS 102298, **isotype**); ex-type living culture MFLUCC 17-2665.

Notes: *Biscogniauxia lithocarpi* (on *Lithocarpus* sp.), *Bi. magna*, *Bi. mangiferae* (*Mangifera indica*) and *Bi. reticulospora* have been introduced from Thailand. *Biscogniauxia magna* has larger ascomata (475–700 × 265–375 µm) compared to *Bi. lithocarpi* (300–400 × 150–200 µm) and *Bi. mangiferae* (310–430 ×

185–225 µm) (Ju et al. 1998; Vasilyeva et al. 2012), but are similar in size when compare to *Bi. schweinitzii* (400–700 × 300–500 µm). *Biscogniauxia mangiferae* and *Bi. schweinitzii* have inconspicuous carbonaceous tissues beneath perithecia, while *Bi. magna* has a thick layer. *Biscogniauxia reticulospora* differs from our strain by its comparatively larger ascospores (27–34 × 14–15.5 µm) with surface ornamentations and reticulations (Ju and Rogers 2001). Combined gene phylogenies showed that *Bi. magna* clusters with *Bi. mangiferae* with strong statistical support (100%). The ITS and LSU bp comparisons of *Bi. magna* and *Bi. mangiferae* (MFLU 18-0827) show 94% (13/578 gaps) and 99% (0/863 gaps) similarities, respectively. Here, we introduce *Bi. magna* as a new species based on distinct morphology and phylogeny.

Biscogniauxia petrensis Z.F. Zhang, F. Liu & L. Cai, in Zhang, Liu, Zhou, Liu, Liu & Cai, Persoonia 39: 11 (2017)

Index Fungorum number: IF818247; *Facesoffungi number*: FoF 10201; Fig. 20

Saprobic on dead branch of *Osmanthus fragrans*. **Sexual morph**: *Stromata* 8–20 × 5.5–10 mm, applanate, dull brown to black, carbonaceous. *Ascomata* 260–430 × 80–145 µm ($\bar{x}$ = 336 × 104 µm, n = 15), in cross-section ovoid to obpyriform, laterally compressed. *Ostioles* pointed, raised. *Paraphyses* 2.5–5 µm ($\bar{x}$ = 3.8 µm, n = 15) wide, long, numerous, filamentous, flexuous, septate, apex rounded. *Asci* 75–105 × 7.5–9.5 µm ($\bar{x}$ = 91.5 × 8.5 µm, n = 20), 8-spored, unitunicate, cylindrical, short pedicellate, with a 1.7–3.2 × 3–3.7 µm ($\bar{x}$ = 2.4 × 3.4 µm, n = 10), wedge-shaped, apical ring, J+ in Melzer's reagent, apex rounded. *Ascospores* 11–15 × 5.7–7 µm ($\bar{x}$ = 12.7 × 6.3 µm, n = 35), L/W 2.02, uniseriate, hyaline when immature, dark brown to black when mature, ellipsoid, ends rounded, aseptate, 1–2-guttulate, with straight germ slit along the entire spore length. **Asexual morph**: *Hyphae* 2.3–3.7 µm ($\bar{x}$ = 3 µm, n = 25) wide, hyaline to brown, septate, branched, thin-walled aerial mycelia abundant. *Conidiophores* 3–4.5 µm ($\bar{x}$ = 3.5 µm, n = 15) wide, composed of main axis, rough-walled, hyaline to slightly yellowish, sometimes one or more major branches, with conidiogenous cells arising terminally or laterally. *Conidiogenous cells* 5–12 × 2–3.5 µm ($\bar{x}$ = 8 × 2.7 µm, n = 25), swollen at the apex and with conidial secession scars, thin- and rough-walled, cylindrical to oblong, hyaline. *Conidia* 4.3–6.5 × 2–3.5 µm ($\bar{x}$ = 5.3 × 2.6 µm, n = 20), holoblastic, ovoid to clavate, obtuse tip and acute truncated base, hyaline, smooth.

Culture characteristics: Colonies on PDA reaching 50 mm diam. after one week at 25°C, growing fast, flat, circular, dense, margin entire, aerial mycelia, light brown; reverse brown at center with dirty white edges.

Material examined: China, Guizhou Province, Guiyang, Guizhou Academy of Agricultural Sciences (GZAAS), on dead branch of *Osmanthus fragrans* (*Oleaceae*), 12 June 2018, M.C. Samarakoon, SAMC157 (HKAS 102388; MFLU 19-2100); living cultures GZCC 21-0040 = MFLUCC T20-0650.

Notes: Zhang et al. (2017) introduced *Bi. petrensis* from a karst cave based on phylogeny and asexual morphology. Ma et al. (2020) reported *Bi. petrensis* as an endophyte in the root of *Dendrobium harveyanum* in Thailand, and Das et al. (2020) found it in adult mosquitoes from Korea. Conidia of our isolate (4.3–6.5 × 2–3.5 µm) overlap with the type CGMCC 3.17912 (4.5–7.5 × 2.5–4.5 µm) and MFLUCC 14-0151 (3.5 – 5 × 2.5 – 3 µm). The BLAST searches also confirmed that our isolate is similar to *Bi. petrensis*, and here we provided a new host record from *Osmanthus fragrans* in China.

Camillea Fr., Summa veg. Scand., Section Post. (Stockholm): 382 (1849)

Notes: *Camillea* was described to accommodate species with long, erect, hard, carbonaceous, cylindrical, black stromata with light coloured ascospores, which are saprobes on wood with the type species *C. leprieurii* (Laessøe et al. 1989; Daranagama et al. 2018; Hyde et al. 2020b). There are 44 species and four with molecular data under *Camillea* (Hyde et al. 2020b).

Camillea tinctor(Berk.) Læssøe, J. D. Rogers & Whalley, Mycol. Res. 93(2): 145 (1989)

Index Fungorum number: IF135971; *Facesoffungi number*: FoF 02973; Fig. 21

Saprobic on dead bark of *Bauhinia racemosa*. **Sexual morph**: *Stromata* 10–120 × 16–30 × 1.2–2.5 mm, erumpent through bark or wood, solitary or aggregated, elongate to irregular, applanate with slightly convex, often with grooves on the surface, shiny black, carbonaceous, margin raised, rounded. *Ascomata* 1010–1200 × 205–270 µm ($\bar{x}$ = 1155 × 234 µm, n = 15), in cross-section tubular, laterally compressed. *Ostioles* pointed, raised. *Paraphyses* 3.5–8.6 µm ($\bar{x}$ = 5.2 µm, n = 25) wide, long, numerous, filamentous, flexuous, septate, apex rounded. *Asci* 112–146 × 9.5–11.5 µm ($\bar{x}$ = 128.5 × 10.5 µm, n = 20), 8-spored, unitunicate, cylindrical, short pedicellate, with a 4–5.3 × 3.4–3.6 µm ($\bar{x}$ = 4.7 × 3.5 µm, n = 10), wedge-shaped, apical ring, J+ in Melzer's reagent, apex rounded. *Ascospores* 15.5–21 × 6.5–8.3 µm ($\bar{x}$ = 17.6 × 7.5 µm, n = 35), L/W 2.35, uniseriate, hyaline when immature, yellowish brown when mature, inequilaterally fusiform, ends rounded, aseptate. **Asexual morph**: Conidiogenous structure xylocladium-like. *Conidiophores* long, with ampulla in the upper part, 27–40 × 7.5–10 µm ($\bar{x}$ = 33.4 × 8.9 µm, n = 5), pale brown, clavate, smooth. *Conidiogenous cells* 8.5–11 × 2.5–4 µm ($\bar{x}$ = 9.8 × 3.2 µm, n = 8), polyblastic, cylindrical, oblong-elliptical to irregular in shape, compact and continuous on the ampulla, simple or branched, hyaline to pale brown. *Conidia* 4–8 × 1.5–3.1 µm ($\bar{x}$ = 6 × 2.5 µm, n = 15), hyaline, ellipsoidal, aseptate.

Culture characteristics: Colonies on PDA reaching 55 mm diam. after two weeks at 25 ºC, flat, circular, dense, with a smooth surface, margin entire, and white to light brown.

Material examined: Thailand, Nan Province, Doi Phu Kha roadside, on dead bark of *Bauhinia racemosa* (*Fabaceae*), 4 August 2017, M.C. Samarakoon, SAMC043 (MFLU 18-0786; HKAS 102292); living culture MFLUCC 18-0508.

Notes: *Camillea tinctor* exhibits a wide distribution in Thailand, and has been described on various timbers (Thienhirun 1997; Whalley et al. 1999; Suwannasai 2005). There is a slight difference in the size of stromata from different locations with overlapping size ranges of ascomata, asci and ascospores described from different studies (Whalley et al. 1999; Suwannasai 2005; Daranagama et al. 2018). Conspicuous orange staining of the host substrate is often reported, but we did not observe such staining in our specimen, as did San Martín González and Rogers (1993). Our collection is provided as a new host record from dead *Bauhinia racemosa* wood, and there is a need to determine if the fungus affects plants as a pathogen.

Lopadostomataceae Daranag. & K.D. Hyde [as 'Lopadostomaceae'], in Senanayake et al., Fungal Diversity 73: 129 (2015)

Senanayake et al. (2015) introduced *Lopadostomataceae* in *Xylariales* to accommodate *Creosphaeria* and *Lopadostoma*. Lopadostomataceous species are saprobes on corticated and decorticated wood (Senanayake et al. 2015, Daranagama et al. 2018). *Creosphaeria*, *Jumillera*, *Lopadostoma* and *Whalleya* are accepted in the family based on morphology and phylogeny (Hyde et al. 2020b).

Lopadostoma (Nitschke) Traverso, Fl. ital. crypt., Pars 1: Fungi. Pyrenomycetae. *Xylariaceae*, *Valsaceae*, *Ceratostomataceae* 1(2): 169 (1906)

Notes: *Lopadostoma* species have immersed, erumpent from bark, postulate or widely effused stromata, 8-spored, unitunicate, cylindrical asci with J+, apical rings bluing in Melzer's reagent and aseptate, oblong to narrowly ellipsoid ascospores with a germ slit and libertella-like asexual morphs (Jaklitsch et al. 2014). There are 24 species and 11 species with sequence data (Hyde et al. 2020b). LSU-ITS phylogeny provides lower species resolution, and the protein coding genes are important for species delimitation (Jaklitsch et al. 2014; Daranagama et al. 2018).

Lopadostoma quercicola Jaklitsch, J. Fourn. & Voglmayr, in Jaklitsch, Fournier, Rogers & Voglmayr, Persoonia 32: 72 (2014)

Index Fungorum number: IF803810; *Facesoffungi number*: FoF 10202; Fig. 22

Saprobic on dead land branch of *Quercus sp*. **Sexual morph**: *Stromata* 1.8–5.3 × 0.8–3.4 mm, immersed, erumpent from bark, surrounded by a narrow, black, carbonaceous disc as a clypeus, surrounded by reddish brown bark surface, convex, raised, dark grey, entostroma dark, usually black. *Ascomata* 800–1750 × 560–1080 µm ($\bar{x}$ = 1322 × 863 µm, n = 15), clustered in valsoid groups, in cross-section subglobose to flask-shaped. *Ostioles* papillate with inconspicuous ostiolar openings, necks white or pale brown. *Paraphyses* comprising two types, 1) 1.7–3 µm ($\bar{x}$ = 2.2 µm, n = 25) wide, long, numerous, cylindrical, aseptate and guttulate; and 2) 2.8–3.8 µm ($\bar{x}$ = 3.3 µm, n = 20) wide, septate, rarely branched, smooth-walled, constricted at septa. *Asci* 90–135 × 5–7.5 µm ($\bar{x}$ = 113 × 6.3 µm, n = 20), 8-spored, unitunicate, cylindrical, pedicellate, with a 0.7–1.1 × 2.6–2.9 µm ($\bar{x}$ = 0.9 × 2.7 µm, n = 10), ellipsoidal-discoid, apical ring, J+ in Melzer's reagent, apex rounded. *Ascospores* 8.3–11.4 × 3.4–4.4 µm ($\bar{x}$ = 9.5 × 3.9 µm, n = 35), L/W 2.4, uniseriate, hyaline when immature, turning pale brown and dark brown at maturity, oblong to narrowly ellipsoid, symmetrical to slightly inequilateral, aseptate, smooth-walled, with a straight germ slit along the entire spore length, when immature with 2 large guttules. **Asexual morph**: Undetermined.

Culture characteristics: Colonies on PDA reaching 45–48 mm diam. after three weeks at 25 ºC, flat, dense, center raised, cottony, margin undulate, circular, whitish grey; reverse light brown and with dirty white zonations.

Material examined: Italy, Province of Forlì-Cesena, Rocca delle Caminate – Predappio, on dead land branch of *Quercus cerris* (*Fagaceae*), 4 March 2017, E. Camporesi, IT3269 (MFLU 17-0731, HKAS 102368). *ibid*. on dead land branch of *Quercus sp*. (*Fagaceae*), 22 March 2017, E. Camporesi, IT3269A (MFLU 17-0843, HKAS 102314); living culture MFLUCC 17-2673. *ibid*. Near Monte Mirabello – Predappio, on dead land branch of *Quercus sp*. (*Fagaceae*), 12 April 2017, E. Camporesi, IT3269B (MFLU 17-0940, HKAS 102369).

Notes: Jaklitsch et al. (2014) introduced *Lopadostoma quercicola* on *Quercus pubescens* from Austria, and the species is similar in morphology and phylogeny to our new collections. Size and shape of ascospores of our collections (8.3–11.4 × 3.4–4.4 µm) overlap in the range of WU 32079 (holotype) (9.5–12 × 4.3–5 µm). A BLAST search of ITS data of our strains is 100% similar with *L. quercicola* (WU 32079). The known host and geographical distribution is widespread in corticated branches of *Quercus* species from Europe, and from Austria, Croatia, France, Italy and Portugal on *Quercus cerris*, *Q. petraea*, *Q. pubescens*, *Q. robur* and *Quercus suber*. Morphology and phylogeny of our new collections are similar to *Lopadostoma quercicola*, and here we provide a new host record *Quercus cerris* from Italy.

Requienellaceae Boise, Mycologia 78(1): 37 (1986)

Requienellaceae was introduced by Boise (1986) and accepted in *Melanommatales*. *Requienellaceae* species have a widespread distribution as saprobes on dead wood or pathogenic on plants and inhabit bark (Hyde et al. 2020b; Dissanayake et al. 2021b). Jaklitsch et al. (2016) revisited the family and placed it in *Xylariales* based on the morphology and phylogeny of *Acrocordiella* and *Requienella*.

Acrocordiella O.E. Erikss., Mycotaxon 15: 189 (1982)

Notes: *Acrocordiella* was introduced by Eriksson (1982) with the type species *Ac. occulta*. The genus is characterised by solitary or small groups of immersed ascomata without a clypeus, bitunicate-like asci with thick-walled apex and wide ocular chamber, and ellipsoid to oblong ascospores with round or acute ends, with one or several transverse distosepta and large lumina (Jaklitsch et al. 2016). Three *Acrocordiella* species have been accepted with morphology and molecular data (Dissanayake et al. 2021b).

Acrocordiella photiniicola Samarak. & K.D. Hyde, ***sp. nov***.

Index Fungorum number: IF558724; *Facesoffungi number*: FoF 10203; Fig. 23

Etymology: The specific epithet reflects the host genus *Photinia*.

Holotype: MFLU 17-1552

Saprobic on dead branch of *Photinia sp*. **Sexual morph**: *Ascomata* 280–330 × 295–400 µm ($\bar{x}$ = 310 × 360 µm, n = 5), immersed beneath a rudimentary clypeus, visible as black, circular dots, with green algal-like growth around the ostioles, mostly solitary, sometimes aggregated into small groups, in cross-section subglobose or globose, with a rounded or flattened base. *Ostioles* centric, raised, ostiolar canal periphysate. *Peridium* 10–15.5 µm ($\bar{x}$ = 14.2 µm, n =

10) wide, multi-layered, outer layer comprising brown, thick-walled cells of *textura angularis*, inner layer composed of hyaline, thin-walled cells of *textura angularis*. *Paraphyses* 4–7 µm ($\bar{x}$ = 5.5 µm, n = 15) wide, long, numerous, filamentous, flexuous, septate, rarely branched, guttulate, tapering to the ends. *Asci* 90–150 × 9.5–17 µm ($\bar{x}$ = 112 × 14 µm, n = 20), 8-spored, unitunicate, cylindrical, with a short pedicel, simple or knob-like at the base, ascal apex thickened, containing a slightly refractive, inversely funnel-shaped. *Ascospores* 22–34 × 9.5–13.5 µm ($\bar{x}$ = 27.5 × 11.5 µm, n = 25), L/W 2.4, obliquely uniseriate, hyaline when immature, greyish olive when young, olivaceous to medium brown when mature, deteriorated dark brown when over mature, aseptate, inequilateral, narrowly rounded to nearly acute at the ends, 3-distoseptate, 2-large rhomboid lumina in middle, 2-small trapezoid lumina at ends, multi-guttulate, smooth- and thick-walled, lacking a mucilaginous sheath. **Asexual morph**: Undetermined.

Culture characteristics: Colonies on PDA reaching 18–20 mm diam. after five weeks at 25°C, dense, irregular, cottony surface with zonate convex areas, margin lobate, immersed hyphal growth, white; reverse light brown.

Material examined: Thailand, Chiang Rai Province, Muang, Mae Fah Luang University premises, on dead branch of *Photinia sp.* (*Rosaceae*), 7 November 2017, M.C. Samarakoon, SAMC003 (MFLU 17-1552, **holotype**), (HKAS 102287, **isotype**); ex-type living culture MFLUCC 18-0617.

Notes: *Acrocordiella photiniicola* is similar to *Ac. yunnanensis* in having similar sized ascomata (280–330 × 295–400 µmvs 290–325 × 325–355 µm) and peridia (10–15.5 µm vs 10–15 µm). *Acrocordiella occulta* (300–500 × 400–800 µm) and *Ac. omanensis* (745–810 × 645–780 µm) have compartively large ascomata (Jaklitsch et al. 2016, Maharachchikumbura et al. 2018). However, *Ac. yunnanensis* differs from our collection in having wider asci and muriform ascospores with 3–7 distosepta with a mucilaginous sheath (Dissanayake et al. 2021b). Sequences of *Ac. photiniicola* are similar to *Ac. yunnanensis* HKAS 111922 (LSU 95%, 4/864 gaps) and *Ac. omanensis* SQUCC 15091 (LSU 96%, 3/852 gaps). Based on distinct morphology and phylogeny, we introduce *Ac. photiniicola* as a new species.

LSU-ITS phylogenies in Jaklitsch et al. (2016) and Maharachchikumbura et al. (2018) showed that *Acrocordiella* and *Requienella* form distinct clades. With the addition of *Ac. yunnanensis*, LSU-ITS phylogeny showed *Ac. occulta* is not monophyletic and clusters in *Requienella* (Dissanayake et al. 2021b). Similarly, our ITS-LSU and ITS-LSU-*rpb2*-*tub2*-*tef1* combined gene phylogenies confirmed that *Acrocordiella* is not monophyletic, even though they share similar morphologies. Boise (1986) only accepted *Requienella* in *Requienellaceae* and synonymised *Ac. occulta* under *Re. seminuda*. Jaklitsch et al. (2016) revisited *Acrocordiella* and *Requienella* and accepted them as distinct genera based on morphology and phylogeny. *Requienella* can easily be distinguished in having prominent ostioles raised above the host surface, while *Acrocordiella* form inconspicuous spots on the host surface. Further studies are required to reveal the generic boundaries of *Acrocordiella* and *Requienella*.

Vamsapriyaceae Y.R. Sun, Yong Wang bis & K.D. Hyde, in Sun et al., XXX (2021)

Vamsapriyaceae was introduced by Sun et al. (2021) to accommodate *Diabolocovidia*, *Didymobotryum*, *Podosporium* and *Vamsapriya*. Species are commonly found in dead wood, especially bamboo. Previous phylogenetic studies place *Vamsapriya* species as a distinct clade in *Xylariales* (Hyde et al. 2020b; Samarakoon et al. 2020c).

Vamsapriya Gawas & Bhat, Mycotaxon 94: 150 (2006)

Notes: Gawas and Bhat (2005) introduced *Vamsapriya* to accommodate *V. indica* described on dead and decaying bamboo twigs from India. The genus is characterised by catenate, phragmosporous conidia on synnematous conidiophores with non-cicatrised, monotretic conidiogenous cells in the asexual morph. Dai et al. (2017) linked the asexual and sexual morphs of *Vamsapriya* in a multigene phylogeny. Eight *Vamsapriya* species have been described, mostly on dead bamboo substrates, and the genus is accepted in *Xylariaceae* (Hyde et al. 2020b).

Apioclypea was introduced by Hyde (1994), which is characterised by immersed, clypeate ascomata; cylindrical asci with J+/J-, apical ring and hyaline, apiospores covered by a mucilaginous sheath. The morphological comparisons between *Apioclypea* and *Vamsapriya* species showed that both genera have similar morphologies in having immersed, clypeate ascomata, asci with short pedicels and hyaline apiospores with a mucilaginous sheath (Hyde 1994; Hyde et al. 1998; Taylor and Hyde 2003). Two of our new collections clustered with *Vamsapriya* and are morphologically similar to the only known species, *V. bambusicola*. However, *Vamsapriya* has a thinner peridium and asci with J+, apical ring, as compared to *Apioclypea* with thicker peridia and some species with a J-, apical ring (*Api. nonapiospora*, *Api. phoenicicola*). *Apioclypea* has been placed in *Clypeosphaeriaceae* and *Hyponectriaceae* in different studies (Hyde 1994; Hyde et al. 1998; Kang et al. 1999). Kang et al. (1999) re-examined the holotype of the generic type, *Api. livistonae* and mentioned a J-, apical ring, which is J+ in the generic description by Hyde (1994). Currently, *Apioclypea* has seven species but lacking molecular data. *Apioclypea sp.* (HKUCC 6269) LSU sequence available in the GenBank (https://www.ncbi.nlm.nih.gov/nuccore/AY083836.1) is similar to unconfirmed taxa that belong to *Lanceispora*, *Polyancora* (*Xylariales* genera *incertae sedis*) and *Leiosphaerella* (*Pseudomassariaceae*). We treat *Apioclypea* and *Vamsapriya* as distinct genera until molecular data for the type of *Apioclypea* becomes available.

Vamsapriya mucosa Samarak. & K.D. Hyde, ***sp. nov.***

Index Fungorum number: IF558725; *Facesoffungi number*: FoF 10204; Fig. 24

Etymology: The specific epithet reflects the thick mucilaginous sheath.

Holotype: MFLU 18-0103

Saprobic on dead bamboo branch. **Sexual morph**: *Ascomata* 260–300 × 320–380 µm ($\bar{x}$ = 280 × 345 µm, n = 5), immersed, visible as black, circular dots, surrounded by a light brown margin, solitary, scattered, in cross-section subglobose, with mostly flattened base. *Ostioles* centric, raised, ostiolar canal periphysate. *Peridium* 9.5–15.2 µm wide ($\bar{x}$ = 12.5 µm, n = 10), multi-layered, attached to the host with yellow innert substrate, outer layer comprising yellowish

brown, thick-walled cells of *textura angularis*, inner layer composed of hyaline, thin-walled cells of *textura angularis*. *Paraphyses* 1.2–2.8 µm ($\bar{x}$ = 2 µm, n = 15) wide, wider at the base, long, septate, constricted at septa, guttulate, ends tapering, in a gelatinous matrix. *Asci* 80–95 × 5–7.5 µm ($\bar{x}$ = 90 × 6 µm, n = 20), 8-spored, unitunicate, cylindrical, short pedicellate, with a 0.8–1.2 × 2.2–2.6 µm ($\bar{x}$ = 1 × 2.4 µm, n = 10), discoid apical ring, J+ in Melzer's reagent, apex rounded. *Ascospores* 10–14 × 3.5–4.5 µm ($\bar{x}$ = 11.5 × 4 µm, n = 25), L/W 2.8, uniseriate, hyaline, ellipsoidal, constricted, apiosporous; apical cell 1.5–3 µm ($\bar{x}$ = 2.3 µm, n = 25) long, conical; based cell 7.5–10.5 µm ($\bar{x}$ = 9.1 µm, n = 25) length, usually with large guttules, fusiform to broad fusiform, pointed at both ends, surrounded by a 4–10 µm ($\bar{x}$ = 6.5 µm, n = 10) wide mucilaginous sheath when fresh. **Asexual morph**: Undetermined.

Material examined: Thailand, Phayao Province, Phachang Noi, Pong, on dead branch of bamboo (*Poaceae*), 1 September 2017, M.C. Samarakoon, SAMC005 (MFLU 18-0103, **holotype**), (HKAS 102291, **isotype**); ex-type living culture MFLUCC 17-2660.

Notes: *Vamsapriya mucosa* hasa black clypeus covering the ostioles as black dots on the host surface, a yellow ectostroma tightly adhered to the host tissues and the peridium, subglobose, ascomata mostly with flattened bases, asci with J+, apical ring and ascospores with a thick mucilaginous sheath (4–10 µm). The LSU and ITS sequences of *V. mucosa* are similar to *V. bambusicola* MFLUCC 11-0477 (99%, 0/900 gaps; 92%, 9/598 gaps), *V. khunkonensis* MFLUCC 11-0475 (99%, 0/885 gaps; 90%, 26/610 gaps) and *Diabolocovidia claustri* CPC 37593 (99%, 0/864 gaps; 88%, 40/593 gaps). The phylogeny shows that *V. mucosa* forms a distinct clade in *Vamsapriya* (Fig. 1).

Paravamsapriya Samarak. & K.D. Hyde, ***gen. nov.***

Index Fungorum number: IF558726; *Facesoffungi number*: FoF 10205

Etymology: After its morphological similarities to *Vamsapriya*.

Saprobic on dead bamboo branch. **Sexual morph**: *Ascomata* immersed, visible as black, circular dots, with a depressed yellowish brown ring covering a clypeus-like black margin around the ostiolar opening, solitary, scattered, in cross-section subglobose. *Ostioles* centric, ostiolar canal periphysate. *Peridium* multi-layered, easily detached from the host with yellow innert substrate, outer layer comprising yellowish brown, thick-walled, compact cells of *textura angularis*, inner layer composed of hyaline, thin-walled cells of *textura angularis*. *Paraphyses* long, septate. *Asci* 8-spored, unitunicate, cylindrical, short pedicellate, with a flattened, J-, apical ring in Melzer's reagent, apex rounded. *Ascospores* uniseriate or overlapping uniseriate, hyaline, ellipsoidal to fusiform, aseptate, lacking germ slits. **Asexual morph**: Undetermined.

Type: *Paravamsapriya ostiolata* Samarak. & K.D. Hyde

Notes: *Paravamsapriya* is similar to *Vamsapriya* in having immersed ascomata with clypei, periphysate ostiolar canals, a peridium with compact cell layers, septate paraphyses, short pedicellate, cylindrical asci and ascospores lacking a germ slit. There are distinct morphologies in *Paravamsapriya* such as distinct yellow and black margin on the host surface around the ostioles, an easily detachable peridium, and aseptate ascospores. *Capsulospora* is characterised by clypeate, immersed ascomata and aseptate, hyaline ascospores similar to *Paravamsapriya*, but differs in having ascospores covered with mucilaginous sheath, some with germ slits (e.g. *Ca. borneoensis*) and asci with discoid, J+ apical ring (Hyde 1996a; Fröhlich and Hyde 2000). Hyde (1996b) introduced *Arecomyces* to accommodate physalospora-like species with immersed ascomata under a clypeus or pseudostroma, broad cylindrical asci with a refractive apical ring and aseptate, hyaline ascospores covered with a mucilaginous sheath, which are different from *Paravamsapriya*. *Sabalicola* is also different from *Paravamsapriya* in having asci with J+, apical ring and yellowish ascospores with a thin mucilaginous sheath and blunt polar appendages bearing (Hyde 1995b). Based on the distinct morphology and phylogeny, here we introduce a new genus as *Paravamsapriya*.

Paravamsapriya ostiolataSamarak. & K.D. Hyde, ***sp. nov.***

Index Fungorum number: IF558727; *Facesoffungi number*: FoF 10206; Fig. 25

Etymology: The specific epithet reflects the distinct ostioles.

Holotype: MFLU 18-0761

Saprobic on dead bamboo branch. **Sexual morph**: *Ascomata* 450–490 × 490–530 µm ($\bar{x}$ = 475 × 515 µm, n = 5), immersed, visible as black, circular dots, with clypeus-like tissue around the ostiolar opening, surrounded by a light brown, depressed margin, solitary, scattered, in cross-section subglobose. *Ostioles* centric, raised, ostiolar canal periphysate. *Peridium* 20–33 µm ($\bar{x}$ = 27 µm, n = 10) wide, multi-layered, easily detached from the host, with yellow innert substrate, outer layer comprising yellowish brown, thick-walled, compact cells of *textura angularis*, inner layer composed of hyaline, thin-walled cells of *textura angularis*. *Paraphyses* 3.8–6.3 µm ($\bar{x}$ = 5 µm, n = 15) wide, long, septate, constricted at septa, guttulate, ends tapering, in a gelatinous matrix. *Asci* 140–175 × 9.5–15 µm ($\bar{x}$ = 160 × 11.5 µm, n = 20), 8-spored, unitunicate, cylindrical, short pedicellate, with a flattened apical ring, J- in Melzer's reagent, apex rounded. *Ascospores* 23–28 × 7.5–10 µm ($\bar{x}$ = 26.5 × 8.5 µm, n = 25), L/W 3.1, uniseriate or overlapping uniseriate, hyaline, rarely brown, ellipsoidal to fusiform, aseptate, smooth-walled, with 3–4 guttules, pointed, slightly curved with thin mucilaginous caps at both ends, prominent, smooth-perispored, wrinkled with 5% KOH, lack of germ slit. **Asexual morph**: Undetermined.

Material examined: Thailand, Lampang Province, Wang Nuea, on dead branch of bamboo (*Poaceae*), 8 August 2017, M.C. Samarakoon, SAMC055 (MFLU 18-0761, **holotype**), HKAS 102297, **isotype**). *ibid*. SAMC055-2 (MFLU 18-0813, HKAS 102357 **paratypes**).

Notes: *Paravamsapriya ostiolata* is described from a dead branch of bamboo in Thailand, which has distinct ostioles, J- refractive apical rings and hyaline, ellipsoidal to fusiform, aseptate, smooth-perispored ascospores with thin mucilaginous caps at the ends. The combined phylogeny shows that two isolates of *P. ostiolata* form a distinct basal clade in *Vamsapriyaceae* (Fig.1, Clade Xy10).

Xylariaceae Tul. & C. Tul. [as 'Xylariei'], Select. fung. carpol. (Paris) 2: 3 (1863)

Xylariaceous species are distributed worldwide as saprobes, pathogens and endophytes in wood, leaves and fruits or associated with insect vectors. Maharachchikumbura et al. (2016) accepted 87 genera into the family, and Daranagama et al. (2018) accepted 37 genera on the re-examination of herbarium specimens. Following several recent studies, Hyde et al. (2020b) accepted 32 genera in *Xylariaceae*.

Helicogermslita Lodha & D. Hawksw., in Hawksworth & Lodha, Trans. Br. Mycol. Soc. 81(1): 91 (1983)

Notes: Hawksworth and Lodha (1983) introduced *Helicogermslita* to accommodate a xylarialean species with ascospores having spiral germ slits and typified by *He. celastri*. Apart from this, *Helicogermslita* species share stromatic ascomata with white ectostroma and asci with J+, apical rings (Petrini 2003; Daranagama et al. 2018). Nine species have been described based only on morphology.

Helicogermslita clypeata Samarak. & K.D. Hyde, ***sp. nov***.

Index Fungorum number: IF558728; *Facesoffungi number*: FoF 10207; Fig. 26

Etymology: The specific epithet reflects the prominent clypeus.

Holotype: MFLU 18-0852

Saprobic on dead branch. **Sexual morph**: *Ascomata* 550–775 × 600–1040 µm ($\bar{x}$ = 671 × 763 µm, n = 10), immersed, raised areas, visible as black dots, solitary or aggregated, in cross-section subglobose to pyriform. *Clypeus* carbonaceous, black, thick, comprising dark fungal hyphae. *Ostioles* centric or eccentric, ostiolar canal periphysate. *Peridium* 29–45 µm ($\bar{x}$ = 36.5 µm, n = 10) wide, with two cell layers, outer layer comprising reddish brown, thick-walled cells of *textura angularis*, inner layer composed of hyaline, thin-walled cells of *textura angularis*. *Paraphyses* 2.5–5.2 µm ($\bar{x}$ = 3.7 µm, n = 25) wide, wider at the base (up to 9.5 µm wide), longer than the asci, numerous, guttulate, filamentous, septate, constricted at septa. *Asci* 115–145 × 9–11.5 µm ($\bar{x}$ = 128.5 × 10.3 µm, n = 18), 8-spored, unitunicate, cylindrical, pedicellate, apically rounded, with 3.5–4.7 × 2–2.8 µm ($\bar{x}$ = 4 × 2.4 µm, n = 10), J+, wedge- or inverted, hat-shaped, apical ring, bluing in Melzer's reagent. *Ascospores* 13–18.5 × 5.7–7.6 µm ($\bar{x}$ = 16.2 × 6.6 µm, n = 25), L/W 2.45, overlapping uniseriate, hyaline when immature, brown to dark brown when mature, broadly ellipsoidal, aseptate, 1–2-guttulate, lacking a mucilaginous sheath, spiral germ slit extending over the full length. **Asexual morph**: Undetermined.

Material examined: Thailand, Lampang Province, Wang Nuea, on dead branch, 18 August 2017, M.C. Samarakoon, SAMC080 (MFLU 18-0852, **holotype**), (HKAS 102321, **isotype**); ex-type living culture MFLUCC 18-0517.

Notes: *Helicogermslita clypeata* has immersed or semi immersed or rarely superficial ascomata when mature with a prominent clypeus and white ectostroma, J+, wedge- or inverted, hat-shaped, apical ring and broadly ellipsoidal ascospores with spiral germ slits, which are comparable to the generic type of *Helicogermslita* (Hawksworth and Lodha 1983). In addition, the carbonaceous stromatic variations can be observed among the species (Læssøe and Spooner 1993). Ascospores of *He. fleischhakii*, *He. gisbornia*, *He. johnstonii* and *He. mackenziei* bear a cellular appendage, which is lacking in *He. clypeata* (Petrini 2003). *Helicogermslita aucklandica* and *He. clypeata* ascospores are similar in shape with one round spiral germ slit, while they differ in having larger ascospores (19–23.5 × 10–14 µm vs 13–18.5 × 5.7–7.6 µm) (Petrini 2003). *Helicogermslita fleischhakii* and *He. gaudefroyi* have mucilaginous sheath around ascospores, which differs from *He. clypeata* (Læssøe and Spooner 1993; Petrini 2003). *Helicogermslita clypeata* differs from other *Helicogermslita* species in having large asomata with a wide clypeus. *Yuea chusqueicola* possesses spiral germ slits in their ascospores, but differs from *He. clypeata* in having small ascomata, large asci and ascospores covered with a mucilaginous sheath (Eriksson 2003). In addition, *Anthostomella limitata* and *An. umbrinella* have similar ascospores with spiral germ slits, but differ in having a mucilaginous sheath (Hawksworth and Lodha 1983; Lu and Hyde 2000; Petrini 2003). There is no molecular data for *Helicogermslita*, and it has been accepted in *Xylariaceae* based only on morphology.

In our phylogeny, *Helicogermslita clypeata* clusters in *Xylaria* "PO" clade (U'Ren et al. 2016; Konta et al. 2021b) sister to *X. frustulosa* with a high statistical support (92%), which is in *Xylaria sensu lato*. *Xylaria* "PO" clade comprises with *Amphirosellinia*, *Astrocystis*, *Collodiscula*, *Kretzmariella*, *Stilbohypoxylon* and *Xylaria* species. Based on its distinct phylogeny and similar morphology, our collection is introduced as a new species of *Helicogermslita* in *Xylariaceae*. However, *Leptomassaria simplex*, type species of *Leptomassaria* has ascospores with a spiral germ slit and thick mucilaginous sheath similar to *Helicogermslita* (Hawksworth and Lodha 1983; Rappaz 1995). Lu and Hyde (2000) mentioned that *Leptomassaria* differs from *Helicogermslita* in having immersed ascomata and slightly an irregular, wedge-shaped, ascal, apical ring. Daranagama et al. (2018) mentioned the possibility of linking *Helicogermslita* and *Leptomassaria* with observations based on herbarium specimens. In addition, we observed that *Leptomassaria* has poorly developed stromata, larger ascomata, reduced clypei and significant wedge-shaped ascal apical rings as compared to *Helicogermslita*, and thus should be treated as two genera.

Hypocopra (Fr.) J. Kickx f., Fl. Crypt. Flandres (Paris) 1: 362 (1867)

Notes: *Hypocopra* is typified by *Hy. merdaria* and characterised by sessile, clypeoid, or reduced stromata; asci with complex apical rings and mostly aseptate, brown ascospores with a germ slit. *Hypocopra* species exclusively inhabit dung. Krug and Cain (1974) described 14 new species and one combination discovered on different dung types. There are 31 species, including three species with molecular data (Becker et al. 2020).

Hypocopra zeae Samarak. & K.D. Hyde, ***sp. nov***.

Index Fungorum number: IF558729; *Facesoffungi number*: FoF 10208; Fig. 27

Etymology: The specific epithet reflects the host genus *Zea*.

Holotype: MFLU 18-0809

Saprobic on dead culm of *Zea mays*. **Sexual morph**: *Ascomata* 255–305 × 185–290 µm ($\bar{x}$ = 280 × 250 µm, n = 10), immersed, visible as greyish black, raised areas, solitary or aggregated, in cross-section globose to subglobose, sometimes with a flattened base. *Clypeus* carbonaceous, greyish black, thick-walled, short, comprising dark fungal hyphae and host epidermal cells. *Ostioles* centric, ostiolar canal periphysate. *Peridium* 35–50 µm ($\bar{x}$ = 43 µm, n = 10) wide, tightly attached to the host, with two cell layers, outer layer thick, yellowish brown, thick-walled cells of *textura angularis*, inner layer thin, composed of hyaline, thin-walled cells of *textura angularis*. *Paraphyses* 2–5.5 µm ($\bar{x}$ = 3.4 µm, n = 25) wide, wider at the base, longer than the asci, numerous, filamentous, septate, rarely branched, constricted at septa, guttulate, apically blunt. *Asci* 65–85 × 5–7.5 µm ($\bar{x}$ = 73 × 6.5 µm, n = 25), 8-spored, unitunicate, cylindrical, short pedicellate, apically rounded with a 1.5–2 × 2–2.6 µm ($\bar{x}$ = 1.8 × 2.3 µm, n = 15), rectangular to slightly obconic apical ring, J+ in Melzer's reagent. *Ascospores* 8–10 × 3.5–5 µm ($\bar{x}$ = 9 × 4.4 µm, n = 35), L/W 2.04, uniseriate, brown, inequilaterally ellipsoidal, aseptate, 1–2-guttulate, germ slit on ventral side of the ascospore along part of the spore. **Asexual morph**: Undetermined.

Material examined: Thailand, Phayao Province, Phachang Noi, Pong, on dead culm of *Zea mays* (*Poaceae*), 11 September 2017, M.C. Samarakoon, SAMC030 (MFLU 18-0809, **holotype**), (HKAS 102327, **isotype**).

Notes: *Hypocopra zeae* is similar to xylariaceous taxa in having immersed ascomata under a clypeus, septate, hyaline paraphyses, 8-spored, unitunicate, cylindrical asci with a J+, apical ring and uniseriate, brown ascospores with a short germ slit. Anthostomelloid taxa such as *An. eructans*, *An. delitesnems*, and *An. pedemontana* have similar ascospores with a short germ slit, but differs in the J-, apical ring and a mucilaginous sheath, while *An. aquatica* from aquatic habitats has larger ascomata, asci and ascospores (Lu and Hyde 2000). In having immersed ascomata under a clypeus, J+ apical ring and ascospores with a short germ slit, our new collection is similar to *Hypocopra* than *Stromatoneurospora*. The LSU, ITS and *rpb*2 sequences of *Hy. zeae* are similar to *Hy. rostrata* NRRL 66178 (99%, 1/911 gaps), *Podosordaria muli* WSP 167 (89%, 19/585 gaps) and *S. phoenix* BCC82040 (92%, 0/705 gaps) respectively. Single and combined gene phylogenies show that our new collection clusters with *Stromatoneurospora phoenix*. There are few *Hypocopra* species and only *Stromatoneurospora phoenix* with molecular data (Becker et al. 2020). Therefore, the phylogenetic placement could be changed with the addition of new sequence data. Giving priority to morphology, we tentatively place our collection as a *Hypocopra* species. In addition, there are no *Hypocopra* species that have been described from plant substrates. Further collections are required in view of the uncertain taxonomic placement of the *Hy. zeae*.

Nemania Gray, Nat. Arr. Brit. Pl. (London) 1: 516 (1821)

Notes: *Nemania* is a species-rich genus (typified by *Ne. serpens*) including endophytes, saprobes and pathogens (U'Ren et al. 2016; Daranagama et al. 2018; Hyde et al. 2020b). *Nemania* species are characterised by stromata not associated with bark rupturing structures, lacking KOH-extractable pigments and finely papillate ostioles, unitunicate, cylindrical asci, and ascospores with a germ slit in their sexual morph, and geniculosporium-like asexual morph (Daranagama et al. 2018). Currently, there are 55 species and 16 with molecular data (Hyde et al. 2020b; Tibpromma et al. 2021).

Nemania longipedicellata Samarak. & K.D. Hyde, ***sp. nov***.

Index Fungorum number: IF558730; *Facesoffungi number*: FoF 10209; Fig. 28

Etymology: The specific epithet reflects the long pedicellate asci.

Holotype: MFLU 18-0819

Saprobic on dead branch of *Camellia sinensis*. **Sexual morph**: *Stromata* 480–720 × 620–870 µm ($\bar{x}$ = 592 × 768 µm, n = 6), superficial or semi-immersed, single or rarely aggregated, mammiformis, dark brown to black, with conspicuous ascomatal mounds, carbonaceous. *Ascomata* 590–670 × 550–660 µm ($\bar{x}$ = 628 × 608 µm, n = 5), in cross-section globose to sphaerical or sometimes ovoid. *Ostioles* surrounding area slightly flattened, shiny black, conspicuous. *Paraphyses* 1.9–2.8 µm ($\bar{x}$ = 2.3 µm, n = 15) wide, long, cylindrical, septate, constricted at septum, smooth-walled. *Asci* 72–125 × 5.2–8.2 µm ($\bar{x}$ = 93.6 × 6.3 µm, n = 20), spore-bearing part 50–57.5 µm ($\bar{x}$ = 53.8 µm, n = 15), 8-spored, unitunicate, cylindrical, pedicellate, with a 1.5–2.3 × 1.8–2.4 µm ($\bar{x}$ = 2 × 2.2 µm, n = 10), inverted, hat-shaped, apical ring, J+ in Melzer's reagent, apex rounded. *Ascospores* 6.8–9.3 × 3.6–4.7 µm ($\bar{x}$ = 7.8 × 4.1 µm, n = 30), L/W 1.9, uniseriate, hyaline, guttulate when immature, turning pale brown and dark brown when mature, oblong to narrowly ellipsoid, symmetrical to slightly inequilateral, aseptate, smooth-walled, with a straight germ slit along the entire spore length. **Asexual morph**: Undetermined.

Material examined: Thailand, Chiang Mai Province, Tambon Pa Pae, Amphoe Mae Taeng, on dead branch of *Camellia sinensis* (*Theaceae*), 1 September 2017, M.C. Samarakoon, SAMC045 (MFLU 18-0819, **holotype**), (HKAS 102329, **isotype**).

Notes: *Nemania longipedicellata* differs from closely related species with mammiform stromata such as *Ne. kauaiensis*, *Ne. parapauzarii*, and *Ne. thailandensis* in having long pedicellate asci and smaller ascospores (Rogers and Ju 2002; Rogers et al. 2008). *Nemania carbonacea* has long, sterile, hyphoid based asci (ca. 80 vs 45–60µm), and larger ascospores (11.5–15.5 × 5–6.5 vs 6.8–9.3 × 3.6–4.7 µm) compared to *Ne. longipedicellata* (Pouzar 1985). *Nemania pouzarii* ascospores have hyaline, cellular remnants, whereas *Ne. longipedicellata* lacks cellular remnants. *Nemania longipedicellata* sequences are similar to *Ne. macrocarpa* WSP 265 (ITS 91%, 5/378 gaps; *tub*2 80%, 24/488 gaps), *Ne. viridis* MFLU 17-2600 (ITS 90%, 10/393 gaps), *Ne. maritima* HAST 89120401 (*rpb*2 84%, 0/926 gaps) and *Ne. abortiva* BISH 467 (*tub*2 80%, 19/472 gaps). The combined gene phylogeny resulted in *Ne. longipedicellata* as a distinct clade with 99% statistical support. We introduce our collection as a new species among other mammiform stromata forming *Nemania* species based on morphology and phylogeny.

Nemania delonicis Samarak. & K.D. Hyde, ***sp. nov***.

Index Fungorum number: IF558731; *Facesoffungi number*: FoF 10210; Fig. 29

Etymology: The specific epithet reflects the host genus *Delonix*.

Holotype: MFLU 19-2124

Saprobic on dead pod of *Delonix regia*. **Sexual morph**: *Stromata* 5.5–20.4 × 2.5–5.1 × 0.42–0.5 mm ($\bar{x}$ = 15.7 × 3.7 × 0.45 mm, n = 5), superficial, effuse, irregularly elongated, surface greyish black to dull black, incrusted with superficial, carbonaceous tissue immediately beneath the surface, tissue beneath the ascomatal layers inconspicuous, dark brown to black, the tissue between perithecia soft, whitish to brownish. *Ascomata* 270–420 × 325–500 µm ($\bar{x}$ = 354 × 412 µm, n = 8), in cross-section subglobose to laterally flattened, depressed-sphaerical toward margins. *Ostioles* centric,papillate, black, obtusely conical to hemisphaerical. *Paraphyses* 3–7 µm ($\bar{x}$ = 5.3 µm, n = 10) wide, wider at the base, long, cylindrical, septate, smooth-walled, constricted at septa. *Asci* 80–100 × 7.5–8.6 µm ($\bar{x}$ = 92 × 8.2 µm, n = 20), 8-spored, unitunicate, cylindrical, with a short pedicel, with a 2.9–3.4 × 1.8–2.4 µm ($\bar{x}$ = 3.2 × 2.2 µm, n = 10), inverted, hat-shaped, apical ring, J+ in Melzer's reagent, apex rounded. *Ascospores* 10.8–13 × 4.5–5.5 µm ($\bar{x}$ = 11.8 × 5.2 µm, n = 35), L/W 2.3, uniseriate or slightly overlapping, greyish when immature, light to medium brown when mature, ellipsoid-equilateral to oblong, symmetrical to slightly inequilateral, aseptate, smooth-walled, with a straight central germ slit along much less than spore-length. **Asexual morph**: Undetermined.

Material examined: Thailand, Phrae Province, on dead pod of *Delonix regia* (*Fabaceae*), 24 January 2019, M.C. Samarakoon, SAMC200 (MFLU 19-2124, **holotype**), (HKAS 106981, **isotype**).

Notes: *Nemania aenea*, *Ne. beaumontii*, *Ne. caries*, *Ne. chestersii*, *Ne. fusoidispora*, *Ne. plumbea*, *Ne. serpens* and our new collection share effuse, confluent stroma on the host surface (Ju and Rogers 2002). Except for *Ne. delonicis*, all above species have long stipitate asci (Granmo et al. 1999; Ju et al. 2005; Tang et al. 2007; Ariyawansa et al. 2015; Fournier et al. 2018). *Nemania serpens* has long pedicellate asci (135–170 µm) with a J-, apical ring in Melzer's reagent, whereas *Ne. delonicis* has short (80–100 µm) asci with a J+, apical ring. Sequences of *Ne. delonicis* are similar to *Ne. serpens* HAST 235 (ITS 87%, 15/316 gaps; *tub*2 83%, 51/769 gaps; *rpb*2 93%, 0/985 gaps), *Ne. yunnanensis* KUMCC 20-0267 (ITS 94%; 2/210 gaps), *Ne. beaumontii* HAST 405 (tub2 83%, 37/566 gaps) and *Euepixylon sphaeriostomum* JDR 261 (*tub*2 78%, 59/771 gaps; *rpb*2 89%, 2/985 gaps). Phylogenetic analyses of single and combined gene phylogeny show that *Ne. delonicis* is sister to *Ne. serpens* with 100%/1.00 PP statistical support. Based on distinct morphology and phylogeny, we introduce *Ne. delonicis* as a new species.

Nemania paraphysata Samarak. & K.D. Hyde, ***sp. nov***.

Index Fungorum number: IF558732; *Facesoffungi number*: FoF 10211; Fig. 30

Etymology: The specific epithet reflects the distinct trabaculae-like paraphyses.

Holotype: MFLU 19-2121

Saprobic on decayed wood. **Sexual morph**: *Stromata* 880–1100 × 850–1400 µm ($\bar{x}$ = 992 × 1099 µm, n = 5), superficial or semi-immersed, solitary or rarely aggregated, mammiform with broad base, surface blackish brown, with conspicuous ascomatal mounds, carbonaceous tissue immediately beneath the surface and between ascomata, tissue beneath the ascomatal layers inconspicuous, dark brown to black. *Ascomata* 720–850 × 625–870 µm ($\bar{x}$ = 770 × 751 µm, n = 5), in cross-section globose to sphaerical or sometimes ovoid. *Ostioles* centric or eccentric, surrounding area slightly flattened, shiny, black, conspicuous. *Paraphyses* two types, 1) 1.2–2 µm ($\bar{x}$ = 1.6 µm, n = 25) wide, long, numerous, cylindrical, aseptate, trabaculate, smooth-walled; 2) 2.8–4 µm ($\bar{x}$ = 3.5 µm, n = 20) wide, septate, branched, smooth-walled, constricted at septa. *Asci* 65–105 × 7–10 µm ($\bar{x}$ = 88.5 × 8.6 µm, n = 20), 8-spored, unitunicate, cylindrical, short pedicellate, with a 1.7–2.5 × 2.4–3.3 µm ($\bar{x}$ = 2 × 2.8 µm, n = 8), inverted, hat-shaped, apical ring, J+ in Melzer's reagent, apex rounded. *Ascospores* 9.5–14.5 × 5–7.5 µm ($\bar{x}$ = 12.5 × 6.2 µm, n = 35), L/W 2.02, uniseriate, hyaline, guttulate when immature, turning pale brown and dark brown when mature, oblong to narrowly ellipsoid, often with a knob at base, symmetrical to slightly inequilateral, aseptate, smooth-walled, with a straight germ slit along the entire spore length, surrounded by a 0.9–1.9 µm ($\bar{x}$ = 1.4 µm, n = 10) thick, mucilaginous sheath. **Asexual morph**: Undetermined.

Material examined: Thailand, Lampang Province, Wang Nuea, on decayed wood, 7 December 2018, M.C. Samarakoon, SAMC188 (MFLU 19-2121, **holotype**), (HKAS 106978, **isotype**).

Notes: The macro morphology of our collection is similar to *Ne. pouzarii* in having mammiform stromata with a broad base (Rogers and Ju 2002). *Nemania pouzarii* has long asci with a long stipe, while *Ne. paraphysata* has short asci without a stipe (110–120 µm vs 65–105 µm). *Nemania paraphysata* has two types of paraphyses, and one of the types is trabeculae-like. The ITS sequence of *Ne. paraphysata* is similar to *Ne. pouzarii* ATCC 2612 (91%, 12/475 gaps) and *Ne. macrocarpa* CBS 109567 (88%, 22/362 gaps), while *rpb*2 is similar to *Ne. maritima* JF04055 (90%, 0/808 gaps) and *Ne. macrocarpa* WSP 265 (83%, 6/1046 gaps). The phylogenetic analyses show that *Ne. paraphysata* clusters basal to *Ne. pouzarii* and *Ne. thailandica* with 100% statistical support. With the presence of trabeculae-like paraphyses and ascospores with a knob at the base, *Ne. paraphysata* is introduced as a new species.

Nemania thailandensis Samarak. & K.D. Hyde, ***sp. nov***.

Index Fungorum number: IF558733; *Facesoffungi number*: FoF 10212; Fig. 31

Etymology: The specific epithet reflects Thailand, where the species was first collected.

Holotype: MFLU 19-2117

Saprobic on decayed stem. **Sexual morph**: *Stromata* 560–740 × 900–1250 µm ($\bar{x}$ = 653 × 1077 µm, n = 5), superficial or semi-immersed, solitary or aggregated, mammiform with broad base, surface blackish brown, with conspicuous ascomatal mounds, carbonaceous tissue immediately beneath the

surface and between ascomata, tissue beneath the ascomatal layers inconspicuous, dark brown to black. *Ascomata* 410–590 × 625–690 µm ($\bar{x}$ = 504 × 657 µm, n = 5), in cross-section globose to sphaerical or sometimes ovoid. *Ostioles* centric or eccentric, surrounding area slightly flattened, shiny, black, conspicuous. *Paraphyses* 2.5–4 µm ($\bar{x}$ = 3.3 µm, n = 15) wide, long, cylindrical, septate, smooth-walled, constricted at septa. *Asci* 80–110 × 7.5–9.5 µm ($\bar{x}$ = 95 × 8.3 µm, n = 20), 8-spored, unitunicate, cylindrical, short pedicellate, with a 2–3 × 2.2–3.6 µm ($\bar{x}$ = 2.5 × 2.4 µm, n = 10), inverted, hat-shaped, apical ring, J+ in Melzer's reagent, apex rounded. *Ascospores* 10.5–13 × 5.5–7.2 µm ($\bar{x}$ = 11.7 × 6.3 µm, n = 35), L/W 1.86, uniseriate, hyaline, guttulate when immature, turning pale brown to dark brown at maturity, oblong to narrowly ellipsoid, symmetrical to slightly inequilateral, aseptate, smooth-walled, with a straight germ slit along the entire spore length. **Asexual morph**: Undetermined.

Material examined: Thailand, Phayao Province, Phu Sang, on dead stem, 4 December 2018, M.C. Samarakoon, SAMC181 (MFLU 19-2117, **holotype**), (HKAS 106974, **isotype**). *ibid*. Lampang, Wang Nuea District, on dead branch, 7 December 2018, M.C. Samarakoon, SAMC189 (MFLU 19-2122, HKAS 106979 **paratypes**).

Notes: Our two collections share similar morphology and are related to *Ne. pouzarii* and *Ne. paraphysata* in phylogeny. *Nemania thailandensis* has wider stromata, shorter and thicker asci (80–110 × 7.5–9.5 vs 140–185 × 6.5–7 µm), and shorter, sterile, hyphoid ascal base (15–25 vs 60–90 µm) compared to *Ne. carbonacea* (Pouzar 1985; Granmo et al. 1999). *Nemania paraphysata* differs in having trabeculae-like paraphyses and ascospores with a thin mucilaginous sheath around ascospores, which are lacking in *Ne. thailandensis* (this study). Sequences of *Ne. thailandensis* are similar to *Ne. pouzarii* ATCC 2612 (ITS 93%, 10/481 gaps), *Ne. maritima* JF 04055 (ITS 92%, 7/424 gaps; *rpb*2 91%, 2/804 gaps), *Ne. macrocarpa* WSP 265 (ITS 86%, 19/367 gaps; *rpb*2 84%, 12/1034 gaps; *tub*2 83%, 23/668 gaps) and *Ne. primolutea* HAST 91102001 (*rpb*2 84%, 8/1032 gaps). Multigene phylogeny in our study established *Ne. thailandensis* as a distinct clade to *Ne. paraphysata* and *Ne. pouzarii* with 100%/1.00 PP statistical support.

Rosellinia De Not., G. bot. ital. 1(1): 334 (1844)

Notes: *Rosellinia* and *Dematophora* share similar morphology of stromata, asci and ascospores, but differ in the geniculosporium-like asexual morph in *Rosellinia* and dematophora-like asexual morph in *Dematophora* (Petrini 2013; Wittstein et al. 2020). Most species have inconspicuous, small stromata, which can easily be missed in the field, and therefore many of the species described are represented by few collections (Petrini 2013).

Rosellinia markhamiae Sivan., Trans. Br. mycol. Soc. 65(1): 19 (1975)

Index Fungorum number: IF322875; *Facesoffungi number*: FoF 10213; Fig. 32

Saprobic on dead branch. **Sexual morph**: *Subiculum* woolly, dark brown, web-like, embedding the lower parts of the stromata. *Stromata* 570–750 × 750–870 µm ($\bar{x}$ = 657 × 819 µm, n = 6), superficial, solitary or aggregated, mammiform, dark brown to black carbonaceous. *Ectostroma* thick, hard and brittle, black, reduced to the base. *Ascomata* 550–710 × 570–770 µm ($\bar{x}$ = 624 × 685 µm, n = 8), in cross-section globose, immersed in stromal tissue, detached from the stromal wall. *Ostioles* papillate, distinctive, surrounding area slightly flattened, shiny, black, conspicuous. *Paraphyses* 3.2–7.4 µm ($\bar{x}$ = 5.2 µm, n = 15) wide, long, cylindrical, septate, branched, constricted at septa, guttulate. *Asci* 190–265 × 38–57 µm ($\bar{x}$ = 221 × 47 µm, n = 15), 8-spored, unitunicate, cylindrical, short pedicellate, with a 15.3–26.5 × 7.5–10 µm ($\bar{x}$ = 20.2 × 9 µm, n = 10), inverted, hat-shaped, apical ring, when immature, with a 15–18.4 × 9.2–13 µm ($\bar{x}$ = 16.5 × 11.5 µm, n = 6), barrel-shaped, apical ring, when mature, J+ in Melzer's reagent, apex rounded. *Ascospores* 70–105 × 11.5–15 µm ($\bar{x}$ = 86.8 × 13 µm, n = 30), L/W 6.7, overlapping biseriate, hyaline, guttulate when immature, turning yellowish brown to dark brown when mature, asymmetrically ellipsoidal, slightly pinched, ends blunt, aseptate, surrounded at each end by mucilagenous caps, with a straight germ slit along the entire spore length. **Asexual morph**: Undetermined.

Material examined: Thailand, Nan Province, Pua, on dead branch, 29 January 2019, M.C. Samarakoon, SAMC217 (MFLU 19-2137, HKAS 106994).

Notes: Our species is closely related to the *Rosellinia emergens* group as described in Petrini (2013), which consists of ascopores with L/W ≥ 4 and stromata generally < 1 mm × < 1 mm. A morphological comparison of *Ro. capetribulensis*, *Ro. emergens*, *Ro. formosana*, *Ro. longispora*, *Ro. markhamiae*, *Ro. megalosperma* and *Ro. megalospora* clearly placed our specimen in *Ro. markhamiae* (Sivanesan 1975; Bahl et al. 2005; Petrini 2013; Xie et al. 2019). All the above species share a germ slit along the entire ascospore length and are surrounded at each end by slimy caps, except for *Ro. capetribulensis*, which has a straight germ slit and thin mucilaginous sheath and lacks slimy caps. Our specimen is similar to *Ro. markhamiae*, which was described on *Markhamia hildebrandtii* from Tanzania in having overlapping ascospore sizes (70–105 × 11.5–15 µm vs 72–135 × 9–14 µm) and J+ apical ring (15–18.4 × 9.2–13 µm vs 13–15 × 7–11 µm). Here we introduce a new geographical record and the phylogenetic placement of *Ro. markhamiae* from Thailand, although further collections may show this to be a distinct species.

Rosellinia britannica L.E. Petrini, Petrini & S.M. Francis, Sydowia 41: 265 (1989)

Index Fungorum number: IF125863; *Facesoffungi number*: FoF 10214; Fig. 33

Saprobic on dead aerial branch of *Hedera helix*. **Sexual morph**: *Subiculum* woolly, dark brown, web-like, embedding the lower parts of the stromata. *Stromata* 765–940 × 795–1130 µm ($\bar{x}$ = 863 × 965 µm, n = 8), superficial, scattered or densely gregarious, subglobose to cupulate, with conspicuous ascomatal mounds, dark brown to black, carbonaceous, containing a single perithecium. *Ascomata* 590–760 × 575–840 µm ($\bar{x}$ = 671 × 707 µm, n = 8), immersed in stromal tissue, detached from the stromal wall, in cross-section globose. *Ostioles* papillate, surrounding area slightly flattened, black. *Paraphyses* 2.8–5.3 µm ($\bar{x}$ = 3.8 µm, n = 15) wide, wider at the base, long, septate, constricted at the septa, guttulate. *Asci* 160–230 × 7–11 µm ($\bar{x}$ = 196 × 8.9 µm, n = 15), spore-bearing part 130–170 µm ($\bar{x}$ = 149 µm, n = 10), 8-spored, unitunicate, cylindrical, long pedicellate, with a 7–11 × 3.4–4 µm ($\bar{x}$ = 8.8 × 3.7 µm, n = 10), inverted, hat-shaped, apical ring, J+ in Melzer's reagent, apex rounded. *Ascospores* 17–25 × 6.5–9 µm ($\bar{x}$ = 20.8 × 7.7 µm, n = 35), L/W 2.7, uniseriate, hyaline, guttulate

when immature, turning yellowish brown to dark brown when mature, with a large central guttule, aseptate, asymmetrically ellipsoidal with blunt ends, surrounded at each end by mucilagenous caps, with a straight germ slit along the entire spore length. **Asexual morph**: Undetermined.

Material examined: Italy, Province of Forlì-Cesena, Pieve di Rivoschio, on dead aerial branch of *Hedera helix* (*Araliaceae*), 3 May 2017, E. Camporesi, IT3213A (MFLU 17-0987, HKAS 102382). *ibid*. Near Meldola, on dead aerial branch of *Hedera helix* (*Araliaceae*), 12 January 2017, E. Camporesi, IT3213 (MFLU 17-0302, HKAS 102349).

Notes: Our collections are similar to *Rosellinia britannica* in size and shape of the stromata (765–940 × 795–1130 µm vs 600–1000 × 700–1400 µm), ascomata (590–760 × 575–840 µm vs 500–875 × 575–975 µm), asci (160–230 × 7–11 µm vs182–265 × 7–20 µm) and ascospores (17–25 × 6.5–9 µm vs 19.8–27.5 × 5.2–10.4 µm) with ends surrounded by slimy sheaths and a straight germ slit along the entire ascospore length. *Rosellinia mammiformis* differs from *Ro. britannica* in having asci with the smallest spore bearing part length, ascospores and ascal apical ring sizes (Petrini et al. 1989; Petrini 2013). However, it is not clear if the mucilaginous sheath on the flat side of ascospores in mature ascospores is present in our collection, as mentioned in *Ro. britannica*. Petrini (2013) opined that *Ro. britannica* is a synonym for *Ro. marcuccina*, but it is still a separate species in public databases.

Xylariales*, genera *incertae sedis

Notes: Hyde et al. (2020b) accepted 52 genera under *Xylariales* genera *incertae sedis* due to lack of molecular data and uncertainty of sexual asexual morphologies and most of them having only single collections. Three other genera, namely *Catenuliconidia*, *Haploanthostomella* and *Xenoanthostomella,* were added in recent studies (Hyde et al. 2020a; Yuan et al. 2020; Konta et al. 2021). In our study, we have revised the taxonomy and phylogeny of selected *incertae sedis* species, and accept 63 namely; *Adomia*, *Alloanthostomella*, *Appendixia*, *Anthostomella*, *Anungitea*, *Ascotrichella*, *Basifimbria*, *Biporispora*, *Basiseptospora*, *Calceomyces*, *Castellaniomyces*, *Catenuliconidia*, *Chaenocarpus*, *Circinotrichum*, *Cryptostroma*, *Cyanopulvis*, *Diamantinia*, *Gigantospora*, *Guestia*, *Gyrothrix*, *Hadrotrichum*, *Haploanthostomella*, *Idriellopsis*, *Kirstenboschia*, *Lanceispora*, *Lasiobertia*, *Leptomassaria*, *Magnostiolata*, *Melanographium*, *Neoanthostomella*, *Neoidriella*, *Nigropunctata*, *Nipicola*, *Nummauxia*, *Occultitheca*, *Ophiorosellinia*, *Palmicola*, *Pandanicola*, *Paraidriella*, *Paramphisphaeria*, *Paraphysalospora*, *Paucithecium*, *Pidoplitchkoviella*, *Polyancora*, *Polyscytalum*, *Poroleprieuria*, *Poroisariopsis*, *Pseudoanthostomella*, *Pseudophloeospora*, *Pulmosphaeria*, *Pyriformiascoma*, *Roselymyces*, *Sabalicola*, *Spirodecospora*, *Sporidesmina*, *Striatodecospora*, *Surculiseries*, *Synnemadiella*, *Tristratiperidium*, *Xenoanthostomella*, *Xylocrea, Xylotumulus* and *Yuea*.

Anthostomella Sacc., Atti Soc. Veneto-Trent. Sci. Nat., Padova, Sér. 4 4: 84 (1875)

Notes: *Anthostomella* is a species-rich, polyphyletic genus, which is characterised by immersed ascomata beneath a dark clypeus, periphysate ostiolar canals, unitunicate, cylindrical asci with or without a J+, apical ring and mostly brown, aseptate ascospores with or without a dwarf cell or appendages at the ends and presence or absence of a germ slit (Lu and Hyde 2000; Daranagama et al. 2015).

Saccardo (1875) introduced *Anthostomella* with three species; *An. limitata*, *An. tomicoides* and *An. perfidiosa* without designating a type. Different studies have accepted *An. limitata* (Eriksson 1966) and *An. tomicoides* (Francis 1975; Lu and Hyde 2000) as the generic type, emphasizing the generic description provided by Saccardo (1875). Eriksson (1966) interpreted Saccardo (1875)'s description and prioritised the non-appendiculate over appendiculate ascospores. Only *An. limitata* has non-appendiculate ascospores from the original three collections and is accepted as the generic type (Eriksson 1966). Francis (1975) argued that the original generic description is based on both appendiculate and non-appendiculate ascospore morphologies and the absence of clypeus in *An. limitata* is not well-suited to *Anthostomella*. However, *An. limitata* has a blackened clypeus (Lu and Hyde 2000). Following Lu and Hyde (2000) with the lectotype of *An. tomicoides*, Daranagama et al. (2015) accepted *An. tomicoides* as the generic type. Furthermore, Daranagama et al. (2015) provided a reference specimen for appendiculate ascospore bearing *An. formosa* and the clade accepted as *Anthostomella* sensu stricto.

In our phylogeny, there are two distinct *Anthostomella* clades, which are named as "*Anthostomella helicofissa* clade" (Clade Xy24) and "*Anthostomella formosa* clade" (Clade Xy25). Based on morphology and phylogeny, Clade Xy24 consist with *An. helicofissa*, "*Neo. viticola*", "*Neo. ficl*" (Daranagama et al. 2016a; Tennakoon et al. 2021) and *An. lamiacearum* (this study) (Fig. 1) in *Xylariales*. Species in this clade are characterised by inconspicuous, immersed, clypeate ascomata, periphysate ostiolar canals, cylindrical, short pedicellate asci with discoid, J+, apical rings, and brown, ellipsoidal, inequilateral, aseptate ascospores with tapered ends and diagonal or crossed diagonal germ slits. The morphology of taxa in this clade is similar to *An. limitata*(Francis 1975). Re-examination of the holotypes of *An. helicofissa,* "*Neo. viticola*" and "*Neo. fici*" amended and confirmed the morphological affinity to *An. limitata* (Table 4). Anthostomella-like taxa are commonly found on monocotyledons, but species clustering to Clade Xy24 are from dicotyledons. *Anthostomella limitata* has been described on different hosts with majority on dicotyledons, namely *Callistemon* sp., *Conium maculatum*, *Euphorbia cyparissias*, *Galium mollugo*, *Geranium* sp., *Kigelia pinnata*, *Oenanthe crocata*, *Rosa* sp., *Rubus* sp., *Sorbus aucuparia*, *Vitis viniferae* and undetermined *Umbeliferae* sp., and a few monocotyledons, namely *Carex acutiformis*, *C. paniculate*, *C. riparia*, *Chamaerops humilis*, *Daemonorops oxycarpa*, *Iris pseudacorus*, *Typha latifolia* in Argentina, Brunei, Finland, Germany, Italy, Portugal and UK (Francis 1975; Lu and Hyde 2000). Probably, *An. limitata* belongs to Clade Xy24 "*Anthostomella helicofissa* clade" based on morphology and host distribution. In addition, *An. xuanenesis* shares similar morphology to Clade Xy24 in having inconspicuous, immersed ascomata, discoid, J+ apical rings and ascospores with diagonal or crossed diagonal germ slit (Taylor and Hyde 2003).

The previously accepted *Anthostomella* sensu stricto clade in Daranagama et al. (2015) is therefore uncertain. Anthostomella-like, appendiculate ascospores are now accepted in different families as a polyphyletic character (e.g. *Entosordaria*, *Occultitheca*, *Pyriformiascoma*). Therefore, we treated Clade Xy25 as the "*Anthostomella formosa* clade".

Anthostomella lamiacearum Samarak. & K.D. Hyde, ***sp. nov***.

Index Fungorum number: IF558742; *Facesoffungi number*: FoF 10223; Fig. 34

Etymology: The specific epithet reflects the *Lamiaceae* host.

Holotype: MFLU 18-0101

Saprobic on dead branch of *Lamiaceae sp*. **Sexual morph**: *Ascomata* 130–180 × 105–135 µm ($\bar{x}$ = 155 × 125 µm, n = 10), immersed, raised, visible as black area, solitary or aggregated, in cross-section globose to subglobose. *Clypeus* carbonaceous, black, forming blackened areas 7.7–13.6 ($\bar{x}$ = 10.4 µm, n = 5) diam., 1.4–1.8 mm ($\bar{x}$ = 1.6 µm, n = 5) high, effuse, irregularly elongated, surface black. *Ostioles* centric or eccentric, ostiolar canal periphysate. *Peridium* 16–23 µm ($\bar{x}$ = 20 µm, n = 10) wide, with two cell layers, outer layer thick, comprising yellowish brown, thick-walled cells of *textura angularis*, inner layer thin, composed of hyaline, thin-walled cells of *textura angularis*. *Paraphyses* 2–3 µm ($\bar{x}$ = 2.6 µm, n = 15) wide, longer than the asci, numerous, filamentous, septate, branched, constricted at septa, guttulate, apically blunt. *Asci* 65–85 × 5–6.5 µm ($\bar{x}$ = 76 × 5.7 µm, n = 25), 8-spored, unitunicate, cylindrical, short pedicellate, apically rounded, with a 0.8–1.6 × 1.8–2.5 µm ($\bar{x}$ = 1.3 × 2.3 µm, n = 10), discoid, apical ring, J+ in Melzer's reagent. *Ascospores* 9–11.5 × 3–5 µm ($\bar{x}$ = 10 × 4 µm, n = 30), L/W 2.5, uniseriate, brown, inequilaterally ellipsoidal, aseptate, 1–2-guttulate, germ slit sigmoid, along the entire spore length. **Asexual morph**: Undetermined.

Material examined: Thailand, Phayao Province, Phachang Noi, Pong, on dead branch of *Lamiaceae* sp., 11 September 2017, M.C. Samarakoon, SAMC014 (MFLU 18-0101, **holotype**), (HKAS 102325, **isotype**); ex-type living culture MFLUCC 17-2668.

Notes: *Anthostomella lamiacearum* is similar to "*Neo. fici*" and "*Neo. viticola*" in having an overlapping range in the size and shape of ascomata, paraphyses, asci and ascospores. "*Neoanthostomella viticola*" has a thicker peridium (34–53 µm) as compared to "*Neo. fici*" (12–18 µm) and *An. lamiacearum* (16–23 µm) (Daranagama et al. 2016a; Tennakoon et al. 2021). Both "*Neo. fici*" and *An. lamiacearum* have sigmoid germ slits in the ascospores. However, *An. lamiacearum* has aggregated ascomata in a blackened area on the host surface, which is distinct from the other species (Daranagama et al. 2016a). The LSU sequence of *An. lamiacearum* is similar to *Xe. chromolaenae* MFLUCC 17-1484 (99%, 2/899 gaps), *Gyrothrix eucalypti* CPC 36066 (99%, 0/894 gaps) and *An. fici* MFLU 19-2765 (99%, 0/829 gaps), while the ITS sequence is similar to *An. helicofissa* MFLUCC 14-0173 (91%, 17/573 gaps), *G. eucalypti* CPC 36066 (91%, 18/581 gaps), *Calceomyces lacunosus* CBS 633.88 (89%, 16/580 gaps), *Xe. chromolaenae* MFLUCC 17-1484 (88%, 30/589 gaps) and *An. viticola* MFLUCC 16-0243 (88%, 30/538 gaps). Following the distinctive morphology and phylogeny, here we introduce *An. lamiacearum* as a new species.

Additional species placed in "Clade Xy24 "*Anthostomella helicofissa* clade"

Anthostomella helicofissa Daranag., Camporesi & K.D. Hyde, in Daranagama et al., Fungal Diversity 73: 217 (2015)

Index Fungorum number: IF809517; *Facesoffungi number*: FoF 00318

Typus: Italy, Province of Forlì-Cesena, Trivella-Predappio, on *Cornus sanguinea* (*Cornaceae*), 5 January 2014, E. Camporesi IT1627 (MFLU 14-0235, **holotype**); ex–type living culture MFLUCC 14-0173. *ibid*. 5 January 2014, E. Camporesi IT1627 (PDD, **isotype**).

Notes: See Daranagama et al. (2016a) for a detailed description. We re-examined the holotype and amended the species with peridium 12–18.5 µm ($\bar{x}$ = 16 µm, n = 5), asci 80–92 × 7.2–8.6 µm ($\bar{x}$ = 86.4 × 7.8 µm, n = 10), with a 0.9–1.4 × 2.1–2.7 µm ($\bar{x}$ = 1.2 × 2.4 µm, n = 6), discoid, apical ring, J+ in Melzer's reagent, and ascospores 9.5–13.5 × 4–5 µm ($\bar{x}$ = 11.3 × 4.5 µm, n = 15), L/W 2.5. We regenerated the ITS and LSU sequences, and phylogeny shows that *An. helicofissa* clusters with Clade Xy24.

"*Neoanthostomella fici*"Tennakoon, C.H. Kuo & K.D. Hyde, in Tennakoon et al., Fungal Divers. (2021)

Index Fungorum number: IF555757; *Facesoffungi number*: FoF 09379

Typus: Taiwan, Chiayi, Ali Shan Mountain, Fanlu Township area, Dahu forest, dead leaves of *Ficus ampelas* (*Moraceae*), 28 July 2019, D.S. Tennakoon, GSP068 (MFLU 19-2765, **holotype**); ex-type living cultures MFLUCC 20-0165 = NCYUCC 19-0013.

Notes: See Tennakoon et al. (2021) for a detailed description. We re-examined the holotype and confirmed the presence of a discoid, apical ring, J+ in Melzer's reagent in asci and ascospores with sigmoid germ slits. Morphology and phylogeny confirm that "*Neo. fici*" is similar to "*Anthostomella helicofissa* clade".

"*Neoanthostomella viticola*" Daranag., Camporesi & K.D. Hyde, in Daranagama et al., Cryptog. Mycol. 37(4): 524 (2016)

Index Fungorum number: IF552248; *Facesoffungi number*: FoF 02392

Typus: Italy, Province of Forlì-Cesena, Trivella di Predappio, on dead aerial branch of *Vitis vinifera* (*Vitaceae*), 31 December 2014, E. Camporesi, IT 2326 (MFLU 15-0691, **holotype**), (HKAS 95066, **isotype**); ex-type living culture MFLUCC 16-0243.

Notes: See Daranagama et al. (2016a) for a detailed description. We re-examined the holotype and amended the species description including asci with a discoid, apical ring, J+ in Melzer's reagent, and sigmoid germ slit bearing ascospores. The morphology and phylogeny of the "*Neo. viticola*"is similar to the "*Anthostomella helicofissa* clade".

Magnostiolata Samarak. & K.D. Hyde, ***gen. nov***.

Index Fungorum number: IF558734; *Facesoffungi number*: FoF 10215

Etymology: The generic epithet reflects a large funnel shaped ostioles.

Saprobic on dead bamboo. **Sexual morph**: *Ascomata* immersed, visible as black spots, solitary or aggregated, in cross-section globose to subglobose with a flattened base. *Ostioles* centric, ostiolar canal periphysate, inverted funnel-shaped, filled with amorphous, hyaline cells, pointed at apex covered with a black, thick clypeus. *Peridium* with two cell layers, outer layer thick, comprising brown to dark brown, thick-walled cells of *textura angularis*, inner layer thin, composed of hyaline, thin-walled cells of *textura angularis*. *Paraphyses* long, numerous, filamentous, sinuous, septate, constricted at septa, guttulate, embedded in a gelatinous matrix. *Asci* 8-spored, unitunicate, cylindrical, short-pedicellate or sometimes apedicellate, apically rounded, with a discoid, inverted, hat-shaped, apical ring, J+ in Melzer's reagent. *Ascospores* uniseriate, brown to dark brown, aseptate, oblong to broadly ellipsoidal, pointed at distal and blunt at basal end, mostly with a large guttule, with a thick mucilaginous sheath, germ slit on ventral side, straight, along the entire spore length. **Asexual morph**: Undetermined.

Type: *Magnostiolata mucida* Samarak. & K.D. Hyde

Notes: *Magnostiolata* possesses immersed ascomata under a black clypeus, unitunicate asci with a J+, apical ring and brown, ellipsoid ascospores with a germ slit, which is similar to anthostomella-like taxa. Several anthostomella-like taxa were discovered during our study. *Magnostiolata* differs as it has funnel-shaped ostiolar canals, filled with amorphous cells and ascospores covered with a wing-shaped mucilaginous sheath. Since the *Anthstomella* generic type has not been sequenced, we followed morphological comparison to introduce our new collection as a new genus. However, with the available sequence data, the multigene phylogeny also reveals that our new specimen clusters distinctly to *Anthostomella* sensu stricto clade with poor statistical support.

Magnostiolata mucida Samarak. & K.D. Hyde, ***sp. nov***.

Index Fungorum number: IF558735; *Facesoffungi number*: FoF 10216; Fig. 35

Etymology: The specific epithet reflects the wing-shaped mucilaginous sheath around the ascospores.

Holotype: MFLU 19-2133

Saprobic on dead branch of bamboo. **Sexual morph**: *Ascomata* 300–400 × 310–360 µm ($\bar{x}$ = 350 × 328 µm, n = 6), immersed, visible as black spots, solitary or aggregated, in cross-section globose to subglobose with a flattened base. *Ostioles* centric, ostiolar canal periphysate, 125–150 × 210–255 µm ($\bar{x}$ = 135 × 230 µm, n = 6), inverted, funnel-shaped, filled with, amorphous, hyaline cells, pointed at apex covered with a black, thick clypeus. *Peridium* 35–43 µm ($\bar{x}$ = 39 µm, n = 10) wide, with two cell layers, outer layer thick, comprising brown to dark brown, thick-walled cells of *textura angularis*, inner layer thin, composed of hyaline, thin-walled cells of *textura angularis*. *Paraphyses* 2.5–6 µm ($\bar{x}$ = 4.4 µm, n = 20) wide, longer than asci, numerous, filamentous, sinuous, septate, constricted at the septa, guttulate, embedded in a gelatinous matrix. *Asci* 105–170 × 10–15 µm ($\bar{x}$ = 140 × 13 µm, n = 20), 8-spored, unitunicate, cylindrical, short-pedicellate or sometimes apedicellate, apically rounded with a 1.2–1.4 × 2.5–3 µm ($\bar{x}$ = 1.3 × 2.7 µm, n = 10), discoid, inverted, hat-shaped, apical ring, J+ in Melzer's reagent. *Ascospores* 12.5–18 × 6.5–9 µm ($\bar{x}$ = 14× 8 µm, n = 30), L/W 1.75, uniseriate, brown to dark brown, aseptate, oblong to broadly ellipsoidal, with pointed distal and blunt basal ends, mostly with a large guttule, with a 5–8.5 µm ($\bar{x}$ = 6.5 µm, n = 10) up to 15 µm wide, mucilaginous sheath, wing-shaped when immature, constricted at the polar ends, often with a hyaline appendage at the base, germ slit on ventral side of the ascospore, straight, along the entire spore length. **Asexual morph**: Undetermined.

Material examined: Thailand, Nan Province, Pua, on dead branch of bamboo (*Poaceae*), 1 January 2019, M.C. Samarakoon, SAMC213 (MFLU 19-2133 **holotype**), (HKAS 106990 **isotype**).

Notes: *Magnostiolata mucida* and *Anthostomelloides krabiensis* (MFLU 16-0543) formed two clades between *Clypeosphaeriaceae* and *Induratiaceae*, which are morphologically distinct. *Anthostomelloides krabiensis* (MFLU 16-0543) has immersed ascomata in globose cross-section, a central, papillate, periphysate ostiolar canal, asci with wedged-shaped, J+, apical rings and oblong, inequilaterally ellipsoidal ascospores with a germ slit (Tibpromma et al. 2017) and differs from *Ma. mucida*. Sequences of *Ma. mucida* are similar to *Clypeosphaeria mamillana* WU 33598 (LSU 97%, 2/876 gaps; *rpb*2 81%, 8/951 gaps), *Anthostomelloides brabeji* CBS 110128 (LSU 97%, 1/881 gaps), *Ant. krabiensis* MFLUCC 15-0678a (LSU 97%, 1/881 gaps) and *Xylaria eucalypti* CPC 36723 (ITS 87%, 34/580 gaps).

Neoanthostomella D.Q. Dai & K.D. Hyde, in Dai et al. Fungal Divers. 82(1), 1–105 (2017)

Notes: Dai et al. (2017) introduced *Neoanthostomella* with its type *Neo. pseudostromatica*. The genus is characterised by large, blackened, circular to elliptical stromata visible as pustules on the host surface, globose to subglobose, dark brown ascomata, unitunicate, cylindrical asci lacking apical rings and ellipsoid, aseptate, dark brown ascospores with mucilaginous sheath and lacking a germ slit. *Pandanicola* has aseptate, brown ascospores lacking a germ slit, which is similar to *Neoanthstomella*, but differs in having ascomata beneath a black, raised, oval spots as solitary or clustered and ascospores with polar germ pores (Hyde 1994b). "*Neoanthostomella fici*", *Neo. pseudostromatica* and"*Neo. viticola*" are extant species described on *Ficus* sp., bamboo and *Vitis vinifera* from Taiwan, Thailand, and Italy (Daranagama et al. 2016a; Dai et al. 2017; Tennakoon et al. 2021). However, the phylogeny of *Neoanthstomella* is uncertain, and the genus is not monophyletic. Therefore, we re-examined the holotypes to confirm the morphological affinities of these species (see above).

Neoanthostomella bambusicola Samarak. & K.D. Hyde, ***sp. nov***.

Index Fungorum number: IF558736; *Facesoffungi number*: FoF 10217; Fig. 36

Etymology: The specific epithet reflects the bamboo host.

Holotype: MFLU 18-0796

Saprobic on dead branch of bamboo. **Sexual morph**: *Stromata* 1.1–4.3 × 0.84–1.5 mm ($\bar{x}$ = 2.3 × 1.1 µm, n = 6), superficial, solitary or aggregated, effuse, subglobose to ellipsoid, surface black to dull black, incrusted with superficial, thick carbonaceous tissue, with yellowish brown margin. *Ascomata* 220–295 × 220–470 µm ($\bar{x}$ = 254 × 365 µm, n = 10), immersed in the stroma, 3–13 per stroma, randomly arranged, in cross-section subglobose to rounded rectangular with a flattened base. *Ostioles* centric or eccentric, ostiolar canal periphysate. *Peridium* 14–18 µm ($\bar{x}$ = 16.3 µm, n = 10) wide, easily detachable, with two cell layers, outer layer thick, comprising yellowish brown, thick-walled cells of *textura angularis*, inner layer thin, composed of hyaline, thin-walled cells of *textura angularis*. *Paraphyses* 4.5–8 µm ($\bar{x}$ = 6.5 µm, n = 15) wide, long, sparse, filamentous, septate, constricted at septa, guttulate. *Asci* 95–130 × 11.5–16 µm ($\bar{x}$ = 116 × 13.6 µm, n = 20), 8-spored, unitunicate, cylindrical, short pedicellate, with a J-, apical ring, rounded at the apex. *Ascospores* 15–19 × 5.5–7.5 µm ($\bar{x}$ = 16.9 × 6.4 µm, n = 30), L/W 2.6, overlapping uniseriate, hyaline when immature, brown when mature, inequilaterally ellipsoidal, slightly curved, aseptate, 1–2-guttulate, covered with a 2.5–3.3 µm ($\bar{x}$ = 2.8 µm, n = 5) thick mucilaginous sheath, lacking a germ slit. **Asexual morph**: Undetermined.

Material examined: Thailand, Chiang Rai Province, Mae Suai, on dead branch of bamboo (*Poaceae*), 18 August 2017, M.C. Samarakoon, SAMC098 (MFLU 18-0796, **holotype**), (HKAS 102348, **isotype**).

Notes: *Neoanthostomella bambusicola* shares similar morphology to the type *N. pseudostromatica* in having pustule-like stromata, asci with J-, apical ring in Melzer's reagent, and brown, aseptate ascospores with a thick mucilaginous sheath and lacking a germ slit (Dai et al. 2017). Our collection differs from *Neo. pseudostromatica* in having more ascomata per stroma (3–13 vs 2–5), a thick peridium (14–18 µm vs 5–10 µm), wider paraphyses (4.5–8 µm vs 2.5–4 µm) and larger ascospores (15–19 × 5.5–7.5 µm vs 11.5–15× 4–5.5 µm). *Anthostomella smilacis* has flat-based ascomata, similar to *Neo. bambusicola*, but differs in being immersed in the host, and lacking a stroma (Lu and Hyde 2000). "*Neoanthostomella fici*" and "*Neo. viticola*" have immersed ascomata with a clypeus and differ from *Neo. bambusicola* and *Neo. pseudostromatica*. The LSU sequence of *Neo. bambusicola* is similar to *Neo. pseudostromatica* MFLUCC 11-0610 (99%, 1/869 gaps), *Melanographium phoenicis* MFLUCC 18-1481 (95%, 5/869 gaps) and *Xe. chromolaenae* MFLUCC 17-1484 (94%, 9/870 gaps), while the ITS sequence is similar to *Neo. pseudostromatica* MFLU 15-1190 (99%, 0/542 gaps) and *Gyrothrix oleae* CPC 37069 (82%, 43/570 gaps). In our phylogeny, *Neo. bambusicola* clusters with *Neo. pseudostromatica* with a 100%/1.00 PP statistical support. Based on distinct morphology and phylogeny, we introduce *Neo. bambusicola* as a new species.

Nigropunctata Samarak. & K.D. Hyde, ***gen. nov.***

Index Fungorum number: IF558737; *Facesoffungi number*: FoF 10218

Etymology: The epithet reflects the ostioles as black dots on the host.

Saprobic on dead bamboo. **Sexual morph**: *Ascomata* immersed, raised, visible as black dots, solitary or aggregated, in cross-section globose to subglobose. *Ostioles* centric or eccentric, ostiolar canal periphysate, flattened at top, covered with a black, thick clypeus. *Ectostroma* yellow to brown. *Peridium* easily detached from host tissues, with two cell layers, outer layer thick, comprising brown, thick-walled cells of *textura angularis*, inner layer thin, composed of hyaline, thin-walled cells of *textura angularis*. *Paraphyses* long, numerous, filamentous, septate, rarely branched, constricted at septa, guttulate, apically blunt, embedded in a gelatinous matrix. *Asci* 8-spored, unitunicate, cylindrical, short pedicellate, apically rounded, with a discoid, or inverted, hat-shaped, apical ring, J+ in Melzer's reagent. *Ascospores* uniseriate or overlapping uniseriate, brown to dark brown, cylindrical to broadly ellipsoidal, aseptate, 1–2-guttulate, covered with a thick mucilaginous sheath or sheath lacking, germ slit on ventral side, straight, along the entire spore length. **Asexual morph**: Undetermined.

Type: *Nigropunctata bambusicola* Samarak. & K.D. Hyde

Notes: Anthostomella-like taxa are polyphyletic in *Xylariales* with diversified morphologies (Lu and Hyde 2000). Several morpho-molecular studies have introduced anthostomella-like taxa as new genera in an attempt to resolve the polyphyletic nature of *Anthostomella* (Daranagama et al. 2015; 2016a; Konta et al. 2021). Lu and Hyde (2000) emphasised that the position and morphology of ascomata, presence or absence, and shape of the J+/J-, apical ring and ascospore morphology, play a vital role in identifying *Anthostomella* species. However, the type species has not yet been designated formally (proposed *An. limitata* and *An. tomicoides*) and sequenced to provide a phylogenetic affinity (Voglmayr et al. 2018). However, based on morphology, *Nigropunctata* does not fit with either *An. limitata* and *An. tomicoides*. *Nigropunctata* species have immersed ascomata with a thick clypeus; white or yellow ectostroma, cylindrical, short pedicel, apically rounded asci with J+, discoid or inverted, hat-shaped, apical ring and cylindrical to broadly ellipsoidal, aseptate, ascospores with a germ slit, which excludes it from *Anthostomella*. In addition, all *Nigropunctata* species introduced in this study occur on dead bamboo. The multigene phylogeny also reveals that *Nigropunctata* clusters independently in *Xylariales* (Fig. 1; Clade Xy26).

Nigropunctata bambusicolaSamarak. & K.D. Hyde, ***sp. nov.***

Index Fungorum number: IF558738; *Facesoffungi number*: FoF 10219; Fig. 37

Etymology: The specific epithet reflects the bamboo host.

Holotype: MFLU 19-2145

Saprobic on dead branch of bamboo. **Sexual morph**: *Ascomata* 285–315 × 260–340 µm ($\bar{x}$ = 300 × 295 µm, n = 6), immersed, visible as black dots, surrounded by white periphery, solitary or aggregated, in cross-section globose to subglobose with a flattened base. *Ostioles* centric, ostiolar canal periphysate, flattened at top covered with black, thick clypeus. *Ectostroma* yellow. *Peridium* 10–18 µm ($\bar{x}$ = 15 µm, n = 10) wide, with two cell layers, outer layer thick, comprising brown to dark brown, thick-walled cells of *textura angularis*, inner layer thin, composed of hyaline, thin-walled cells of *textura angularis*. *Paraphyses* 3–5 µm ($\bar{x}$ = 3.8 µm, n = 20) wide, longer than the asci, numerous, filamentous, sinuous, septate, constricted at septa, guttulate, embedded in a gelatinous matrix. *Asci* 95–140 × 9.5–12.5 µm ($\bar{x}$ = 120 × 11 µm, n = 20), 8-spored, unitunicate, cylindrical, short-pedicellate or sometimes apedicellate,

apically rounded with 1.7–2 × 4–4.8 µm ($\bar{x}$ = 1.8 × 4.5 µm, n = 8), discoid, inverted hat-shaped, apical ring, J+ in Melzer's reagent. *Ascospores* 13.5–17 × 5.5–9.5 µm ($\bar{x}$ = 15 × 7 µm, n = 30), L/W 2.14, uniseriate, brown to dark brown, oblong to broadly ellipsoidal, aseptate, slightly constricted at center, guttulate, covered with a 2–6 µm ($\bar{x}$ = 4 µm, n = 10) thick, mucilaginous sheath, slightly constricted at center, germ slit on ventral side of the ascospore, straight, along the entire spore length. **Asexual morph**: Undetermined.

Material examined: Thailand, Chiang Rai Province, Amphoe Mueang Chiang Rai, on dead branch of bamboo (*Poaceae*), 15 June 2019, M.C. Samarakoon, SAMC228 (MFLU 19-2145, **holotype**), (HKAS 107002, **isotype**). *ibid*. Nan Province, Pua, on dead branch of bamboo (*Poaceae*), 29 January 2019, M.C. Samarakoon, SAMC214 (MFLU 19-2134, HKAS 106991, **paratypes**).

Notes: Two of our specimens share a close morphological similarity to *An. fragellariae*, *An. leucobasis* and *An. oblongata* in having immersed ascomata visible as black dots, cylindrical, short pedicellate asci and oblong to broadly ellipsoidal ascospores with a mucilaginous sheath (Lu and Hyde 2000). *Nigropunctata bambusicola* differs in having small ascomata, large, discoid-inverted, hat-shaped (1.7–2 × 4–4.8 µm) ascal apical rings and a thicker mucilaginous sheath (2–6 µm) compared to *An. fragellariae* (1.3–1.5 × 2.5–3 µm; 0.5 – 2.5 µm). *Anthostomella leucobasis* and *An. oblongata* have a thick peridium (20–25 and 27.5–37.5 µm) compared to *Ni. bambusicola* (10–18 µm). *Anthostomella oblongata* has asci with J-, apical ring and oblong-ellipsoidal ascospores, which differ from *Ni. bambusicola*. The LSU sequence of *Ni. bambusicola* is similar to *Melanographium phoenicis* MFLUCC 18-1481 (96%, 3/798 gaps), *Fasciatispora nypae* MFLUCC 11-0382 (93%, 16/895 gaps), *Xenoanthostomella chromolaenae* MFLUCC 17-1484 (96%, 3/797 gaps) and *Entosordaria perfidiosa* WU 35981 (94%, 8/851 gaps), while the ITS sequence is 87% (13/549 gaps) similar to *Mel. phoenicis* MFLU 18-1587. Morphology and phylogeny of the two collections identify these as separate species in *Nigropunctata*.

Nigropunctata nigrocircularisSamarak. & K.D. Hyde, ***sp. nov***.

Index Fungorum number: IF558739; *Facesoffungi number*: FoF 10220; Fig. 38

Etymology: The specific epithet reflects the black circular patch around the ostioles.

Holotype: MFLU 19-2130

Saprobic on dead branch of bamboo. **Sexual morph**: *Ascomata* 450–535 × 455–560 µm ($\bar{x}$ = 490 × 515 µm, n = 5), immersed, ostioles raised, visible as black dots, surrounded by round black patch of released spores, solitary or aggregated, in cross-section globose to subglobose. *Ostioles* centric, ostiolar canal periphysate, at top covered with black, thick-walled clypeus. *Ectostroma* yellow. *Peridium* 11–20 µm ($\bar{x}$ = 14.5 µm, n = 10) wide, easily detached from host tissues, with two cell layers, outer layer thick, comprising brown, thick-walled cells of *textura angularis*, inner layer thin, composed of hyaline, thin-walled cells of *textura angularis*. *Paraphyses* 2.5–4 µm ($\bar{x}$ = 3.4 µm, n = 20) wide, longer than the asci, numerous, filamentous, septate, rarely branched, constricted at septa, guttulate, apically blunt, embedded in a gelatinous matrix. *Asci* 125–170 × 8–10.5 µm ($\bar{x}$ = 145 × 9 µm, n = 20), 8-spored, unitunicate, cylindrical, short pedicellate, apically rounded, with 1.2–2.5 × 3.2–3.6 µm ($\bar{x}$ = 1.7 × 3.4 µm, n = 5), discoid, inverted, hat-shaped, apical ring, J+ in Melzer's reagent. *Ascospores* 12.5–19 × 5–8 µm ($\bar{x}$ = 15.5 × 6.4 µm, n = 40), L/W 2.4, uniseriate, brown to dark brown, cylindrical to broadly ellipsoidal, aseptate, 1–2-guttulate, covered with a 3–4.5 µm ($\bar{x}$ = 3.8 µm, n = 5) thick, mucilaginous sheath, germ slit on ventral side of the ascospore, straight, along the entire spore length. **Asexual morph**: Undetermined.

Material examined: Thailand, Phrae Province, on dead branch of bamboo (*Poaceae*), 24 January 2019, M.C. Samarakoon, SAMC208 (MFLU 19-2130, **holotype**), (HKAS 106987, **isotype**).

Notes: *Nigropunctata nigrocircularis* is similar to *Anthostomella oblongata*, which appears as black dots on the host. *Anthostomella fragellariae*, *An. leucobasis* and *An. oblongata* and *Ni. bambucicola* have close morphological similarity to *Ni. nigrocircularis* with cylindrical, short pedicellate asci and oblong to broadly ellipsoidal ascospores with a mucilaginous sheath (Lu and Hyde 2000). However, *Ni. nigrocircularis* has a J+, apical ring and a straight side of the ascospores covered with a thick sheath, while *An. oblongata* has J-, apical ring and concave side of the ascospores, covered with thin sheath. *Nigropunctata nigrocircularis* has large ascomata 450–535 × 455–560 µm vs 250–360 × 300–420 µm) and long asci (125–170 µm vs 100–115 µm) compared to *An. fragellariae*. The LSU sequence of *Ni. nigrocircularis* is similar to *Ni. thailandica* MFLU 19-2118 (97%, 1/949 gaps), *Ni. bambusicola* MFLU 19-2145 (96%, 2/890 gaps) and *Melanographium phoenicis* MFLUCC 18-1481 (97%, 2/857), while the ITS is similar to *Ni. bambusicola* MFLU 19-2145 (88%, 24/530 gaps) and *Mel. phoenicis* MFLU 18-1587 (86%, 23/510 gaps). In the combined gene phylogeny, *Ni. nigrocircularis* forms a distinct clade basal to *Nigropunctata* species. Based on distinct morphology and phylogeny, we introduce *Ni. nigrocircularis* as a new species.

Nigropunctata thailandicaSamarak. & K.D. Hyde, ***sp. nov***.

Index Fungorum number: IF558740; *Facesoffungi number*: FoF 10221; Fig. 39

Etymology: The specific epithet reflects of Thailand, where the species was first collected.

Holotype: MFLU 19-2118

Saprobic on dead branch of bamboo. **Sexual morph**: *Ascomata* 615–830 × 770–965 µm ($\bar{x}$ = 734 × 880 µm, n = 6), immersed, visible as black dots surrounded by yellowish brown, sunken periphery, solitary or rarely aggregated, in cross-section globose to subglobose. *Ostioles* centric ostiolar canal periphysate, at top covered with black, thick, reduced clypeus. *Ectostroma* yellowish brown. *Peridium* 10–14 µm ($\bar{x}$ = 12.4 µm, n = 8) wide, easily detachable, with two cell layers, outer layer thin, comprising brown to dark brown, cells of *textura angularis*, inner layer thin, composed of hyaline, thin-walled cells of *textura angularis*. *Paraphyses* 2.8–5.5 µm ($\bar{x}$ = 4 µm, n = 20) wide, wider at the base (up to 7.5 µm), longer than the asci, numerous, filamentous, sinuous, septate, constricted at septa, guttulate, embedded in a gelatinous matrix. *Asci* 120–155 × 11–16 µm ($\bar{x}$ = 140 × 14.2 µm, n = 15), 8-spored, unitunicate,

cylindrical, short-pedicellate, apically rounded with a 4.5–6 µm ($\bar{x}$ = 5.4 µm, n = 5) wide, J+, discoid, apical ring, initially bluing in Melzer's reagent then becoming faint or colour disappearing. *Ascospores* 15–18.5 × 7–11.5 µm ($\bar{x}$ = 17 × 9 µm, n = 25), L/W 1.8, uniseriate, brown to dark brown, oblong to broadly ellipsoidal, aseptate, guttulate, covered with a 2–4.5 µm ($\bar{x}$ = 3.4 µm, n = 10), thick mucilaginous sheath, slightly constricted at center, germ slit on ventral side of the ascospore, straight, along the entire spore length. **Asexual morph**: Undetermined.

Material examined: Thailand, Phayao Province, Phu Sang, on dead branch of bamboo (*Poaceae*), 4 December 2018, M.C. Samarakoon, SAMC182 (MFLU 19-2118, **holotype**), (HKAS 106975, **isotype**).

Notes: *Nigropunctata thailandica* has the largest ascomata (615–830 × 770–965 µm) when compared to other *Nigropunctata* species, *An. flagellariae* and *An. tenacis* (Lu and Hyde 2000). *Anthostomella tenacis* has globose ascomata with smaller asci (65–90 × 6–9 µm) and ascospores (7.5–12.5 × 5–6.5 µm) as compared to *Ni. thailandica* (120–155 × 11–16 µm; 15–18.5 × 7–11.5 µm). The LSU sequence of *Ni. thailandica* is similar to *Ni. nigrocircularis* MFLU 19-2130 (97%, 1/949 gaps), *Melanographium phoenicis* MFLUCC 18-1481 (97%, 2/872 gaps) and *Ni. bambusicola* MFLU 19-2145 (96%, 5/891 gaps), while the ITS is similar to *Ni. bambusicola* MFLU 19-2145 (89%, 21/581 gaps). *Nigropunctata thailandica* forms a distinct clade sister to *Ni. bambusicola* with medium statistical support, and here we introduce *Ni. thailandica* as a new species.

Occultitheca J.D. Rogers & Y.M. Ju, Sydowia 55(2): 359 (2003)

Notes: *Occultitheca* is a monospecific genus typified by *O. costaricensis* identified from decayed wood in Costa Rica (Rogers and Ju 2003). The genus is characterised by immersed ascomata, short pedicellate asci with J+, apical ring, and brown ascospores with hyaline dwarf cells and a straight germ slit. Rogers and Ju (2003) emphasised the large distance between the uppermost ascospore and the ascus apex as a key feature of the genus.

Occultitheca rosae Samarak., Jian K. Liu & K.D. Hyde, ***sp. nov***.

Index Fungorum number: IF558741; *Facesoffungi number*: FoF 10222; Fig. 40

Etymology: The specific epithet reflects the host genus *Rosa*.

Holotype: HKAS 102393

Saprobic on dead branch of *Rosa sp*. **Sexual morph**: *Ascomata* 360–385 × 350–420 µm ($\bar{x}$ = 370 × 385 µm, n = 10), immersed, solitary or aggregated, slightly raising host surface, in cross-section globose to subglobose. *Clypeus* carbonaceous, black, thick-walled, short, comprising dark fungal hyphae and host epidermal cells. *Ostioles* centric, ostiolar canal periphysate. *Peridium* 18–25 µm ($\bar{x}$ = 22 µm, n = 8) wide, tightly attached to the host, with two cell layers, outer layer thick, comprising yellowish brown, thick-walled cells of *textura angularis*, inner layer thin, composed of hyaline, thin-walled cells of *textura angularis*. *Paraphyses* 3–6.5 µm ($\bar{x}$ = 4.4 µm, n = 25) wide, wider at the base, longer than the asci, filamentous, septate, constricted at the septa, guttulate, embedded in gelatinous matrix. *Asci* 90–140 × 11–13 µm ($\bar{x}$ = 117 × 12 µm, n = 20), 8-spored, unitunicate, cylindrical, short pedicellate, apically rounded, with 3.5–4.5 × 2.8–3.2 µm ($\bar{x}$ = 4 × 3 µm, n = 10), rectangular to slightly obconic, apical ring, J+ in Melzer's reagent. *Ascospores* 16.5–20 × 6.5–8 µm ($\bar{x}$ = 18 × 7 µm, n = 30), L/W 2.6, uniseriate, brown, inequilaterally oblong-ellipsoidal, apical cell 15–18 µm ($\bar{x}$ = 16.7 µm, n = 25) long, usually with large guttules, sometimes covered with a thin mucilaginous sheath, large brown cell polar with a thick mucilaginous cap clearly visible when immature, germ slit on ventral side of the ascospore, straight, along the entire spore length, with a small, hyaline, rounded, basal cell, 1.5–2.2 µm ($\bar{x}$ = 1.7 µm, n = 25). **Asexual morph**: Undetermined.

Material examined: China, Guizhou, Guiyang, Tongxin, Yan Lou, on dead branch of *Rosa sp*. (*Rosaceae*), 17 June 2018, M.C. Samarakoon, SAMC162 (HKAS 102393, **holotype**), (MFLU 19-2105, **isotype**).

Notes: There are several *Anthostomella* species that have asci with a J+, apical ring, ascospores comprising a large brown cell with a straight germ slit and apical or basal hyaline dwarf cell, such as *An. foveolaris*, *An. hemileuca, An. tomicoides* and *An. unguiculata* and differ with a short distance between the uppermost ascospore and the ascus apex as a key feature of the genus (Lu and Hyde 2000; Rogers and Ju 2003). *Anthostomella tomicoides* has a very short germ slit, while *Occultitheca rosae* has a straight germ slit along the entire spore length (Lu and Hyde 2000). In addition, *An. clypeata* and *An. clypeoides* are similar to *Occultitheca rosae* in having immersed, clypeate ascomata, J+, apical ring and ascospores with a brown large and hyaline dwarf cell. However, both species lack germ slits and *An. clypeoides* has a mucilaginous sheath in their ascospores that differs from *Occultitheca rosae* (Lu and Hyde 2000; Lee and Crous 2003). Francis (1975) described *An. sabiniana* on *Pinus sabiniana* needles, which is similar to *Occultitheca rosae* in having clypeate, immersed ascomata, a J+ apical ring, inequilateral, ellipsoidal, brown ascospores with a large and thickened cap at the polar end, staright germ slit and mucilaginous sheath, and short distance between the uppermost ascospore and the ascus apex. *Occultitheca rosae* mostly has 1–2 individual ascomata, which differs from *O. costaricensis* in having 2–12 ascomata in a cluster. In addition, *O. rosae* differs from *O. costaricensis* in having ascospores with a thin mucilaginous sheath. The LSU sequence of *O. rosae* is similar to *Clypeosphaeria oleae* CPC 36779 (98%, 2/722 gaps), *Xylaria eucalypti* CPC 36723 (97%, 2/723 gaps), *Fasciatispora cocoes* MFLUCC 18-1445 (96%, 5/714 gaps) and *Barrmaelia rappazii* WU36926 (96%, 11/738 gaps). However, no molecular data is available for *Occultitheca costaricensis* and following the morphological comparison, we introduce a new *Occultitheca* species and provide a tentative phylogenetic placement for the genus.

Pseudoanthostomella Daranag., Camporesi & K.D. Hyde, in Daranagama et al., Cryptog. Mycol. 37(4): 527 (2016)

Notes: Daranagama et al. (2016a) introduced *Pseudoanthostomella*, with its type *Ps. pini-nigrae,* to accommodate anthostomella-like species. *Pseudoanthostomella* is similar to *Anthostomella* in having blackened, conical to dome-shaped, semi-immersed to immersed ascomata, which mostly solitary or rarely aggregated in small groups, while differes from *Anthostomella* in having an eccentric, periphysate, ostiolar canals, distinctly clavate asci and

ascospores with straight germ slit (Daranagama et al. 2016a). Furthermore, *Pseudoanthostomella* differs from *Neoanthostomella* in having asci with J+, apical ring and ascospores with germ slits and differs from *Alloanthostomella* in having aseptate, pigmented ascospores with germ slits. In this study, we revisited *Pseudoanthostomella* by re-examination of the holotype (Daranagama et al. 2016a).

Pseudoanthostomella pini-nigrae Daranag., Camporesi & K.D. Hyde, in Daranagama et al., Cryptog. Mycol. 37(4): 530 (2016)

Index Fungorum number: IF552250; *Facesoffungi number*: FoF 02390; Fig. 41

Saprobic on dead aerial branch of *Cytisus sp*. **Sexual morph**: *Ascomata* 235–320 × 230–305 µm ($\bar{x}$ = 275 × 255 µm, n = 10), immersed, visible as black, raised area, solitary, in cross-section globose to subglobose, with flattened top. *Clypeus* carbonaceous, black, thick-walled, short, comprising dark fungal hyphae and host epidermal cells. *Ostioles* centric or eccentric, ostiolar canal periphysate. *Peridium* 21–30 µm ($\bar{x}$ = 25.5 µm, n = 15) wide, with two cell layers, outer layer comprising yellowish brown, thick-walled cells of *textura angularis*, inner layer composed of hyaline, thin-walled cells of *textura angularis*. *Paraphyses* 2.8–4.8 µm ($\bar{x}$ = 3.7 µm, n = 20) wide, wider at the base, slightly shorter than the asci, numerous, guttulate, filamentous, septate, branched, constricted at septa, apically blunt. *Asci* 95–125 × 10–13.5 µm ($\bar{x}$ = 110 × 12 µm, n = 20), 8-spored, unitunicate, cylindrical to clavate, pedicel short or absent, apically rounded, with a 1.6–2.2 × 4.5–5.6 µm ($\bar{x}$ = 1.9 × 5 µm, n = 5), J+, discoid, inverted, hat-shaped, apical ring, bluing in Melzer's reagent. *Ascospores* 12.5–16 × 7.5–9 µm ($\bar{x}$ = 14.5 × 8.3 µm, n = 25), L/W 1.75, overlapping uniseriate, dark brown to black, broadly ellipsoidal, aseptate, 1–2-guttulate, covered with a 2–3 µm ($\bar{x}$ = 2.5 µm, n = 5) thick, mucilaginous sheath, germ slit on ventral side of the ascospore, straight, along the entire spore length. **Asexual morph**: Undetermined.

Material examined: Italy, Province of Arezzo, Casuccia di Micheli - Quota, on the dead aerial branch of *Cytisus sp*. (*Fabaceae*), 19 October 2015, Camporesi Erio, IT2652 (MFLU 15-3608, HKAS 102309); living culture MFLUCC 18-0614. UK, Hampshire, Stanstead House, on the dead leaf of a cultivated plant (phormium-like), 28 August 2017, E.B.G. Jones, GJ422-1 (MFLU 18-0877, HKAS 102306).

Notes: We studied two collections of *Ps. pini-nigrae* collected on dead aerial branches of *Cytisus sp*. and a dead leaf of a cultivated plant from Italy and the UK. Both collections possess centric or eccentric and periphysate ostiolar canals, cylindrical to clavate asci and ascospores with straight germ slit. MFLU 15-3608 (Italy) has a noticeable black patch on the host surface and centric/eccentric ostioles as compare to MFLU 18-0877 (UK), which has only a centric ostiole. However, this could be probably due to the texture of the host tissue. These two collections are similar to the holotype of *Ps. pini-nigrae* in having globose-subglobose ascomata beneath a clypeus, a two-layered peridium, 8-spored, unitunicate, cylindrical-clavate, short pedicellate asci with a discoid-inverted, hat-shaped, J+, apical ring and broadly ellipsoidal ascospores with a thick mucilaginous sheath and a straight germ slit on the ventral side of the ascospore along the entire spore length (Daranagama et al. 2016a). We re-examined holotypes of *Ps. delitescens*, *Ps. pini-nigrae*, *Ps. senecionicola* and *Ps. thailandica*.The species cluster with *Ps. pini-nigrae* and share similar characters, such as globose to subglobose ascomata; cylindrical-clavate asci with J+, apical rings and equilateral ellipsoidal ascospores with a straight germ slit along the entire spore length. The overlapping measurements are given in Table 5. However, the presence of clypeus varies from prominent to rudimentary, which may due to the host texture.

Xenoanthostomella Mapook & K.D. Hyde, in Hyde et al., Fungal Diversity 100: 235 (2020)

Notes: *Xenoanthostomella* was introduced by Hyde et al. (2020a) with the type *Xe. chromolaenae* on *Chromolaena odorata* from Thailand. The genus has immersed ascomata beneath a clypeus, cylindrical to broadly filiform asci and aseptate, broadly fusiform ascospores. Based on phylogenetic uncertainty, *Xenoanthostomella* has been accepted in *Xylariales*, genera *incertae sedis* (Hyde et al. 2020a). In our multigene phylogeny, Clade Xy23 comprises *Calceomyces*, *Ceratocladium*, *Circinotrichum*, *Gyrothrix* and *Xenoanthostomella* (Fig. 1). However, only *Calceomyces lacunosus* (CBS 633.88) has type sequences (Wendt et al. 2018). Even though *Xenoanthostomella* is morphologically similar to "*Anthostomella helicofissa* clade", we here treat it as a separate genus until further studies are undertaken.

Xenoanthostomella chromolaenae Mapook & K.D. Hyde, in Hyde et al., Fungal Diversity 100: 237 (2020)

Index Fungorum number: IF556908; *Facesoffungi number*: FoF 06796; Fig. 42

Saprobic on dead rachis of *Nephrolepis sp*. (*Nephrolepidaceae*). **Sexual morph**: *Stromata* 150–190 × 220–310 µm ($\bar{x}$ = 173 × 260 µm, n = 5), superficial, solitary or rarely aggregated, in cross-section subglobose to mammiform, with conspicuous ascomatal mounds, base somewhat applanate, carbonaceous, dark brown to black. *Ascomata* 95–137 × 145–190 µm ($\bar{x}$ = 116.5 × 168.5 µm, n = 5), in cross-section globose to subglobose. *Ostioles* centric, surrounding area slightly flattened, shiny black, conspicuous, ostiolar canal periphysate. *Paraphyses* 2.2–3.1 µm ($\bar{x}$ = 2.6 µm, n = 15) wide, long, cylindrical, septate, smooth-walled. *Asci* 64–80 × 6.4–8.5 µm ($\bar{x}$ = 71.6 × 7.2 µm, n = 20), 8-spored, unitunicate, cylindrical, short pedicellate, with a 0.5–0.8 × 1.9–2.2 µm ($\bar{x}$ = 0.6 × 2.1 µm, n = 5), discoid, apical ring, J+ in Melzer's reagent, apex rounded. *Ascospores* 9–12 × 3.4–5 µm ($\bar{x}$ = 10.4 × 4 µm, n = 30), L/W 2.6, uniseriate, hyaline, guttulate, pale brown and dark brown, oblong to narrowly ellipsoid, symmetrical to slightly inequilateral, slightly curved, aseptate, with a spiral germ slit along the entire spore length. **Asexual morph**: Undetermined.

Material examined: Thailand, Nan Province, on dead rachis of *Nephrolepis sp*. (*Nephrolepidaceae*), 4 August 2017, M.C. Samarakoon, SAMC051 (MFLU 18-0840, HKAS 102303).

Notes: Our specimenhas superficial, mammiform, stromata, whereas the holotype of *Xe. chromolaenae* has immersed clypeate stromata. We re-examined the holotype of *Xe. chromolaenae* (MFLU 20-0048) and confirmed the presence of a J+, discoid, apical ring in the asci and ascospores with a sigmoid germ slit (which were not described in the original description). Morphological comparison shows that both collections have an overlapping range in dimensions of paraphyses (2.5–4 µm vs 2.2–3.1 µm), J+, discoid, apical ring bearing asci (60–98 × 5–7.5 µm vs 64–80 × 6.4–8.5 µm) and ascospores (10.5–14 × 4–5.5 µm vs 9–12 × 3.4–5 µm) with sigmoid germ slits (Hyde et al. 2020a). However, our specimendiffers from the *Xe. chromolaenae* holotype in having superficial, stromatic, larger ascomata. The superficial and immersed stromatic character might be due to the hard surface of the rachis of *Nephrolepis* sp., while a dead

stem of *Chromolaena odorata* has a soft surface. *Anthostomella limitata*, *An. spiralis* and *An. xuanenesis* have similar cylindrical asci with J+, discoid, apical rings and ascospores with sigmoid/diagonal germ slits, but differ in having immersed ascomata under a clypeus as compare to a superficial stroma in *Xe. chromolaenae* (Francis 1975; Lu and Hyde 2000; Taylor and Hyde 2003). The LSU and ITS sequences of our specimen is identical similar to *Xe. chromolaenae* (MFLUCC 17-1484). Based on similar morphology and phylogeny, here we provide a new host record, *Nephrolepis sp.* for *Xe. chromolaenae*. If these are the same species, it would be that *Xe. chromolaenae* has jumped to the introduced weed *Chromolaena odorata* from *Nephrolepis sp.* (a fern), the latter may be its original host.

Discussion

Stromatic variation in xylarialean taxa

A stroma is an aggregation of vegetative mycelium with more or less differentiation, mainly based on the properties of the substrate or on the factors affecting growth, which cause variations in the type or amount of mycelium produced (Wehmeyer 1926; Læssøe and Spooner 1993). The formation of a stroma begins with the development and differentiation of immersed mycelium, appearing as a blackening of the substrate surface and followed by proliferation of mycelia (Wehmeyer 1926). The marginal zone comprises blackened tissues that protect the stromatic areas and provide nutrition for the developing ascomata (Wehmeyer 1926). A pseudostroma is an altered form of stromata consisting of host and fungus tissues (Læssøe and Spooner 1993) and probably is an intermediate evolutionary form between a clypeus and true stromata. Early mycologists used the position, structure, and arrangement of perithecia and stromata to distinguish the families of ascomycetous taxa (Barr 1987). It is important to discuss the varying characters of the stromata than fixed types of stroma i.e. valsoid, eutypoid (Wehmeyer 1926).

Several conspicuous stromatic genera are accommodated in the xylarialean taxa, ranging from firm, compact, external regions and an inner region of stromata composed of loosely interwoven hyphae or pseudoparenchymatous cells (Barr 1990). The texture of stromata varies from fleshy, brittle and carbonaceous to tough and woody with different sterile and fertile regions. The diverse shapes and size of the stromata can range from sessile to stalked, subglobose or globose and erumpent from the substrate or superficial. The forms are crustose, applanate or pulvinate, and sometimes effuse. The pigmentation and shape of the final stromata structure can be recognizable as the ectostroma and entostroma, or in the incorporation of substrate cells known as a pseudostroma (Barr 1990). Such stromatic features are essential for macroscopic identification of xylarialean fungi (Rogers 1979; Barr 1987).

In the family *Diatrypaceae*, extensive use is made of stromatic characters for generic segregation (Glawe and Jacobs 1987). Acero et al. (2004) grouped stromata of diatrypaceous taxa into diatrypoid, eutypoid and valsoid. However, it is emphasised that the evolutionary relationship among those stromatic characters among genera are not well-defined. The factors affecting the development of stromata, such as host species, substrate structure and environmental humidity, might be a reason for intra and interspecific stromatic variations (Rappaz 1987). However, in some xylarialean classifications, the colour of stromatic tissue between ostiolar necks or the presence or absence of a black stromatic line around individual ascomatal clusters are vital characters for species delimitation, rather than the diameter of stromata, the number of ascomata and their size (Barr 1987; Jaklitsch et al. 2014).

A clypeus is a form of modified stromatic features with stromatic tissue or melanised hyphae developing above the immersed or semi-immersed ascomata, which is shield-shaped and variable in development (Læssøe and Spooner 1993). Sometimes, several stromata are contained within a region of the substrate delimited from noninfected tissues by a blackened ventral and sometimes a dorsal zone or line (Barr 1990). Since stromatic tissues are formed from vegetative hyphae, they are considered a stable character (Barr 1990). In past studies that were published before molecular evidence, many taxa were lumped in *Anthostomella* or *Xylaria* in *Xylariales*, which were classified, based on stromatic characters, either being conspicuous (*Xylaria*) or inconspicuous (*Anthostomella*) stromata (Lu and Hyde 2000; Peršoh et al. 2009; Hsieh et al. 2010; Daranagama et al. 2018).

Even though the stromatic characters are easy to observe, they have sometimes been ignored, misinterpreted or overemphasised (Rogers 1979). The stromatic characters, such as size, shape, colour and external roughness, are sometimes highly variable and difficult to use for taxon identification (Rogers 1979). Thus, it is important to correlate other microscopic characters, such as conidial features, asci, and ascospores (Rogers 1979). Furthermore, Rogers (1979) suggested that the superficial stromatic nature of *Xylariaceae* and *Sordariaceae* probably originated from an astromatic common ancestor through similar environmental conditions. Even though there is a need to use stromatic variations for generic delimitation of some xylarialean taxa, the family level stromatic variations are more important for general identifications (Daranagama et al. 2018).

Significant aspects of micro characters

Besides the stromatic characteristics, amyloid reactions and the shape and size of the ascal apical ring are used for xylarialean taxa identification. The ascal apical ring evolved for the ejaculation of ascospores and is a character of most xylarialean taxa. Exceptions have formed in xylarialean taxa and have most likely been lost due to lifestyle adaptions. Suwannasai et al. (2012) proposed six types of apical ring, stacks of small rings (e.g. *Hypocopra*, *Poronia*), discoid or triangular (e.g. *Hypoxylon*, *Daldinia*), broad to discoid (e.g. *Biscogniauxia*), rhomboid to diamond-shaped (e.g. *Camillea*), inverted hat or urn-shaped (e.g. *Xylaria*, *Rosellinia*, *Kretzschmaria* and *Nemania*), and no visible apical ring under the light microscope (*Rhopalostroma* and *Ascotricha*). According to the reaction of the apical ring in Melzer's reagent, they are consistently iodine positive, consistently iodine-negative and vary in reaction (Suwannasai et al. 2012). The different ring types are likely to have evolved across *xylarialean* taxa and should reflect distinct genera when rings are distinct. We observed that the apical ring in some specimens stained blue with Melzer's reagent for only a short time. This may lead to misidentification in those taxa having a J-, apical ring (e.g. *Nigropunctata bambusicola*, *Pseudoanthostomella senecionicola*) when the species delimitation is based on the amyloid reaction. The amyloid reaction is constant within most taxa, but the interpretation can be problematic. However, positive reactions will continue to be a cardinal character for xylarialean taxa

in delimiting species (Rogers 1979). In addition, the ascus stipe length is also important in xylarialean taxonomy (Hsieh et al. 2010). This study introduces *Nemania longipedicellata* with a characteristically long pedicel among closely related mammiform stromata forming *Nemania* species.

The number of ascospores per ascus, colour, septation and the germ slit play a vital role in the identification of xylarialean taxa. The number of ascospores is usually eight but may vary from four to polysporous (Barr 1990). Diatrypaceous generic delimitation is determined by the number of ascospores per ascus as a key character (Barr 1990; Carmarán et al. 2006; Senwanna et al. 2017; Konta et al. 2020a).

Another important character is the germ slit, through which the germ tube emerges. It is a typical structure in *Xylariomycetidae*, but is also found in other *Sordariomycetes* families (e.g. *Auratiopycnidiellaceae*, *Ceratostomataceae*, *Coniochaetaceae*, *Lasiosphaeriaceae*) (Hyde et al. 2020b) and even some *Dothideomycetes* (e.g. *Botryosphaeriaceae*, *Venturiaceae*) (Hongsanan et al. 2021). The germ slit or germ pore of the ascospores is a constant and diagnostic feature for certain xylarialean species (Beckett 1979). Generally, if the ascospore lacks a germ slit, it appears as light (less melanised) than those having it (Suwannasai 2005). This is due to the germ slit development process linked with the pigment deposition described in Beckett (1979). The germ slits are characterised by their shape, position on the spore, orientation along the long axis of the spore, and length. We observed straight to sigmoid, full ascospore length or less, concave or convex sided germ slits from our collections during our study. Interestingly, we observed an equatorial and scattered distribution of germ pores in *Paraxylaria* as described above. The nature of the germ slit is distinct and likely to be a good character to differentiate between genera. The colour of the ascospores is generally a reflection of their habitat, as they need to be protected from UV light (Wong et al. 2019).

Generally, ascospores are brown to dark brown or hyaline, aseptate, septate or apiosporous and infrequently have a dwarf cell (Barr 1990). Ascospore appendages are important in spore dispersal (Jones and Moss 1978) and ascospores with distinct characters are likely to reflect distinct genera. More frequently, immature ascospores have cellular appendages, which can contribute to the characterization of species (Rogers 1979). Appendages in *Xylariomycetidae*, however, often occur and may not reflect generic status.

Paleomycological evidence of xylarialean taxa

Fossil remains of fungi and the taxonomic placement with extant taxa are useful for the reconstruction of past ecological conditions (van Geel and Aptroot 2006; Samarakoon et al. 2019; Saxena et al. 2021). This is one of the challenges in the divergence time estimations and the ancestral reconstructions in xylarialean taxa, as there are very few taxonomically well-placed fossil specimens. Poinar (2014) described *Xylaria antiqua* from Tertiary Dominican amber (15–20 MYA), which has close affinity to extant *X. allantoidea* and *X. grandis* in having similar shaped ascospores and longitudinal germ slits. In addition, several other fossil ascospores have been identified, which are similar to extant xylarialean taxa. Saxena et al. (2021) reviewed fossil ascospores and accepted 55 *Hypoxylonites* species, which are similar to extant *Hypoxylon* (*Hypoxylaceae*) and one *Nigrospora* (*Apiosporaceae*). van Geel and Aptroot (2006) described *Amphisphaerella dispersella* (*Coniocessiaceae*) fossil spores in the early Holocene deposits in the Netherlands with the characteristic equatorially arranged germ pores. Similarly, *Palaeoamphisphaerella pirozynskii* has been discovered from India aged to the Miocene, which is characterised by 8–10 equatorial germ pores similar to extant *Paraxylaria*. In addition, Saxena et al. (2021) accepted another two *Palaeoamphisphaerella,* namely *P. keralensis* and *P. tankensis*. However, it is important to research the integrated approach to identify taxonomically well-placed fossil xylarialean fungi for future studies (Samarakoon et al. 2019).

Evolution and ancestral character reconstruction of Xylariomycetidae

Based on selected taxon sampling, *Amphisphaeriales* and *Xylariales* diverged around 150.5 (115–180) MYA within well-supported clades during the period of rapid divergence in the Early Mesozoic. The ancestral character analysis show the earlier *Xylariomycetidae* to have evolved around 159 (124–193) MYA with ancestral ancestors with astromatic forms and hyaline, aseptate ascospores, which lacked germ slits. *Amphisphaeriales* remained mostly as astromatic forms with aseptate and hyaline ascospores and are mostly known only as asexual morphs. Therefore, the unidentified morphologies are separately denoted in the analysis. In our ancestral character reconstruction based on seven stromatic characters, the immersed or semi-immersed inconspicuous ascomata with a prominent or rudimentary carbonaceous clypeus were an ancestral character of *Xylariomycetidae*. The divergence of ascomata types into different stromatic forms and ascospore modifications mainly occurred during the Cretaceous (66–145 MYA). The hypoxyloid (100–164 MYA), pseudostroma (95–156 MYA), bipartite and applanate (72–128 MYA), xylarioid (69–119 MYA) and rosellinoid (52.5–88.5 MYA) stromata types appear to have developed mostly during the Cretaceous period. The pseudostromatic character found in some diatrypaceous evolved may have an intermediate development of the stromatic and astromatic development, which needs further characterizations to investigate unidentified sexual morphs. Brown ascospores are common in *Xylariales*, but first appeared in *Amphisphaeriaceae*, *Melogrammataceae* and *Sporocadaceae* during the early Cretaceous (94–155 MYA) (Fig. 2). The hyaline apiospores and filiform ascospores may have appeared as separate lineages basal to *Xylariaceae*. The ascospore germ slit appeared only in *Xylariales* during the Cretaceous (95–156 MYA) after the divergence of *Lopadostomataceae*.

The ancestral character state reconstruction plays an important role in a better understanding of morphological character evolution (Schmitt et al. 2009). The methodology has been used in various studies on fungi to show, lifestyles and nutritional modes (Thiyagaraja et al. 2020; 2021), morphological characterization of ascospores (Rathnayaka et al. 2021) and appressoria (Chethana et al. 2021b), and geographical and host distributions (Píchová et al. 2018; Zhu et al. 2019). Even though the xylarialean taxa are highly diversified, no study of the ancestral character state reconstruction through molecular data has been performed.

Rogers (2000) hypothesised that the aseptate ascospores with a germ slit, “truly xylariaceous” evolved from dark coloured one septate ascospores that lacked a germ slit, while passing several complex evolutionary stages. Considering the stromatic nature of *Xylariaceae* and *Sordariaceae* taxa, Rogers (1979)

suggested that these two lineages may have evolved from astromatic ancestors, probably with bicellular ascospores. This is an important initiative to develop a hypothesis of the ancestor of *Xylariomycetidae*.

It has been theoreticised that fungi may have moved from aquatic to land environments in ancient times as symbionts of plants (Krings et al. 2012; Lutzoni et al. 2018). If this was the case, the early *Ascomycota* are likely to have been endophytes in symbiosis with plants and have subsequently evolved as saprobes and pathogens or maintained two or three of these lifestyles. The wide taxonomic distribution of viaphytes, i.e. fungi that undergo an interim stage as leaf endophytes and after leaf senescence, colonize other woody substrates via hyphal growth, suggests that viaphytic dispersal may be a deeply ancestral trait (U'Ren et al. 2016; Nelson et al. 2020). There is a broader host range for endophytic lifestyle compared to saprotrophs (Whalley 1996; U'Ren et al. 2016; Nelson et al. 2020). Xylarialean taxa can be found in living, asymptomatic leaves of angiosperms, gymnosperms, and bryophytes with close phylogenetic relationships (Davis et al. 2003; U'Ren et al. 2016). Interestingly, some of the taxa that appeared on freshly fallen branches or even on branches still attached to the parent tree (Whalley 1996), may have undergone rapid lifestyle changes. This shows that xylarialean taxa evolved as astromatic forms from endophytes and diversified into stromatic forms as adaptations to different conditions. The question then arises how the endophytic species appear as saprobes. This might be a result of the endophytes emerging from spores from saprobes. Rodrigues et al. (1993) tested a high degree of genetic diversity of endophytic *X. cubensis*, isolated from leaves of the Brazilian rainforest palm *Euterpe oleracea*. This is possibly due to the spore origin of endophytes. Ju et al. (2018) described the possibility of wind-borne xylariaceous fungal spores to establish endophytic associations. Furthermore, Ju et al. (2018) mentioned the efficiency of the modern molecular techniques in tracing propagules and infections rather than using tedious cultural procedures. However, the studies on biochemical mechanisms and transition of the saprobe to endophyte are poorly researched (Promputtha et al. 2007, Zhou et al. 2018).

Rodriguez and Redman (2008) pointed out that both symbiosis and pathogens invade the host and remain dormant until favourable environmental factors. This is a vital strategy to exploit plant nutrients effectively (Davis et al. 2003). Some saprobic *Ascomycota* produce appressoria and that is evidence towards endophytic lifestyles and would also indicate that many saprobes may be host-specific (Chethana et al. 2021a,b). *Oxydothis* the early colonizers of palms, and *Linocarpon*, which are very common on degrading palm fronds, have been shown to produce appressoria (Konta et al. 2016; 2017). More endophytic taxa can be recovered from senescent leaves or decomposing leaves, wood, bark, fruits or flowers, and endophytism could be a stage to a complex lifecycle that can involve interactions with diverse host lineages (U'Ren et al. 2016). This provides evidence that endophytic fungi are the ancestral forms of saprobic nutritional modes. Xylarialean taxa however, show a wide range of host-substrate invasions of 1) living leaves and stems, often fruiting on living host material (e.g. *Anthostomella*), of 2) living stems as opportunists and rapidly and widely colonizing the host and fruiting (e.g. *Daldinia*, *Biscogniauxia*, *Camillea*, *Hypoxylon*), of 3) primarily as saprobes and then facultative parasites causing serious diseases (e.g. *Dematophora necatrix*, *Kretzschmaria clavus*, *Xylaria*), of 4) living as endophytes and often fruit on decayed material (e.g. *Nemania*, *Xylaria*), of 5) fruit on seeds and fruits with specific and discrete host-fungal relationships (e.g. *Xylaria*), of 6) invading dung (e.g. *Hypocopra*, *Podosordaria*, *Poronia*), of 7) associated with ant and termite nests, of 8) inhabiting litter and organic soils, and, of 9) damaging pathogens (e.g. *Entoleuca*, *Rosellinia*) (Rogers 2000). Voglmayr et al. (2019) emphasised the endophytic lifestyle as the primary stage of *Leptosillia* lined with ascomatal development as saprobes, while pathogenicity as the secondary evolved character.

Even though the exact ancestral state of xylarialean taxa is unclear, the stromatic nature of the taxa might have evolved for successful parasitism and saprotrophism in dry sites (Rogers 1979). Thus, the early xylarialeans were probably endophytes that formed simple anthostomella-like ascomata with small clypei on the host surface and later evolved into other stromatic forms. The rapid morphological diversifications resulted in the Cretaceous radiation of angiosperms (Rogers 2000; Phillips et al. 2019) and probably with multiple independent diversifications. Rogers (1979) suggested that *Collodiscula* was as a primitive xylarialean taxon due to its two-celled ascospores, and in having *Astrocystis* as the nearest relative (Ju and Rogers 1990). Septate to aseptate, ascospores may have evolved, which is evident from the cellular appendages in some immature ascospores in xylarialean taxa. However, an independent evolution from aseptate to septate ascospores may have occured due to rapid diversification. Another example is long, filiform, aseptate ascospores of *Linosporopsis*. Voglmayr and Beenken (2020) mentioned that *Linosporopsis* are saprobes and endophytes, but not pathogens, and have unusual ascospore morphologies borne in asci in astromatic, clypeate ascomata. Furthermore, Voglmayr and Beenken (2020) proposed that it is not surprising that independently evolved leaf-inhabiting species of various ascomycete lineages occurred.

Much work needs to be carried out on *Xylariomycetidae* as the classification is only now being resolved (Senanayake et al. 2015; Daranagama et al. 2018; Wendt et al. 2018; Konta et al. 2021). If as theoreticised above, the stromatic *Xylariomycetidae* evolved from astromatic ancestors, it would be interesting to research chemical profiles of a range of genera. The stromatic form is known to produce an array of chemical compounds that are probably useful in deterring insect predation (Becker and Stadler 2021), but what about the ancestral clypeate forms? Was there an evolution of chemicals produced in the astromatic forms as composed with those with stroma? The former would have been protected by the host plant and developed simple clypei for protection from UV light. Even though, as early predictions, the stromata development may have been related to moisture conservation, however, the stromatic forms would have needed insecticidal chemicals to prevent insect and other pest predations.

In summary, astromatic, clypeate ascomata with aseptate, hyaline ascospores lacking a germ slit may probably be the ancestral *Xylariomycetidae*, which evolved as the result of plant fungal endophytic associations. The Cretaceous period with rapid diversification of angiosperms may have affected the diversification of xylarialean fungi with several independent lineages.

Conclusion

Before molecular data, most of the xylarialean taxa were classified based on their stromatic nature e.g. anthostomelloid (with indistinct stromata), hypoxyloid (with pulvinate atromata), rosellinioid (stroma with a single ascomata) and xylarioid (with well-developed stromata). Other forms had distinct characters, e.g. *Astrocystis* (star-shaped, split ectostroma) and diatrypoid taxa were placed in *Diatrypaceae*. With the molecular data, the criteria for taxonomic classification changed from previous schemes. It revealed that we could not use a stalk-like or well-developed stromata to place all taxa in *Xylaria*. *Xylaria* is polyphyletic and contains many distinct genera, and the well-developed stromata has evolved on multiple occasions. Therefore, we should not be conservative and should

introduce higher ranks for xylarioid taxa (see Konta et al. 2020b; Maharachchikumbura et al. 2021). Similarly, taxa with poorly developed stromata with clypei or even lacking external structures should not be lumped in *Anthotomella*. Recent studies using molecular data have shown poorly develop stromata to be polyphyletic and found across *Xylariales*. The clypeus or immersed ascomata, lacking a well-developed stroma, is a primitive character and cannot be used to delimit genera without a combination of other characters, including molecular data. Furthermore, stromatic variations will not be a key character to introduce higher ranks, but the type of ring, the colour of the ascospores, and the presence or absence of the type of germ slit will be important in xylarialean taxa.

Declarations

Acknowledgements

This study was supported by the Joint Fund of the National Natural Science Foundation of China and the Karst Science Research Center of Guizhou province (Grant No. U1812401). Kevin D. Hyde thanks the Thailand Research grants entitled “Impact of climate change on fungal diversity and biogeography in the Greater Mekong Subregion” (grant no: RDG6130001), Thailand Science Research and Innovation (TSRI) grant entitled "Macrofungi diversity research from the Lancang-Mekong watershed and surrounding areas (grant no: DBG6280009), and Chaing Mai University for the award of Visiting Professor. This research work was supported by the Mushroom Research Foundation (MRF), Chiang Mai University. Timur Bulgakov was supported by the State Research Task of the Subtropical Scientific Centre of the Russian Academy of Sciences (Theme No. 0492-2021-0007). Gareth Jones is supported under the Distinguished Scientist Fellowship Program (DSFP), King Saud University, Kingdom of Saudi Arabia. The authors extend their gratitude to Hiran Ariyawansa, Eleni Gentekaki, Samantha C. Karunarathna, Thilini Chethana, Shaun Pennycook, Saranyaphat Boonmee and Dinushani A. Daranagama for their valuable suggestions. We thank the technical staff of the Center of Excellence in Fungal Research, Sornram Sukpisit, Wilawan Punyaboon and Witchuda Taliam for their invaluable assistance. Feng Yao, Asha J. Dissanayake and Ning-Guo Liu are thanked for their valuable assistance.

Conflicts of Interest: The authors declare no conflict of interest.

References

1. Acero FJ, González V, Sánchez-Ballesteros J, Rubio V, Checa J, Bills GF, Salazar O, Platas G, Peláez F (2004) Molecular phylogenetic studies on the *Diatrypaceae* based on rDNA-ITS sequences. Mycologia 96:249–259
2. Altschul SF, Gish W, Miller W, Myers EW, Lipman DJ (1990) Basic Local Alignment Search Tool. J Mol Biol 215:403–410
3. Ariyawansa HA, Hyde KD, Jayasiri SC, Buyck B, Chethana KWT, Dai DQ, Dai YC, Daranagama DA, Jayawardena RS, Lücking R, Ghobad-Nejhad M, Niskanen T, Thambugala KM, Voigt K, Zhao RL, Li GJ, Doilom M, Boonmee S, Yang ZL, Cai Q, Cui YY, Bahkali AH, Chen J, Cui BK, Chen JJ, Dayarathne MC, Dissanayake AJ, Ekanayaka AH, Hashimoto A, Hongsanan S, Jones EBG, Larsson E, Li WJ, Li QR, Liu JK, Luo ZL, Maharachchikumbura SSN, Mapook A, McKenzie EHC, Norphanphoun C, Konta S, Pang KL, Perera RH, Phookamsak R, Phukhamsakda C, Pinruan U, Randrianjohany E, Singtripop C, Tanaka K, Tian CM, Tibpromma S, Abdel-Wahab MA, Wanasinghe DN, Wijayawardene NN, Zhang JF, Zhang H, Abdel-Aziz FA, Wedin M, Westberg M, Ammirati JF, Bulgakov TS, Lima DX, Callaghan TM, Callac P, Chang CH, Coca LF, Dal Forno M, Dollhofer V, Fliegerová K, Greiner K, Griffith GW, Ho HM, Hofstetter V, Jeewon R, Kang JC, Wen TC, Kirk PM, Kytövuori I, Lawrey JD, Xing J, Li H, Liu ZY, Liu XZ, Liimatainen K, Lumbsch HT, Matsumura M, Moncada B, Nuankaew S, Parnmen S, de Azevedo Santiago ALCM, Sommai S, Song Y, de Souza CAF, de Souza-Motta CM, Su HY, Suetrong S, Wang Y, Wei SF, Wen TC, Yuan HS, Zhou LW, Réblová M, Fournier J, Camporesi E, Luangsa-ard JJ, Tasanathai K, Khonsanit A, Thanakitpipattana D, Somrithipol S, Diederich P, Millanes AM, Common RS, Stadler M, Yan JY, Li XH, Lee HW, Nguyen TTT, Lee HB, Battistin E, Marsico O, Vizzini A, Vila J, Ercole E, Eberhardt U, Simonini G, Wen HA, Chen XH (2015) Fungal diversity notes 111–252 taxonomic and phylogenetic contributions to fungal taxa. Fungal Divers 75:1–248
4. Asgari B, Zare R (2011) Contribution to the taxonomy of the genus *Coniocessia* (*Xylariales*). Mycol Prog 10:189–206
5. Bahl J (2006) Molecular evolution of three morphologically similar families in the *Xylariomycetidae* (*Apiosporaceae*, *Clypeosphaeriaceae*, *Hyponectriaceae*). The University of Hong Kong. Pokfulam Road, Hong Kong SAR
6. Bahl J, Jeewon R, Hyde KD (2005) Phylogeny of *Rosellinia capetribulensis sp. nov*. and its allies (*Xylariaceae*). Mycologia 97:1102–1110
7. Barr ME (1987) Prodromus to class Loculoascomycetes. United States of America Hamilton I. Newell, Inc, Amherst, Massachusetts
8. Barr ME (1990) Prodromus to nonlichenized, pyrenomycetous members of class Hymenoascomycetes. Mycotaxon XXXIX:43–184
9. Barr ME (1994) Notes on the *Amphisphaeriaceae* and related families. Mycotaxon 51:191–224
10. Barr ME, Rogers JD, Ju YM (1993) Revisionary studies in the *Calosphaeriaceae*. Mycotaxon 48:529–535
11. Becker K, Stadler M (2021) Recent progress in biodiversity research on the *Xylariales* and their secondary metabolism. Jpn J Antibiot 74:1–23
12. Becker K, Wongkanoun S, Wessel A, Bills GF, Stadler M, Luangsa-ard JJ (2020) Phylogenetic and chemotaxonomic studies confirm the affinities of *Stromatoneurospora phoenix* to the coprophilous *Xylariaceae*. J Fungi 6:144
13. Beckett A (1979) Ultrastructure and development of the ascospore germ slit in *Xylaria longipes*. Trans Brit Mycol Soc 72:269–276
14. Boise J (1986) *Requienellaceae*, a new family of Loculoascomycetes. Mycologia 78:37–41
15. Bonthond G, Sandoval-Denis M, Groenewald JZ, Crous PW (2018) *Seiridium* (*Sporocadaceae*): an important genus of plant pathogenic fungi. Persoonia 40:96–118
16. Capella-Gutierrez S, Silla-Martinez JM, Gabaldon T (2009) trimAl: a tool for automated alignment trimming in large-scale phylogenetic analyses. Bioinformatics 25:1972–1973
17. Carmarán CC, Romero AI, Giussani LM (2006) An approach towards a new phylogenetic classification in *Diatrypaceae*. Fungal Divers 23:67–87

18. Cesati V, de Notaris G (1863) Schema di classificazione degli sferiacei italici aschigeri più o meno appartenenti al genere Sphaeria nell'antico significato attribuitoglda Persoon. Comment Soc Crittogamia Ital 1:177–240
19. Chethana KW, Jayawardena RS, Chen YJ, Konta S, Tibpromma S, Phukhamsakda C, Abeywickrama PD, Samarakoon MC, Senwanna C, Mapook A, Tang X, Gomdola D, Marasinghe DS, Padaruth OD, Balasuriya A, Xu J, Lumyong S, Hyde KD (2021a) Appressorial interactions with host and their evolution. Fungal Divers https://doi.org/10.1007/s13225-021-00487-5
20. Chethana KWT, Jayawardena RS, Chen Y.-J, Konta S, Tibpromma S, Abeywickrama PD, Gomdola D, Balasuriya A, Xu J, Lumyong S, Hyde KD (2021b) Diversity and function of appressoria. Pathogens 10:746
21. Crous PW, Groenewald JZ (2013) A phylogenetic re-evaluation of *Arthrinium*. IMA Fungus 4:133–154
22. Crous PW, Wingfield MJ, Chooi YH, Gilchrist CLM, Lacey E, Pitt JI, Roets F, Swart WJ, Cano-Lira JF, Valenzuela-Lopez N, Hubka V, Shivas RG, Stchigel AM, Holdom DG, Jurjević Ž, Kachalkin AV, Lebel T, Lock C, Martín MP, Tan YP, Tomashevskaya MA, Vitelli1 JS, Baseia IG, Bhatt VK, Brandrud TE, De Souza JT, Dima B, Lacey HJ, Lombard L, Johnston PR, Morte A, Papp V, Rodríguez A, Rodríguez-Andrade E, Semwal KC, Tegart L, Abad ZG, Akulov A, Alvarado P, Alves A, Andrade JP, Arenas F, Asenjo C, Ballarà J, Barrett MD, Berná LM, Berraf-Tebbal A, Bianchinotti MV, Bransgrove K, Burgess TI, Carmo FS, Chávez R, Čmoková A, Dearnaley JDW, de A. Santiago ALCM, Freitas-Neto JF, Denman S, Douglas B, Dovana F, Eichmeier A, Esteve-Raventós F, Farid A, Fedosova AG, Ferisin G, Ferreira RJ, Ferrer A, Figueiredo CN, Figueiredo YF, Reinoso-Fuentealba CG, Garrido-Benavent I, Cañete-Gibas CF, Gil-Durán C, Glushakova AM, Gonçalves MFM, González M, Gorczak M, Gorton C, Guard FE, Guarnizo AL, Guarro J, Gutiérrez M, Hamal P, Hien LT, Hocking AD, Houbraken J, Hunter GC, Inácio CA, Jourdan M, Kapitonov V, Kelly L, Khanh TN, Kisło K, Kiss L, Kiyashko A, Kolařík M, Kruse J, Kubátová A, Kučera V, Kučerová I, Kušan I, Lee HB, Levicán G, Lewis A, Liem NV, Liimatainen K, Lim HJ, Lyons MN, Maciá-Vicente JG, Magaña-Dueñas V, Mahiques R, Malysheva EF, Marbach PAS, Marinho P, Matočec N, McTaggart AR, Mešić A, Morin L, Muñoz-Mohedano JM, Navarro-Ródenas A, Nicolli CP, Oliveira RL, Otsing E, Ovrebo CL, Pankratov TA, Paños A, Paz-Conde A, Pérez-Sierra A, Phosri C, Pintos Á, Pošta A, Prencipe S, Rubio E, Saitta A, Sales LS, Sanhueza L, Shuttleworth LA, Smith J, Smith ME, Spadaro D, Spetik M, Sochor M, Sochorová Z, Sousa JO, Suwannasai N, Tedersoo L, Thanh HM, Thao LD, Tkalčec Z, Vaghefi N, Venzhik AS, Verbeken A, Vizzini A, Voyron S, Wainhouse M, Whalley AJS, Wrzosek M, Zapata M, Zeil-Rolfe I, Groenewald JZ (2020) Fungal Planet description sheets: 1042–1111. Persoonia 44:301–459
23. Dai DQ, Phookamsak R, Wijayawardene NN, Li WJ, Bhat DJ, Xu JC, Taylor JE, Hyde KD, Chukeatirote E (2017) Bambusicolous fungi. Fungal Divers 82:1–105
24. Daranagama DA, Camporesi E, Liu XZ, Jeewon R, Liu X, Stadler M, Lumyong S, Hyde KD (2016b) Taxonomic rearrangement of *Anthostomella* (*Xylariaceae*) based on multigene phylogenies and morphology. Cryptogam Mycol 37:509–538
25. Daranagama DA, Camporesi E, Tian Q, Liu X, Chamyuang S, Stadler M, Hyde KD (2015) *Anthostomella* is polyphyletic comprising several genera in *Xylariaceae*. Fungal Divers 73:203–238
26. Daranagama DA, Hyde KD, Sir EB, Thambugala KM, Tian Q, Samarakoon MC, Mckenzie EHC, Jayasiri SC, Tibpromma S, Bhat JD, Liu XZ, Stadler M (2018) Towards a natural classification and backbone tree for *Graphostromataceae*, *Hypoxylaceae*, *Lopadostomataceae* and *Xylariaceae*. Fungal Divers 88:1–165
27. Daranagama DA, Jones EBG, Liu XZ, To-anun C, Stadler M, Hyde KD (2016b) Mycosphere Essays 13 – Do xylariaceous macromycetes make up most of the *Xylariomycetidae*? Mycosphere 7:582–601
28. Das K, Kim JH, Choi KS, Seung-Yeol L, Hee-Young J (2020) A new report of *Biscogniauxia petrensis* isolated from mosquitoes in Korea. Korean J Med Mycol 48:87–93
29. Davis EC, Franklin JB, Shaw AJ, Vilgalys R (2003) Endophytic *Xylaria* (*Xylariaceae*) among liverworts and angiosperms: phylogenetics, distribution, and symbiosis. Am J Bot 90:1661–1667
30. Dayarathne MC, Phookamsak R, Hyde KD, Manawasinghe IS, To-anun C, Jones EBG (2016) *Halodiatrype*, a novel diatrypaceous genus from mangroves with *H. salinicola* and *H. avicenniae spp. nov*. Mycosphere 7:612–627
31. de Almeida DAC, Gusmão LFP, Miller AN (2016) Taxonomy and molecular phylogeny of *Diatrypaceae* (*Ascomycota*, *Xylariales*) species from the Brazilian semi-arid region, including four new species. Mycol Prog 15:53
32. Dissanayake AJ, Bhunjun CS, Maharachchikumbura SSN, Liu JK (2020) Applied aspects of methods to infer phylogenetic relationships amongst fungi. Mycosphere 11:2652–2676
33. Dissanayake LS, Maharachchikumbura SSN, Mortimer PE, Hyde KD, Kang JC (2021b) *Acrocordiella yunnanensis sp. nov*. (*Requienellaceae*, *Xylariales*) from Yunnan, China. Phytotaxa 487:103–113
34. Dissanayake LS, Wijayawardene NN, Dayarathne MC, Samarakoon MC, Dai DQ, Hyde KD, Kang JC (2021a) *Paraeutypella guizhouensis gen. et sp. nov*. and *Diatrypella longiasca sp. nov*. (*Diatrypaceae*) from China. Biodivers Data J 9:e63864
35. Eriksson OE (1966) On *Anthostomella* Sacc., *Entosordaria* (Sacc.) Hohn. and some related genera (Pyrenomycetes). Sven Bot Tidskr 60:315–324
36. Eriksson OE (1982) Notes on ascomycetes and coelomycetes from NW Europe. Mycotaxon 15:189–202
37. Eriksson OE (1983) Outline of the ascomycetes - 1983. Systema Ascomycetum 2:1–37
38. Eriksson OE (2003) *Yuea*, a new genus in *Xylariales*. Mycotaxon 85:313–317
39. Eriksson OE, Baral HO, Currah RS, Hansen K, Kurtzman CP, Rambold G, Laessøe T (2003) Outline of *Ascomycota* - 2003. Myconet 9:1–89
40. Eriksson OE, Winka K (1997) Supraordinal taxa of *Ascomycota*. Myconet 1:1–16
41. Farr DF, Rossman AY (2021) Fungal Databases, U.S. National Fungus Collections, ARS, USDA. https://nt.ars-grin.gov/fungaldatabases (Accessed on 10 March 2021)

42. Feng Y, Liu JK, Lin CG, Chen YY, Xiang MM, Liu ZY (2021) Additions to the genus *Arthrinium* (*Apiosporaceae*) from bamboos in China. Front. Microbiol. 12:661281.
43. Fournier J, Lechat C, Courtecuisse R (2018) The genera *Kretzschmariella* and *Nemania* (*Xylariaceae*) in Guadeloupe and Martinique (French West Indies). Ascomycete.org 10:1–47
44. Francis SM (1975) *Anthostomella* Sacc. (Part 1). Mycol Pap 139:1–97
45. Fries EM (1849) Summa Vegetabilium Scandinaviae (in Latin) Sectio posterior. Uppsala, Sweden: Typographia Academica. 259–572
46. Fröhlich J, Hyde KD (2000) Palm microfungi, Fungal Diversity Research Series. Fungal Diversity Press, Hong Kong
47. Gafforov Y (2017) A preliminary checklist of Ascomycetous microfungi from Southern Uzbekistan. Mycosphere 8:660–696
48. Gawas P, Bhat DJ (2005) *Vamsapriya indica gen. et sp. nov.*, a bambusicolous, synnematous fungus from India. Mycotaxon 94:149–154
49. Glawe A, Jacobs KA (1987) Taxonomic notes on *Eutypella vitis*, *Cryptosphaeria populina*, and *Diatrype stigma*. Mycologia 79:135–139
50. Granmo A, Læssøe T, Schumacher T (1999) The genus *Nemania* s.l. (*Xylariaceae*) in Norden. Sommerfeltia 27:1–96
51. Hall TA (1999) BioEdit: a user-friendly biological sequence alignment editor and analysis program for Windows 95/98/NT. Nucleic Acids Symp Ser 41:95–98
52. Hawksworth DL, Eriksson OE (1986) The names of accepted orders of Ascomycetes. Systema Ascomycetum 5:175–184
53. Hawksworth DL, Lodha BC (1983) *Helicogermslita*, a new stromatic Xylariaceous genus with a spiral germ slit from India. Trans Brit Mycol Soc 81:91–96
54. Hennings P (1902) Fungi blumenavienses II. Hedwigia 41:1–33
55. Hongsanan S, Hyde KD, Phookamsak R, Wanasinghe DN, McKenzie HCE, Sarma VV, Boonmee S, Lücking R, Pem D, Bhat JD, Liu N, Tennakoon DS, Karunarathna A, Jiang SH, Jones EBG, Phillips AJL, Manawasinghe I, Tibpromma S, Jayasiri SC, Sandamali D, Jayawardena RS, Wijayawardene NN, Ekanayaka AH, Jeewon R, Lu YZ, Dissanayake AJ, Zeng XY, Luo Z, Tian Q, Phukhamsakda C, Thambugala KM, Dai D, Chethana TKW, Ertz D, Doilom M, Liu JK, Pérez-Ortega S, Suija A, Senwanna C, Wijesinghe SN, Konta S, Niranjan M, Zhang SN, Ariyawansa HA, Jiang HB, Zhang JF, de Silva NI, Thiyagaraja V, Zhang H, Bezerra JDP, Miranda-Gonzáles R, Aptroot A, Kashiwadani H, Harishchandra D, Aluthmuhandiram JVS, Abeywickrama PD, Bao DF, Devadatha B, Wu HX, Moon KH, Gueidan C, Schumm F, Bundhun D, Mapook A, Monkai J, Chomnunti P, Samarakoon MC, Suetrong S, Chaiwan N, Dayarathne MC, Jing Y, Rathnayaka AR, Bhunjun CS, Xu J, Zheng J, Liu G, Feng Y, Xie N (2020) Refined families of *Dothideomycetes*: *Dothideomycetidae* and *Pleosporomycetidae*. Mycosphere 11:1553–2107
56. Hongsanan S, Maharachchikumbura SSN, Hyde KD, Samarakoon MC, Jeewon R, Zhao Q, Al-Sadi AM, Bahkali AH (2017) An updated phylogeny of *Sordariomycetes* based on phylogenetic and molecular clock evidence. Fungal Divers 84:25–41
57. Hsieh HM, Lin CR, Fang MJ, Rogers JD, Fournier J, Lechat C, Ju YM (2010) Phylogenetic status of *Xylaria* subgenus *Pseudoxylaria* among taxa of the subfamily *Xylarioideae* (*Xylariaceae*) and phylogeny of the taxa involved in the subfamily. Mol Phylogenet Evol 54:957–969
58. Huelsenbeck JP, Ronquist F (2001) MRBAYES: Bayesian inference of phylogenetic trees. Bioinformatics 17:754–755
59. Hyde KD (1991) A new amphisphaeriaceous fungus from intertidal fronds of *Nypa fruticans*. Trans Mycol Soc Japan 32:265–271
60. Hyde KD (1994a) Fungi from rachides of *Livistona* in the Western Province of Papua New Guinea. Bot J Linn Soc 116:315–324
61. Hyde KD (1994b) Fungi from *Pandanus*. I. *Pandanicola gen. nov*. from Australia and the Philippine Islands. Sydowia 46:35–40
62. Hyde KD (1995a) Fungi from palms. XIX. *Appendicospora coryphae*, a new name for *Apiosporella coryphae*. Sydowia 47:31–37
63. Hyde KD (1995b) Fungi from palms. XV. *Sabalicola gen. nov*., and a new combination for *Anthostomella sabalensioides*. Nova Hedwig 60:595–598
64. Hyde KD (1996a) Fungi from palms. XXVII. *Capsulospora gen. nov*., with three new species. Sydowia 48:111–121
65. Hyde KD (1996b) Fungi from palms. XXXIII. *Arecomyces gen. nov*., with seven new species. Sydowia 48:224–240
66. Hyde KD, Dong Y, Phookamsak R, Jeewon R, Bhat DJ, Jones EBG, Liu NG, Abeywickrama PD, Mapook A, Wei D, Perera RH, Manawasinghe IS, Pem D, Bundhun D, Karunarathna A, Ekanayaka AH, Bao DF, Li J, Samarakoon MC, Chaiwan N, Lin CG, Phutthacharoen K, Zhang SN, Senanayake IC, Goonasekara ID, Thambugala KM, Phukhamsakda C, Tennakoon DS, Jiang HB, Yang J, Zeng M, Huanraluek N, Liu JK, Wijesinghe SN, Tian Q, Tibpromma S, Brahmanage RS, Boonmee S, Huang SK, Thiyagaraja V, Lu YZ, Jayawardena RS, Dong W, Yang EF, Singh SK, Singh SM, Rana S, Lad SS, Anand G, Devadatha B, Niranjan M, Sarma VV, Liimatainen K, Aguirre-Hudson B, Niskanen T, Overall A, Alvarenga RLM, Gibertoni TB, Pfliegler WP, Horváth E, Imre A, Alves AL, Santos ACdaS, Tiago PV, Bulgakov TS, Wanasinghe DN, Bahkali AH, Doilom M, Elgorban AM, Maharachchikumbura SSN, Rajeshkumar KC, Haelewaters D, Mortimer PE, Zhao Q, Lumyong S, Xu J, Jun Sheng J (2020a) Fungal diversity notes 1151–1276: taxonomic and phylogenetic contributions on genera and species of fungal taxa. Fungal Divers 100:5–277
67. Hyde KD, Fröhlich J (1997) A new species of *Appendicospora* from Hong Kong. Mycoscience 38:395–397
68. Hyde KD, Fröhlich J, Taylor JE (1998) Fungi from palms XXXVI - Reflections on unitunicate ascomycetes with apiospores. Sydowia 50:21–80
69. Hyde KD, Jones EBG (1992) Intertidal mangrove fungi: *Pedumispora gen. nov*. (*Diaporthales*). Mycol Res 96:78–80
70. Hyde KD, Maharachchikumbura SS, Hongsanan S, Samarakoon MC, Lücking R, Pem D, Harishchandra D, Jeewon R, Zhao RL, Xu JC, Liu JK (2017) The ranking of fungi: a tribute to David L. Hawksworth on his 70th birthday. Fungal Divers 84:1–23
71. Hyde KD, Norphanphoun C, Maharachchikumbura SSN, Bhat DJ, Jones EBG, Bundhun D, Chen YJ, Bao DF, Boonmee S, Calabon MS, Chaiwan N, Chethana KWT, Dai DQ, Dayarathne MC, Devadatha B, Dissanayake AJ, Dissanayake LS, Doilom M, Dong W, Fan XL, Goonasekara ID, Hongsanan S, Huang SK, Jayawardena RS, Jeewon R, Karunarathna A, Konta S, Kumar V, Lin CG, Liu JK, Liu NG, Luangsa-ard J, Lumyong S, Luo ZL, Marasinghe DS, McKenzie EHC, Niego AGT, Niranjan M, Perera RH, Phukhamsakda C, Rathnayaka AR, Samarakoon MC, Samarakoon SMBC, Sarma VV, Senanayake IC, Shang QJ, Stadler M, Tibpromma S, Wanasinghe DN, Wei DP, Wijayawardene NN, Xiao YP, Yang J, Zeng XY, Zhang SN, Xiang MM (2020b) Refined families of *Sordariomycetes*. Mycosphere 11:305–1059

72. Jaklitsch WM, Fournier J, Rogers JD, Voglmayr H (2014) Phylogenetic and taxonomic revision of *Lopadostoma*. Persoonia 32:52–82
73. Jaklitsch WM, Gardiennet A, Voglmayr H (2016) Resolution of morphology-based taxonomic delusions: *Acrocordiella*, *Basiseptospora*, *Blogiascospora*, *Clypeosphaeria*, *Hymenopleella*, *Lepteutypa*, *Pseudapiospora*, *Requienella*, *Seiridium* and *Strickeria*. Persoonia 37:82–105
74. Jaklitsch WM, Voglmayr H (2012) Phylogenetic relationships of five genera of *Xylariales* and *Rosasphaeria gen. nov.* (*Hypocreales*). Fungal Divers 52:75–98
75. Jayasiri SC, Hyde KD, Abd-Elsalam KA, Abdel-Wahab MA, Ariyawansa HA, Bhat J, Buyck B, Dai YC, Ertz D, Hidayat I, Jeewon R, Jones EBG, Karunarathna SC, Kirk P, Lei C, Liu JK, Maharachchikumbura SSN, McKenzie E, Ghobad-Nejhad M, Nilsson H, Pang KL, Phookamsak R, Rollins AW, Romero AI, Stephenson S, Suetrong S, Tsui CKM, Vizzini A, Wen TC, De Silva NI, Promputtha I, Kang JC (2015) The Faces of Fungi database: fungal names linked with morphology, phylogeny and human impacts. Fungal Divers 74:3–18
76. Jones EBG, Moss ST (1978) Ascospore appendages of marine ascomycetes: an evaluation of appendages as taxonomic criteria. Mar Biol 49:11–26
77. Ju YM, Rogers JD (1990) *Astrocystis* reconsidered. Mycologia 82:342–349
78. Ju YM, Rogers JD (2001) New and interesting *Biscogniauxia* taxa, with a key to the world species. Mycol Res 105:1123–1133
79. Ju YM, Rogers JD (2002) The genus *Nemania* (*Xylariaceae*). Nova Hedwig 74:75–120
80. Ju YM, Rogers JD, Hsieh HM (2005) New *Hypoxylon* and *Nemania* species from Costa Rica and Taiwan. Mycologia 97:562–567
81. Ju YM, Rogers JD, Hsieh HM (2018) *Xylaria* species associated with fallen fruits and seeds. Mycologia 110:726–749
82. Ju YM, Rogers JD, San Martín F, Granmo A (1998) The genus *Biscogniauxia*. Mycotaxon 66:1–98
83. Kang JC, Hyde KD, Kong RYC (1999) Studies on the *Amphisphaeriales* I. The *Clypeosphaeriaceae*. Mycoscience 40:151–164
84. Kang JC, Kong RYC, Hyde KD (1998) Studies on the *Amphisphaeriales* I. *Amphisphaeriaceae* (*sensu stricto*) and its phylogenetic relationships inferred from 5.8S rDNA and ITS2 sequences. Fungal Divers 1:147–157
85. Kang JC, Kong RYC, Hyde KD (2002) Phylogeny of *Amphisphaeriaceae* (*sensu stricto*) and related taxa revisited based on nrDNA sequences. Mycotaxon LXXXXI:321–330
86. Katoh K, Rozewicki J, Yamada KD (2019) MAFFT online service: multiple sequence alignment, interactive sequence choice and visualization. Brief Bioinform 20:1160–1166
87. Kirk PM, Cannon PF, Minter DW, Stalpers JA (2008) Ainsworth & Bisby's Dictionary of the Fungi, 10th Edition. CABI Publishing, Wallingford, UK
88. Kirschstein W (1934) Remarks on a collection of British species of *Rosellinia* and a redistribution of the species of that genus. Trans Brit Mycol Soc 18:302–307
89. Konta S, Hongsanan S, Eungwanichayapant PD, Liu JK, Jeewon R, Hyde KD, Maharachchikumbura SSN, Boonmee S (2017) *Leptosporella* (*Leptosporellaceae fam. nov.*) and *Linocarpon* and *Neolinocarpon* (*Linocarpaceae fam. nov.*) are accommodated in *Chaetosphaeriales*. Mycosphere 8:1943–1974
90. Konta S, Hongsanan S, Tibpromma S, Thongbai B, Maharachchikumbura SSN, Bahkali AH, Hyde KD, Boonmee S (2016) An advance in the endophyte story: *Oxydothidaceae fam. nov.* with six new species of *Oxydothis*. Mycosphere 7:1425–1446
91. Konta S, Hyde KD, Eungwanichayapant PD, Karunarathna SC, Samarakoon MC, Xu J, Dauner LAP, Aluthwattha ST, Lumyong S, Tibpromma S (2021) Multigene phylogeny reveals *Haploanthostomella elaeidis gen. et sp. nov.* and familial replacement of *Endocalyx* (*Xylariales*, *Sordariomycetes*, *Ascomycota*). Life 11:486
92. Konta S, Hyde KD, Phookamsak R, Xu JC, Maharachchikumbura SSN, Daranagama DA, McKenzie EHC, Boonmee S, Tibpromma S, Eungwanichayapant PD, Samarakoon MC, Lu YZ (2020b) Polyphyletic genera in *Xylariaceae* (*Xylariales*): *Neoxylaria gen. nov.* and *Stilbohypoxylon*. Mycosphere 11:2629–2651
93. Konta S, Maharachchikumbura SSN, Senanayake IC, McKenzie EHC, Stadler M, Boonmee S, Phookamsak R, Jayawardena RS, Senwanna C, Hyde KD, Elgorban AM, Eungwanichayapant PD (2020a) A new genus *Allodiatrype*, five new species and a new host record of diatrypaceous fungi from palms (*Arecaceae*). Mycosphere 11:239–268
94. Krings M, Taylor TT, Dotzler N (2012) Fungal endophytes as a driving force in land plant evolution: Evidence from the fossil record. In: Southworth D. (ed) Biocomplexity of Plant–Fungal Interactions. John Wiley & Sons, Inc, pp 5–27
95. Krug JC, Cain RF (1974) New species of *Hypocopra* (*Xylariaceae*). Can J Bot 52:809–843
96. Laessøe T, Rogers JD, Whalley AJS (1989) *Camillea*, *Jongiella* and light-spored species of *Hypoxylon*. Mycol Res 93:121–155
97. Læssøe T, Spooner BM (1993) *Rosellinia* & *Astrocystis* (*Xylariaceae*): New species and generic concepts. Kew Bull 49:1–70
98. Lee S, Crous PW (2003) New species of *Anthostomella* on fynbos, with a key to the genus in South Africa. Mycol Res 107:360–370
99. Liu F, Bonthond G, Groenewald JZ, Cai L, Crous PW (2019) *Sporocadaceae*, a family of coelomycetous fungi with appendage-bearing conidia. Stud Mycol 92:287–415
100. Liu JK, Hyde KD, Jones EBG, Ariyawansa HA, Bhat DJ, Boonmee S, Maharachchikumbura S, McKenzie EHC, Phookamsak R, Phukhamsakda C, Shenoy BD, Abdel-Wahab MA, Buyck B, Chen J, Chethana KWT, Singtripop C, Dai DQ, Dai YC, Daranagama DA, Dissanayake AJ, Doliom M, D'souza MJ, Fan XL, Goonasekara ID, Hirayama K, Hongsanan S, Jayasiri SC, Jayawardena RS, Karunarathna SC, Li WJ, Mapook A, Norphanphoun C, Pang KL, Perera RH, Peršoh D, Pinruan U, Senanayake IC, Somrithipol S, Suetrong S, Tanaka K, Thambugala KM, Tian Q, Tibpromma S, Udayanga D, Wijayawardena NN, Wanasinghe D, Wisitrassameewong K, Abdel-Aziz FA, Adamčík S, Bahkali AH, Boonyuen N, Bulgakov T, Callac P, Chomnunti P, Greiner K, Hashimoto A, Hofstetter V, Kang JC, Lewis D, Li XH, Liu XX, Liu ZY, Matumura M, Mortimer PE, Rambold G, Randrianjohany E, Sato G, Sri-Indrasutdhi V, Tian CM,

Verbeken A, von Brackel W, Wang Y, Wen TC, Xu JC, Yan JY, Zhao RL, Camporesi E (2015) Fungal diversity notes 1–110: taxonomic and phylogenetic contributions to fungal species. Fungal Divers 72:1–197

101. Liu YJ, Whelen S, Hall BD (1999) Phylogenetic relationships among ascomycetes: evidence from an RNA polymerse II subunit. Mol Biol Evol 16:1799–1808
102. Lu BS, Hyde KD (2000) A world monograph of *Anthostomella*, Fungal Diversity Research Series. Fungal Diversity Press
103. Lu BS, Hyde KD, Liew ECY (2000) Eight new species of *Anthostomella* from South Africa. Mycol Res 104:742–754
104. Lumbsch HT, Huhndorf SM (2010) Myconet Volume 14. Part One. Outline of *Ascomycota*—2009. Part Two. Notes on Ascomycete Systematics. Nos. 4751–5113. Fieldiana Life and Earth Sci 1:1–64
105. Lutzoni F, Nowak MD, Alfaro ME, Reeb V, Miadlikowska J, Krug M, Arnold AE, Lewis LA, Swofford DL, Hibbett D, Hilu K, James TY, Quandt D, Magallón S (2018) Contemporaneous radiations of fungi and plants linked to symbiosis. Nat Commun 9:5451
106. Ma XY, Nontachaiyapoom S, Hyde KD, Jeewon R, Doilom M, Chomnunti P, Kang JC (2020) *Biscogniauxia dendrobii sp. nov*. and *B. petrensis* from *Dendrobium* orchids and the first report of cytotoxicity (towards A549 and K562) of *B. petrensis* (MFLUCC 14-0151) in vitro. South African J Bot 134:382–393
107. Maharachchikumbura SSN, Chen Y, Ariyawansa HA, Hyde KD, Haelewaters D, Perera RH, Samarakoon MC, Wanasinghe DN, Bustamante DE, Liu JK, Lawrence DP, Cheewangkoon R, Stadler M (2021) Integrative approaches for species delimitation in *Ascomycota*. Fungal Diversity, https://doi.org/10.1007/s13225-021-00486-6.
108. Maharachchikumbura SSN, Hyde KD, Jones EBG, McKenzie EHC, Bhat DJ, Dayarathne MC, Huang SK, Norphanphoun C, Senanayake IC, Perera RH, Shang QJ, Xiao YP, D'souza MJ, Hongsanan S, Jayawardena RS, Daranagama DA, Konta S, Goonasekara ID, Zhuang WY, Jeewon R, Phillips AJL, AbdelWahab MA, Al-Sadi AM, Bahkali AH, Boonmee S, Boonyuen N, Cheewangkoon R, Dissanayake AJ, Kang JC, Li QR, Liu JK, Liu XZ, Liu ZY, Luangsa-ard JJ, Pang KL, Phookamsak R, Promputtha I, Suetrong S, Stadler M, Wen TC, Wijayawardene NN (2016) Families of *Sordariomycetes*. Fungal Divers 79:1–317
109. Maharachchikumbura SSN, Hyde KD, Perera RH, Al-Sadi AM (2018) *Acrocordiella omanensis sp. nov*. (*Requienellaceae*, *Xylariales*) from the Sultanate of Oman. Phytotaxa 338:294–300
110. Mathiassen G (1993) Corticolous and lignicolous Pyrenomycetes s.lat. (Ascomycetes) on *Salix* along a mid-Scandinavian transect. Oslo
111. Mehrabi M, Hemmti R, Vasilyeva LN, Trouillas FP (2016) *Diatrypella macrospora sp. nov*. and new records of diatrypaceous fungi from Iran. Phytotaxa 252:43–55
112. Müller E, von Arx JA (1962) Die Gattungen der didymosphoren pyrenomyceten. Beiträge zur Krytogamenflora der Schweiz 11:1–922
113. Munk A (1953) The system of the Pyrenomycetes: a contribution to a natural classification of the group Sphacriales sensu Lindau., Dansk bota. Copenhagen
114. Nees von Esenbeck CG (1816) Das system der pilze und schwämme. Wurzburg, Germany
115. Nelson A, Vandegrift R, Carroll GC, Roy BA (2020) Double lives: transfer of fungal endophytes from leaves to woody substrates. PeerJ 8:e9341
116. Nguyen LT, Schmidt HA, von Haeseler A, Minh BQ (2015) IQ-TREE: a fast and effective stochastic algorithm for estimating maximum-likelihood phylogenies. Mol Biol Evol 32:268–274
117. Nitschke TRJ (1869) Grundlage eines Systems der Pyrenomyceten. Verhandlungen des Naturhistorischen Vereins der Preuss Rheinlande, Westfalens und des Regierungsbezirks Osnabrück 262:70–77
118. Nylander JAA (2004) MrModeltest v2. Program distributed by the author. Evolutionary Biology Centre, Uppsala University
119. O'Donnell K, Cigelnik E (1997) Two divergent intragenomic rDNA ITS2 Types within a monophyletic lineage of the fungus *Fusarium* are nonorthologous. Mol Biol Evol 7:103–116
120. Perera RH, Maharachchikumbura SSN, Jones EBG, Bahkali AH, Elgorban AM, Liu JK, Liu ZY, Hyde KD (2017) *Delonicicola siamense gen. et sp. nov*. (*Delonicicolaceae fam. nov*., *Delonicicolales ord. nov*.), a saprobic species from *Delonix regia* seed pods. Cryptogam Mycol 38:321–340
121. Peršoh D, Melcher M, Graf K, Fournier J, Stadler M, Rambold G (2009) Molecular and morphological evidence for the delimitation of *Xylaria hypoxylon*. Mycologia 101:256–268
122. Petrini LE (2003) *Rosellinia* and related genera in New Zealand. New Zeal J Bot 41:71–138
123. Petrini LE (2013) *Rosellinia* – a world monograph. J. Cramer in der Gebr. Borntraeger Verlagsbuchhandlung, Berlin
124. Petrini LE, Petrini O, Francis SM (1989) On *Rosellinia mammaeformis* and other related species. Sydowia 41:257–276
125. Phillips AJ, Hyde KD, Alves A, Liu JK (2019) Families in *Botryosphaeriales*: a phylogenetic, morphological and evolutionary perspective. Fungal Divers 94:1–22
126. Phookamsak R, Hyde KD, Jeewon R, Bhat DJ, Jones EBG, Maharachchikumbura SSN, Raspé O, Karunarathna SC, Wanasinghe DN, Hongsanan S, Doilom M, Tennakoon DS, Machado AR, Firmino AL, Ghosh A, Karunarathna A, Mešić A, Dutta AK, Thongbai B, Devadatha B, Norphanphoun C, Senwanna C, Wei D, Pem D, Ackah FK, Wang GN, Jiang HB, Madrid H, Lee HB, Goonasekara ID, Manawasinghe IS, Kušan I, Cano J, Gené J, Li J, Das K, Acharya K, Raj KNA, Latha KPD, Chethana KWT, He MQ, Dueñas M, Jadan M, Martín MP, Samarakoon MC, Dayarathne MC, Raza M, Park MS, Telleria MT, Chaiwan N, Matočec N, de Silva NI, Pereira OL, Singh PN, Manimohan P, Uniyal P, Shang QJ, Bhatt RP, Perera RH, Alvarenga RLM, Nogal-Prata S, Singh SK, Vadthanarat S, Oh SY, Huang SK, Rana S, Konta S, Paloi S, Jayasiri SC, Jeon SJ, Mehmood T, Gibertoni TB, Nguyen TTT, Singh U, Thiyagaraja V, Sarma VV, Dong W, Yu XD, Lu YZ, Lim YW, Chen Y, Tkalčec Z, Zhang ZF, Luo ZL, Daranagama DA, Thambugala KM, Tibpromma S, Camporesi E, Bulgakov TS, Dissanayake AJ, Senanayake IC, Dai DQ, Tang LZ, Khan S, Zhang H, Promputtha I, Cai L, Chomnunti P, Zhao RL, Lumyong S, Boonmee S, Wen TC, Mortimer PE, Xu J (2019) Fungal diversity notes 929–1035: taxonomic and phylogenetic contributions on genera and species of fungi. Fungal Divers 95:1–273

127. Píchová K, Pažoutová S, Kostovčík M, Chudíčková M, Stodůlková E, Novák P, Flieger M, van der Linde E, Kolařík M (2018) Evolutionary history of ergot with a new infrageneric classification (*Hypocreales*: *Clavicipitaceae*: *Claviceps*). Mol Biol Evol 123:73–87
128. Pintos Á, Alvarado P (2021) Phylogenetic delimitation of *Apiospora* and *Arthrinium*. Fungal Syst Evol 7:197–221
129. Poinar GO (2014) *Xylaria antiqua sp. nov.* (*Ascomycota*: *Xylariaceae*) in Dominican Amber. J Bot Res Inst Texas 8:145–149
130. Pouzar Z (1985) Reassessment of *Hypoxylon serpens*-complex I. Česká Mykol 39:15–25
131. Promputtha I, Lumyong S, Dhanasekaran V, McKenzie EHC, Hyde KD, Jeewon R (2007) A phylogenetic evaluation of whether endophytes become saprotrophs at host senescence. Microb Ecol 53:579–590
132. Rambaut A (2012) FigTree: Tree figure drawing tool 2006–2012, version 1.4.0. Institute of Evolutionary Biology, University of Edinburgh, Edinburgh
133. Rambaut A, Suchard MA, Xie D, Drummond AJ (2013) Tracer version 1.6. University of Edinburgh. [Online]. available at http://tree.bio.ed.ac.uk/software/tracer. (Accessed on 01 June 2021)
134. Rappaz F (1987) Taxonomie et momenclature des Diatrypacees à asques octospores. Mycol Helv 2:285–648
135. Rappaz F (1995) *Anthostomella* and related xylariaceous fungi on hardwoord from Europe and North America. Mycol Helv 7:99–168
136. Rashmi M, Kushveer JS, Sarma VV (2019) A worldwide list of endophytic fungi with notes on ecology and diversity. Mycosphere 10:798–1079
137. Rathnayaka AR, Chethana KWT, Phillips AJL, Liu JK, Samarakoon MC, Hyde KD (2021) Re-evaluating of *Botryosphaeriales*: Ancestral character analyses of selected characters and evolution of nutritional modes (prep)
138. Rehner SA, Samuels GJ (1994) Taxonomy and phylogeny of *Gliocladium* analysed from nuclear large subunit ribosomal DNA sequences. Mycol Res 98:625–634
139. Rodrigues KF, Leuchtmann L, Petrini O (1993) Endophytic species of *Xylaria*: cultural and isozymic studies. Sydowia 45:116–138
140. Rodriguez R, Redman R (2008) More than 400 million years of evolution and some plants still can't make it on their own: plant stress tolerance via fungal symbiosis. J Exp Bot 59:1109–1114
141. Rogers JD (1979) The *Xylariaceae*: Systematic, biological and evolutionary aspects. Mycologia 71:1–42
142. Rogers JD (2000) Thoughts and musings on tropical *Xylariaceae*. Mycol Res 104:1412–1420
143. Rogers JD, Hidalgo A, Fernández FA, Huhndorf SM (2004) *Ophiorosellinia costaricensis gen. et sp. nov.*, a xylariaceous fungus with scolecosporous ascospores. Mycologia 96:172–174
144. Rogers JD, Ju YM (2002) *Nemania pouzarii*, a new species from Oahu Island, Hawaii. Czech Mycol 54:79–81
145. Rogers JD, Ju YM (2003) *Occultitheca costaricensis gen. et sp. nov.* and *Apiocamarops pulvinata sp. nov.* from Costa Rica. Sydowia 55:359–364
146. Rogers JD, Vasilyeva L, Hay FO (2008) New *Xylariaceae* from Hawaii and Texas (USA). Sydowia 60:277–286
147. Saccardo PA (1875) Conspectus generum Pyrenomycetum Italicorum. Atti della Accademia Scientifica Veneto-Trentino-Istriana Già 4:77–100
148. Samarakoon BC, Wanasinghe DN, Samarakoon MC, Phookamsak R, McKenzie EHC, Chomnunti P, Hyde KD, Lumyong S, Karunarathna SC (2020a) Multi-gene phylogenetic evidence suggests *Dictyoarthrinium* belongs in *Didymosphaeriaceae* (*Pleosporales*, *Dothideomycetes*) and *Dictyoarthrinium musae sp. nov.* on *Musa* from Thailand. MycoKeys 71:101–118
149. Samarakoon MC, Hyde KD, Hongsanan S, McKenzie EHC, Ariyawansa HA, Promputtha I, Zeng XY, Tian Q, Liu JK (2019a) Divergence time calibrations for ancient lineages of *Ascomycota* classification based on a modern review of estimations. Fungal Divers 96:285–346
150. Samarakoon MC, Hyde KD, Promputtha I, Hongsanan S, Ariyawansa HA, Maharachchikumbura SSN, Daranagama DA, Stadler M, Mapook A (2016) Evolution of *Xylariomycetidae* (*Ascomycota*: *Sordariomycetes*). Mycosphere 7:1746–1761
151. Samarakoon MC, Liu JK, Hyde KD, Promputtha I (2019b) Two new species of *Amphisphaeria* (*Amphisphaeriaceae*) from northern Thailand. Phytotaxa 391:207–217
152. Samarakoon MC, Maharachchikumbura SSN, Liu JK, Hyde KD, Promputtha I, Stadler M (2020b) Molecular phylogeny and morphology of *Amphisphaeria* (= *Lepteutypa*) (*Amphisphaeriaceae*). J Fungi 6:174
153. Samarakoon MC, Thongbai B, Hyde KD, Brönstrup M, Beutling U, Lambert C, Miller AN, Liu JK, Promputtha I, Stadler M (2020c) Elucidation of the life cycle of the endophytic genus *Muscodor* and its transfer to *Induratia* in *Induratiaceae fam. nov.*, based on a polyphasic taxonomic approach. Fungal Divers 101:177–210
154. San Martín González F, Rogers JD (1993) *Biscogniauxia* and *Camillea* in Mexico. Mycotaxon 47:229–258
155. Saxena RK, Wijayawardene NN, Dai DQ, Hyde KD, Kirk PM (2021) Diversity in fossil fungal spores. Mycosphere 12:670–874
156. Schmitt I, Prado R del, Grube M, Lumbsch HT (2009) Repeated evolution of closed fruiting bodies is linked to ascoma development in the largest group of lichenized fungi (*Lecanoromycetes*, *Ascomycota*). Mol Phylogenetics Evol 52:34–44
157. Senanayake IC, Bhat JD, Cheewangkoon R and Xie N (2020) Bambusicolous *Arthrinium* species in Guangdong Province, China. Front. Microbiol. 11:602773.
158. Senanayake IC, Maharachchikumbura SSN, Hyde KD, Bhat JD, Jones EBG, McKenzie EHC, Dai DQ, Daranagama DA, Dayarathne MC, Goonasekara ID, Konta S, Li WJ, Shang Q, Stadler M, Wijayawardene NN, Xiao YP, C. Norphanphoun C, Li Q, Liu XL, Bahkali A, Kang J, Wang Y, Wen T, Wendt L, Xu J, Camporesi E (2015) Towards unraveling relationships in *Xylariomycetidae* (*Sordariomycetes*). Fungal Divers 73:73–144
159. Senanayake IC, Rathnayaka AR, Marasinghe DS, Calabon MS, Gentekaki E, Lee HB, Hurdeal VG, Pem D, Dissanayake LS, Wijesinghe SN, Bundhun D, Nguyen TT, Goonasekara ID, Abeywickrama PD, Bhunjun CS, Jayawardena RS, Wanasinghe DN, Jeewon R, Bhat DJ, Xiang MM (2020) Morphological approaches in studying fungi: collection, examination, isolation, sporulation and preservation. Mycosphere 11:2678–2754

160. Senwanna C, Phookamsak R, Doilom M, Hyde KD, Cheewangkoon R (2017) Novel taxa of *Diatrypaceae* from Para rubber (*Hevea brasiliensis*) in northern Thailand; introducing a novel genus *Allocryptovalsa*. Mycosphere 8:1835–1855
161. Shang QJ, Hyde KD, Phookamsak R, Doilom M, Bhat DJ, Maharachchikumbura SSN, Promputtha I (2017) *Diatrypella tectonae* and *Peroneutypa mackenziei spp. nov*. (*Diatrypaceae*) from northern Thailand. Mycol Prog 16:463–476
162. Sivanesan A (1975) New ascomycetes and some revisions. Trans Brit Mycol Soc 65:19–27
163. Smith GJD, Liew ECY, Hyde KD (2003) The *Xylariales*: a monophyletic order containing 7 families. Fungal Divers 13:185–218
164. Suchard MA, Lemey P, Baele G, Ayres DL, Drummond AJ, Rambaut A (2018) Bayesian phylogenetic and phylodynamic data integration using BEAST 1.10. Virus Evol 4:vey016
165. Sullivan TS, Gottel NR, Basta N, Jardine PM, Schadt CW (2012) Firing range soils yield a diverse array of fungal isolates capable of organic acid production and Pb mineral solubilization. Appl Environ Microbiol 78:6078–6086
166. Suwannasai N (2005) Molecular taxonomic studies of selected members of the *Xylariaceae* (Fungi). Suranaree University of Technology, Thailand
167. Suwannasai N, Whalley MA, Whalley AJS, Thienhirun S, Sihanonth P (2012) Ascus apical apparatus and ascospore characters in *Xylariaceae*. IMA Fungus 3:125–133
168. Tanaka K, Hirayama K, Yonezawa H, Sato G, Toriyabe A, Kudo H, Hashimoto A, Matsumura M, Harada Y, Kurihara Y, Shirouzu T, Hosoya T (2015) Revision of the *Massarineae* (*Pleosporales*, *Dothideomycetes*). Stud Mycol 82:75–136
169. Tang AMC, Jeewon R, Hyde KD (2007) Phylogenetic relationships of *Nemania plumbea sp. nov*. and related taxa based on ribosomal ITS and RPB2 sequences. Mycol Res 111:392–402
170. Tang AMC, Jeewon R, Hyde KD (2009) A re-evaluation of the evolutionary relationships within the *Xylariaceae* based on ribosomal and protein-coding gene sequences. Fungal Divers 34:127–155
171. Taylor JE, Hyde KD (2003) Microfungi of tropical and temperate palms, Fungal Diversity Research Series. Fungal Diversity Press
172. Tennakoon DS, Kuo CH, Maharachchikumbura SSN, Thambugala KM, Gentekaki E, Phillips AJL, Bhat DJ, N. Wanasinghe DN, de Silva NI, Promputtha I, Hyde KD (2021) Taxonomic and phylogenetic contributions to *Celtis formosana*, *Ficus ampelas*, *F. septica*, *Macaranga tanarius* and *Morus australis* leaf litter inhabiting microfungi. Fungal Divers 108:1–215
173. Thienhirun S (1997) A Preliminary Account of the *Xylariaceae* of Thailand. Liverpool John Moores University. UK
174. Thiyagaraja V, Lücking R, Ertz D, Karunarathna SC, Wanasinghe DN, Lumyong S, Hyde KD (2021) The evolution of life modes in *Stictidaceae*, with three novel taxa. J Fungi 7:105
175. Thiyagaraja V, Lücking R, Ertz D, Wanasinghe DN, Karunarathna SC, Camporesi E, Hyde KD (2020) Evolution of non-lichenized, saprotrophic species of *Arthonia* (*Ascomycota*, *Arthoniales*) and resurrection of *Naevia*, with notes on *Mycoporum*. Fungal Divers 102:205–224
176. Tibpromma S, Daranagama DA, Boonmee S, Promputtha I, Nontachaiyapoom S, Hyde KD (2017) *Anthostomelloides krabiensis gen. et sp. nov*. (*Xylariaceae*) from *Pandanus odorifer* (*Pandanaceae*). Turk J Botany 41:107–116
177. Tibpromma S, McKenzie EHC, Karunarathna SC, Mortimer PE, Xu J, Hyde KD, Hu DM (2021) Volatile constituents of endophytic fungi isolated from *Aquilaria sinensis* with descriptions of two new species of *Nemania*. Life 11:363
178. Trifinopoulos J, Nguyen LT, von Haeseler A, Minh BQ (2016) W-IQ-TREE: a fast-online phylogenetic tool for maximum likelihood analysis. Nucleic Acids Res 44:W232–W235
179. Trouillas FP, Hand FP, Inderbitzin P, Gubler WD (2015) The genus *Cryptosphaeria* in the western United States: taxonomy, multilocus phylogeny and a new species, *C. multicontinentalis*. Mycologia 107:1304–1313
180. U'Ren JM, Miadlikowska J, Zimmerman NB, Lutzoni F, Stajich JE, Arnold AE (2016) Contributions of North American endophytes to the phylogeny, ecology, and taxonomy of *Xylariaceae* (*Sordariomycetes*, *Ascomycota*). Mol Phylogenet Evol 98:210–232
181. van Geel B, Aptroot A (2006) Fossil ascomycetes in Quaternary deposits. Nova Hedwig 82:313–329
182. Vasilyeva LN, Ma HX (2014) Diatrypaceous fungi in north-eastern China. 1. *Cryptosphaeria* and *Diatrype*. Phytotaxa 186:261–270
183. Vasilyeva LN, Stephenson SL (2009) The genus *Diatrype* (*Ascomycota*, *Diatrypaceae*) in Arkansas and Texas (USA). Mycotaxon 107:307–313
184. Vasilyeva LN, Stephenson SL (2014) Notes on pyrenomycetous fungi in the Mountain Lake area of southwestern Virginia. Mycosphere 5:218–227
185. Vasilyeva LN, Stephenson SL, Hyde KD, Bahkali AH (2012) Some stromatic pyrenomycetous fungi from northern Thailand - 1. *Biscogniuxia*, *Camillea* and *Hypoxylon* (*Xylariaceae*). Fungal Divers 55:65–76
186. Vilgalys R, Hester M (1990) Rapid genetic identification and mapping of enzymatically amplified ribosomal DNA from several *Cryptococcus* species. J Bacteriol 172:4238–4246
187. Voglmayr H, Aguirre-Hudson MB, Wagner HG, Tello S, Jaklitsch WM (2019) Lichens or endophytes? The enigmatic genus *Leptosillia* in the *Leptosilliaceae fam. nov*. (*Xylariales*), and *Furfurella gen. nov*. (*Delonicicolaceae*). Persoonia 42:228–260
188. Voglmayr H, Beenken L (2020) *Linosporopsis*, a new leaf-inhabiting scolecosporous genus in *Xylariaceae*. Mycol Prog 19:205–222
189. Voglmayr H, Friebes G, Gardiennet A, Jaklitsch WM (2018) *Barrmaelia* and *Entosordaria* in *Barrmaeliaceae* (*fam. nov.*, *Xylariales*) and critical notes on Anthostomella-like genera based on multigene phylogenies. Mycol Prog 17:155–177
190. Walker JD (2019) GSA Geologic Time Scale v. 5.0. Elsevier
191. Wanasinghe DN, Phukhamsakda C, Hyde KD, Jeewon R, Lee HB, Jones EBG, Tibpromma S, Tennakoon DS, Dissanayake AJ, Jayasiri SC, Gafforov Y, Camporesi E, Bulgakov TS, Ekanayake AH, Perera RH, Samarakoon MC, Goonasekara ID, Mapook A, Li WJ, Senanayake IC, Li J, Norphanphoun C, Doilom

D, Bahkali AH, Xu J, Mortimer PE, Tibell L, Tibell S, Karunarathna SC (2018) Fungal diversity notes 709–839: taxonomic and phylogenetic contributions to fungal taxa with an emphasis on fungi on *Rosaceae*. Fungal Divers 89:1–236

192. Wang M, Liu F, Crous PW, Cai L (2017) Phylogenetic reassessment of *Nigrospora:* ubiquitous endophytes, plant and human pathogens. Persoonia 39:118–142
193. Wang M, Tan XM, Liu F, Cai L (2018) Eight new *Arthrinium* species from China. MycoKeys 34:1–24
194. Wang YZ, Aptroot A, Hyde KD (2004) Revision of the Ascomycete genus *Amphisphaeria*, The Fungal Diversity Research Series. Hong Kong SAR, China
195. Wang YZ, Hyde KD (1999) *Hyponectria buxi* with notes on the *Hyponectriaceae*. Fungal Divers 3:159–172
196. Wehmeyer LE (1926) A biologic and phylogenetic study of the stromatic *Sphaeriales*. Am J Bot 13:575–645
197. Wendt L, Sir EB, Kuhnert E, Heitkämper S, Lambert C, Hladki AI, Romero AI, Luangsa-ard JJ, Srikitikulchai P, Peršoh D, Stadler M (2018) Resurrection and emendation of the *Hypoxylaceae*, recognised from a multigene phylogeny of the *Xylariales*. Mycol Prog 17:115–154
198. Whalley AJS (1996) The xylariaceous way of life. Mycol Res 100:897–922
199. Whalley MA, Whalley AJS, Thienhirun S, Sihanonth P (1999) *Camillea malaysianensis sp. nov*. and the distribution of *Camillea* in Southeast Asia. Kew Bull 54:715
200. White TJ, Bruns T, Lee S, Taylor J (1990) Amplification and direct sequencing of fungal ribosomal rna genes for phylogenetics. In: PCR Protocols. Elsevier, pp 315–322
201. Wijayawardene NN, Hyde KD, Al-Ani LKT, Tedersoo L, Haelewaters D, Rajeshkumar KC, Zhao RL, Aptroot A, Leontyev DV, Saxena RK, Tokarev YS, Dai DQ, Letcher PM, Stephenson SL, Ertz D, Lumbsch HT, Kukwa M, Issi IV, Madrid H, Phillips AJL, Selbmann L, Pfliegler WP, Horváth E, Bensch K, Kirk PM, Kolaříková K, Raja HA, Radek R, Papp V, Dima V, Ma J, Malosso E, Takamatsu S, Rambold G, Gannibal PB, Triebel D, Gautam AK, Avasthi S, Suetrong S, Timdal E, Fryar SC, Delgado G, Réblová M, Doilom M, Dolatabadi S, Pawłowska J, Humber RA, Kodsueb R, Sánchez-Castro I, Goto BT, Silva DKA, de Souza FA, Oehl F, da Silva GA, Silva IR, Błaszkowski J, Jobim K, Maia LC, Barbosa FR, Fiuza PO, Divakar PK, Shenoy BD, Castañeda-Ruiz RF, Somrithipol S, Lateef AA, Karunarathna SC, Tibpromma S, Mortimer PE, Wanasinghe DN, Phookamsak R, Xu J, Wang Y, Tian F, Alvarado P, Li DW, Kušan I, Matočec N, Maharachchikumbura SSN, Papizadeh M, Heredia G, Wartchow F, Bakhshi M, Boehm E, Youssef N, Hustad VP, Lawrey JD, Santiago ALCMA, Bezerra JDP, Souza-Motta CM, Firmino AL, Tian Q, Houbraken J, Hongsanan S, Tanaka K, Dissanayake AJ, Monteiro JS, Grossart HP, Suija A, Weerakoon G, Etayo J, Tsurykau A, Vázquez V, Mungai P, Damm U, Li QR, Zhang H, Boonmee S, Lu YZ, Becerra AG, Kendrick B, Brearley FQ, Motiejūnaitė J, Sharma B, Khare R, Gaikwad S, Wijesundara DSA, Tang LZ, He MQ, Flakus A, Rodriguez-Flakus P, Zhurbenko MP, McKenzie EHC, Stadler M, Bhat DJ, Liu JK, Raza M, Jeewon R, Nassonova ES, Prieto M, Jayalal RGU, Erdoğdu M, Yurkov A, Schnittler M, Shchepin ON, Novozhilov YK, Silva-Filho AGS, Liu P, Cavender JC, Kang Y, Mohammad S, Zhang LF, Xu RF, Li YM, Dayarathne MC, Ekanayaka AH, Wen TC, Deng CY, Pereira OL, Navathe S, Hawksworth DL, Fan XL, Dissanayake LS, Kuhnert E, Grossart HP, Thines M (2020) Outline of Fungi and fungus-like taxa. Mycosphere 11:1060–1456
202. Winter G (1887) Die Pilze Deutschlands, Oesterreichs und der Schweiz. 2 Abt., Ascomyceten: Gymnoasceen und Pyrenomyceten. Rabenhorst's Kryptogamen-Flora von Deutschland, Oesterreich und der Schweiz 2:1–928
203. Wittstein K, Cordsmeier A, Lambert C, Wendt L, Sir EB, Weber J, Wurzler N, Petrini LE, Stadler M (2020) Identification of *Rosellinia* species as producers of cyclodepsipeptide PF1022 A and resurrection of the genus *Dematophora* as inferred from polythetic taxonomy. Stud Mycol 96:1–16
204. Wong HJ, Mohamad-Fauzi N, Rizman-Idid M, Convey P, Alias SA (2019) Protective mechanisms and responses of micro-fungi towards ultraviolet-induced cellular damage. Polar Sci 20:19–34
205. Xie X, Liu L, Zhang X, Long Q, Shen X, Boonmee S, Kang J, Li Q (2019) Contributions to species of *Xylariales* in China—2. *Rosellinia pervariabilis* and *R. tetrastigmae spp. nov*., and a new record of *R. caudata*. Mycotaxon 134:183–196
206. Yu Y, Harris AJ, Blair C, He X (2015) RASP (Reconstruct Ancestral State in Phylogenies): A tool for historical biogeography. Mol Phylogenet Evol 87:46–49
207. Yuan HS, Lu X, Dai YC, Hyde KD, Kan YH, Kušan I, He SH, Liu NG, Sarma VV, Zhao CL, Cui BK, Yousaf N, Sun G, Liu SY, Wu F, Lin CG, Dayarathne MC, Gibertoni TB, Conceição LB, Garibay-Orijel R, Villegas-Ríos M, Salas-Lizana R, Wei TZ, Qiu JZ, Yu ZF, Phookamsak R, Zeng M, Paloi S, Bao DF, Abeywickrama PD, Wei DP, Yang J, Manawasinghe IS, Harishchandra D, Brahmanage RS, de Silva NI, Tennakoon DS, Karunarathna A, Gafforov Y, Pem D, Zhang SN, de Azevedo Santiago ALCM, Bezerra JDP, Dima B, Acharya K, Alvarez-Manjarrez J, Bahkali AH, Bhatt VK, Brandrud TE, Bulgakov TS, Camporesi E, Cao T, Chen YX, Chen YY, Devadatha B, Elgorban AM, Fan LF, Du X, Gao L, Gonçalves CM, Gusmão LFP, Huanraluek N, Jadan M, Jayawardena Khalid AN, Langer E, Lima DX, de Lima-Júnior NC, de Lira CRS, Liu JK, Liu S, Lumyong S, Luo ZL, Matočec N, Niranjan M, Oliveira-Filho JRC, Papp V, Pérez-Pazos E, Phillips AJP, Qiu PL, Ren Y, Ruiz RFC, Semwal KC, Soop K, de Souza CAF, Souza-Motta CM, Sun LH, Xie ML, Yao YJ, Zhao Q, Zhou LW (2020) Fungal diversity notes 1277–1386: taxonomic and phylogenetic contributions to fungal taxa. Fungal Divers 104:1–266
208. Yuan ZQ, Zhao ZY (1992) *Anthostomella* on *Lonicera* in China. Sydowia 44:85–89
209. Zhang N, Castlebury LA, Miller AN, Huhndorf SM, Schoch CL, Seifert KA, Rossman AY, Rogers JD, Kohlmeyer J, Volkmann-Kohlmeyer B, Volkmann-Kohlmeyer B, Sung GH (2006) An overview of the systematics of the *Sordariomycetes* based on a four-gene phylogeny. Mycologia 98:1076–1087
210. Zhang ZF, Liu F, Zhou X, Liu XZ, Liu SJ, Cai L (2017) Culturable mycobiota from Karst caves in China, with descriptions of 20 new species. Persoonia 39:1–31
211. Zhaxybayeva O, Gogarten JP (2002) Bootstrap, Bayesian probability and maximum likelihood mapping: exploring new tools for comparative genome analyses. BMC Genomics 3:4
212. Zhou J, Li X, Huang PW, Dai CC (2018) Endophytism or saprophytism: Decoding the lifestyle transition of the generalist fungus *Phomopsis liquidambari*. Microbiol Res 206:99–112
213. Zhu L, Song J, Zhou JL, Si J, Cui BK (2019) Species diversity, phylogeny, divergence time, and biogeography of the genus *Sanghuangporus* (*Basidiomycota*). Front Microbiol 10:812

Tables

Table 1 Genes/DNA loci amplified in this study with respective PCR primers and protocols

Gene/loci	PCR primers (forward/reverse)	PCR protocol	References
ITS	ITS5/ITS4	94°C/30 s, 56°C/50 s, 72°C/60 s	White et al. (1990)
LSU	LR0R/LR5	94°C/30 s, 55°C/50 s, 72°C/60 s	Vilgalys and Hester (1990)
SSU	NS1/NS4	94°C/30 s, 54°C/50 s, 72°C/60 s	White et al. (1990)
*rpb*2	fRPB2-5f/fRPB2-7cR	95°C/45 s, 57°C/50 s, 72°C/90 s	Liu et al. (1999)
*tub*2	T1/T22	95°C/60 s, 54°C/110 s, 72°C/120 s	O'Donnell and Cigelnik (1997)
*tef*1	EF1-983F/EF1-2218R	94°C/30 s, 55°C/50 s, 72°C/60 s	Rehner and Samuels (1994)

Initial denaturation at 95°C for 5 min and final extension at 72°C for 10 min with 35 cycles for all gene regions

Table 2 GenBank accession numbers obtained in this study

Taxon	Specimen no.	Country	Host	ITS	LSU	*rpb2*	*tub2*	*tef1*	SSU
Acrocordiella photiniicola	MFLU 17-1552	Thailand	Unidentified	MW240627	MW240556	MW658617	MW775583	MW759507	–
Acrocordiella photiniicola	HKAS 102287	Thailand	Unidentified	MW240628	MW240557	–	MW775584	–	–
Allocryptovalsa sichuanensis	HKAS 107017	China	Unidentified	MW240633	MW240563	MW658624	MW775592	MW759517	MW2629
Amphisphaeria parvispora	MFLU 18-0767	Thailand	Unidentified	MW240644	MW240574	MW658631	MW775601	MW759532	–
Anthostomella lamiacearum	MFLU 18-0101	Thailand	*Lamiaceae sp.*	MW240669	MW240599	MW658648	–	–	–
Anthostomella lamiacearum	HKAS 102325	Thailand	*Lamiaceae sp.*	MW240670	MW240600	MW658649	–	–	–
Apiospora guiyangensis	HKAS 102403	China	Unidentified grass	MW240647	MW240577	MW658634	MW775604	MW759535	–
Apiospora sichuanensis	HKAS 107008	China	*Poaceae*	MW240648	MW240578	MW658635	MW775605	MW759536	–
Appendicospora hongkongensis	HKAS 107015	China	Palm	MW240651	MW240581	MW658638	MW775609	MW759539	MW2629
Biscogniauxia magna	MFLU 18-0850	Thailand	Unidentified	MW240616	MW240545	MW342620	MW775577	MW759498	–
Biscogniauxia petrensis	HKAS 102388	China	*Osmanthus sp.*	MW240615	MW240544	MW342619	MW775576	MW759497	–
Camillea tinctor	MFLU 18-0786	Thailand	*Bauhinia racemosa*	MW240614	MW240543	MW342618	MW775575	–	–
Diatrype disciformis	MFLU 17-1549	Italy	Unidentified	MW240629	MW240559	MW658621	–	MW759513	MW2629
Eutypa camelliae	HKAS 107022	China	*Camelia japonica*	MW240634	MW240564	MW658625	MW775593	MW759518	–
Eutypa camelliae	MFLU 20-0182HT	China	*Camelia japonica*	MW240635	MW240565	–	MW775594	MW759519	–
Fasciatispora cocoes	MFLU 19-2143	Thailand	*Cocos nucifera*	MW240618	MW240547	MW658611	MW775578	MW759499	MW2629
Fasciatispora cocoes	HKAS 107000	Thailand	*Cocos nucifera*	MW240619	MW240548	MW658612	MW775579	MW759500	–
Helicogermslita clypeata	MFLU 18-0852	Thailand	Unidentified	MW240666	MW240596	MW658647	MW775614	MW759549	–
Helicogermslita clypeata	HKAS 102321	Thailand	Unidentified	MW240667	MW240597	–	MW775615	MW759550	–
Hypocopra zeae	MFLU 18-0809	Thailand	*Zea mays*	MW240671	MW240601	MW658650	MW775616	MW759551	–
Lopadostoma quercicola	MFLU 17-0731	Italy	*Quercus cerris*	MW240637	MW240567	MW658627	MW775597	MW759522	–
Lopadostoma quercicola	MFLU 17-0843	Italy	*Quercus sp.*	MW240638	MW240568	MW658628	MW775598	–	–
Lopadostoma quercicola	MFLU 17-0940	Italy	*Quercus sp.*	MW240639	MW240569	MW658629	MW775599	MW759523	–
Magnostiolata mucida	MFLU 19-2133	Thailand	Bamboo	MW240673	MW240603	MW658652	MW775618	MW759553	MW2629
Melanostictus longiostiolatus	MFLU 19-2146	Thailand	Unidentified	MW240636	MW240566	MW658626	MW775595	MW759520	MW2629
Melanostictus thailandicus	MFLU 19-2123	Thailand	Unidentified	MW240630	MW240560	MW658622	MW775590	MW759514	–
Melogramma campylosporum	MFLU 17-0348	Italy	*Corylus avellana*	MW240645	MW240575	MW658632	MW775602	MW759533	–
Melogramma campylosporum	MFLU 18-0778	Russia	*Corylus avellana*	MW240646	MW240576	MW658633	MW775603	–	–
Nemania delonicis	MFLU 19-	Thailand	*Delonix regia*	MW240613	MW240542	MW342617	MW775574	MW759496	MW2629

	2124								
Nemania longipedicellata	MFLU 18-0819	Thailand	*Camelia sinensis*	MW240612	MW240541	MW342616	MW775573	MW759495	–
Nemania paraphysata	MFLU 19-2121	Thailand	Unidentified	MW240609	MW240538	MW342613	–	MW759492	–
Nemania thailandensis	MFLU 19-2122	Thailand	Unidentified	MW240610	MW240539	MW342614	MW775571	MW759493	MW2629
Nemania thailandensis	MFLU 19-2117	Thailand	Unidentified	MW240611	MW240540	MW342615	MW775572	MW759494	–
Neoamphisphaeria hyalinospora	MFLU 19-2131	Thailand	Unidentified	MW240649	MW240579	MW658636	MW775607	MW759537	–
Neoamphisphaeria hyalinospora	HKAS 106988	Thailand	Unidentified	MW240650	MW240580	MW658637	MW775608	MW759538	–
Neoanthostomella bambusicola	MFLU 18-0796	Thailand	Bamboo	MW240657	MW240587	MW658641	MW775610	MW759543	–
Nigropunctata bambusicola	MFLU 19-2134	Thailand	Bamboo	MW240662	MW240592	MW658644	–	MW759547	–
Nigropunctata bambusicola	MFLU 19-2145	Thailand	Bamboo	MW240664	MW240594	MW658646	–	MW759548	–
Nigropunctata nigrocircularis	MFLU 19-2130	Thailand	Bamboo	MW240661	MW240591	–	MW775612	MW759546	–
Nigropunctata thailandica	MFLU 19-2118	Thailand	Bamboo	MW240659	MW240589	MW658643	–	MW759544	MW2629
Nigropunctata thailandica	HKAS 106975	Thailand	Bamboo	MW240660	MW240590	–	–	MW759545	–
Occultitheca rosae	HKAS 102393	China	*Rosa sp.*	MW240672	MW240602	MW658651	MW775617	MW759552	–
Paravamsapriya ostiolata	MFLU 18-0761	Thailand	Bamboo	MW240624	MW240553	–	MW775581	MW759505	–
Paravamsapriya ostiolata	MFLU 18-0813	Thailand	Bamboo	MW240625	MW240554	–	MW775582	–	–
Paraxylaria xylostei	MFLU 17-1636	Italy	*Lonicera sp.*	MW240640	MW240570	–	MW820914	MW759524	–
Paraxylaria xylostei	MFLU 17-1645	Italy	*Lonicera sp.*	MW240641	MW240571	–	MW820915	MW759525	–
Paraxylaria xylostei	HKAS 102313	Italy	*Lonicera sp.*	MW240642	MW240572	–	MW820916	–	–
Peroneutypa leucaenae	MFLU 18-0816	Thailand	*Leucaena leucocephala*	MW240631	MW240561	–	MW775591	MW759515	–
Pseudoanthostomella pini-nigrae	MFLU 18-0877	UK	Unidentified	MW240654	MW240584	MW658639	MW820918	MW759541	–
Pseudoanthostomella pini-nigrae	MFLU 15-3608	Italy	*Cytisus sp.*	MW240655	MW240585	MW658640	MW820919	MW759542	–
Pseudoanthostomella pini-nigrae	HKAS 102309	Italy	*Cytisus sp.*	MW240656	MW240586	–	MW820920	–	–
Rosellinia britannica	MFLU 17-0302	Italy	*Hedera helix*	MW240605	MW240534	MW342609	MW775568	MW759490	–
Rosellinia britannica	HKAS 102349	Italy	*Hedera helix*	MW240606	MW240535	MW342610	MW775569	–	–
Rosellinia britannica	MFLU 17-0987	Italy	*Hedera helix*	MW240607	MW240536	MW342611	MW775570	–	–
Rosellinia markhamiae	MFLU 19-2137	Thailand	Unidentified	MW240608	MW240537	MW342612	–	MW759491	–
Seiridium italicum	MFLU 16-1315	Italy	Unidentified	MW240643	MW240573	MW658630	MW775600	MW759527	–
Vamsapriya mucosa	MFLU 18-0103	Thailand	Bamboo	MW240622	MW240551	MW658614	MW775580	MW759503	–
Xenoanthostomella chromolaenae	MFLU 18-0840	Thailand	*Nehrolepis sp.*	MW240668	MW240598	–	–	–	–

**Amphisphaeria camelliae*	HKAS 107021	China	*Camellia japonica*	–	–	–	–	MW759530	–
**Amphisphaeria curvaticonidia*	MFLU 18-0789	Thailand	Unidentified	–	–	–	–	MW759529	–
**Amphisphaeria flava*	MFLU 18-0102	Thailand	Unidentified	–	–	–	–	MW759528	–
**Amphisphaeria micheliae*	HKAS 107012	China	*Magnolia alba*	–	–	–	–	MW759531	–
**Anthostomella formosa*	MFLUCC 14-0170	Italy	*Pinus sylvestris*	MW240652	MW240582	–	MW820917	MW759540	–
**Anthostomella helicofissa*	MFLUCC 14-0173	Italy	*Cornus sanguinea*	MW240653	MW240583	–	–	–	–
**Arthrinium phragmites*	MFLU 17-0310	Italy	*Arundo plinii*	–	–	–	MW775606	MW759534	–
**Diatrypella tectonae*	MFLU 15-3430	Thailand	*Tectona grandis*	–	–	MW658618	MW775585	MW759508	–
**Eutypa flavovirens*	MFLU 15-0741	Thailand	Unidentified	–	–	–	MW775588	MW759511	–
**Eutypa linearis*	MFLU 15-1186	Thailand	Bamboo	–	–	MW658619	MW775586	MW759509	–
**Eutypa linearis*	MFLUCC 15-0198	Thailand	Bamboo	–	MW240558	MW658620	MW775587	MW759510	–
**Hypomontagnella monticulosa*	MFLU 18-0822	Thailand	*Leucaena leucocephala*	–	–	–	–	MW820912	–
**Induratia thailandica*	MFLU 18-0784	Thailand	Unidentified	–	–	–	–	MW759555	–
**Induratia ziziphi*	MFLU 18-0105	Thailand	*Ziziphus sp.*	–	–	–	–	MW759556	–
**Lopadostoma gastrinum*	MFLU 17-0941	Italy	*Quercus sp.*	–	–	–	MW775596	MW759521	–
**Monochaetia ilexae*	HKAS 92492	China	*Ilex sp.*	–	–	–	–	MW759526	–
**Peroneutypa diminutiasca*	MFLU 17-1187	Thailand	Unidentified	–	–	–	MW775589	MW759512	–
**Pseudoanthostomella senecionicola*	MFLUCC 15-0013	Italy	*Senecio sp.*	MW240674	MW240604	MW658653	MW820913	MW759554	–
**Vamsapriya khunkonensis*	MFLUCC 11-0475	Thailand	*Dendrocalamus giganteus*	MW240620	MW240549	–	–	MW759501	–

"-" Sequences were not obtained; "*" Regenerated sequences from previously published taxa.

Table 3 Characters used in ancestral character state analysis

Character	Description
Character 1	Aggregated ascomata in a conspicuous, stalked or sessile, carbonaceous stroma (e.g. *Xylaria*, *Daldinia*)
Character 2	Aggregated ascomata in a conspicuous, erumpent, effuse, bipartite, carbonaceous stroma with a smooth surface (e.g. *Biscogniauxia*, *Camillea*)
Character 3	Aggregated or single ascomata in a conspicuous, pulvinate, discoid, effused-pulvinate, unipartite, carbonaceous stroma (e.g. *Hypoxylon*)
Character 4	Aggregated or single ascomata in a semi-immersed, erumpent or superficial, pseudostroma (e.g. *Datrype*, *Furfurella*, *Lopadostoma*, *Melogramma*)
Character 5	Mostly single ascomata in an erumpent or superficial carbonaceous stroma (e.g. *Astrocystis*, *Rosellinia*)
Character 6	Aggregated or single ascomata, mostly immersed or semi-immersed, inconspicuous, prominent or rudimentary carbonaceous clypeus (e.g. *Amphisphaeria*, *Anthostomella*, *Arthrinium*, *Seiridium*)
Character 7	Aggregated or single, superficial or semi immersed ascomata (e.g. *Iodosphaeria*, *Leptosillia*)

Table 4 Synopsis of related anthostomella-like taxa in Clade Xy24

Species	Ascomata (μm)	Peridium (μm)	Paraphyses (μm)	Asci (μm)	Ascospors (μm)	Apical ring (μm)	Germ slit	Sheath
An. helicofissa	150–195 × 170–200	12–18.5	3.5	80–92 × 7.2–8.6	9.5–13.5 × 4–5	J+, 1.2 × 2.4	sigmoid	no
An. lamiacearum	130–180 × 105–135	16–23	2–3	65–85 × 5–6.5	9–11.5 × 3–5	J+	sigmoid	no
An. limitata	125–207 × 104–220	16	2	66–95 × 6–8	8–12 × 4–5	J+, 1 × 3	sigmoid	no
An. spiralis	165–275 × 170–285	7.5–14.5	2.5–3.8	95–142.5 × 9.5–11.3	12–14.5 × 5–5.5	J+, 3.1–5	sigmoid	have
An. xuanenesis	185–218 × 202–240	10–30	2.4–4	74–106 × 6–7.6	12–17 × 4–5.6	J+, 1.2-1.6 × 2.8-4	sigmoid, not full-length	no
Ant. brabeji	500 × 530	30–37.5	1.5–2.5	105–122.5 × 6–8	14.5–16 × 5–6	J+, 1.5–2 × 2–2.5	not observed	no
"*Neo. ficî*"	100–150 × 80–120	12–18	2.5–3	60–70 × 5–6	10–12 × 4–5	J+	sigmoid	no
"*Neo. viticola*"	160–203 × 180–225	34-53	2.5–3.4	85–117 × 5–7	5.7–11 × 3.4–4.8	J+	sigmoid	no

Table 5 Synopsis of related anthostomella-like taxa in Clade Xy25

Species	Ascomata (μm)	Peridium (μm)	Paraphyses (μm)	Asci (μm)	Ascospores (μm)	Ascospores L/W	Sheath (μm)	Host
An. thailandica	150–200 × 140–155	14–22	4.2–6.5	87–118 × 14.1–17.8	12–17 × 5.5–9	2.14	2.6–4.4	Grass
Ant. forlìcesenica	250–280 × 200–250	15–20	5	95–120 × 13–16	13–15 × 6–7	2.23	1.5–3.8	*Spartium junceum*
Ps. conorum	250 ×330	15-22.5	4-5	125-150 × 14-15	14–19 × 7.5–10	1.96	2–3	*Salix* sp., *Helleborus, Artemisia, Pinus sylvestris*, *Galium fruticosum*, *Urginea maritima*, *Coronilla glauca*, *Mesembryanthemum edule*, *Cytisus fontanensius*, *Laurus nobilis*
Ps. delitescens	340-360 × 285-320	18-30	4-5	120-145 × 10-15	14–17 × 8–10	1.6	2.9–3.1	*Pinus nigra*
Ps. pini-nigrae	250-275 × 330-350	17-25	5	90-120 × 11-13.5	10–15 × 8.5–12	1.4	3–3.4	*Pinus nigra*
Ps. pini-nigrae (MFLU 15-3608)	230–305 × 235–320	21–30	2.8–4.8	95–125 × 10–13.5	12.5–16 × 7.5–9	1.75	2–3	*Cytisus* sp.
Ps. pini-nigrae (MFLU 18-0877)	265–335 × 315–345	32–40	3.8–4.8	100–120 × 11–14.5	11–15 × 7–9.5	1.55	2.4–4	Phormium-like
Ps. senecionicola	160-215 × 206-240	18-20	3-4	70-98 × 14-17	10–16 × 8–10	1.66	3.2–4	*Senecio* sp.

Figures

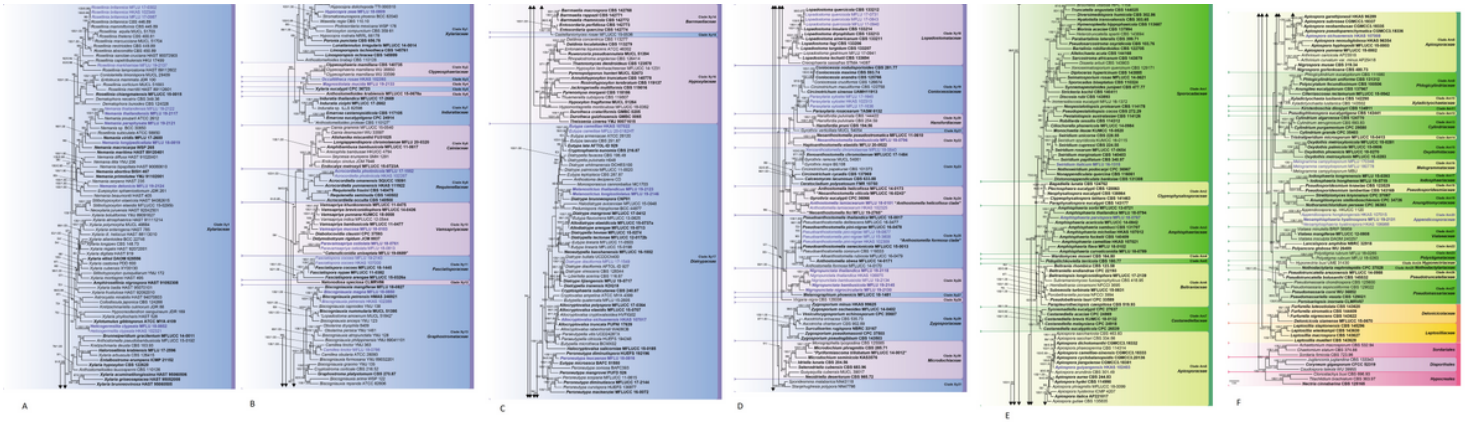

Figure 1

Phylogram generated from maximum likelihood analysis based on combined ITS-LSU-rpb2-tub2-tef1 sequence data. Four hundred seventy-eight strains are included in the combined sequence analyses, which comprise 4830 characters with gaps. Single gene analyses were also performed and topology and clade stability compared from combined gene analyses. Nine taxa from Diaporthales, Hypocreales and Sordariales are used as out group taxa. Tree topology from ML analysis was similar to BI analysis. The best scoring RAxML tree with a final likelihood value of −233649.5773 is presented. The matrix had 2174 (45.01% of all sites) number of constant or ambiguous constant, 2178 number of parsimony informative sites and 3303 number of distinct site patterns. Estimated base frequencies were as follows; A = 0.2702, C = 0.2562, G = 0.2394, T = 0.2342; substitution rates AC = 0.9872, AG = 2.6813, AT = 1.0632, CG = 1.2043, CT = 5.5710, GT = 1.000; gamma distribution shape parameter α = 0.492847. Bootstrap support values for ML equal to or greater than 60%, PP equal to or greater than 0.9 (ML/PP) are given above or below the nodes. The newly generated sequences are in blue. Type collections are in bold.

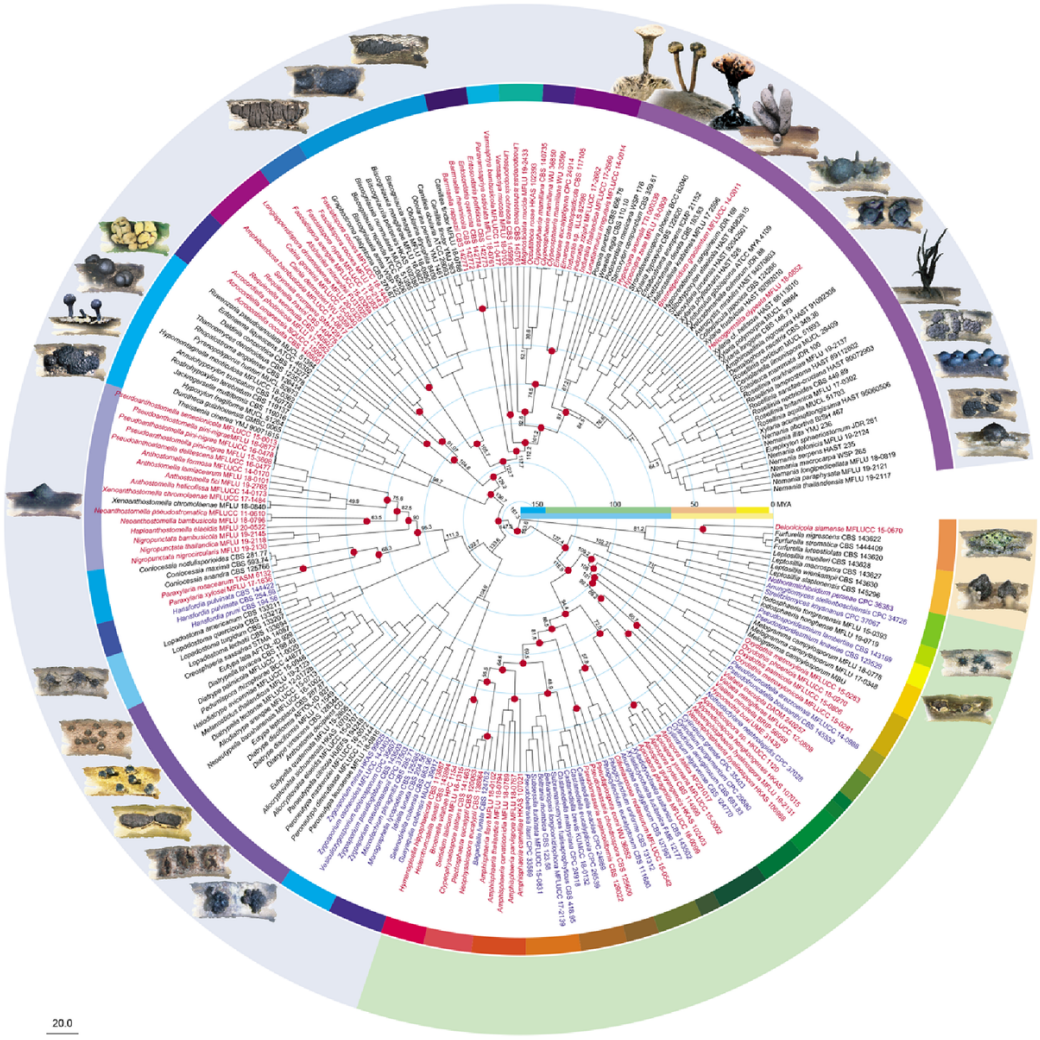

Figure 2

Ancestral character state analysis focusing on stromatic characters in Xylariomycetidae, using Bayesian Binary MCMC method. Taxa with the Character 6 are shown in red, and unknown character are shown in blue. Dark red dots in nodes show the highest percentage of the node distribution with stromatic Character 6. The respective colour code represents each family in three orders, Amphisphaeriales (green), Delonicicolales (orange) and Xylariales (blue). Selected stromatic characters are given modified from previous publications (Deepna Latha and Manimohan 2012; Daranagama et al. 2018; Voglmayr et al. 2019a; Becker et al. 2020; Konta et al. 2020).

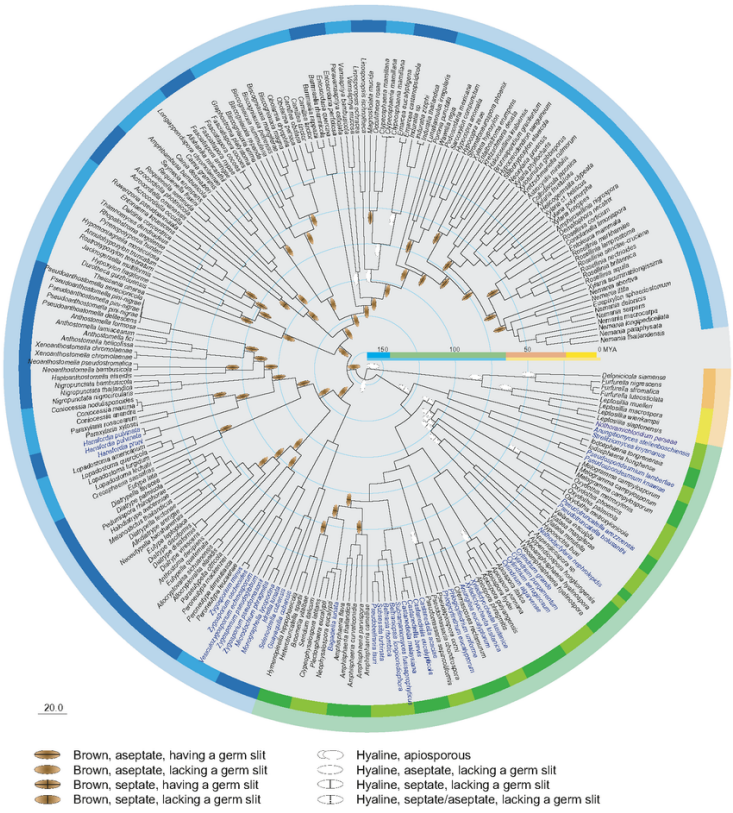

Figure 3

Ancestral character state analysis focusing on ascospore characters in Xylariomycetidae, using Bayesian Binary MCMC method. Taxa with unidentified sexual morph are shown in blue. Ascospore character is given in nodes based on the highest percentage of the node distribution according to the legend. The respective colour code represents each family in three orders, Amphisphaeriales (green), Delonicicolales (orange) and Xylariales (blue).

Figure 4

Amphisphaeria parvispora (MFLU 18-0767, holotype). a Substrate. b,c Ascomata in dead substrate. d Section through ascoma. e Peridium. f Section through ostiole. g Paraphyses. h–l Asci. m Apical ring blueing in Melzer's reagent. n–u Ascospores. Scale bars: a = 1 cm, b,c = 1000 µm, d = 100 µm, e,f,h–l = 20 µm, m–u = 10 µm, g = 5 µm.

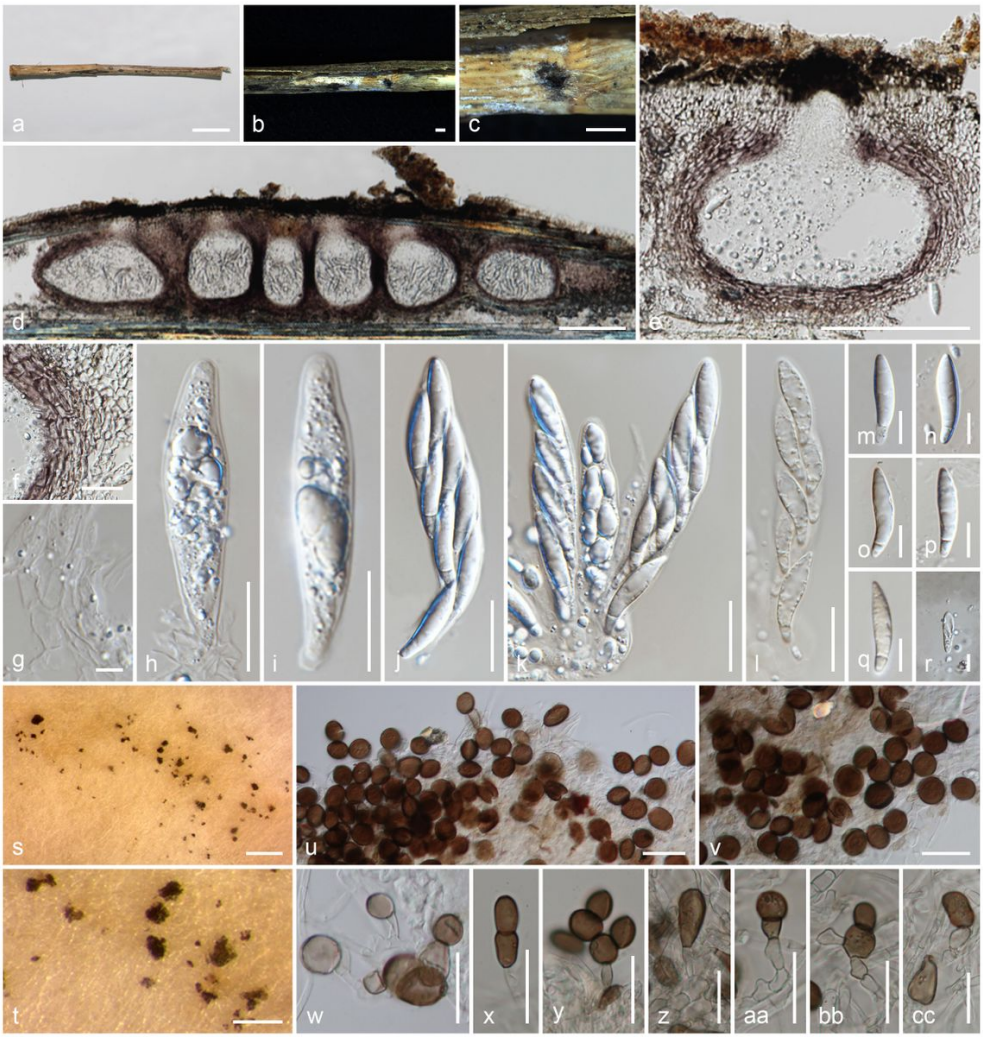

Figure 5

Apiospora guiyangensis (HKAS 102403, holotype; CGMCC3.20365, ex-type living culture). a Substrate. b,c Stroma in dead substrate. d Longitudinal section through stroma. e Section through ascoma. f Peridium. g Paraphyses. h–l Asci (l in Melzer's reagent). m–r Ascospores (r in Indian ink). s,t Conidiomata in culture. u–cc Conidia and conidiogenous cells. Scale bars: a = 1 cm, b,c = 1000 µm, s = 500 µm, t = 200 µm, d,e = 100 µm, f,h–l,u–cc = 20 µm, m–r = 10 µm, g = 5 µm.

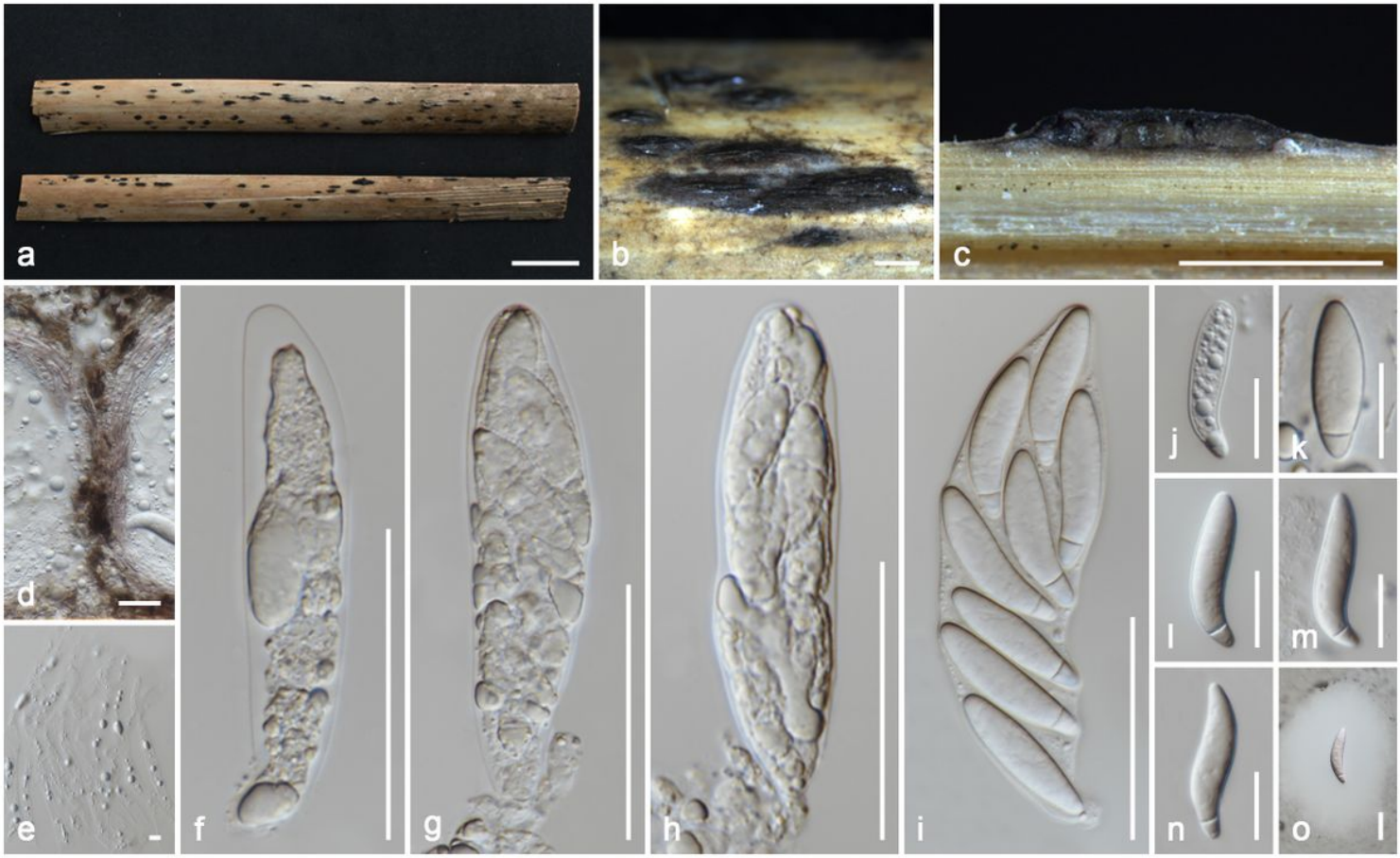

Figure 6

Apiospora sichuanensis (HKAS 107008, holotype). a Substrate. b Stroma in dead substrate. c Longitudinal section through stroma. d Peridium. e Paraphyses. f–i Asci. j–o ascospores (o in Indian ink). Scale bars: a = 1 cm, b,c = 1000 µm, f–i = 50 µm, d,j–o = 20 µm, e = 5 µm.

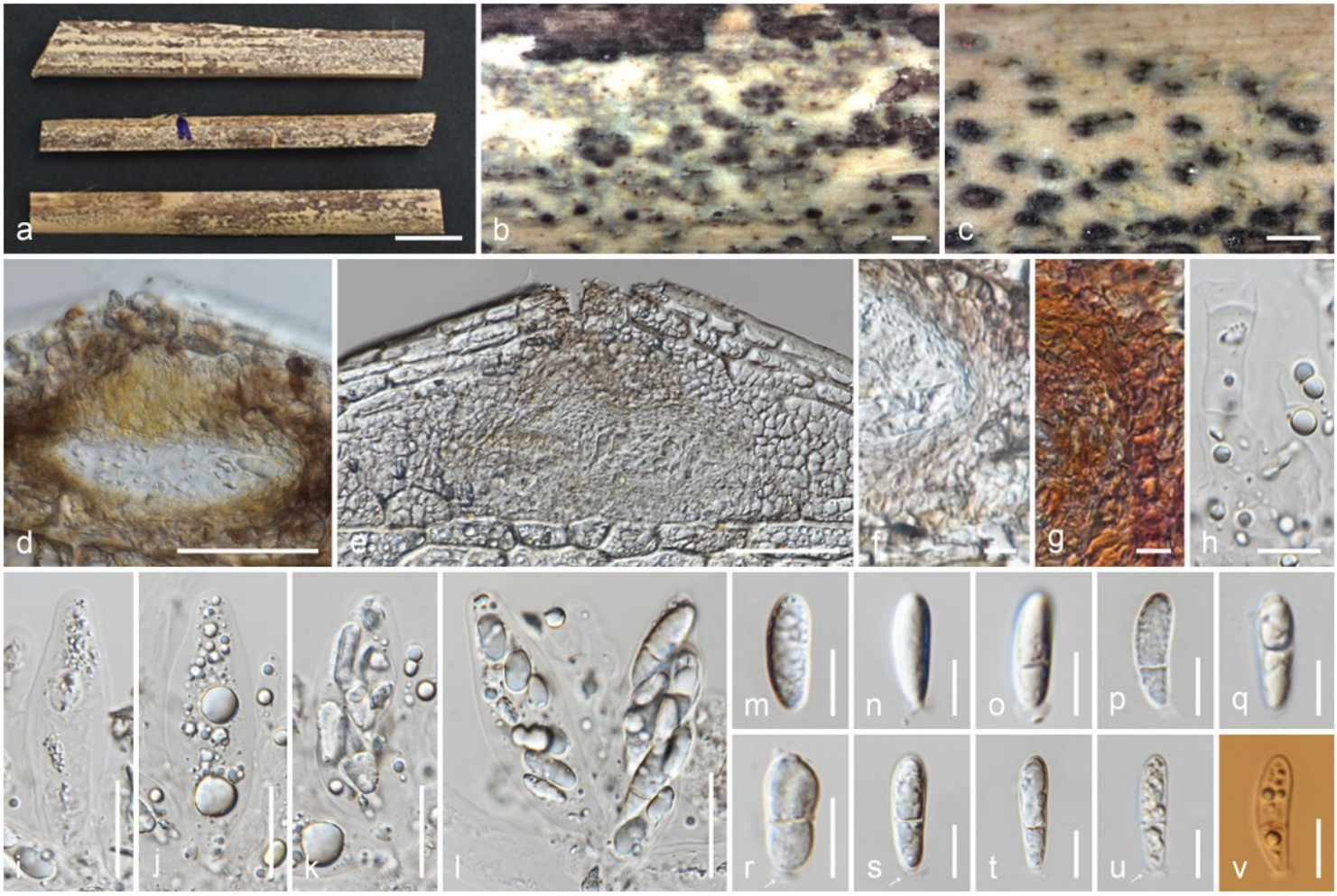

Figure 7

Appendicospora hongkongensis (HKAS 107015, reference specimen). a Substrate. b,c Ascomata in dead substrate. d,e Section through ascoma. f,g Peridium (g in Congo red). h Paraphyses. i–l Asci. m–v Ascospores (v in Congo red). Scale bars: a = 1 cm, b,c = 500 µm, d,e = 50 µm, i–l = 20 µm, f–h,m–v = 10 µm.

Figure 8

Neoamphisphaeria hyalinospora (MFLU 19-2131, holotype). a Substrate. b,c Ascomata in dead substrate. d,e Section through ascoma. f Peridium. g Paraphyses. h–l Asci. m Apical ring in Melzer's reagent. n Apical ring in Congo red. o–r Ascospores (r in Melzer's reagent). Scale bars: a = 1 cm, b,c = 1000 µm, d,e = 100 µm, f,h–l = 20 µm, g,m–r = 10 µm.

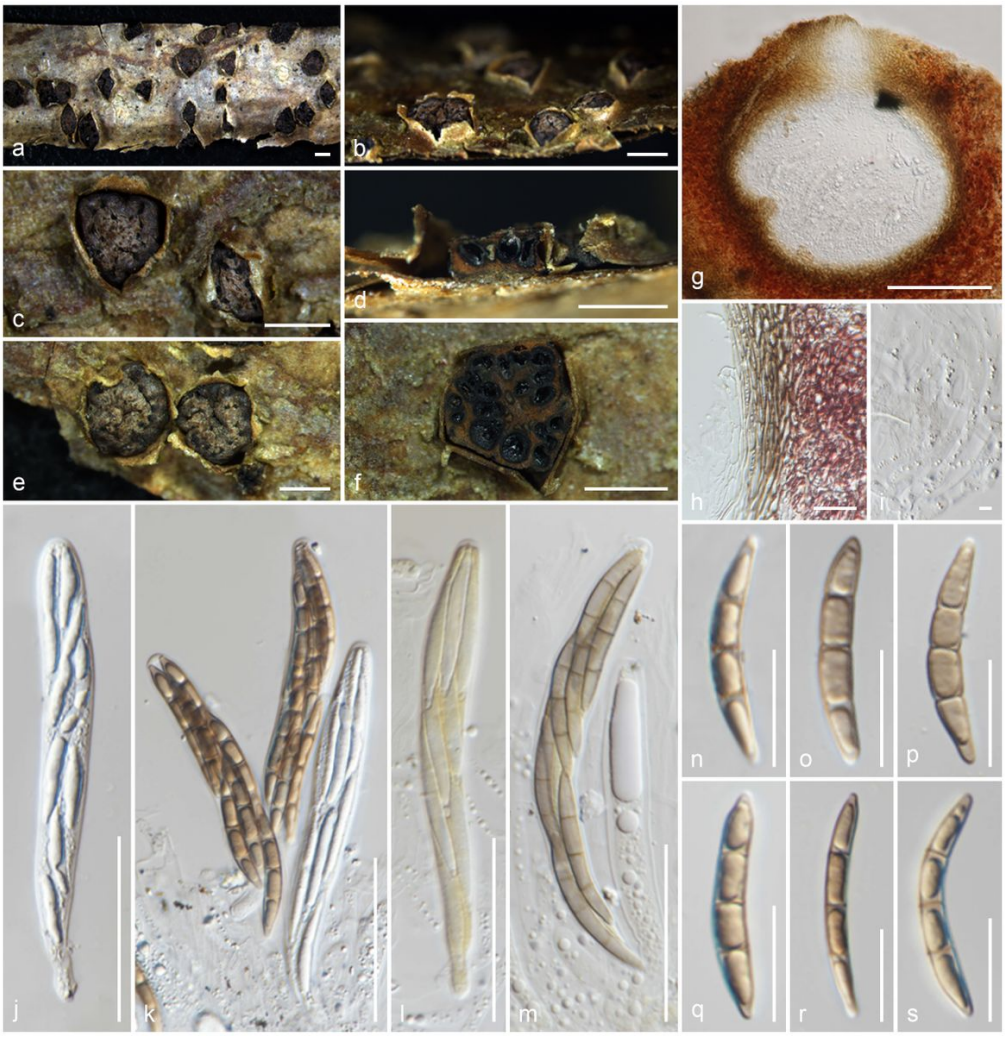

Figure 9

Melogramma campylosporum (MFLU 17-0348). a Substrate. b,c,e Stromata in dead substrate. d,f Sections through stroma (d vertical, f horizontal). g Section through ascoma. h Peridium. i Paraphyses. j–m Asci (l,k in Melzer's reagent). n–s Ascospores. Scale bars: a–f = 1000 µm, g = 100 µm, j–m = 50 µm, h,n–s = 20 µm, i = 5 µm.

Figure 10

Seiridium italicum (MFLU 16-1315, holotype). a Substrate, b,c Ascomata in dead substrate. d Section through ascoma. e Peridium. f Section through ostiole. g Paraphyses. h–l Asci. m–t Ascospores (t in Melzer's reagent). Scale bars: a–b = 1000 µm, d = 100 µm, e,f,h–l = 20 µm, m–t = 10 µm, g = 5 µm.

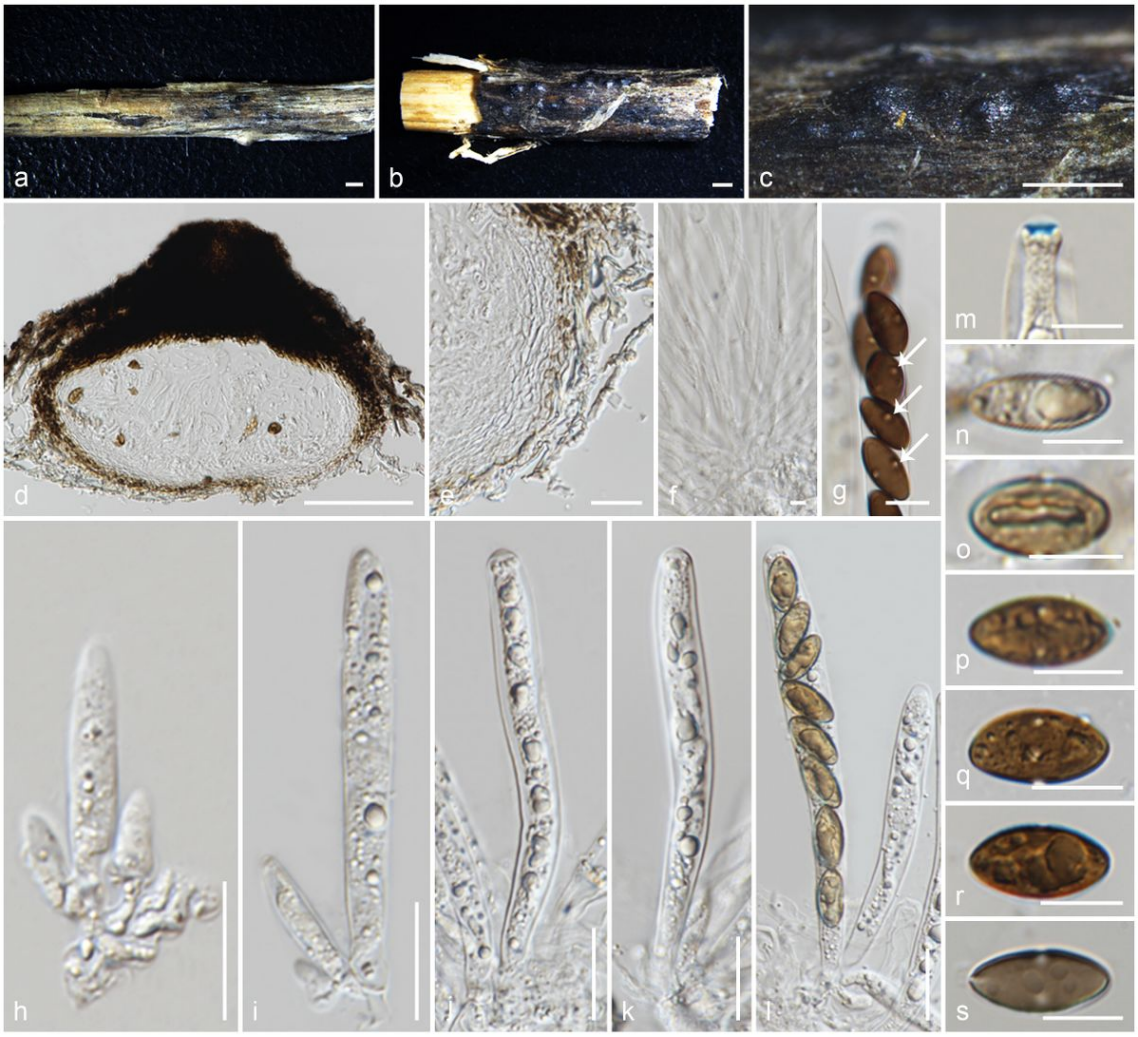

Figure 11

Paraxylaria xylostei (MFLU 17-1636). a Substrate, b,c Ascomata in dead substrate. d Section through ascoma. e Peridium. f Paraphyses. g–l Asci (g in Melzer's reagent, white arrows show germ pores). m Apical ring blueing in Melzer's reagent. n–s Ascospores. Scale bars: a–c = 1000 µm, d = 100 µm, e,h–l = 20 µm, g,m–s = 10 µm, f = 5 µm.

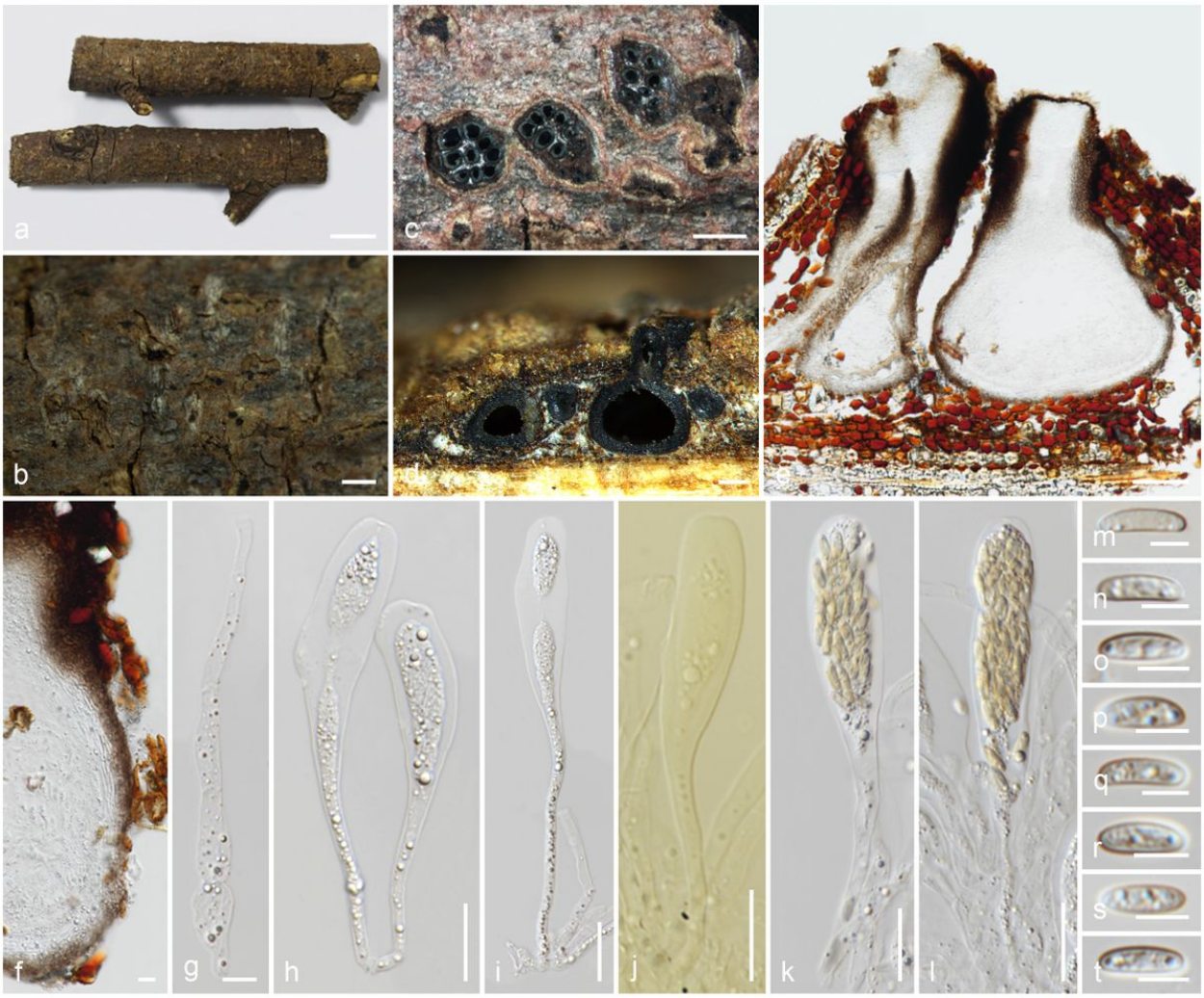

Figure 12

Allocryptovalsa sichuanensis (HKAS 107017, holotype). a Substrate. b Ascomata in wood. c–e Sections through ascomata (c horizontal, d vertical). f Peridium. g Paraphyses. h–l Asci (j in Melzer's reagent). m–t Ascospores. Scale bars: a = 1 cm, b,c = 1000 µm, d = 200 µm, e = 100 µm, f,h–l = 20 µm, g = 10 µm, m–t = 5 µm.

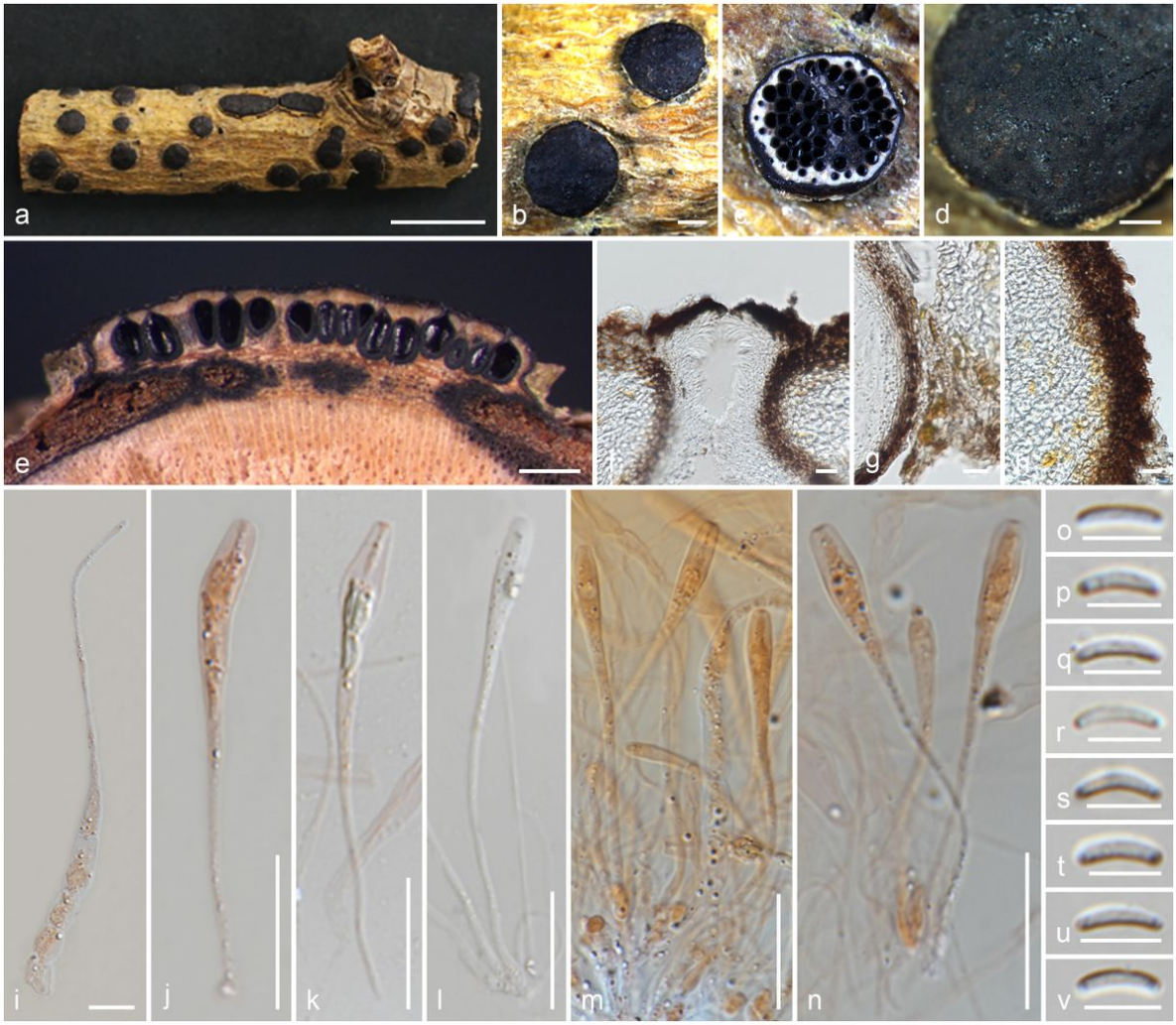

Figure 13

Diatrype disciformis (MFLU 17-1549). a Substrate. b,d Stromata in dead substrate. c,e Section through stroma (c horizontal, e vertical). f Section through ostiole. g Peridium. h Stroma wall. i Paraphyses (in Congo red). j–n Asci (i–k,m,n in Congo red). o–v Ascospores. Scale bars: a = 1 cm, b = 1000 µm, c–e = 500 µm, j–n = 20 µm, f–h,i = 10 µm, o–v = 5 µm.

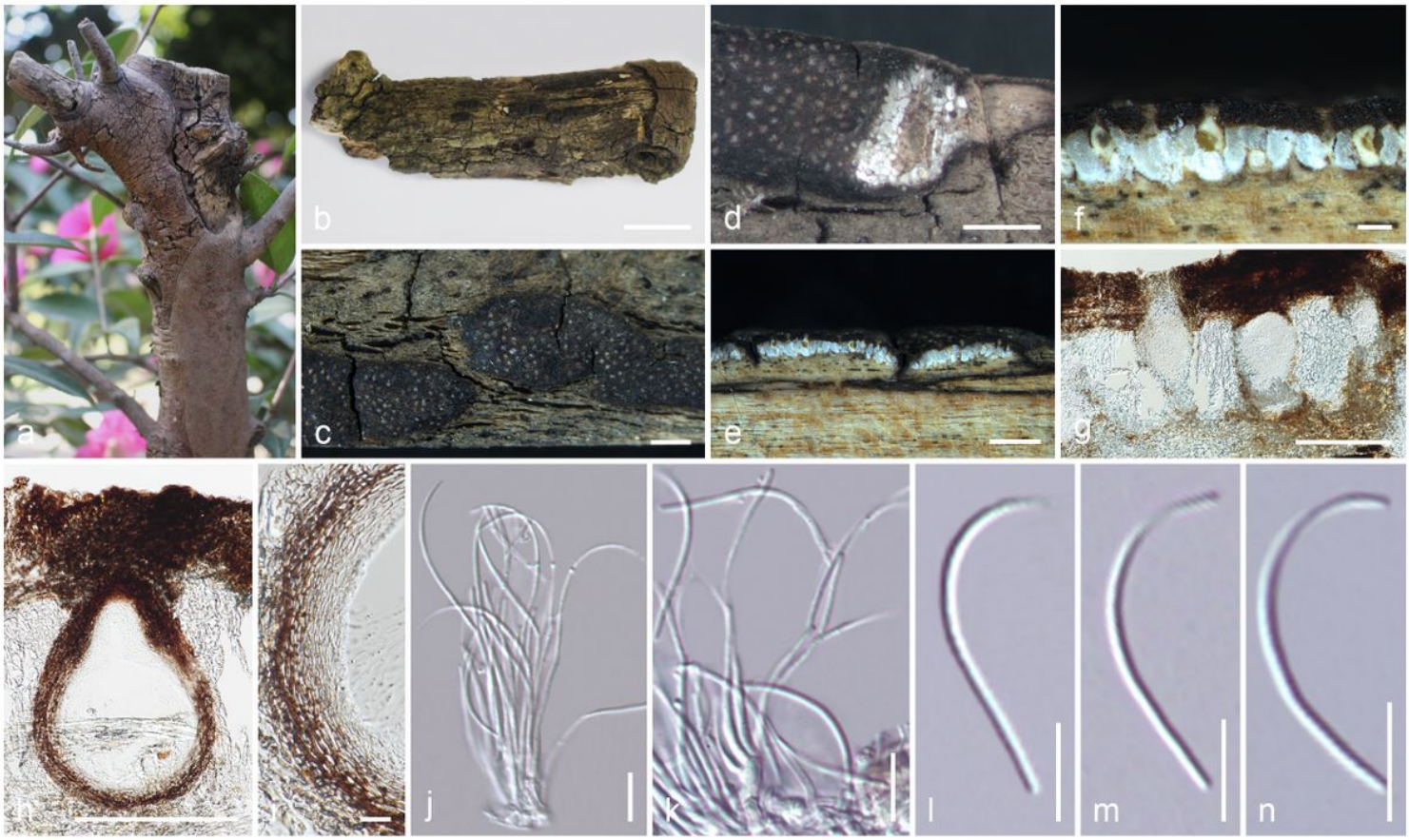

Figure 14

Eutypa camelliae (HKAS 107022, holotype). a Host (Camellia japonica). b Substrate. c,d Stromata in dead substrate. e–h Section through stroma. i Peridium of ascomata. j,k Conidiophores and conidia on stromata. l–n Conidia. Scale bars: b = 1 cm, c–e = 1000 µm, f–h = 200 µm, i = 20 µm, j–n = 10 µm.

Figure 15

Melanostictus longiostiolatus (MFLU 19-2146, holotype). a Substrate. b Ascomata in dead substrate. c–e Section through ascomata (c horizontal, d,e vertical). f Peridium. g Paraphyses. h–k Asci. l Apical ring. m–p Ascospores (o,p in Congo red). Scale bars: a = 1 cm, b,c = 1000 µm, d,e = 200 µm, f,h–k = 20 µm, g,l = 10 µm, m–p = 5 µm.

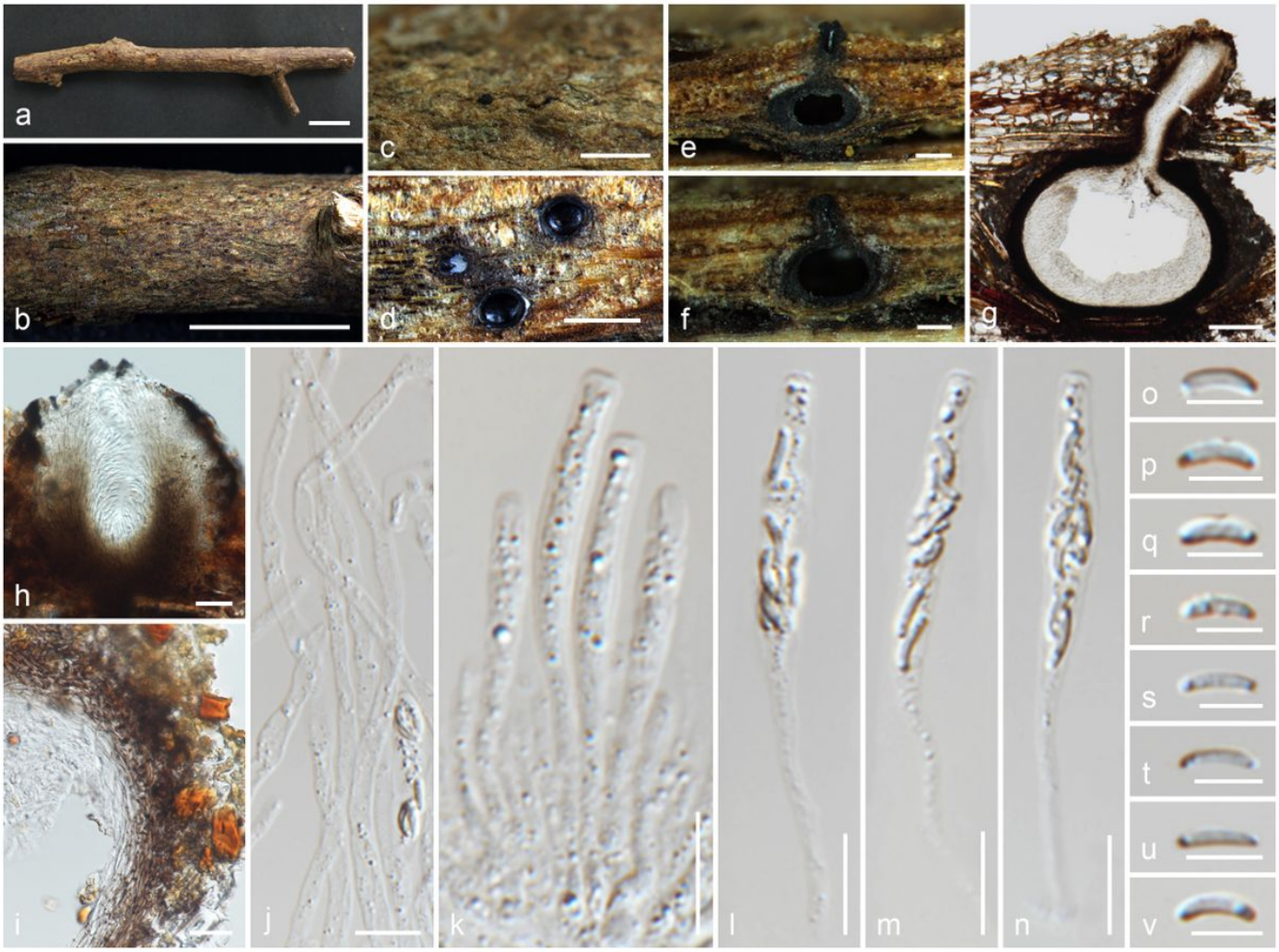

Figure 16

Melanostictus thailandicus (MFLU 19-2123, holotype). a Substrate. b,c Ascomata in dead substrate. d–g Sections through ascomata (d in horizontal, e–g in vertical). h Section through ostiole. i Peridium. j Paraphyses. k–n Asci. o–v Ascospores. Scale bars: a,b = 1 cm, c,d = 1000 µm, e,f = 200 µm, g = 100 µm, h,i = 20 µm, j–n = 10 µm, o–v = 5 µm.

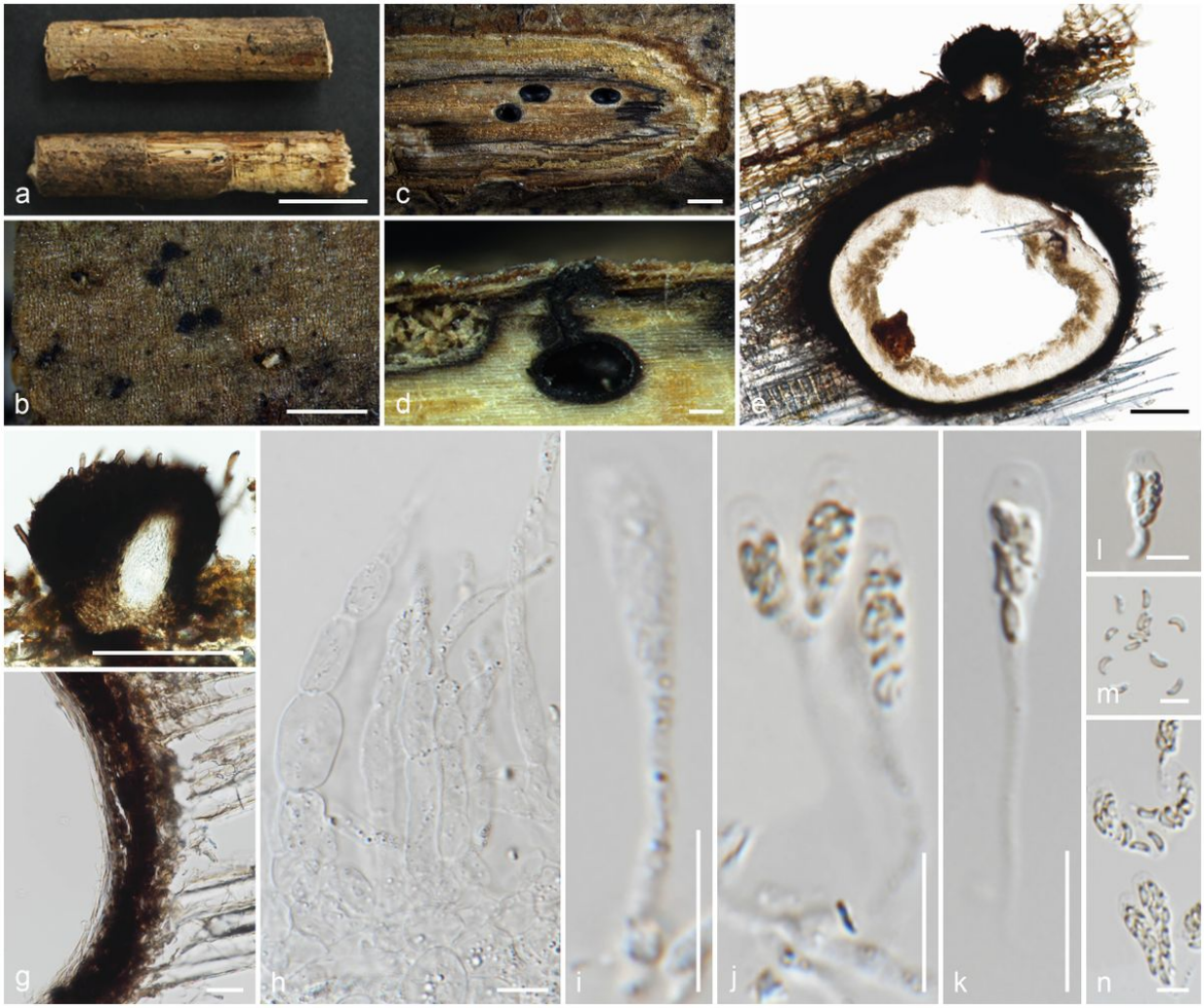

Figure 17

Peroneutypa leucaenae (MFLU 18-0816, holotype). a Substrate, b Ascomata in dead substrate, c–e Section through ascomata (c horizontal, d,e vertical), f Section through the ostiole. g Peridium. h Paraphyses. i–k Asci. l Apical ring blueing in Melzer's reagent. m,n Ascospores. Scale bars: a = 1 cm, b,c = 1000 µm, d = 200 µm, e,f = 100 µm, g = 20 µm, h–k = 10 µm, l–n = 5 µm.

Figure 18

Fasciatispora cocoes (MFLU 19-2143). a Substrate. b,c Ascomata in dead substrate. d,e Section through ascoma. f Peridium. g Paraphyses. h–m Asci. n Apical ring blueing in Melzer's reagent. o–u Ascospores (o in Indian ink). Scale bars: a = 1 cm, c = 1000 µm, d,e = 100 µm, h–m = 20 µm, f,n–u = 10 µm, g = 5 µm.

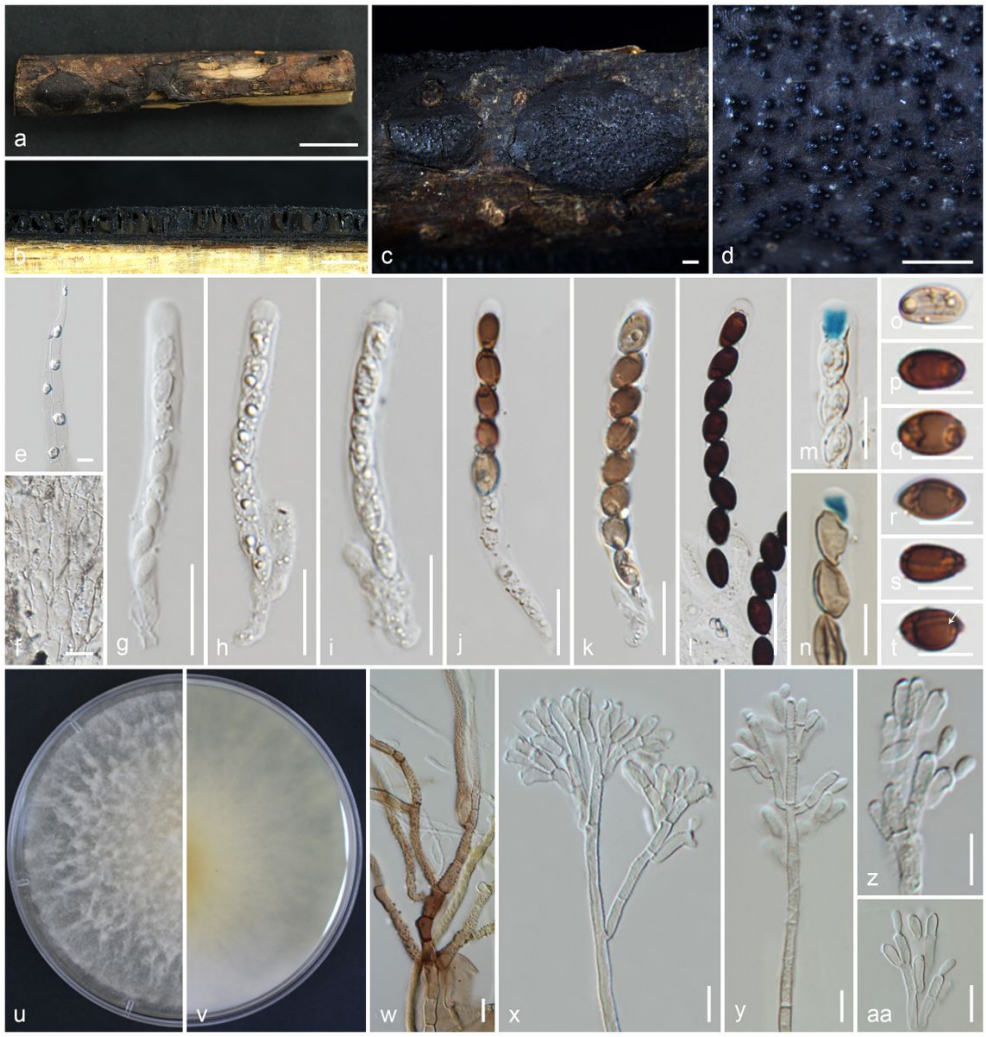

Figure 19

Biscogniauxia magna (MFLU 18-0850, holotype; MFLUCC 17-2665, ex-type living culture). a Substrate. b Section through stroma showing ascomata. c,d Stromatal surface. e Paraphyses. f Inner layer of the peridium. g–l Asci (paraphyses in f). m,n Apical ring blueing in Melzer's reagent. o–t Ascospores (germ slit shows in white arrow), u Upper view. v Reverse view of the one-week-old colony on PDA. w–aa Conidia, conidiogenous cells, and conidiophores. Scale bars: a = 1 cm, b–d = 1000 µm, g–l = 20 µm, e,f,m–t,w–aa = 10 µm.

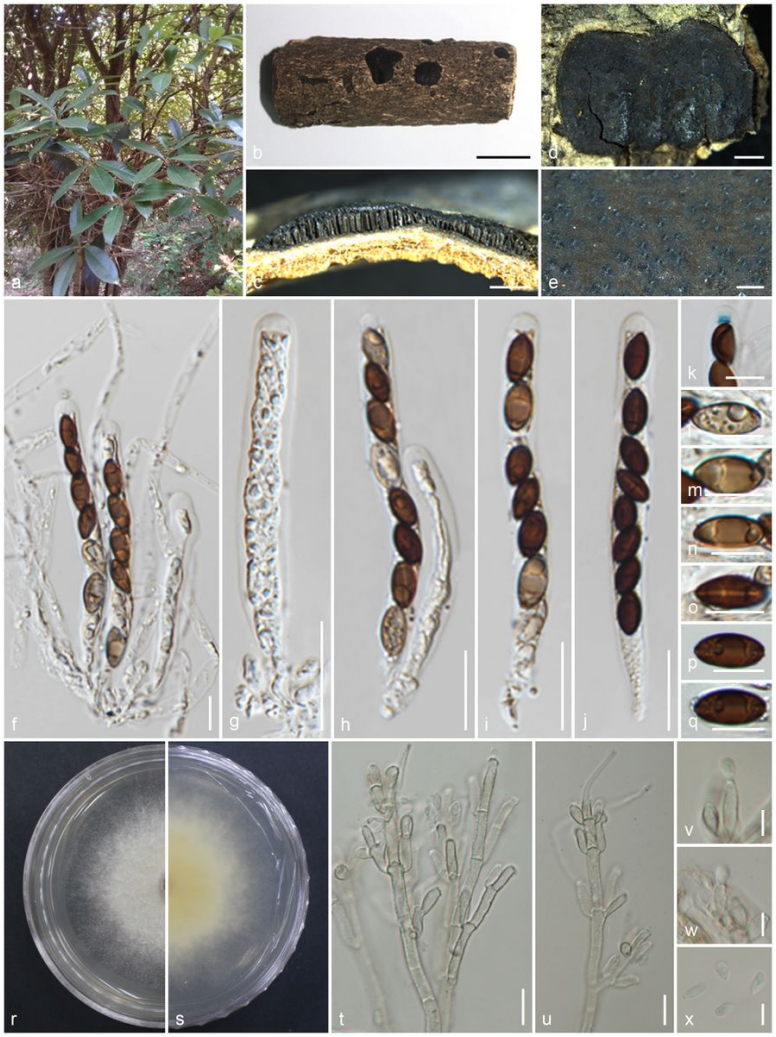

Figure 20

Biscogniauxia petrensis (HKAS 102388; GZCC 21-0040, living culture). a Host (Osmanthus fragrans). b Substrate. c Section through stroma showing ascomata. d,e Stromatal surface. f–j Asci (paraphyses in f). k Apical ring blueing in Melzer's reagent. l–q Ascospores (germ slit in o). r Upper view. s Reverse view of the one-week-old colony on PDA. t–x Conidia, conidiogenous cells, and conidiophores. Scale bars: b = 1 cm, c,d = 1000 µm, e = 500 µm, g = 20 µm, f,h–q,t,u = 10 µm, v–x = 5 µm.

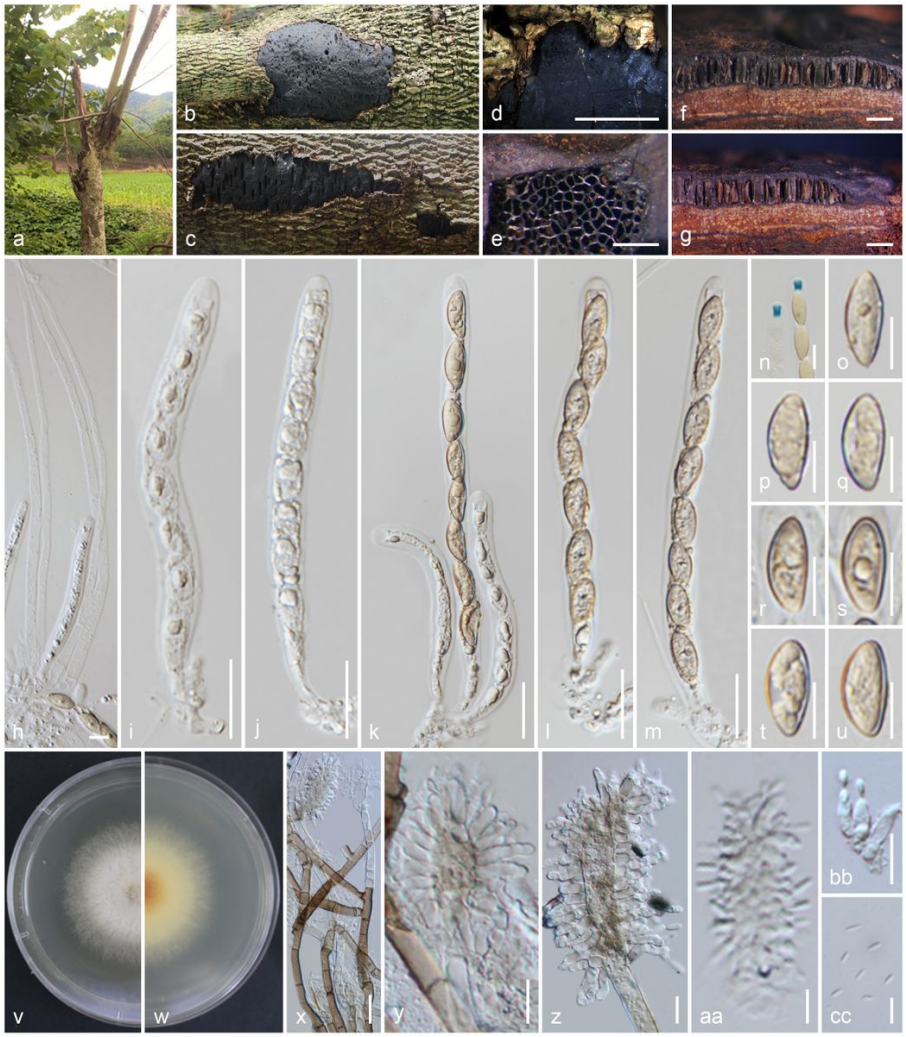

Figure 21

Camillea tinctor (MFLU 18-0786; MFLUCC 18-0508, living culture). a Host (Bauhinia racemosa). b–d Stromatal surface on the substrate. e–g Section through stroma showing ascomata (e in horizontal, f,g in vertical). h Paraphyses. i–m Asci, n. apical ring blueing in Melzer's reagent. o–u Ascospores. v Upper view. w Reverse view of the one-week-old colony on PDA. x–cc Conidia, conidiogenous cells, and conidiophores. Scale bars: d = 1 cm, e–g = 1000 µm, i–m,x = 20 µm, h,n–u,y–cc = 10 µm.

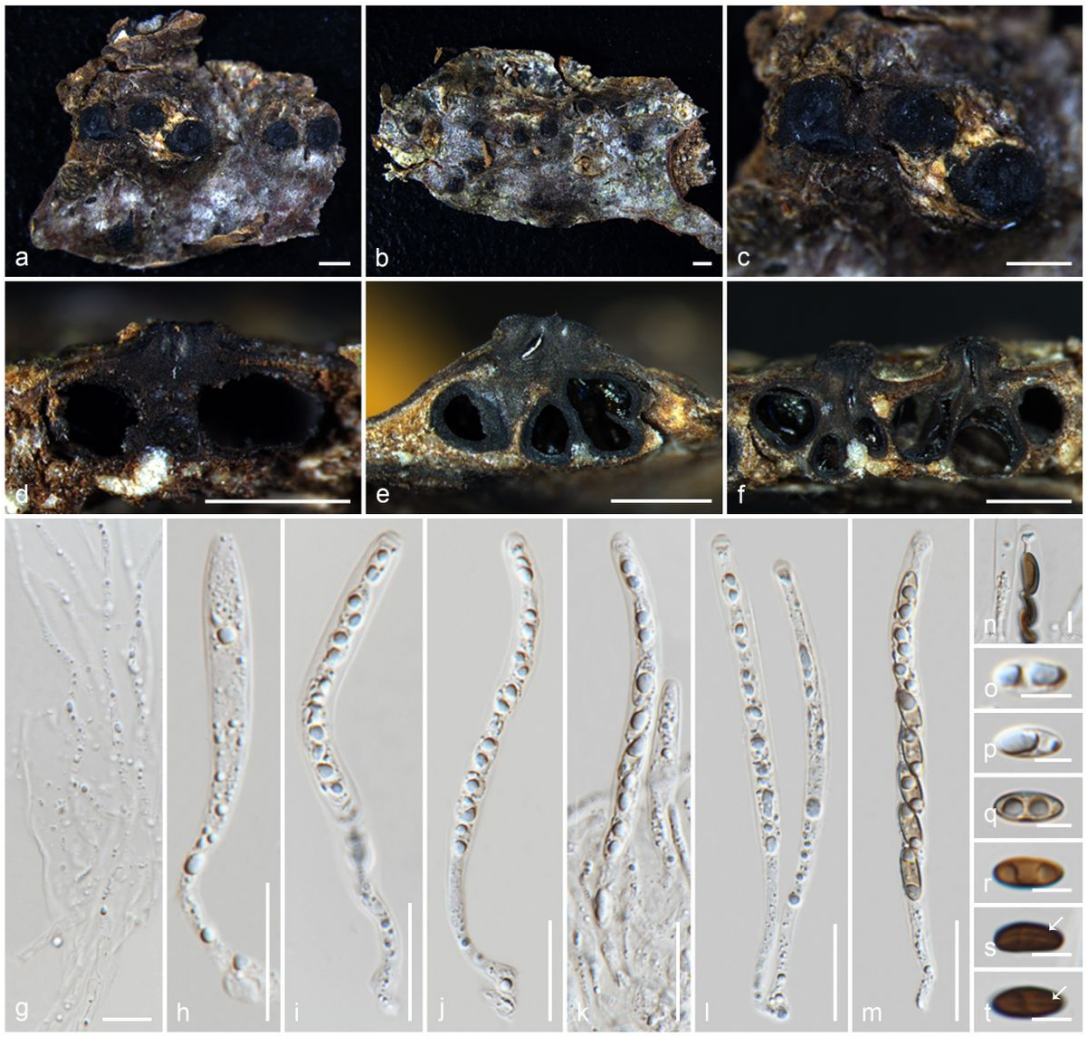

Figure 22

Lopadostoma quercicola (MFLU 17-0731). a–c Stromata in dead substrate. d–f Section through stroma. g Paraphyses. h–m Asci. n Apical ring blueing in Melzer's reagent. o–t Ascospores (white arrows show germ slits). Scale bars: a–f = 1000 µm, h–m = 20 µm, g = 10 µm, n–t = 5 µm.

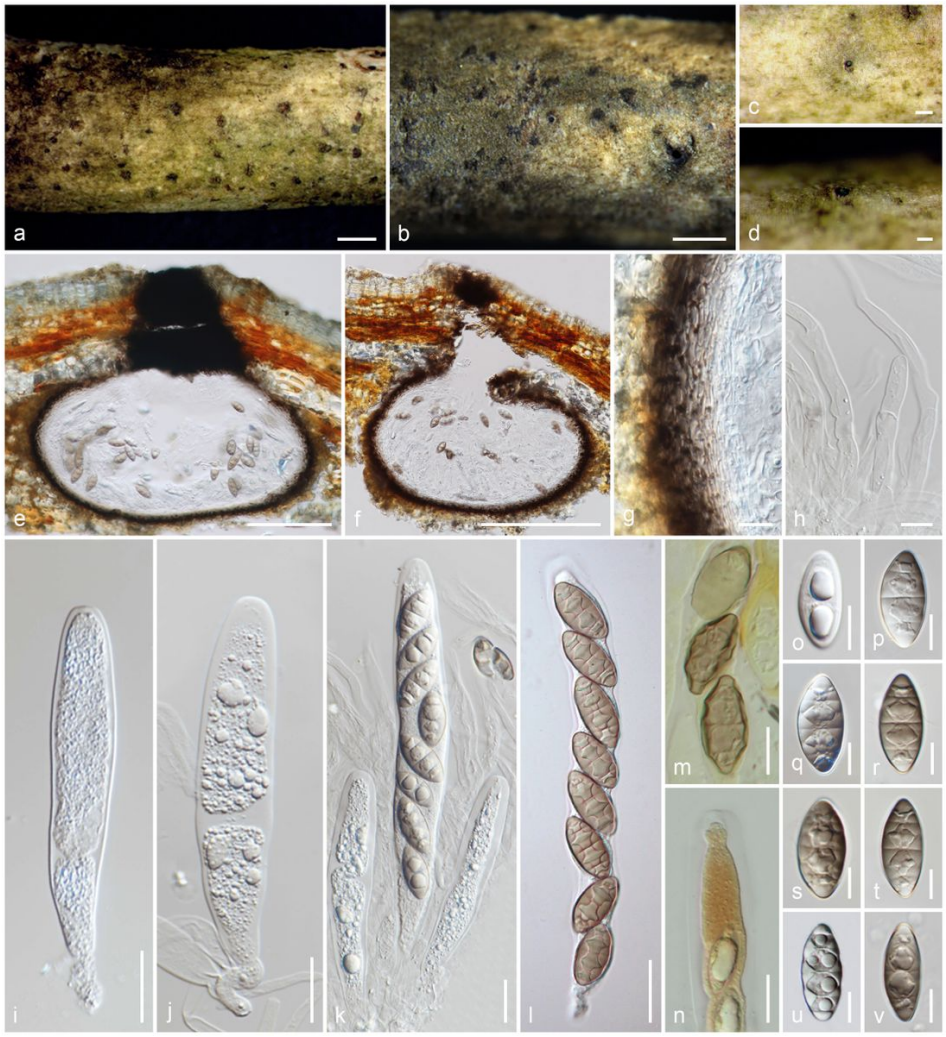

Figure 23

Acrocordiella photiniicola (MFLU 17-1552, holotype). a Substrate. b–d Ascomata in branches. e,f Section through ascoma. g Peridium. h Paraphyses. i–l Asci. m Ascospores in 5% KOH. n Apical ring in Melzer's reagent. o–v Ascospores. Scale bars: a,b = 1000 µm, c = 200 µm, d–f = 100 µm, i–l = 20 µm, g,h,m–v = 10 µm.

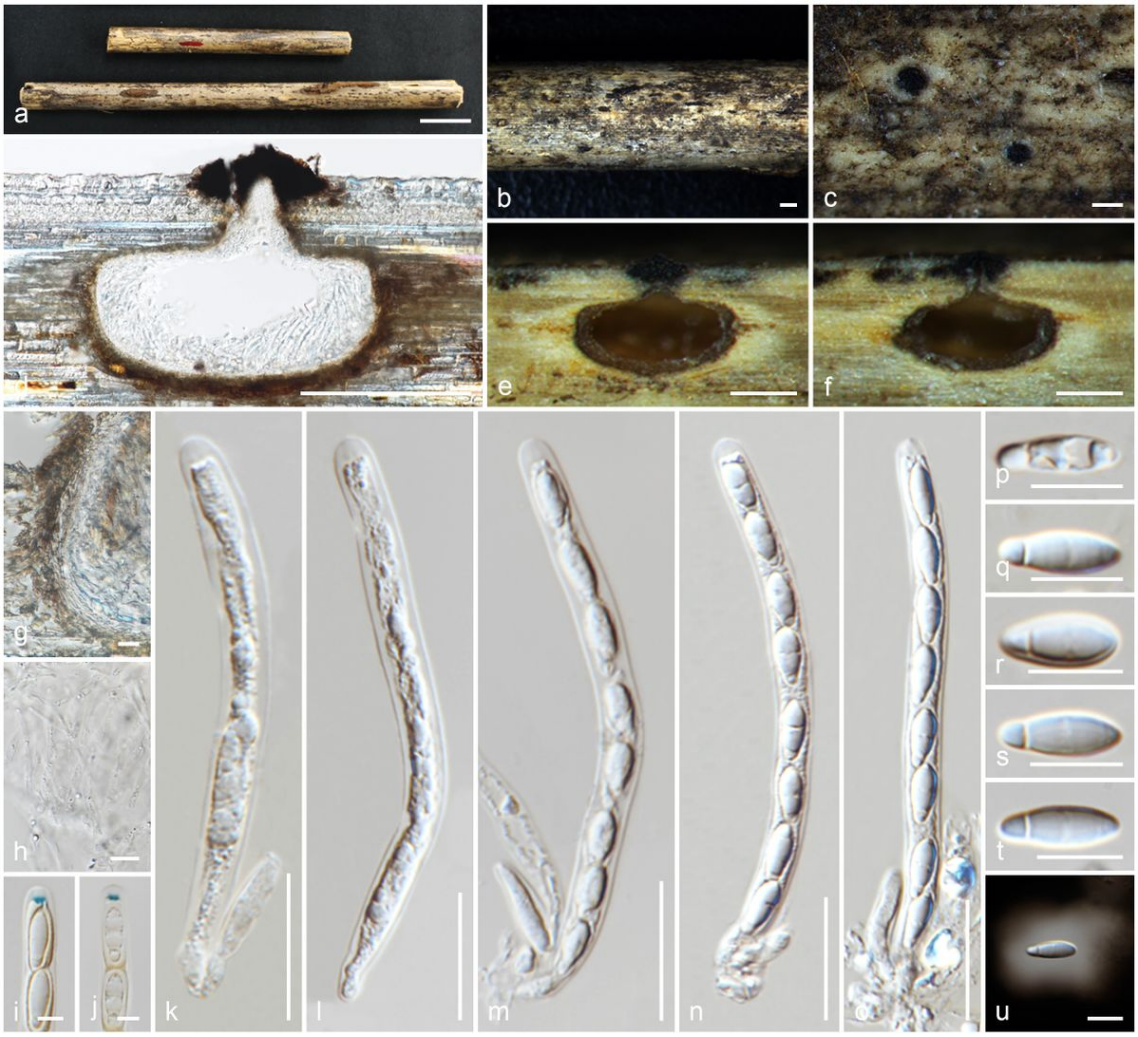

Figure 24

Vamsapriya mucosa (MFLU 18-0103, holotype). a Substrate. b,c Ascomata in wood. d–f Section through ascoma. g Peridium. h Paraphyses. i,j Apical ring blueing in Melzer's reagent. k–o Asci. p–u Ascospores (u in Indian ink). Scale bars: a = 1 cm, b = 1000 µm, c–f = 200 µm, k–o = 20 µm, g,h,p–u = 10 µm, i,j = 5 µm.

Figure 25

Paravamsapriya ostiolata (MFLU 18-0761, holotype). a Substrate. b,c Ascomata in wood. d–f Section through ascoma. g Peridium. h Paraphyses. i–l Asci. m–s Ascospores (q in 5% KOH, r in Congo red, s in Indian ink, white arrows show mucilaginous polar ends), t J- apical ring in Melzer's reagent. Scale bars: a = 1 cm, b = 1000 µm, c–e = 500 µm, f = 200 µm, g,i–l = 20 µm, h,m–t = 10 µm.

Figure 26

Helicogermslita clypeata (MFLU 18-0852, holotype). a substrate. b,c Ascomata in branches. d–f Section through ascoma. g Peridium. h Paraphyses. i–l Asci. m Apical ring blueing in Melzer's reagent. n–t Ascospores (white arrows show germ slits). Scale bars: a = 1 cm, b,c = 1000 µm, d,e = 200 µm, f = 100 µm, i–l = 20 µm, g,h = 10 µm, m–t = 5 µm.

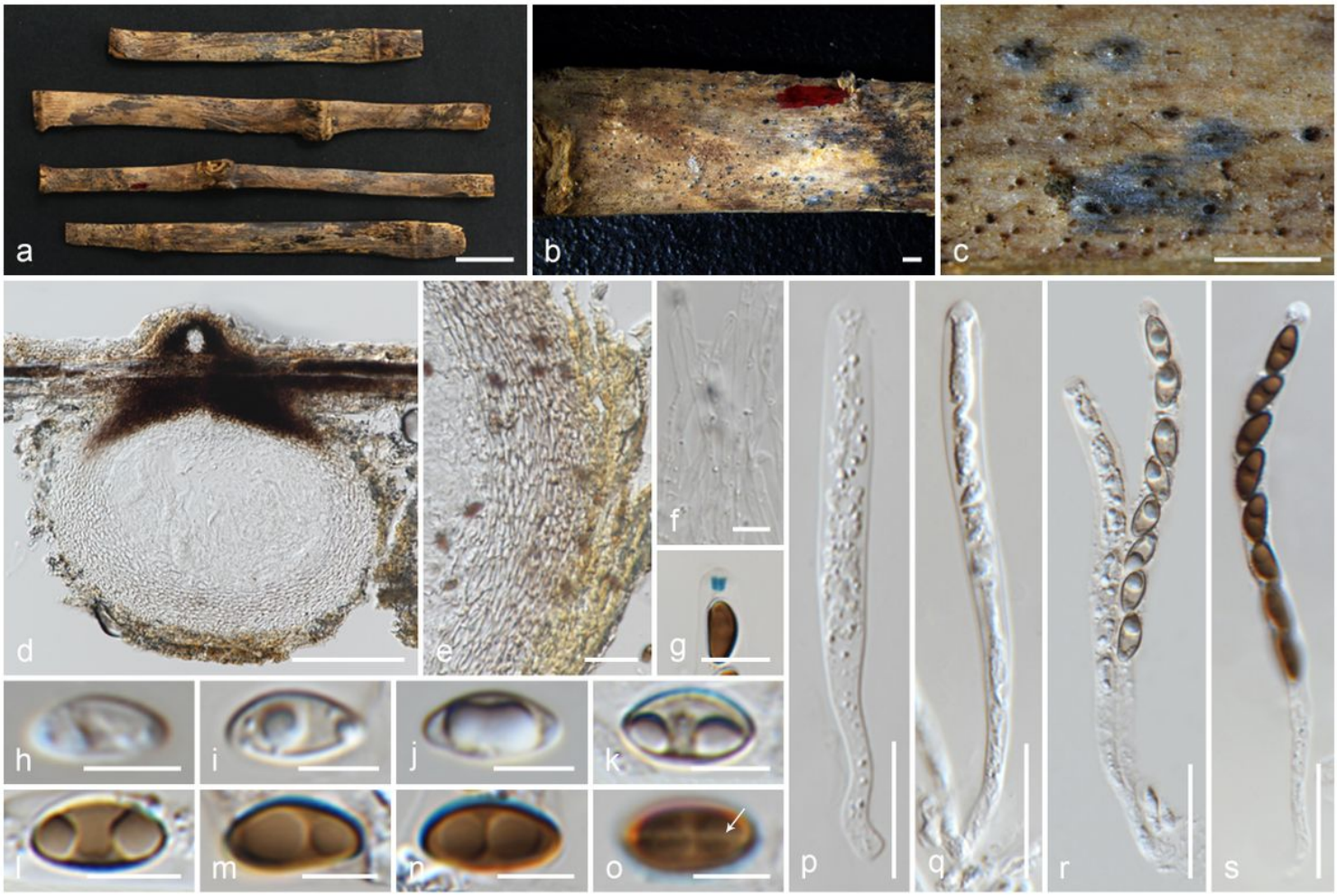

Figure 27

Hypocopra zeae (MFLU 18-0809, holotype). a Substrate. b,c Ascomata in dead substrate. d Section through ascoma. e Peridium. f Paraphyses. g Apical ring blueing in Melzer's reagent. h–o Ascospores (white arrow shows germ slit). p–s Asci. Scale bars: a–c = 1000 µm, d = 100 µm, e,p–s = 20 µm, f,g = 10 µm, h–o = 5 µm.

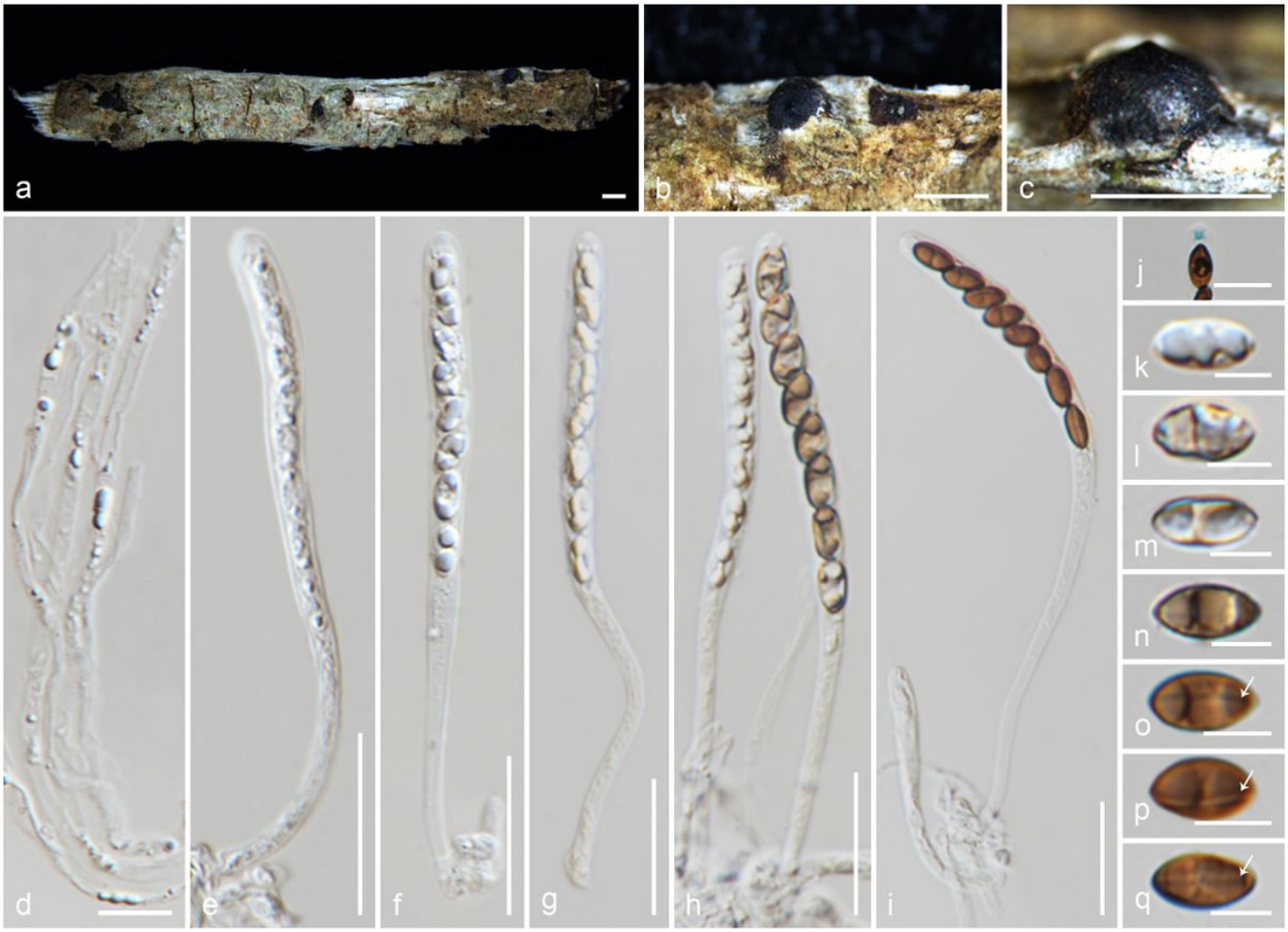

Figure 28

Nemania longipedicellata (MFLU 18-0819, holotype). a Substrate. b,c Stromata in dead substrate. d Paraphyses. e–i Asci. j Apical ring blueing in Melzer's reagent. k–q Ascospores (white arrows show germ slits). Scale bars: a–c = 1000 µm, e–i = 20 µm, d,j = 10 µm, k–q = 5 µm.

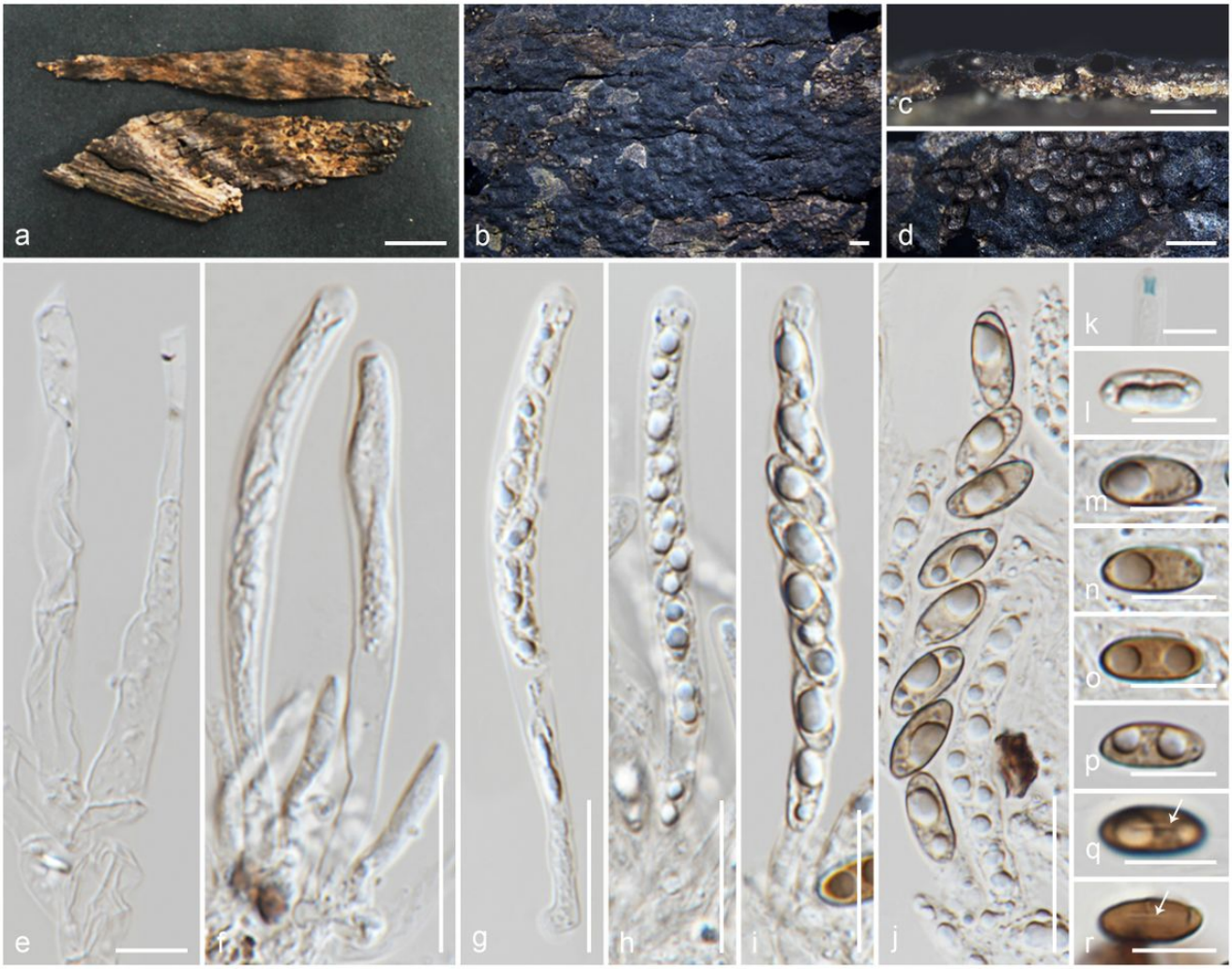

Figure 29

Nemania delonicis (MFLU 19-2124, holotype). a,b Stromata in dead substrate. c,d Section through stromata (c vertical, d horizontal), e Paraphyses. f–j Asci. k Apical ring blueing in Melzer's reagent. l–r Ascospores (white arrows show germ slits). Scale bars: a = 1 cm, b–d = 1000 µm, f–j = 20 µm, e,k–r = 10 µm.

Figure 30

Nemania paraphysata (MFLU 19-2121, holotype). a Substrate. b,c Stromata in wood. d,e Section through stroma. f Paraphyses. g–j Asci. k Apical ring blueing in Melzer's reagent. l–q Ascospores (germ slit in white arrow; q in Indian ink). Scale bars: a = 1 cm, b–e = 1000 µm, g–j = 20 µm, f = 10 µm, k–q = 5 µm.

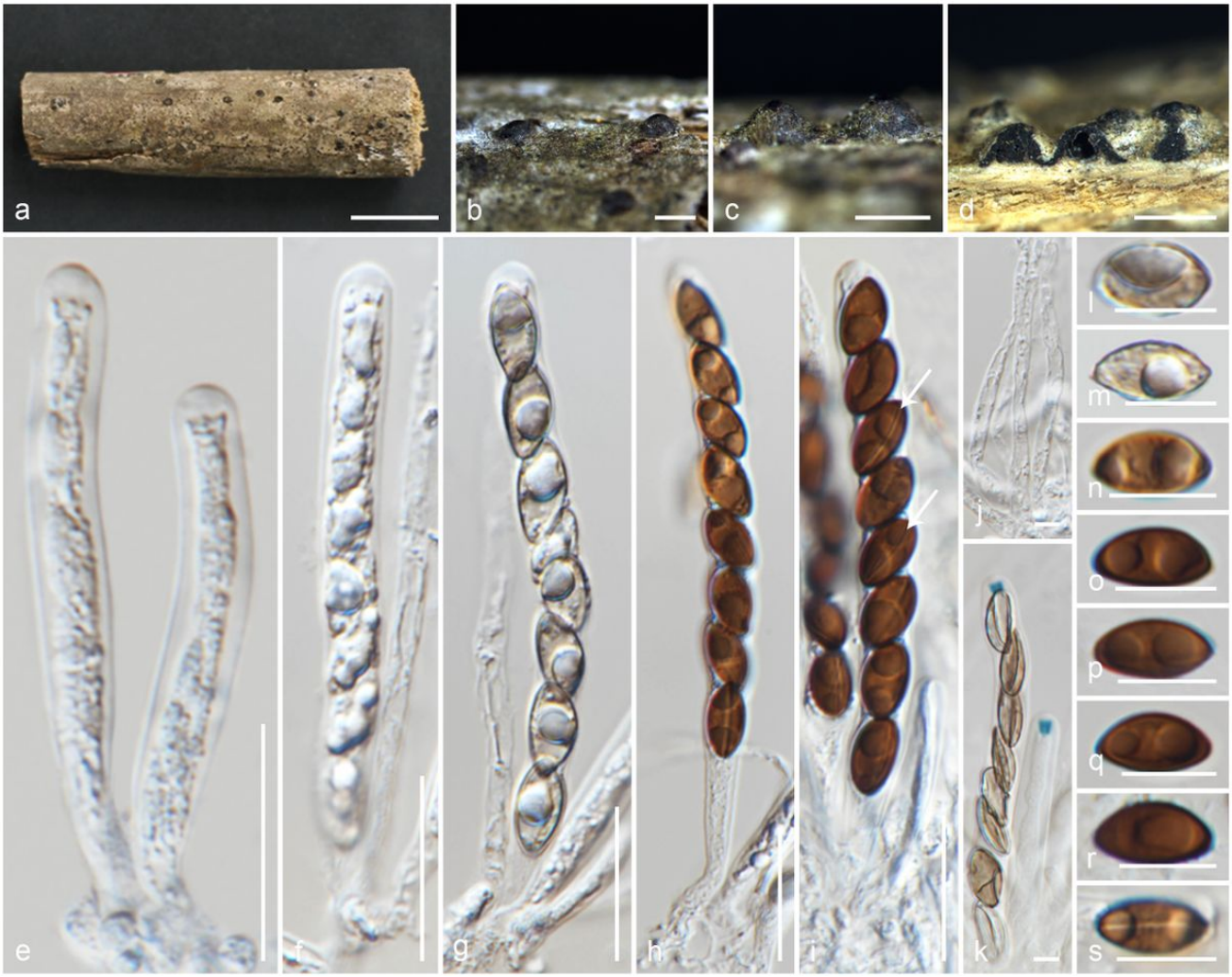

Figure 31

Nemania thailandensis (MFLU 19-2117, holotype). a substrate. b,c Stromata in wood. d Sections through stromata. e–i Asci. j Paraphyses. k Apical ring blueing in Melzer's reagent. l–s Ascospores. Scale bars: a = 1 cm, b–d = 1000 µm, e–i = 20 µm, l–s = 10 µm, j,k = 5 µm.

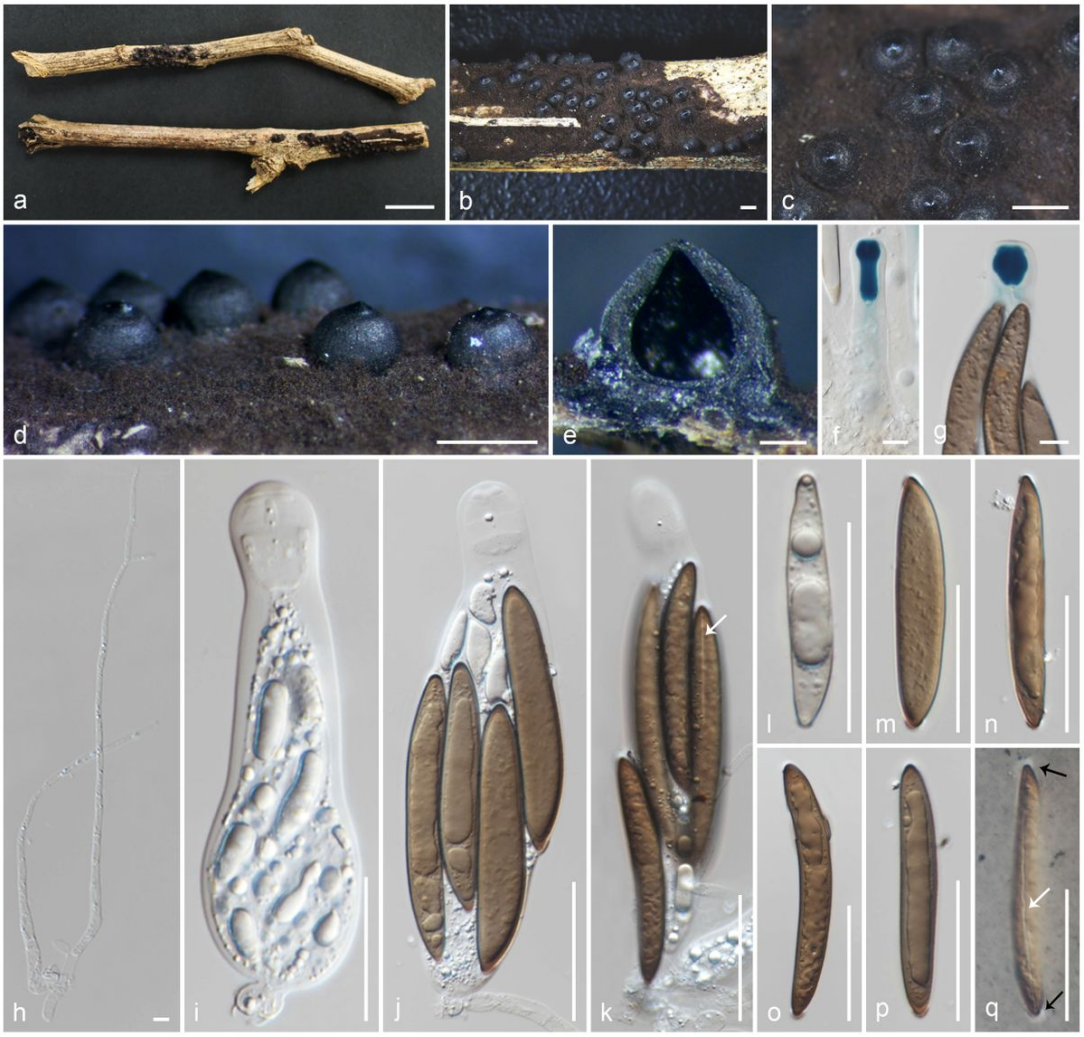

Figure 32

Rosellinia markhamiae (MFLU 19-2137). a Substrate. b–d Stromata in dead substrate. e Section through stroma. f,g Apical ring blueing in Melzer's reagent. h Paraphyses. i–k Asci. l–q Ascospores (white arrows show germ slits, black arrows show ascospore apical sheaths, q in Indian ink). Scale bars: a = 1 cm, b–d = 1000 µm, e = 200 µm, i–q = 50 µm, f–h = 10 µm.

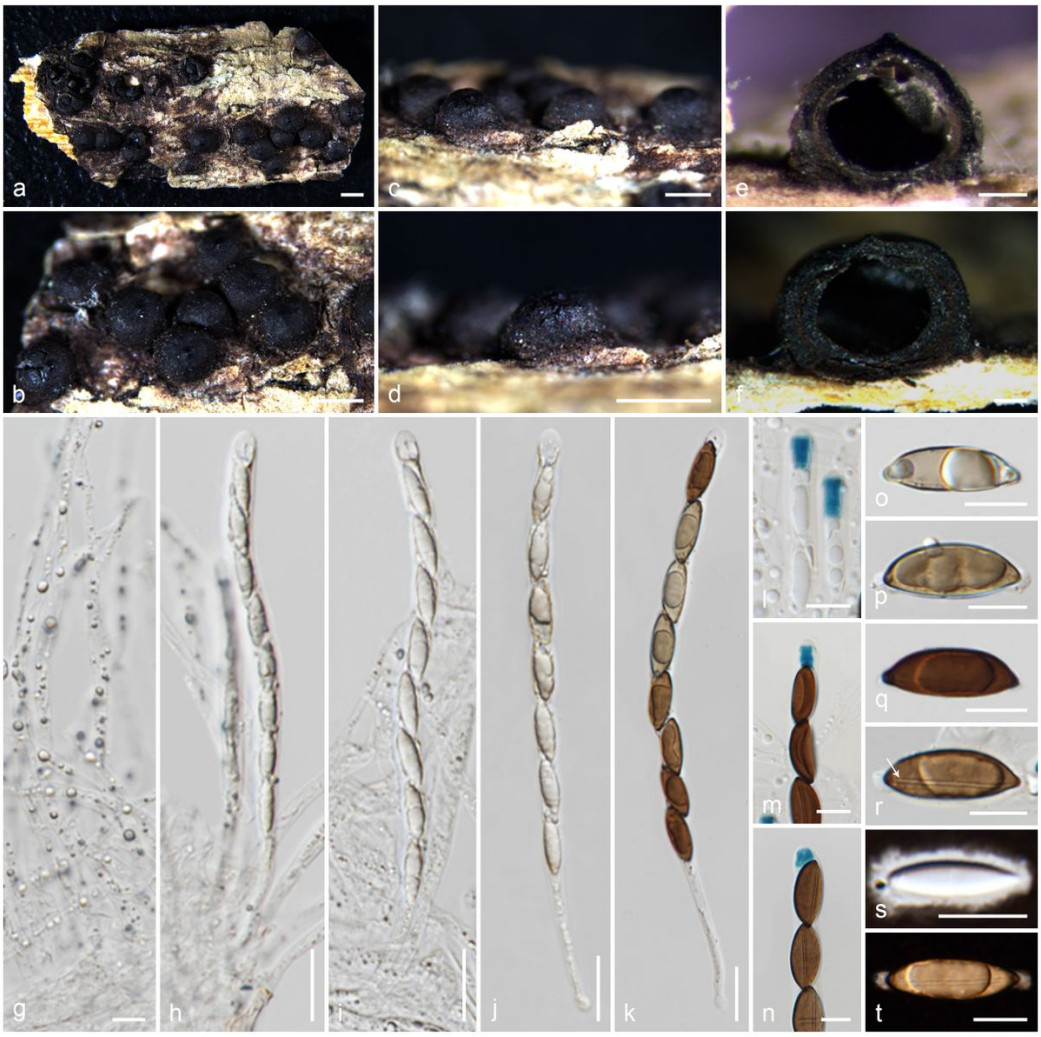

Figure 33

Rosellinia britannica (MFLU 17-0987). a–d Stromata in dead substrate. e,f Section through stroma. g Paraphyses. h–k Asci. l–n Apical ring blueing in Melzer's reagent. o–t Ascospores (germ slit shows in white arrow, s,t in Indian ink). Scale bars: a–d = 1000 µm, e,f = 200 µm, h–k = 20 µm, g,l–t = 10 µm.

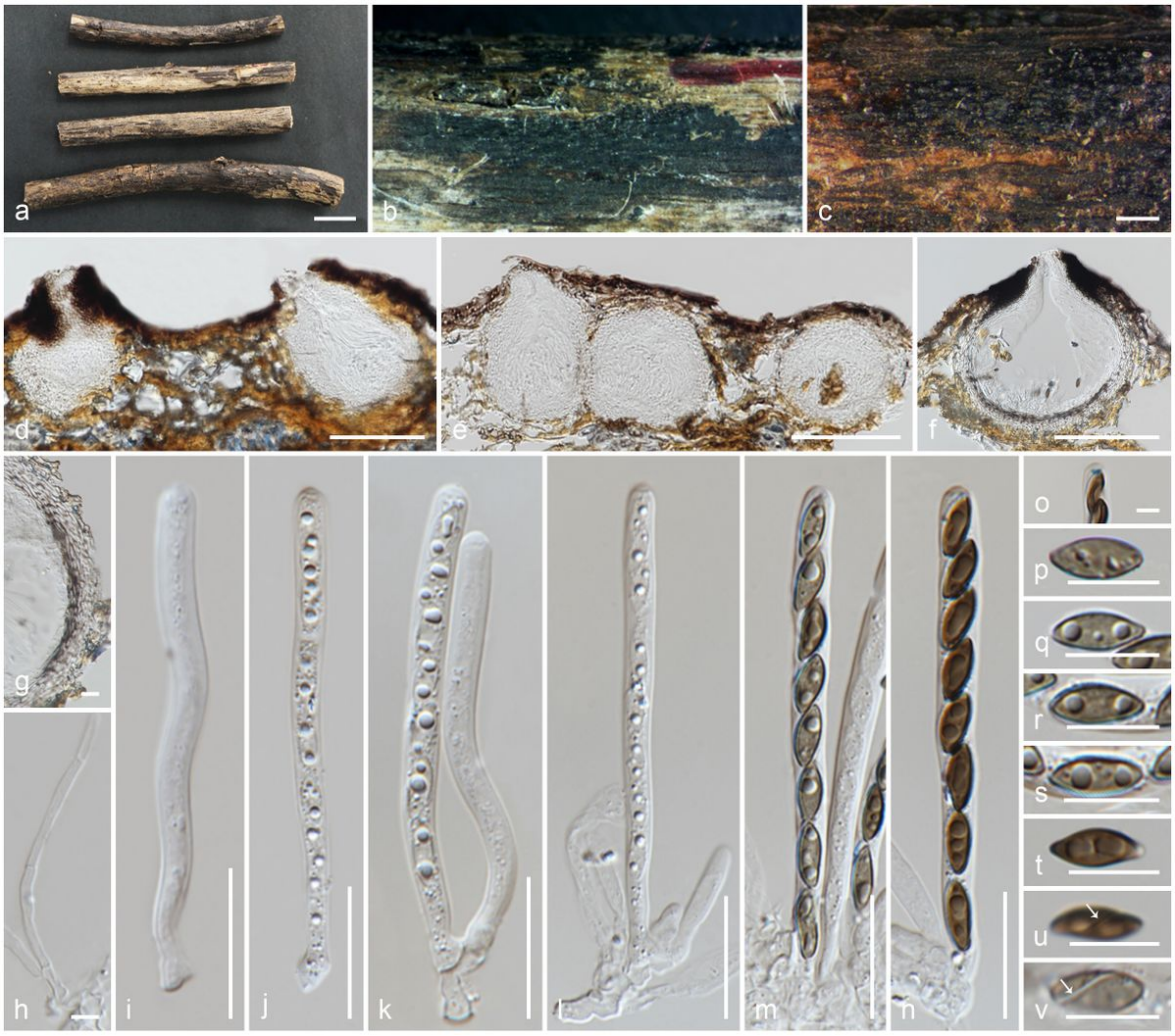

Figure 34

Anthostomella lamiacearum (MFLU 18-0101, holotype). a Substrate. b,c Ascomata in dead substrate. d–f Section through ascomata. g Peridium. h Paraphyses. i–n Asci. o Apical ring blueing in Melzer's reagent. p–v Ascospores (white arrows show germ slits). Scale bars: a = 1 cm, c = 500 µm, d–f = 100 µm, i–n = 20 µm, g,p–v = 10 µm, h,o = 5 µm.

Figure 35

Magnostiolata mucida (MFLU 19-2133, holotype). a Substrate. b,c Ascomata in dead substrate. d–f Sections through ascomata. g Peridium. g Paraphyses. h,i Apical ring blueing in Melzer's reagent (white arrow shows germ slit). j–m Asci (k with paraphyses). n–u Ascospores (u in Indian ink). Scale bars: a = 1 cm, b,c = 1000 µm, d,e = 200 µm, f = 100 µm, j–m = 20 µm, g–i,n–u = 10 µm.

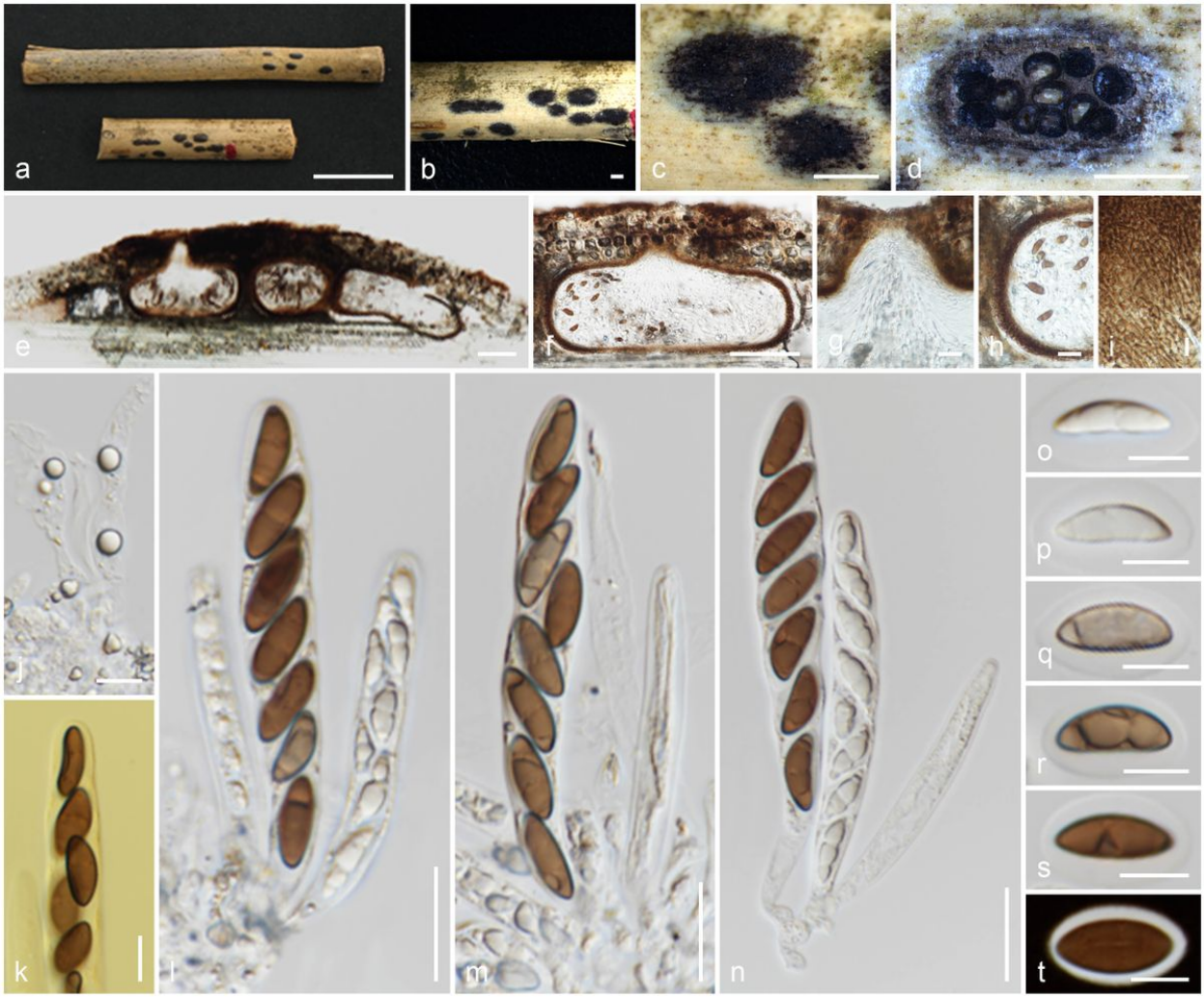

Figure 36

Neoanthostomella bambusicola (MFLU 18-0796, holotype). a Substrate. b–d Stromata on branches (d horizontal). e,f Sections through ascomata. g Section through ostiole. h Peridium. i Inner layer of the peridium. j Paraphyses. k Asci in Melzer's reagent. l–n Asci. o–t Ascospores (t in Indian ink). Scale bars: a = 1 cm, b–d = 1000 µm, e,f = 100 µm, g,h,l–n = 20 µm, i–k,o–t = 10 µm.

Figure 37

Nigropunctata bambusicola (MFLU 19-2145, holotype). a Substrate. b,c Ascomata in dead substrate. d,e Sections through ascomata. f Peridium. g Paraphyses. h–k Asci. l Apical ring blueing in Melzer's reagent. m–r Ascospores (germ slit shows in white arrow, q,r in Indian ink). Scale bars: a,b = 1 cm, c = 1000 µm, d = 500 µm, e = 100 µm, f = 20 µm, g–r = 10 µm.

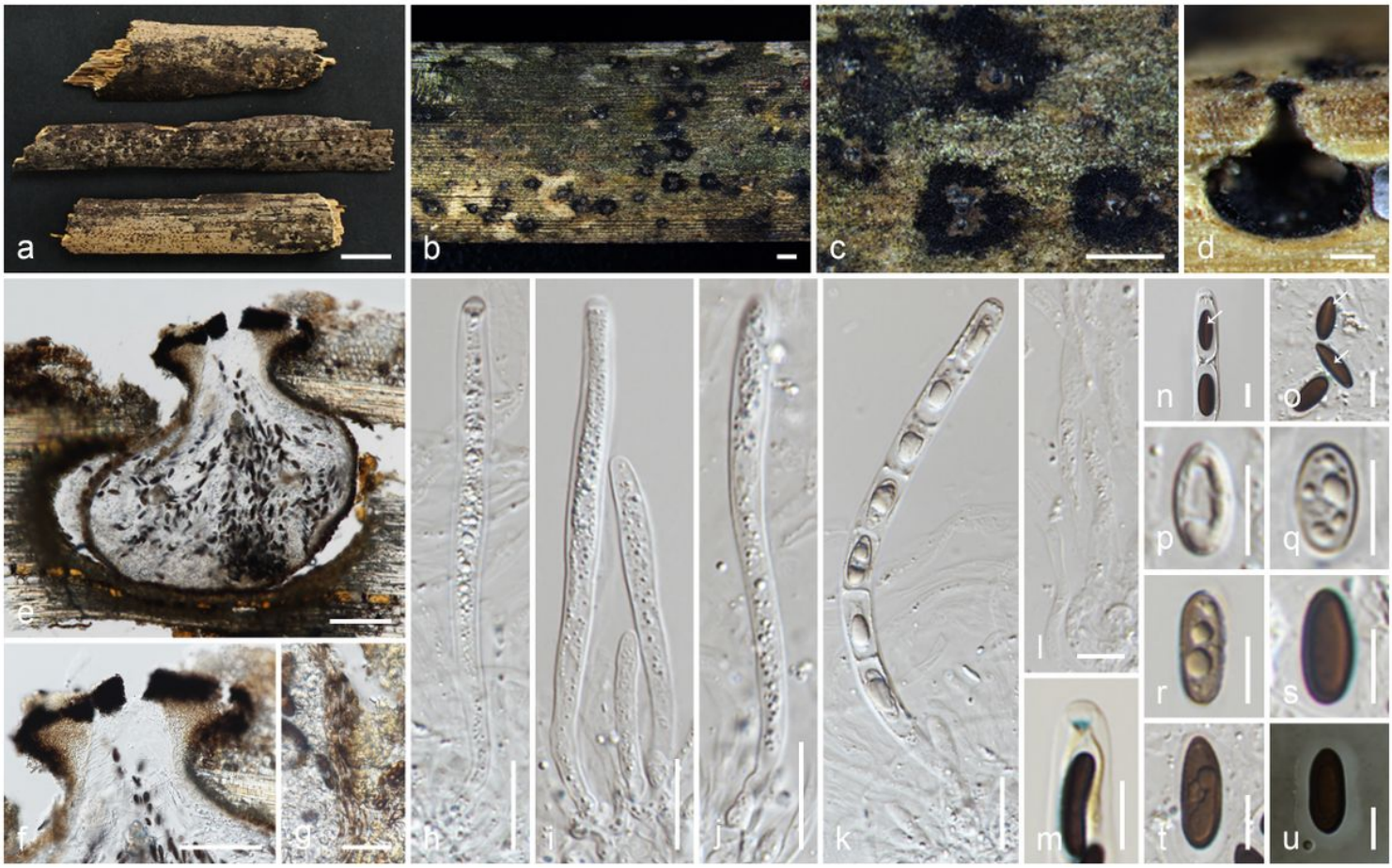

Figure 38

Nigropunctata nigrocircularis (MFLU 19-2130, holotype). a Substrate. b,c ascomata in dead substrate. d,e Sections through ascoma. f Section through ostiole. g Peridium. h–k Asci. l Paraphyses. m Apical ring blueing in Melzer's reagent. n–u Ascospores (white arrows show germ slits, u in Indian ink). Scale bars: a = 1 cm, b,c = 1000 µm, d = 200 µm, e,f = 100 µm, g–k = 20 µm, l–u = 10 µm.

Figure 39

Nigropunctata thailandica (MFLU 19-2118, holotype). a Substrate. b,c Ascomata in dead substrate. d,e Sections through ascomata. f Peridium. g Paraphyses. h–l Asci. m Apical ring blueing in Melzer's reagent. n–t Ascospores. Scale bars: a = 1 cm, b,c = 1000 µm, d = 200 µm, e = 100 µm, f,h–l = 20 µm, g,m–t = 10 µm.

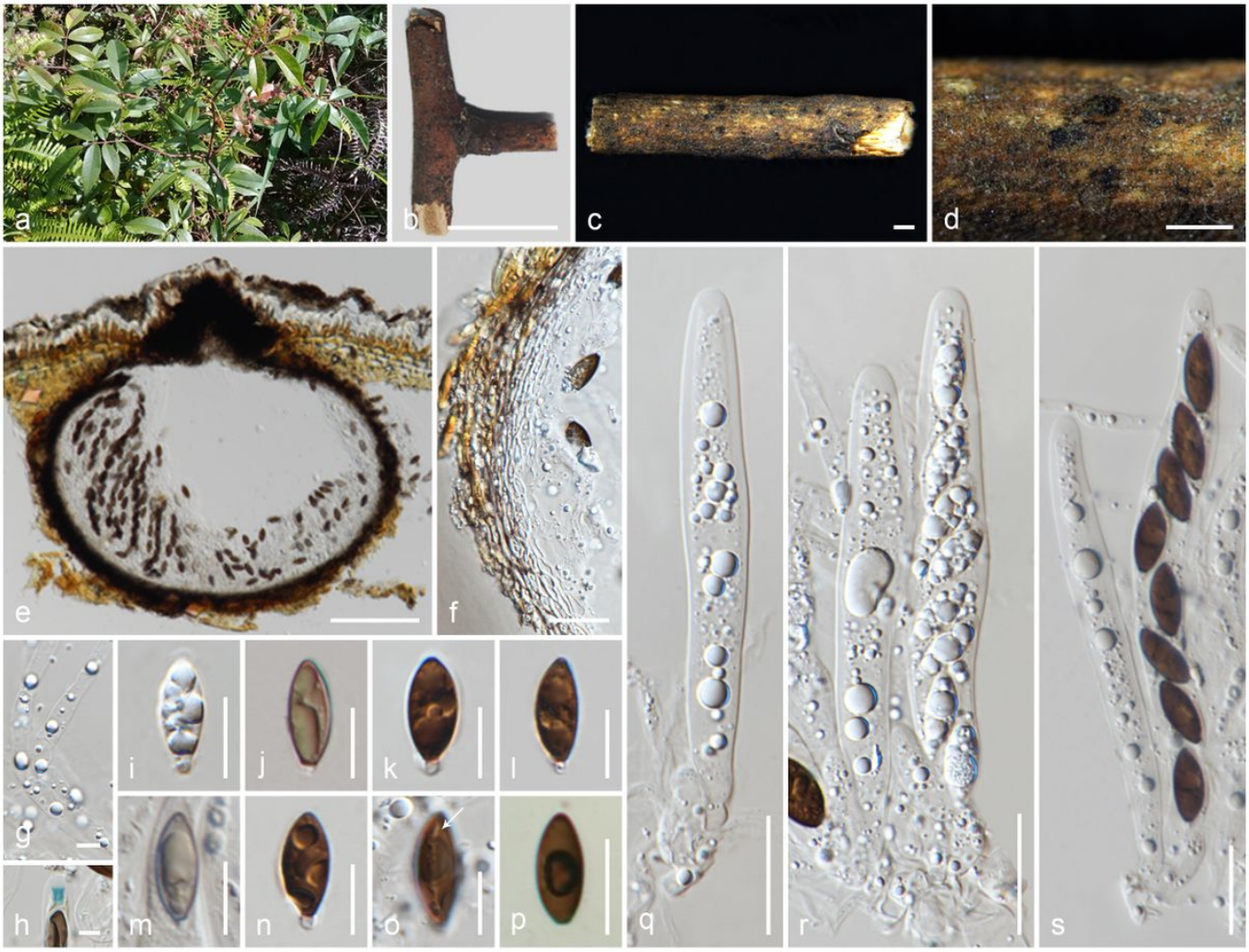

Figure 40

Occultitheca rosae (HKAS 102393, holotype). a Host (Rosa sp.). b Substrate. c,d Ascomata in dead substrate. e Section through ascoma. f Peridium. g Paraphyses. h Apical ring blueing in Melzer's reagent. i–p Ascospores (germ slit shows in white arrow, p in Melzer's reagent). q–s Asci. Scale bars: b = 1 cm, c,d = 1000 µm, e = 100 µm, f,q–s = 20 µm, i–p = 10 µm, g,h = 5 µm.

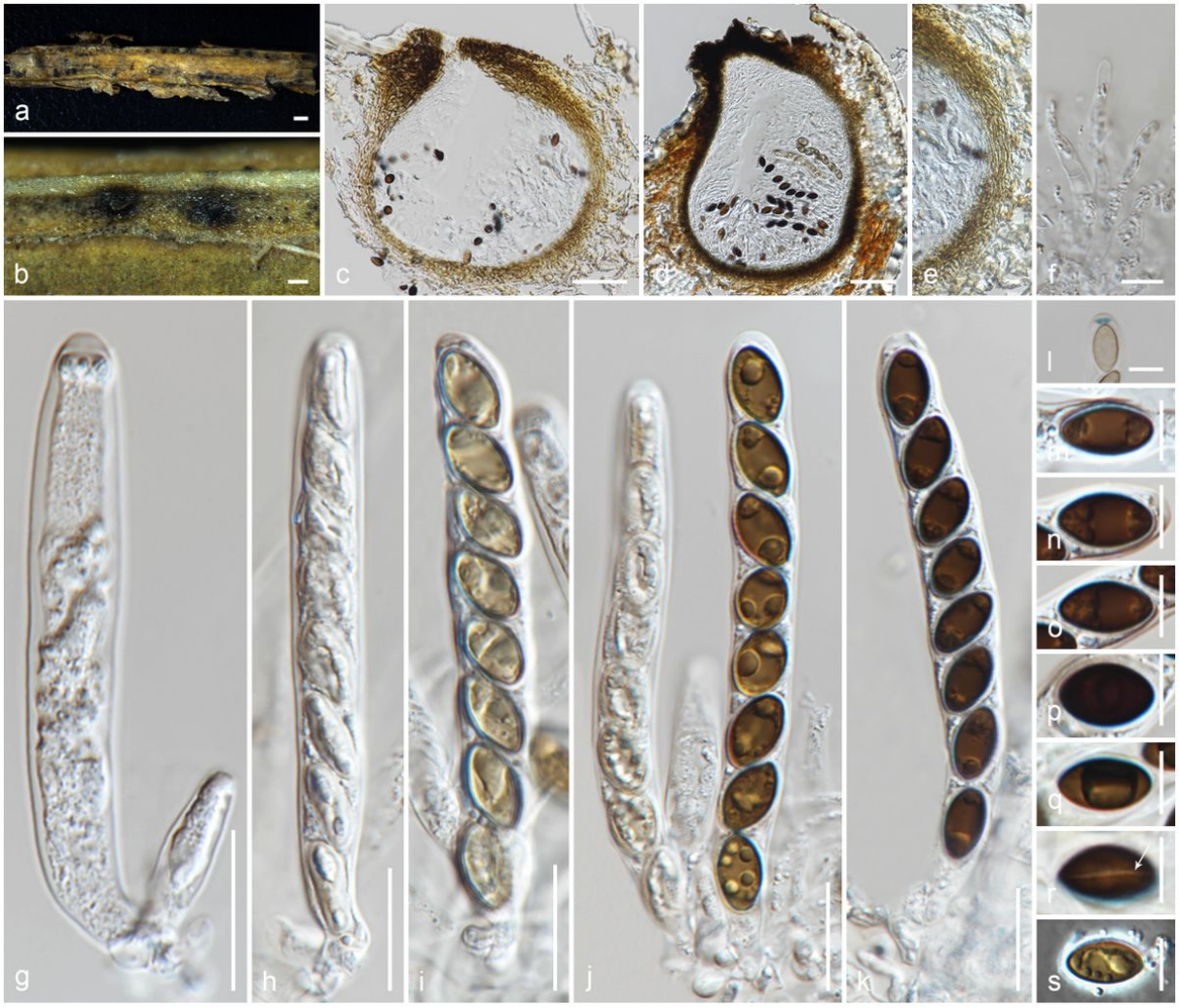

Figure 41

Pseudoanthostomella pini-nigrae (MFLU 15-3608). a Substrate. b Ascomata in substrate. c–d Sections through ascoma. e Peridium. f Paraphyses. g–k Asci. l Apical ring blueing in Melzer's reagent. m–s Ascospores (white arrows show germ slits, s in Indian ink). Scale bars: a = 1000 µm, b = 200 µm, c,d = 50 µm, e,g–k = 20 µm, f,l–s = 10 µm.

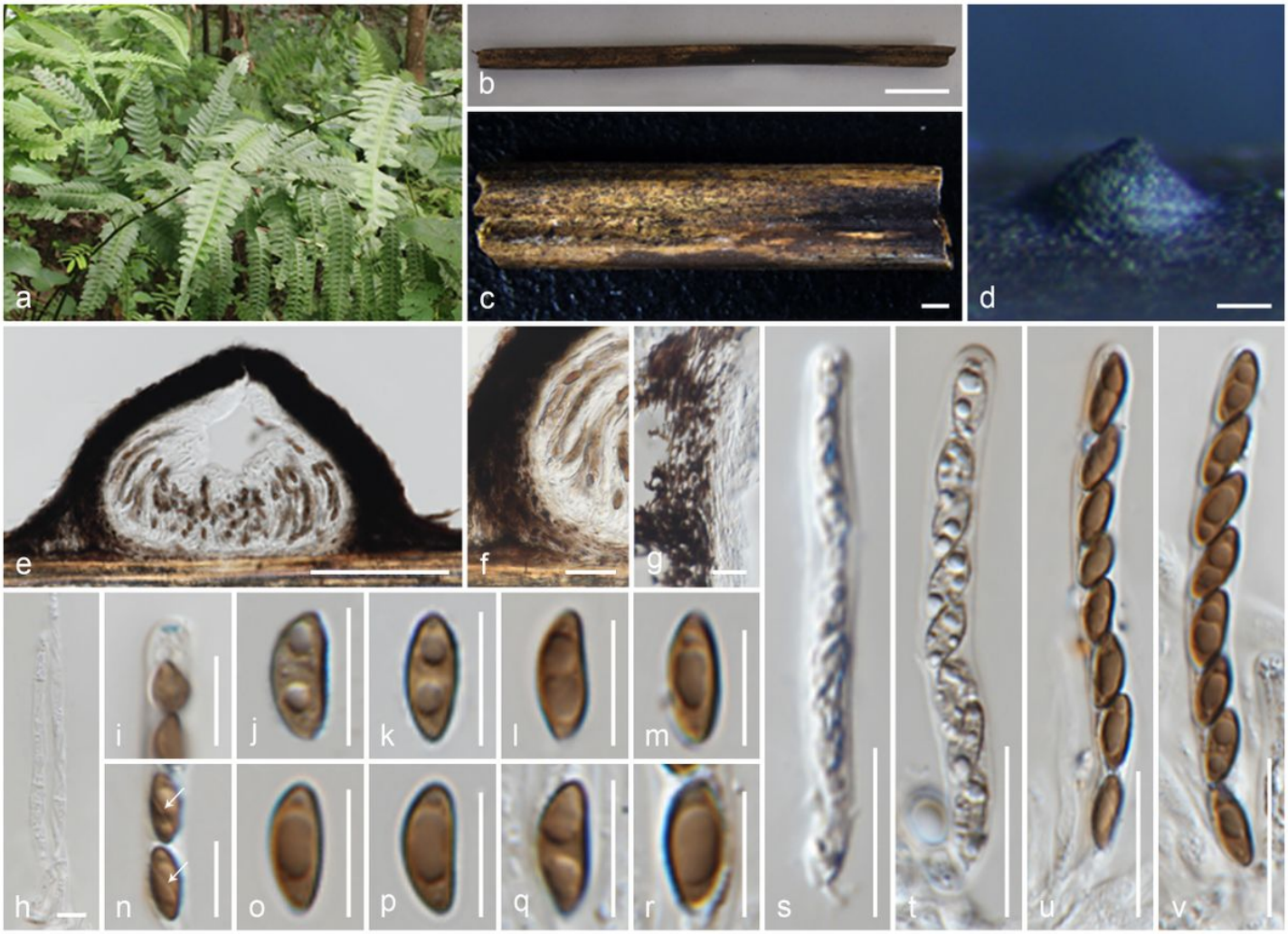

Figure 42

Xenoanthostomella chromolaenae (MFLU 18-0840). a Host (Nephrolepis sp.). b substrate. c,d Stromata in dead substrate. e Section through stroma. f,g Peridium. h paraphyses. i Apical ring blueing in Melzer's reagent. j–r Ascospores (white arrows show germ slits). s–v Asci. Scale bars: b = 1 cm, c = 1000 µm, d,e = 100 µm, f,s–v = 20 µm, g,i–r = 10 µm, h = 5 µm.

Supplementary Files

This is a list of supplementary files associated with this preprint. Click to download.

- Supplementary1.xlsx
- Supplementary2.xlsx